FERMILAB-FN-0815-E

arXiv:0704.3575v1 [hep-ex] 26 Apr 2007

Averages of b-hadron Properties at the End of 2006

Heavy Flavor Averaging Group (HFAG)*

April 26, 2007

Abstract

This article reports world averages for measurements on b-hadron properties obtained by the Heavy Flavor Averaging Group (HFAG) using the available results at the end of 2006. In the averaging, the input parameters used in the various analyses are adjusted (rescaled) to common values, and all known correlations are taken into account. The averages include lifetimes, neutral meson mixing parameters, parameters of semileptonic decays, branching fractions of B decays to final states with open charm, charmonium and no charm, and measurements related to CP asymmetries.

*The HFAG members involved in producing the averages for the end of 2006 update are: E. Barberio, R. Bernhard, S. Blyth, G. Cavoto, P. Chang, F. Di Lodovico, S. Eidelman, T. Gershon, R. Godang, R. Harr, H. Lacker, A. Limosani, C.-J. Lin, O. Long, V. Luth, S. Prell, O. Schneider, J. Smith, S. Tosi, K. Trabelsi, R. Van Kooten, C. Voena, and C. Weiser.

Contents

1 Introduction **4**

2 Methodology **5**

3 b-hadron production fractions, lifetimes and mixing parameters **13**

3.1 b-hadron production fractions . . . 13

3.1.1 b-hadron production fractions in $\Upsilon(4S)$ decays . . . 13

3.1.2 b-hadron production fractions in $\Upsilon(5S)$ decays . . . 15

3.1.3 b-hadron production fractions at high energy . . . 16

3.2 b-hadron lifetimes . . . 19

3.2.1 Lifetime measurements, uncertainties and correlations . . . 20

3.2.2 Inclusive b-hadron lifetimes . . . 21

3.2.3 B^0 and B^+ lifetimes and their ratio . . . 23

3.2.4 B_s^0 lifetime . . . 25

3.2.5 B_c^+ lifetime . . . 27

3.2.6 Λ_b^0 and b-baryon lifetimes . . . 28

3.2.7 Summary and comparison with theoretical predictions . . . 30

3.3 Neutral B-meson mixing . . . 31

3.3.1 B^0 mixing parameters . . . 31

3.3.2 B_s^0 mixing parameters . . . 37

4 Measurements related to Unitarity Triangle angles **46**

4.1 Introduction . . . 46

4.2 Notations . . . 48

4.2.1 CP asymmetries . . . 48

4.2.2 Time-dependent CP asymmetries in decays to CP eigenstates . . . 48

4.2.3 Time-dependent CP asymmetries in decays to vector-vector final states . 49

4.2.4 Time-dependent asymmetries in decays to self-conjugate multiparticle final states . . . 50

4.2.5 Time-dependent CP asymmetries in decays to non-CP eigenstates . . . 52

4.2.6 Time-dependent CP asymmetries in the B_s System . . . 57

4.2.7 Asymmetries in $B \to D^{(*)}K^{(*)}$ decays . . . 58

4.3 Common inputs and error treatment . . . 59

4.4 Time-dependent asymmetries in $b \to c\bar{c}s$ transitions . . . 60

4.4.1 Time-dependent CP asymmetries in $b \to c\bar{c}s$ decays to CP eigenstates . 60

4.4.2 Time-dependent transversity analysis of $B^0 \to J/\psi K^{*0}$ . . . 61

4.4.3 Time-dependent CP asymmetries in $B^0 \to D^{*+}D^{*-}K_S^0$ decays . . . 62

4.4.4 Time-dependent analysis of $B_s^0 \to J/\psi\phi$ . . . 62

4.5 Time-dependent CP asymmetries in colour-suppressed $b \to c\bar{u}d$ transitions . . . 63

4.6 Time-dependent CP asymmetries in charmless $b \to q\bar{q}s$ transitions . . . 64

4.6.1 Time-dependent CP asymmetries in charmless $b \to q\bar{q}s$ decays to CP eigenstates . . . 65

4.6.2 Time-dependent Dalitz plot analysis of $B^0 \to K^+K^-K^0$ decays . . . 67

4.7 Time-dependent CP asymmetries in $b \to c\bar{c}d$ transitions . . . 67

4.8 Time-dependent CP asymmetries in $b \to q\bar{q}d$ transitions . . . 68

4.9 Time-dependent asymmetries in $b \to s\gamma$ transitions . . . 69
4.10 Time-dependent CP asymmetries in $b \to u\overline{u}d$ transitions . . . 70
4.11 Time-dependent CP asymmetries in $b \to c\overline{u}d/u\overline{c}d$ transitions . . . 73
4.12 Rates and asymmetries in $B^{\mp} \to D^{(*)}K^{(*)\mp}$ decays . . . 74
4.12.1 D decays to CP eigenstates . . . 74
4.12.2 D decays to suppressed final states . . . 74
4.12.3 D decays to multiparticle self-conjugate final states . . . 75

5 Semileptonic B decays 87
5.1 Common set of input parameters . . . 87
5.2 Exclusive CKM-favored decays . . . 87
5.2.1 $\overline{B}^0 \to D^{*+}\ell^-\overline{\nu}$ . . . 87
5.2.2 $\overline{B}^0 \to D^+\ell^-\overline{\nu}$ . . . 89
5.3 Inclusive CKM-favored decays . . . 92
5.3.1 Inclusive Semileptonic Branching Fraction for $B^0/B^+ \to X\ell\nu_\ell$ . . . 92
5.3.2 Ratio of $\mathcal{B}(B^+ \to X\ell^+\nu_\ell)$ to $\mathcal{B}(B^0 \to X^-\ell^+\nu_\ell)$ . . . 93
5.3.3 Branching Fractions for $B^+ \to X\ell^+\nu_\ell$ and $B^0 \to X^-\ell^+\nu_\ell$ . . . 94
5.3.4 $|V_{cb}|$ Determined from $B \to X\ell\overline{\nu}$ . . . 95
5.4 Exclusive CKM-suppressed decays . . . 96
5.5 Inclusive CKM-suppressed decays . . . 98
5.5.1 BLNP . . . 99
5.5.2 DGE . . . 100
5.5.3 BLL . . . 103
5.5.4 Summary . . . 103

6 Charmless B-decay branching fractions and their asymmetries 108
6.1 Mesonic charmless decays . . . 108
6.2 Radiative and leptonic decays . . . 113
6.3 $B \to s\gamma$ . . . 117
6.4 Baryonic decays . . . 118
6.5 B_s decays . . . 120
6.6 Charge asymmetries . . . 120
6.7 Polarization measurements . . . 123

7 B Decays to open charm and charmonium final states 125

8 Summary 154

1 Introduction

Flavor dynamics is an important element in understanding the nature of particle physics. The accurate knowledge of properties of heavy flavor hadrons, especially b hadrons, plays an essential role for determination of the Cabibbo-Kobayashi-Maskawa (CKM) matrix [1]. Since asymmetric-energy e^+e^- B factories started their operation, the size of available B meson samples has dramatically increased and the accuracies of measurements have been improved. Tevatron experiments also started to provide rich results on B hadron decays with increased Run II data samples.

The Heavy Flavor Averaging Group (HFAG) has been formed in 2002, continuing the activities of LEP Heavy Flavor Steering group [2], to provide averages for measurements of b-flavor related quantities.

The HFAG is currently organized into five subgroups:

- the "Lifetime and Mixing" group provides averages for b-hadron lifetimes, b-hadron fractions in $\Upsilon(4S)$ decay and high energy collisions, and various parameters in B^0 and B_s^0 oscillation (mixing);
- the "Semileptonic B Decays" group provides averages for inclusive and exclusive B-decay branching fractions, and estimates of the CKM matrix elements $|V_{cb}|$ and $|V_{ub}|$;
- the "$CP(t)$ and Unitarity Triangle Angles" group provides averages for time-dependent CP asymmetry parameters and angles of the B unitarity triangle;
- the "Rare Decays" group provides averages of branching fractions and their asymmetries between B and $\overline{B}$ for charmless mesonic, radiative, leptonic, and baryonic B decays;
- the "B to Charm Decays" group provides averages of branching fractions for B decays to final states involving open charm mesons or charmonium.

The first two subgroups continue the activities from LEP working groups with some reorganization (merging four groups into two groups). The latter three groups have been newly formed to provide averages for results which are available from B factory experiments. The five HFAG subgroups consist of representatives and contact persons from the experimental groups: *BABAR*, Belle, CDF, CLEO, DØ, and LEP. As of the writing of this document a sixth HFAG subgroup which deals with the physics of charm hadrons is being initiated. First averages from the Charm subgroup are available for the Winter 2007 conferences on the HFAG web page and will be included in the next update of this document.

This article is an update of the *End of 2005* HFAG document [3], and we report the world averages using the available results at the end of 2006. All results that are publicly available, including recent preliminary results, are used in the averages. We do not use preliminary results which remain unpublished for a long time or for which no publication is planned. Close contacts have been established between representatives from the experiments and members of different subgroups in charge of the averages, to ensure that the data are prepared in a form suitable for combinations.

We do not scale the error of an average (as is presently done by the Particle Data Group [4]) in case $\chi^2/\text{dof} > 1$, where dof is the number of degrees of freedom in the average calculation. In such a case, we examine the systematics of each measurement and try to understand them.

Unless we find possible systematic discrepancies between the measurements, we do not make any special treatment for the calculated error. We provide the confidence level of the fit as an indicator for the consistency of the measurements included in the average. We attach a warning message in case that some special treatment was necessary to calculate the average or the approximation used in the average calculation may not be good enough (*e.g.*, Gaussian error is used in averaging although the likelihood indicates non-Gaussian behavior).

Section 2 describes the methodology for calculating averages for various quantities used by the HFAG. In the averaging, the input parameters used in the various analyses are adjusted (rescaled) to common values, and, where possible, known correlations are taken into account. The general philosophy and tools for calculations of averages are presented. Sections 3–7 describe the averaging of the quantities from each of the subgroups mentioned above. A brief summary of the averages described in this article is given in Sec. 8.

The complete listing of averages and plots described in this article are also available on the HFAG web page:

`http://www.slac.stanford.edu/xorg/hfag` and

`http://belle.kek.jp/mirror/hfag` (KEK mirror site).

2 Methodology

The general averaging problem that HFAG faces is to combine the information provided by different measurements of the same parameter, to obtain our best estimate of the parameter's value and uncertainty. The methodology described here focuses on the problems of combining measurements performed with different systematic assumptions and with potentially-correlated systematic uncertainties. Our methodology relies on the close involvement of the people performing the measurements in the averaging process.

Consider two hypothetical measurements of a parameter x, which might be summarized as

$$x = x_1 \pm \delta x_1 \pm \Delta x_{1,1} \pm \Delta x_{2,1} \ldots$$
$$x = x_2 \pm \delta x_2 \pm \Delta x_{1,2} \pm \Delta x_{2,2} \ldots \ ,$$

where the δx_k are statistical uncertainties, and the $\Delta x_{i,k}$ are contributions to the systematic uncertainty. One popular approach is to combine statistical and systematic uncertainties in quadrature

$$x = x_1 \pm (\delta x_1 \oplus \Delta x_{1,1} \oplus \Delta x_{2,1} \oplus \ldots)$$
$$x = x_2 \pm (\delta x_2 \oplus \Delta x_{1,2} \oplus \Delta x_{2,2} \oplus \ldots)$$

and then perform a weighted average of x_1 and x_2, using their combined uncertainties, as if they were independent. This approach suffers from two potential problems that we attempt to address. First, the values of the x_k may have been obtained using different systematic assumptions. For example, different values of the B^0 lifetime may have been assumed in separate measurements of the oscillation frequency Δm_d. The second potential problem is that some contributions of the systematic uncertainty may be correlated between experiments. For example, separate measurements of Δm_d may both depend on an assumed Monte-Carlo branching fraction used to model a common background.

The problems mentioned above are related since, ideally, any quantity y_i that x_k depends on has a corresponding contribution $\Delta x_{i,k}$ to the systematic error which reflects the uncertainty

Δy_i on y_i itself. We assume that this is the case, and use the values of y_i and Δy_i assumed by each measurement explicitly in our averaging (we refer to these values as $y_{i,k}$ and $\Delta y_{i,k}$ below). Furthermore, since we do not lump all the systematics together, we require that each measurement used in an average have a consistent definition of the various contributions to the systematic uncertainty. Different analyses often use different decompositions of their systematic uncertainties, so achieving consistent definitions for any potentially correlated contributions requires close coordination between HFAG and the experiments. In some cases, a group of systematic uncertainties must be lumped to obtain a coarser description that is consistent between measurements. Systematic uncertainties that are uncorrelated with any other sources of uncertainty appearing in an average are lumped with the statistical error, so that the only systematic uncertainties treated explicitly are those that are correlated with at least one other measurement via a consistently-defined external parameter y_i. When asymmetric statistical or systematic uncertainties are quoted, we symmetrize them since our combination method implicitly assumes parabolic likelihoods for each measurement.

The fact that a measurement of x is sensitive to the value of y_i indicates that, in principle, the data used to measure x could equally-well be used for a simultaneous measurement of x and y_i, as illustrated by the large contour in Fig. 1(a) for a hypothetical measurement. However, we often have an external constraint Δy_i on the value of y_i (represented by the horizontal band in Fig. 1(a)) that is more precise than the constraint $\sigma(y_i)$ from our data alone. Ideally, in such cases we would perform a simultaneous fit to x and y_i, including the external constraint, obtaining the filled (x, y) contour and corresponding dashed one-dimensional estimate of x shown in Fig. 1(a). Throughout, we assume that the external constraint Δy_i on y_i is Gaussian.

In practice, the added technical complexity of a constrained fit with extra free parameters is not justified by the small increase in sensitivity, as long as the external constraints Δy_i are sufficiently precise when compared with the sensitivities $\sigma(y_i)$ to each y_i of the data alone. Instead, the usual procedure adopted by the experiments is to perform a baseline fit with all y_i fixed to nominal values $y_{i,0}$, obtaining $x = x_0 \pm \delta x$. This baseline fit neglects the uncertainty due to Δy_i, but this error can be mostly recovered by repeating the fit separately for each external parameter y_i with its value fixed at $y_i = y_{i,0} + \Delta y_i$ to obtain $x = \tilde{x}_{i,0} \pm \delta\tilde{x}$, as illustrated in Fig. 1(b). The absolute shift, $|\tilde{x}_{i,0} - x_0|$, in the central value of x is what the experiments usually quote as their systematic uncertainty Δx_i on x due to the unknown value of y_i. Our procedure requires that we know not only the magnitude of this shift but also its sign. In the limit that the unconstrained data is represented by a parabolic likelihood, the signed shift is given by

$$\Delta x_i = \rho(x, y_i) \frac{\sigma(x)}{\sigma(y_i)} \Delta y_i \ , \tag{1}$$

where $\sigma(x)$ and $\rho(x, y_i)$ are the statistical uncertainty on x and the correlation between x and y_i in the unconstrained data. While our procedure is not equivalent to the constrained fit with extra parameters, it yields (in the limit of a parabolic unconstrained likelihood) a central value x_0 that agrees to $\mathcal{O}(\Delta y_i/\sigma(y_i))^2$ and an uncertainty $\delta x \oplus \Delta x_i$ that agrees to $\mathcal{O}(\Delta y_i/\sigma(y_i))^4$.

In order to combine two or more measurements that share systematics due to the same external parameters y_i, we would ideally perform a constrained simultaneous fit of all data samples to obtain values of x and each y_i, being careful to only apply the constraint on each y_i once. This is not practical since we generally do not have sufficient information to reconstruct the unconstrained likelihoods corresponding to each measurement. Instead, we perform the two-step approximate procedure described below.

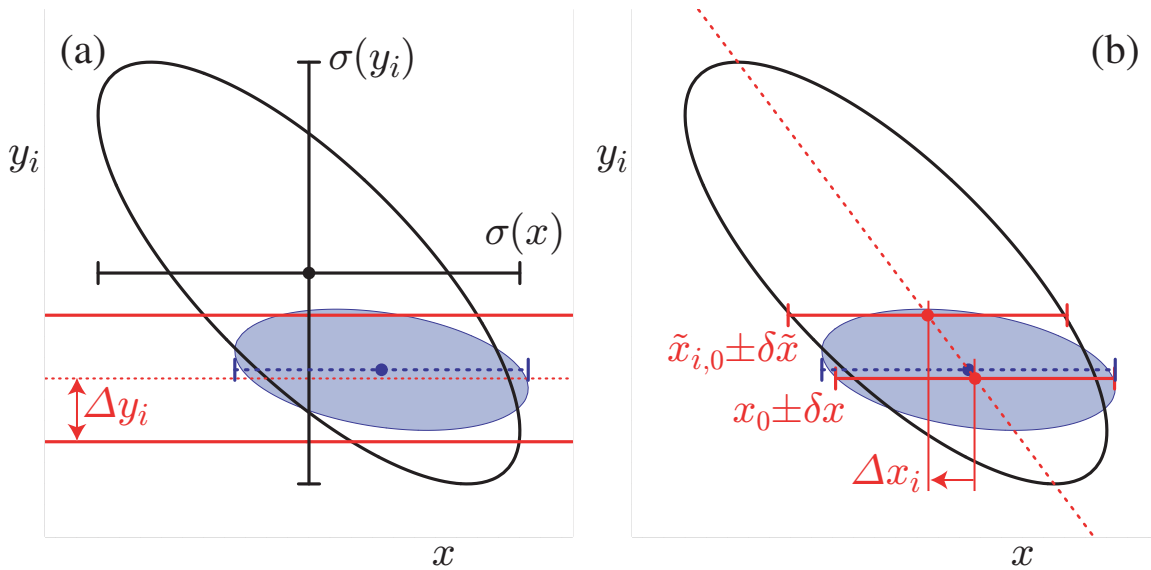

Figure 1: The left-hand plot, (a), compares the 68% confidence-level contours of a hypothetical measurement's unconstrained (large ellipse) and constrained (filled ellipse) likelihoods, using the Gaussian constraint on y_i represented by the horizontal band. The solid error bars represent the statistical uncertainties, $\sigma(x)$ and $\sigma(y_i)$, of the unconstrained likelihood. The dashed error bar shows the statistical error on x from a constrained simultaneous fit to x and y_i. The right-hand plot, (b), illustrates the method described in the text of performing fits to x only with y_i fixed at different values. The dashed diagonal line between these fit results has the slope $\rho(x, y_i)\sigma(y_i)/\sigma(x)$ in the limit of a parabolic unconstrained likelihood. The result of the constrained simultaneous fit from (a) is shown as a dashed error bar on x.

Figs. 2(a,b) illustrate two statistically-independent measurements, $x_1 \pm (\delta x_1 \oplus \Delta x_{i,1})$ and $x_2 \pm (\delta x_i \oplus \Delta x_{i,2})$, of the same hypothetical quantity x (for simplicity, we only show the contribution of a single correlated systematic due to an external parameter y_i). As our knowledge of the external parameters y_i evolves, it is natural that the different measurements of x will assume different nominal values and ranges for each y_i. The first step of our procedure is to adjust the values of each measurement to reflect the current best knowledge of the values y'_i and ranges $\Delta y'_i$ of the external parameters y_i, as illustrated in Figs. 2(c,b). We adjust the central values x_k and correlated systematic uncertainties $\Delta x_{i,k}$ linearly for each measurement (indexed by k) and each external parameter (indexed by i):

$$x'_k = x_k + \sum_i \frac{\Delta x_{i,k}}{\Delta y_{i,k}} \left(y'_i - y_{i,k}\right) \tag{2}$$

$$\Delta x'_{i,k} = \Delta x_{i,k} \cdot \frac{\Delta y'_i}{\Delta y_{i,k}} \ . \tag{3}$$

This procedure is exact in the limit that the unconstrained likelihoods of each measurement is parabolic.

The second step of our procedure is to combine the adjusted measurements, $x'_k \pm (\delta x_k \oplus \Delta x'_{k,1} \oplus \Delta x'_{k,2} \oplus \ldots)$ using the chi-square

$$\chi^2_{\rm comb}(x, y_1, y_2, \ldots) \equiv \sum_k \frac{1}{\delta x_k^2} \left[x'_k - \left(x + \sum_i (y_i - y'_i) \frac{\Delta x'_{i,k}}{\Delta y'_i} \right) \right]^2 + \sum_i \left(\frac{y_i - y'_i}{\Delta y'_i} \right)^2 \ , \tag{4}$$

and then minimize this χ^2 to obtain the best values of x and y_i and their uncertainties, as illustrated in Fig. 3. Although this method determines new values for the y_i, we do not report them since the $\Delta x_{i,k}$ reported by each experiment are generally not intended for this purpose (for example, they may represent a conservative upper limit rather than a true reflection of a 68% confidence level).

For comparison, the exact method we would perform if we had the unconstrained likelihoods $\mathcal{L}_k(x, y_1, y_2, \ldots)$ available for each measurement is to minimize the simultaneous constrained likelihood

$$\mathcal{L}_{\rm comb}(x, y_1, y_2, \ldots) \equiv \prod_k \mathcal{L}_k(x, y_1, y_2, \ldots) \prod_i \mathcal{L}_i(y_i) \ , \tag{5}$$

with an independent Gaussian external constraint on each y_i

$$\mathcal{L}_i(y_i) \equiv \exp\left[-\frac{1}{2} \left(\frac{y_i - y'_i}{\Delta y'_i} \right)^2 \right] \ . \tag{6}$$

The results of this exact method are illustrated by the filled ellipses in Figs. 3(a,b), and agree with our method in the limit that each $\mathcal{L}_k$ is parabolic and that each $\Delta y'_i \ll \sigma(y_i)$. In the case of a non-parabolic unconstrained likelihood, experiments would have to provide a description of $\mathcal{L}_k$ itself to allow an improved combination. In the case of some $\sigma(y_i) \simeq \Delta y'_i$, experiments are advised to perform a simultaneous measurement of both x and y so that their data will improve the world knowledge about y.

The algorithm described above is used as a default in the averages reported in the following sections. For some cases, somewhat simplified or more complex algorithms are used and noted in

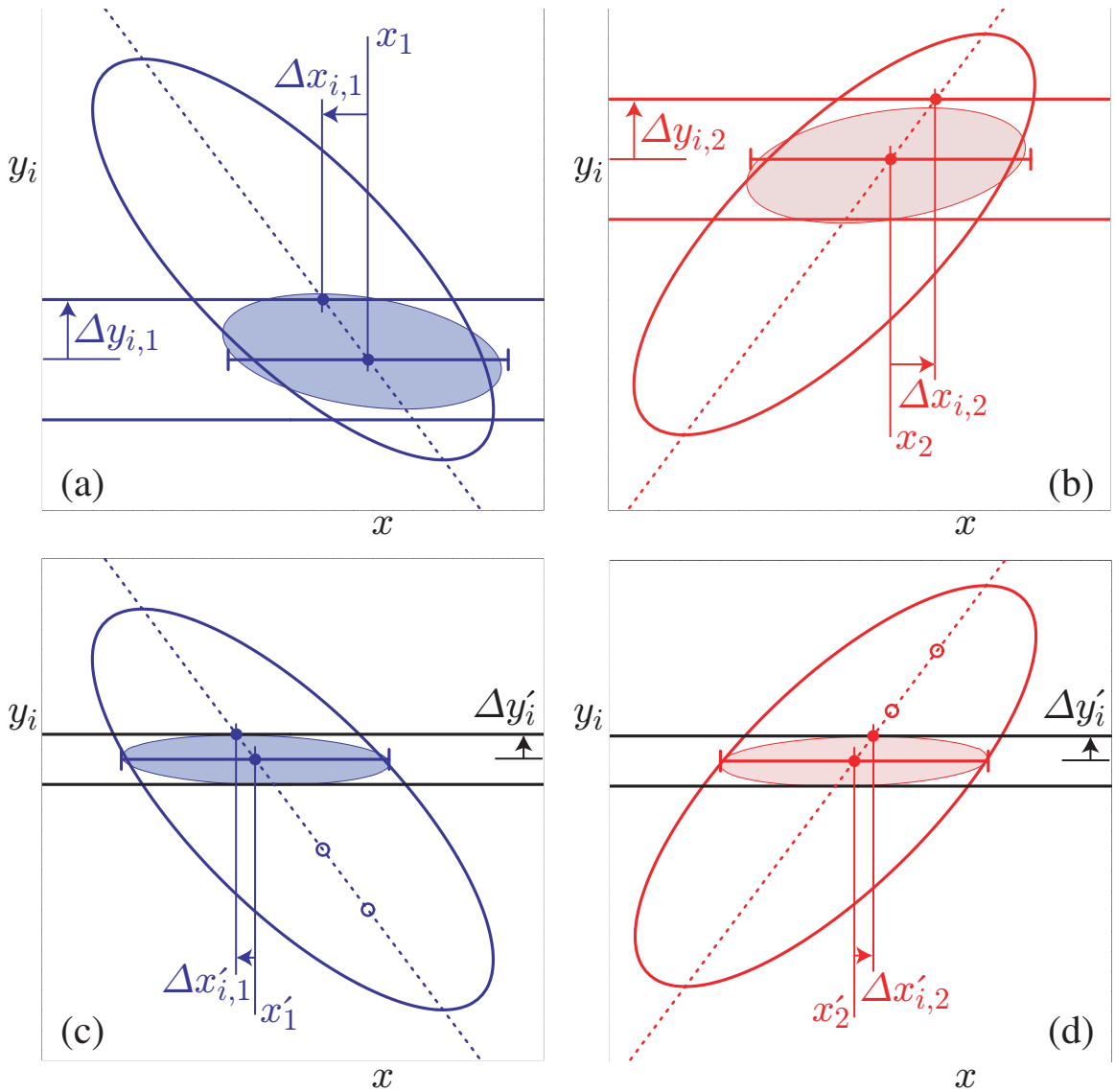

Figure 2: The upper plots, (a) and (b), show examples of two individual measurements to be combined. The large ellipses represent their unconstrained likelihoods, and the filled ellipses represent their constrained likelihoods. Horizontal bands indicate the different assumptions about the value and uncertainty of y_i used by each measurement. The error bars show the results of the approximate method described in the text for obtaining x by performing fits with y_i fixed to different values. The lower plots, (c) and (d), illustrate the adjustments to accommodate updated and consistent knowledge of y_i described in the text. Hollow circles mark the central values of the unadjusted fits to x with y fixed, which determine the dashed line used to obtain the adjusted values.

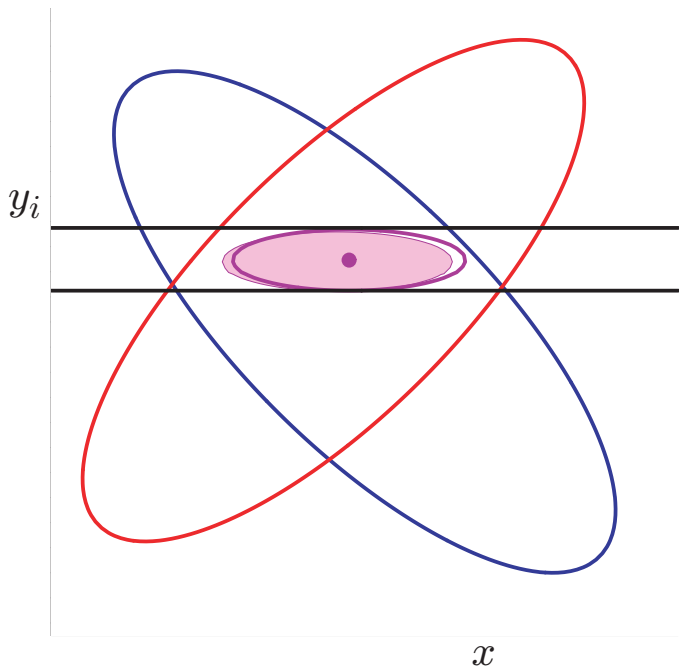

Figure 3: An illustration of the combination of two hypothetical measurements of x using the method described in the text. The ellipses represent the unconstrained likelihoods of each measurement and the horizontal band represents the latest knowledge about y_i that is used to adjust the individual measurements. The filled small ellipse shows the result of the exact method using $\mathcal{L}_{\text{comb}}$ and the hollow small ellipse and dot show the result of the approximate method using χ^2_{comb}.

the corresponding sections. Some examples for extensions of the standard method for extracting averages are given here. These include the case where measurement errors depend on the measured value, i.e. are relative errors, unknown correlation coefficients and the breakdown of error sources.

For measurements with Gaussian errors, the usual estimator for the average of a set of measurements is obtained by minimizing the following χ^2:

$$\chi^2(t) = \sum_i^N \frac{(y_i - t)^2}{\sigma_i^2}, \tag{7}$$

where y_i is the measured value for input i and σ_i^2 is the variance of the distribution from which y_i was drawn. The value $\hat{t}$ of t at minimum χ^2 is our estimator for the average. (This discussion is given for independent measurements for the sake of simplicity; the generalization to correlated measurements is straightforward, and has been used when averaging results.) The true σ_i are unknown but typically the error as assigned by the experiment $\sigma_i^{\rm raw}$ is used as an estimator for it. Caution is advised, however, in the case where $\sigma_i^{\rm raw}$ depends on the value measured for y_i. Examples of this include an uncertainty in any multiplicative factor (like an acceptance) that enters the determination of y_i, i.e. the $\sqrt{N}$ dependence of Poisson statistics, where $y_i \propto N$ and $\sigma_i \propto \sqrt{N}$. Failing to account for this type of dependence when averaging leads to a biased average. Biases in the average can be avoided (or at least reduced) by minimizing the following χ^2:

$$\chi^2(t) = \sum_i^N \frac{(y_i - t)^2}{\sigma_i^2(\hat{t})}. \tag{8}$$

In the above $\sigma_i(\hat{t})$ is the uncertainty assigned to input i that includes the assumed dependence of the stated error on the value measured. As an example, consider a pure acceptance error, for which $\sigma_i(\hat{t}) = (\hat{t}/y_i) \times \sigma_i^{\rm raw}$. It is easily verified that solving Eq. 8 leads to the correct behavior, namely

$$\hat{t} = \frac{\sum_i^N y_i^3/(\sigma_i^{\rm raw})^2}{\sum_i^N y_i^2/(\sigma_i^{\rm raw})^2},$$

i.e. weighting by the inverse square of the fractional uncertainty, $\sigma_i^{\rm raw}/y_i$.

It is sometimes difficult to assess the dependence of $\sigma_i^{\rm raw}$ on $\hat{t}$ from the errors quoted by experiments.

Another issue that needs careful treatment is the question of correlation among different measurements, e.g. due to using the same theory for calculating acceptances. A common practice is to set the correlation coefficient to unity to indicate full correlation. However, this is not a "conservative" thing to do, and can in fact lead to a significantly underestimated uncertainty on the average. In the absence of better information, the most conservative choice of correlation coefficient between two measurements i and j is the one that maximizes the uncertainty on $\hat{t}$ due to that pair of measurements:

$$\sigma^2_{\hat{t}(i,j)} = \frac{\sigma_i^2\,\sigma_j^2\,(1-\rho_{ij}^2)}{\sigma_i^2 + \sigma_j^2 - 2\,\rho_{ij}\,\sigma_i\,\sigma_j}, \tag{9}$$

namely

$$\rho_{ij} = \min\left(\frac{\sigma_i}{\sigma_j}, \frac{\sigma_j}{\sigma_i}\right), \tag{10}$$

which corresponds to setting $\sigma^2_{\hat{t}(i,j)} = \min(\sigma_i^2, \sigma_j^2)$. Setting $\rho_{ij} = 1$ when $\sigma_i \neq \sigma_j$ can lead to a significant underestimate of the uncertainty on $\hat{t}$, as can be seen from Eq. 9.

Finally, a note on the breakdown of the error sources contributing to the overall uncertainty on the average. The overall covariance matrix is constructed from a number of individual sources, e.g. $\mathbf{V} = \mathbf{V_{stat}} + \mathbf{V_{sys}} + \mathbf{V_{th}}$. The variance on the average $\hat{t}$ can be written

$$\sigma^2_{\hat{t}} = \frac{\sum_{i,j} \left(\mathbf{V^{-1}} \left[\mathbf{V_{stat}} + \mathbf{V_{sys}} + \mathbf{V_{th}}\right] \mathbf{V^{-1}}\right)_{ij}}{\left(\sum_{i,j} V^{-1}_{ij}\right)^2} = \sigma^2_{stat} + \sigma^2_{sys} + \sigma^2_{th}. \tag{11}$$

Written in this form, one can readily determine the contribution of each source of uncertainty to the overall uncertainty on the average. This breakdown of the uncertainties is used in the following sections.

Following the prescription described above, the central values and errors are rescaled to a common set of input parameters in the averaging procedures, according to the dependency on any of these input parameters. We try to use the most up-to-date values for these common inputs and the same values among the HFAG subgroups. For the parameters whose averages are produced by the HFAG, we use the updated values in the current update cycle. For other external parameters, we use the most recent PDG values.

The parameters and values used in this update cycle are listed in each subgroup section.

3 b-hadron production fractions, lifetimes and mixing parameters

Quantities such as b-hadron production fractions, b-hadron lifetimes, and neutral B-meson oscillation frequencies have been studied for many years at high-energy colliders, namely at LEP and SLC (e^+e^- colliders at $\sqrt{s} = m_Z$) as well as at the first version of the Tevatron ($p\overline{p}$ collider at $\sqrt{s} = 1.8$ TeV). In the last few years, precise measurements of the B^0 and B^+ lifetimes, as well as of the B^0 oscillation frequency, have also been performed at the asymmetric B factories, KEKB and PEPII (e^+e^- colliders at $\sqrt{s} = m_{\Upsilon(4S)}$). In most cases, these basic quantities, although interesting by themselves, can now be seen as necessary ingredients for the more complicated and refined analyses being currently performed at the asymmetric B factories and at the upgraded Tevatron ($\sqrt{s} = 1.96$ TeV), in particular the time-dependent CP asymmetry measurements. It is therefore important that the best experimental values of these quantities continue to be kept up-to-date and improved. Recently new measurements of B_s^0 mixing parameters have been performed at the Tevatron, with similar or sometimes better precision than the "old" measurements of B^0 mixing parameters.

In several cases, the averages presented in this chapter are needed and used as input for the results given in the subsequent chapters. Within this chapter, some averages need the knowledge of other averages in a circular way. This coupling, which appears through the b-hadron fractions whenever inclusive or semi-exclusive measurements have to be considered, has been reduced significantly in the last years with increasingly precise exclusive measurements becoming available. To cope with this circularity, a rather involved averaging procedure had been developed, in the framework of the former LEP Heavy Flavour Steering Group. This is still in use now (details can be found in [2]), although simplifications can be envisaged in the future when even more precise exclusive measurements become available.

3.1 b-hadron production fractions

We consider here the relative fractions of the different b-hadron species found in an unbiased sample of weakly-decaying b hadrons produced under some specific conditions. The knowledge of these fractions is useful to characterize the signal composition in inclusive b-hadron analyses, or to predict the background composition in exclusive analyses. Many analyses in B physics need these fractions as input. We distinguish here the following three conditions: $\Upsilon(4S)$ decays, $\Upsilon(5S)$ decays, and high-energy collisions (including Z^0 decays).

3.1.1 b-hadron production fractions in $\Upsilon(4S)$ decays

Only pairs of the two lightest (charged and neutral) B mesons can be produced in $\Upsilon(4S)$ decays, and it is enough to determine the following branching fractions:

$$f^{+-} = \Gamma(\Upsilon(4S) \to B^+B^-)/\Gamma_{\rm tot}(\Upsilon(4S))\,, \tag{12}$$

$$f^{00} = \Gamma(\Upsilon(4S) \to B^0\overline{B}^0)/\Gamma_{\rm tot}(\Upsilon(4S))\,. \tag{13}$$

In practice, most analyses measure their ratio

$$R^{+-/00} = f^{+-}/f^{00} = \Gamma(\Upsilon(4S) \to B^+B^-)/\Gamma(\Upsilon(4S) \to B^0\overline{B}^0)\,, \tag{14}$$

Table 1: Published measurements of the B^+/B^0 production ratio in $\Upsilon(4S)$ decays, together with their average (see text). Systematic uncertainties due to the imperfect knowledge of $\tau(B^+)/\tau(B^0)$ are included.

Experiment and year	Ref.	Decay modes or method	Published value of $R^{+-/00} = f^{+-}/f^{00}$	Assumed value of $\tau(B^+)/\tau(B^0)$
CLEO, 2001	[5]	$J/\psi K^{(*)}$	$1.04 \pm 0.07 \pm 0.04$	1.066 ± 0.024
BABAR, 2002	[6]	$(c\bar{c})K^{(*)}$	$1.10 \pm 0.06 \pm 0.05$	1.062 ± 0.029
CLEO, 2002	[7]	$D^*\ell\nu$	$1.058 \pm 0.084 \pm 0.136$	1.074 ± 0.028
Belle, 2003	[8]	dilepton events	$1.01 \pm 0.03 \pm 0.09$	1.083 ± 0.017
BABAR, 2004	[9]	$J/\psi K$	$1.006 \pm 0.036 \pm 0.031$	1.083 ± 0.017
Average			1.021 ± 0.034 (tot)	1.076 ± 0.008

which is easier to access experimentally. Since an inclusive (but separate) reconstruction of B^+ and B^0 is difficult, specific exclusive decay modes, $B^+ \to x^+$ and $B^0 \to x^0$, are usually considered to perform a measurement of $R^{+-/00}$, whenever they can be related by isospin symmetry (for example $B^+ \to J/\psi K^+$ and $B^0 \to J/\psi K^0$). Under the assumption that $\Gamma(B^+ \to x^+) = \Gamma(B^0 \to x^0)$, *i.e.* that isospin invariance holds in these B decays, the ratio of the number of reconstructed $B^+ \to x^+$ and $B^0 \to x^0$ mesons is proportional to

$$\frac{f^{+-}\,\mathcal{B}(B^+ \to x^+)}{f^{00}\,\mathcal{B}(B^0 \to x^0)} = \frac{f^{+-}\,\Gamma(B^+ \to x^+)\,\tau(B^+)}{f^{00}\,\Gamma(B^0 \to x^0)\,\tau(B^0)} = \frac{f^{+-}}{f^{00}}\,\frac{\tau(B^+)}{\tau(B^0)}\,, \tag{15}$$

where $\tau(B^+)$ and $\tau(B^0)$ are the B^+ and B^0 lifetimes respectively. Hence the primary quantity measured in these analyses is $R^{+-/00}\,\tau(B^+)/\tau(B^0)$, and the extraction of $R^{+-/00}$ with this method therefore requires the knowledge of the $\tau(B^+)/\tau(B^0)$ lifetime ratio.

The published measurements of $R^{+-/00}$ are listed in Table 1 together with the corresponding assumed values of $\tau(B^+)/\tau(B^0)$. All measurements are based on the above-mentioned method, except the one from Belle, which is a by-product of the B^0 mixing frequency analysis using dilepton events (but note that it also assumes isospin invariance, namely $\Gamma(B^+ \to \ell^+\mathrm{X}) = \Gamma(B^0 \to \ell^+\mathrm{X})$). The latter is therefore treated in a slightly different manner in the following procedure used to combine these measurements:

- each published value of $R^{+-/00}$ from CLEO and *BABAR* is first converted back to the original measurement of $R^{+-/00}\,\tau(B^+)/\tau(B^0)$, using the value of the lifetime ratio assumed in the corresponding analysis;
- a simple weighted average of these original measurements of $R^{+-/00}\,\tau(B^+)/\tau(B^0)$ from CLEO and *BABAR* (which do not depend on the assumed value of the lifetime ratio) is then computed, assuming no statistical or systematic correlations between them;
- the weighted average of $R^{+-/00}\,\tau(B^+)/\tau(B^0)$ is converted into a value of $R^{+-/00}$, using the latest average of the lifetime ratios, $\tau(B^+)/\tau(B^0) = 1.076 \pm 0.008$ (see Sec. 3.2.3);
- the Belle measurement of $R^{+-/00}$ is adjusted to the current values of $\tau(B^0) = 1.527 \pm 0.008$ ps and $\tau(B^+)/\tau(B^0) = 1.076 \pm 0.008$ (see Sec. 3.2.3), using the quoted systematic uncertainties due to these parameters;

- the combined value of $R^{+-/00}$ from CLEO and *BABAR* is averaged with the adjusted value of $R^{+-/00}$ from Belle, assuming a 100% correlation of the systematic uncertainty due to the limited knowledge on $\tau(B^+)/\tau(B^0)$; no other correlation is considered.

The resulting global average,

$$R^{+-/00} = \frac{f^{+-}}{f^{00}} = 1.021 \pm 0.034\,, \tag{16}$$

is consistent with an equal production of charged and neutral B mesons.

On the other hand, the *BABAR* collaboration has performed a direct measurement of the f^{00} fraction using a novel method, which does not rely on isospin symmetry nor requires the knowledge of $\tau(B^+)/\tau(B^0)$. Its analysis, based on a comparison between the number of events where a single $B^0 \to D^{*-}\ell^+\nu$ decay could be reconstructed and the number of events where two such decays could be reconstructed, yields [10]

$$f^{00} = 0.487 \pm 0.010\,(\text{stat}) \pm 0.008\,(\text{syst})\,. \tag{17}$$

The two results of Eqs. (16) and (17) are of very different natures and completely independent of each other. Their product is equal to $f^{+-} = 0.497 \pm 0.021$, while another combination of them gives $f^{+-} + f^{00} = 0.984 \pm 0.031$, compatible with unity. Assuming[1] $f^{+-} + f^{00} = 1$, also consistent with CLEO's observation that the fraction of $\Upsilon(4S)$ decays to $B\overline{B}$ pairs is larger than 0.96 at 95% CL [12], the results of Eqs. (16) and (17) can be averaged (first converting Eq. (16) into a value of $f^{00} = 1/(R^{+-/00} + 1)$) to yield the following more precise estimates:

$$f^{00} = 0.493 \pm 0.007\,, \quad f^{+-} = 1 - f^{00} = 0.507 \pm 0.007\,, \quad \frac{f^{+-}}{f^{00}} = 1.030 \pm 0.029\,. \tag{18}$$

3.1.2 *b*-hadron production fractions in $\Upsilon(5S)$ decays

Hadronic events produced in e^+e^- collisions at the $\Upsilon(5S)$ energy can be classified into three categories: light-quark continuum events, $b\overline{b}$ continuum events, and $\Upsilon(5S)$ events. The latter two cannot be distinguished and are expected to always produce one of the following final states with a pair of b-flavored mesons: $B\overline{B}$, $B\overline{B}^*$, $B^*\overline{B}$, $B^*\overline{B}^*$, $B\overline{B}\pi$, $B\overline{B}^*\pi$, $B^*\overline{B}\pi$, $B^*\overline{B}^*\pi$, $B\overline{B}\pi\pi$, $B_s^0\overline{B}_s^0$, $B_s^0\overline{B}_s^{0*}$, $B_s^{0*}\overline{B}_s^0$ or $B_s^{0*}\overline{B}_s^{0*}$, where B denotes a B^0 or B^+ meson and $\overline{B}$ denotes a $\overline{B}^0$ or B^- meson. The excited states decay via $B^* \to B\gamma$ and $B_s^{0*} \to B_s^0\gamma$. We define here $f_s(\Upsilon(5S))$ as the fraction of $B_s^{0(*)}\overline{B}_s^{0(*)}$ events over all events with a pair of b-flavored mesons at the $\Upsilon(5S)$ energy:

$$f_s(\Upsilon(5S)) = \frac{\sigma(e^+e^- \to B_s^{0(*)}\overline{B}_s^{0(*)})}{\sigma(e^+e^- \to \Upsilon(5S) \text{ or } b\overline{b}X)} \quad \text{at } \sqrt{s} = m(\Upsilon(5S))\,. \tag{19}$$

The CLEO and Belle collaborations have recently published measurements of several inclusive $\Upsilon(5S)$ branching fractions, $\mathcal{B}(\Upsilon(5S) \to D_sX)$, $\mathcal{B}(\Upsilon(5S) \to \phi X)$, $\mathcal{B}(\Upsilon(5S) \to D^0X)$, and $\mathcal{B}(\Upsilon(5S) \to B\overline{B}X)$, from which they extract the model-dependent estimates of $f_s(\Upsilon(5S))$

[1] Two non-$B\overline{B}$ decay modes of the $\Upsilon(4S)$, $\Upsilon(4S) \to \Upsilon(1S)\pi^+\pi^-$ and $\Upsilon(4S) \to \Upsilon(2S)\pi^+\pi^-$, have now been observed with branching fractions of the order of 10^{-4} [11], corresponding to a partial width several times larger than that in the e^+e^- channel. However, this can still be neglected and the assumption $f^{+-} + f^{00} = 1$ remains valid in the present context of the determination of f^{+-} and f^{00}.

Table 2: Published values of $f_s(\Upsilon(5S))$ and their average.

Experiment, year and dataset	Ref.	Decay modes or method	Published value of $f_s(\Upsilon(5S))$
CLEO, 2006, $0.42\,\mathrm{fb}^{-1}$	[13]	$\Upsilon(5S) \to D_s X$	$0.168 \pm 0.026^{+0.067}_{-0.034}$
	[13]	$\Upsilon(5S) \to \phi X$	$0.246 \pm 0.029^{+0.110}_{-0.053}$
	[13]	$\Upsilon(5S) \to B\overline{B}X$	$0.411 \pm 0.100 \pm 0.092$
	[13]	CLEO average of above 3	$0.21^{+0.06}_{-0.03}$
Belle, 2006, $1.86\,\mathrm{fb}^{-1}$	[14]	$\Upsilon(5S) \to D_s X$	$0.179 \pm 0.014 \pm 0.041$
	[14]	$\Upsilon(5S) \to D^0 X$	$0.181 \pm 0.036 \pm 0.075$
	[14]	Belle average of above 2	$0.180 \pm 0.013 \pm 0.032$
Average of all above after adjustments to inputs of Table 3			$0.199 \pm 0.011 \pm 0.030$

Table 3: External inputs on which the $f_s(\Upsilon(5S))$ average is based.

Branching fraction	Value	Explanation and reference
$\mathcal{B}(B \to D_s X) \times \mathcal{B}(D_s \to \phi\pi)$	0.00381 ± 0.00015	world average [4, 15]
$\mathcal{B}(B_s^0 \to D_s X)$	0.92 ± 0.11	model-dependent estimate [15]
$\mathcal{B}(D_s \to \phi\pi)$	0.044 ± 0.006	[4]
$\mathcal{B}(B \to D^0 X) \times \mathcal{B}(D^0 \to K\pi)$	0.0243 ± 0.0010	[4]
$\mathcal{B}(B_s^0 \to D^0 X)$	0.08 ± 0.07	model-dependent estimate [15]
$\mathcal{B}(D^0 \to K\pi)$	0.0380 ± 0.0007	[4]
$\mathcal{B}(B \to \phi X)$	0.0344 ± 0.0012	world average [4, 13]
$\mathcal{B}(B_s^0 \to \phi X)$	0.161 ± 0.024	model-dependent estimate [13]

reported in Table 2. This extraction requires the knowledge of several other branching fractions, which are listed in Table 3 together with their most recent values. Before being averaged, the CLEO and Belle results are adjusted to these new external inputs. The world average of $f_s(\Upsilon(5S))$ taking into account all systematic correlations introduced by the use of common external inputs, as well as the experiment-specific correlations due to the estimated number of $b\overline{b}$ events, is

$$f_s(\Upsilon(5S)) = 0.199 \pm 0.032\,. \tag{20}$$

This production of B_s^0 mesons at the $\Upsilon(5S)$ is observed to be dominated by the $B_s^{0*}\overline{B}_s^{0*}$ channel [16, 17], with $\sigma(e^+e^- \to B_s^{0*}\overline{B}_s^{0*})/\sigma(e^+e^- \to B_s^{0(*)}\overline{B}_s^{0(*)}) = (93^{+7}_{-9} \pm 1)\%$ [17].

3.1.3 *b*-hadron production fractions at high energy

At high energy, all species of weakly-decaying b hadrons can be produced, either directly or in strong and electromagnetic decays of excited b hadrons. We assume here that the fractions of these different species are the same in unbiased samples of high-p_{T} b jets originating from Z^0 decays or from $p\overline{p}$ collisions at the Tevatron. This hypothesis is plausible considering that, in both cases, the last step of the jet hadronization is a non-perturbative QCD process occurring at

the scale of $\Lambda_{\rm QCD}$. On the other hand, there is no strong argument to claim that these fractions should be strictly equal, so this assumption should be checked experimentally. Although the available data is not sufficient at this time to perform a significant check, it is expected that more data from Tevatron Run II may improve this situation and allow one to confirm or disprove this assumption with reasonable confidence. Meanwhile, the attitude adopted here is that these fractions are assumed to be equal at all high-energy colliders until demonstrated otherwise by experiment.[2] However, as explained below, the measurements performed at LEP and at the Tevatron show slight discrepancies. Therefore we present two sets of averages: one set including only measurements performed at LEP, and a second set including measurements performed at both LEP and Tevatron.

Contrary to what happens in the charm sector where the fractions of D^+ and D^0 are different, the relative amount of B^+ and B^0 is not affected by the electromagnetic decays of excited B^{+*} and B^{0*} states and strong decays of excited B^{+**} and B^{0**} states. Decays of the type $B_s^{0**} \to B^{(*)}K$ also contribute to the B^+ and B^0 rates, but with the same magnitude if mass effects can be neglected. We therefore assume equal production of B^+ and B^0. We also neglect the production of weakly-decaying states made of several heavy quarks (like B_c^+ and other heavy baryons) which is known to be very small. Hence, for the purpose of determining the b-hadron fractions, we use the constraints

$$f_u = f_d \quad \text{and} \quad f_u + f_d + f_s + f_{\rm baryon} = 1\,, \tag{21}$$

where f_u, f_d, f_s and $f_{\rm baryon}$ are the unbiased fractions of B^+, B^0, B_s^0 and b baryons, respectively.

The LEP experiments have measured $f_s \times \mathcal{B}(B_s^0 \to D_s^- \ell^+ \nu_\ell X)$ [18], $\mathcal{B}(b \to \Lambda_b^0) \times \mathcal{B}(\Lambda_b^0 \to \Lambda_c^+ \ell^- \overline{\nu}_\ell X)$ [19,20] and $\mathcal{B}(b \to \Xi_b^-) \times \mathcal{B}(\Xi_b^- \to \Xi^- \ell^- \overline{\nu}_\ell X)$ [21,22][3] from partially reconstructed final states including a lepton, $f_{\rm baryon}$ from protons identified in b events [24], and the production rate of charged b hadrons [25]. The various b-hadron fractions have also been measured at CDF using electron-charm final states [26] and double semileptonic decays with $\phi\ell$ and $K^*\ell$ final states [27]. All these published results[4] have been combined following the procedure and assumptions described in [2], to yield $f_u = f_d = 0.404 \pm 0.011$, $f_s = 0.093 \pm 0.018$ and $f_{\rm baryon} = 0.099 \pm 0.019$ under the constraints of Eq. (21). Following the PDG prescription, we have scaled the combined uncertainties on these fractions by 1.1 to account for slight discrepancies in the input data. Repeating the combination using LEP data only, we obtain $f_u = f_d = 0.406 \pm 0.010$, $f_s = 0.088 \pm 0.016$ and $f_{\rm baryon} = 0.100 \pm 0.017$ and find that no scaling factor is necessary. For these combinations other external inputs are used, *e.g.* the branching ratios of B mesons to final states with a D, D^* or D^{**} in semileptonic decays, which are needed to evaluate the fraction of semileptonic B_s^0 decays with a D_s^- in the final state.

Time-integrated mixing analyses performed with lepton pairs from $b\overline{b}$ events produced at high-energy colliders measure the quantity

$$\overline{\chi} = f'_d\,\chi_d + f'_s\,\chi_s\,, \tag{22}$$

where f'_d and f'_s are the fractions of B^0 and B_s^0 hadrons in a sample of semileptonic b-hadron decays, and where χ_d and χ_s are the B^0 and B_s^0 time-integrated mixing probabilities. Assuming

[2]It is not unlikely that the b-hadron fractions in low-$p_{\rm T}$ jets at a hadronic machine be different; in particular, beam-remnant effects may enhance the b-baryon production.

[3]The DELPHI result of Ref. [22] is considered to supersede an older one [23].

[4]Preliminary measurements [28] performed by CDF with Run II data have not been included here.

Table 4: Time-integrated mixing probability $\overline{\chi}$ (defined in Eq. (22)), and fractions of the different b-hadron species in an unbiased sample of weakly-decaying b hadrons, obtained from both direct and mixing measurements. Measurements performed in Z decays are included in both sets of averages.

Quantity		in Z decays	at high energy
Mixing probability	$\overline{\chi}$	0.1259 ± 0.0042	0.1284 ± 0.0069
B^+ or B^0 fraction	$f_u = f_d$	0.402 ± 0.009	0.401 ± 0.010
B^0_s fraction	f_s	0.104 ± 0.009	0.106 ± 0.013
b baryon fraction	$f_{\rm baryon}$	0.091 ± 0.015	0.092 ± 0.018
Correlation between f_s and $f_u = f_d$		-0.534	-0.517
Correlation between $f_{\rm baryon}$ and $f_u = f_d$		-0.860	-0.798
Correlation between $f_{\rm baryon}$ and f_s		$+0.029$	-0.104

that all b hadrons have the same semileptonic decay width implies $f'_i = f_i R_i$, where $R_i = \tau_i/\tau_b$ is the ratio of the lifetime τ_i of species i to the average b-hadron lifetime $\tau_b = \sum_i f_i \tau_i$. Hence measurements of the mixing probabilities $\overline{\chi}$, χ_d and χ_s can be used to improve our knowledge of f_u, f_d, f_s and $f_{\rm baryon}$. In practice, the above relations yield another determination of f_s obtained from $f_{\rm baryon}$ and mixing information,

$$f_s = \frac{1}{R_s} \frac{(1+r)\overline{\chi} - (1 - f_{\rm baryon} R_{\rm baryon})\chi_d}{(1+r)\chi_s - \chi_d}\,, \tag{23}$$

where $r = R_u/R_d = \tau(B^+)/\tau(B^0)$.

The published measurements of $\overline{\chi}$ performed by the LEP experiments have been combined by the LEP Electroweak Working Group to yield $\overline{\chi} = 0.1259 \pm 0.0042$ [29]. This can be compared with the Tevatron average, $\overline{\chi} = 0.147 \pm 0.011$, obtained from a CDF measurement with Run I data [30] and from a recent DØ measurement with Run II data [31]. The two averages deviate from each other by $1.8\,\sigma$; this could be an indication that the production fractions of b hadrons at the Z peak or at the Tevatron are not the same. Although this discrepancy is not very significant it should be carefully monitored in the future. We choose to combine these two results in a simple weighted average, assuming no correlations, and, following the PDG prescription, we multiply the combined uncertainty by 1.8 to account for the discrepancy. Our world average is then $\overline{\chi} = 0.1284 \pm 0.0069$.

Introducing the $\overline{\chi}$ average in Eq. (23), together with our world average $\chi_d = 0.1877 \pm 0.0024$ (see Eq. (53) of Sec. 3.3.1), the assumption $\chi_s = 1/2$ (justified by Eq. (83) in Sec. 3.3.2), the best knowledge of the lifetimes (see Sec. 3.2) and the estimate of $f_{\rm baryon}$ given above, yields $f_s = 0.121 \pm 0.019$ (or $f_s = 0.114 \pm 0.012$ using only LEP data), an estimate dominated by the mixing information. Taking into account all known correlations (including the one introduced by $f_{\rm baryon}$), this result is then combined with the set of fractions obtained from direct measurements (given above), to yield the improved estimates of Table 4, still under the constraints of Eq. (21). As can be seen, our knowledge on the mixing parameters substantially reduces the uncertainty on f_s, and this even in the case of the world averages where a rather strong deweighting was introduced in the computation of $\overline{\chi}$. It should be noted that the results are correlated, as indicated in Table 4.

3.2 *b*-hadron lifetimes

In the spectator model the decay of b-flavored hadrons H_b is governed entirely by the flavor changing $b \to Wq$ transition ($q = c, u$). For this very reason, lifetimes of all b-flavored hadrons are the same in the spectator approximation regardless of the (spectator) quark content of the H_b. In the early 1990's experiments became sophisticated enough to start seeing the differences of the lifetimes among various H_b species. The first theoretical calculations of the spectator quark effects on H_b lifetime emerged only few years earlier.

Currently, most of such calculations are performed in the framework of the Heavy Quark Expansion, HQE. In the HQE, under certain assumptions (most important of which is that of quark-hadron duality), the decay rate of an H_b to an inclusive final state f is expressed as the sum of a series of expectation values of operators of increasing dimension, multiplied by the correspondingly higher powers of $\Lambda_{\rm QCD}/m_b$:

$$\Gamma_{H_b \to f} = |CKM|^2 \sum_n c_n^{(f)} \left(\frac{\Lambda_{\rm QCD}}{m_b}\right)^n \langle H_b|O_n|H_b\rangle, \tag{24}$$

where $|CKM|^2$ is the relevant combination of the CKM matrix elements. Coefficients $c_n^{(f)}$ of this expansion, known as Operator Product Expansion [32], can be calculated perturbatively. Hence, the HQE predicts $\Gamma_{H_b \to f}$ in the form of an expansion in both $\Lambda_{\rm QCD}/m_b$ and $\alpha_s(m_b)$. The precision of current experiments makes it mandatory to go to the next-to-leading order in QCD, *i.e.* to include correction of the order of $\alpha_s(m_b)$ to the $c_n^{(f)}$'s. All non-perturbative physics is shifted into the expectation values $\langle H_b|O_n|H_b\rangle$ of operators O_n. These can be calculated using lattice QCD or QCD sum rules, or can be related to other observables via the HQE [33]. One may reasonably expect that powers of $\Lambda_{\rm QCD}/m_b$ provide enough suppression that only the first few terms of the sum in Eq. (24) matter.

Theoretical predictions are usually made for the ratios of the lifetimes (with $\tau(B^0)$ chosen as the common denominator) rather than for the individual lifetimes, for this allows several uncertainties to cancel. The precision of the current HQE calculations (see Refs. [34–36] for the latest updates) is in some instances already surpassed by the measurements, *e.g.* in the case of $\tau(B^+)/\tau(B^0)$. Also, HQE calculations are not assumption-free. More accurate predictions are a matter of progress in the evaluation of the non-perturbative hadronic matrix elements and verifying the assumptions that the calculations are based upon. However, the HQE, even in its present shape, draws a number of important conclusions, which are in agreement with experimental observations:

- The heavier the mass of the heavy quark the smaller is the variation in the lifetimes among different hadrons containing this quark, which is to say that as $m_b \to \infty$ we retrieve the spectator picture in which the lifetimes of all H_b's are the same. This is well illustrated by the fact that lifetimes are rather similar in the b sector, while they differ by large factors in the c sector ($m_c < m_b$).

- The non-perturbative corrections arise only at the order of $\Lambda^2_{\rm QCD}/m_b^2$, which translates into differences among H_b lifetimes of only a few percent.

- It is only the difference between meson and baryon lifetimes that appears at the $\Lambda^2_{\rm QCD}/m_b^2$ level. The splitting of the meson lifetimes occurs at the $\Lambda^3_{\rm QCD}/m_b^3$ level, yet it is enhanced by a phase space factor $16\pi^2$ with respect to the leading free b decay.

To ensure that certain sources of systematic uncertainty cancel, lifetime analyses are sometimes designed to measure a ratio of lifetimes. However, because of the differences in decay topologies, abundance (or lack thereof) of decays of a certain kind, *etc.*, measurements of the individual lifetimes are more common. In the following section we review the most common types of the lifetime measurements. This discussion is followed by the presentation of the averaging of the various lifetime measurements, each with a brief description of its particularities.

3.2.1 Lifetime measurements, uncertainties and correlations

In most cases lifetime of an H_b is estimated from a flight distance and a $\beta\gamma$ factor which is used to convert the geometrical distance into the proper decay time. Methods of accessing lifetime information can roughly be divided in the following five categories:

1. ***Inclusive (flavor blind) measurements***. These measurements are aimed at extracting the lifetime from a mixture of b-hadron decays, without distinguishing the decaying species. Often the knowledge of the mixture composition is limited, which makes these measurements experiment-specific. Also, these measurements have to rely on Monte Carlo for estimating the $\beta\gamma$ factor, because the decaying hadrons are not fully reconstructed. On the bright side, these usually are the largest statistics b-hadron lifetime measurements that are accessible to a given experiment, and can, therefore, serve as an important performance benchmark.

2. **Measurements in semileptonic decays of a specific H_b**. W from $b \to Wc$ produces $\ell\nu_l$ pair ($\ell = e, \mu$) in about 21% of the cases. Electron or muon from such decays is usually a well-detected signature, which provides for clean and efficient trigger. c quark from $b \to Wc$ transition and the other quark(s) making up the decaying H_b combine into a charm hadron, which is reconstructed in one or more exclusive decay channels. Knowing what this charmed hadron is allows one to separate, at least statistically, different H_b species. The advantage of these measurements is in statistics, which usually is superior to that of the exclusively reconstructed H_b decays. Some of the main disadvantages are related to the difficulty of estimating lepton+charm sample composition and Monte Carlo reliance for the $\beta\gamma$ factor estimate.

3. ***Measurements in exclusively reconstructed hadronic decays***. These have the advantage of complete reconstruction of decaying H_b, which allows one to infer the decaying species as well as to perform precise measurement of the $\beta\gamma$ factor. Both lead to generally smaller systematic uncertainties than in the above two categories. The downsides are smaller branching ratios, larger combinatoric backgrounds, especially in $H_b \to H_c\pi(\pi\pi)$ and multi-body H_c decays, or in a hadron collider environment with non-trivial underlying event. $H_b \to J/\psi H_s$ are relatively clean and easy to trigger on $J/\psi \to \ell^+\ell^-$, but their branching fraction is only about 1%.

4. ***Measurements at asymmetric B factories***. In the $\Upsilon(4S) \to B\overline{B}$ decay, the B mesons (B^+ or B^0) are essentially at rest in the $\Upsilon(4S)$ rest frame. This makes lifetime measurements impossible with experiments such as CLEO, in which $\Upsilon(4S)$ produced at rest. At asymmetric B factories the $\Upsilon(4S)$ meson is boosted resulting in B and $\overline{B}$ moving nearly parallel to each other. The lifetime is inferred from the distance Δz separating B and $\overline{B}$ decay vertices and $\Upsilon(4S)$ boost known from colliding beam energies.

In order to determine the charge of the B mesons in each event, one of the them is fully reconstructed in semileptonic or fully hadronic decay modes. The other B is typically not fully reconstructed, only the position of its decay vertex is determined from the remaining tracks in the event. These measurements benefit from very large statistics, but suffer from poor Δz resolution.

5. ***Direct measurement of lifetime ratios***. This method has so far been only applied in the measurement of $\tau(B^+)/\tau(B^0)$. The ratio of the lifetimes is extracted from the dependence of the observed relative number of B^+ and B^0 candidates (both reconstructed in semileptonic decays) on the proper decay time.

In some of the latest analyses, measurements of two (*e.g.* $\tau(B^+)$ and $\tau(B^+)/\tau(B^0)$) or three (*e.g.* $\tau(B^+)$, $\tau(B^+)/\tau(B^0)$, and Δm_d) quantities are combined. This introduces correlations among measurements. Another source of correlations among the measurements are the systematic effects, which could be common to an experiment or to an analysis technique across the experiments. When calculating the averages, such correlations are taken into account per general procedure, described in Ref. [37].

3.2.2 Inclusive *b*-hadron lifetimes

The inclusive b hadron lifetime is defined as $\tau_b = \sum_i f_i \tau_i$ where τ_i are the individual species lifetimes and f_i are the fractions of the various species present in an unbiased sample of weakly-decaying b hadrons produced at a high-energy collider.[5] This quantity is certainly less fundamental than the lifetimes of the individual species, the latter being much more useful in comparisons of the measurements with the theoretical predictions. Nonetheless, we perform the averaging of the inclusive lifetime measurements for completeness as well as for the reason that they might be of interest as "technical numbers."

In practice, an unbiased measurement of the inclusive lifetime is difficult to achieve, because it would imply an efficiency which is guaranteed to be the same across species. So most of the measurements are biased. In an attempt to group analyses which are expected to select the same mixture of b hadrons, the available results (given in Table 5) are divided into the following three sets:

1. measurements at LEP and SLD that accept any b-hadron decay, based on topological reconstruction (secondary vertex or track impact parameters);

2. measurements at LEP based on the identification of a lepton from a b decay; and

3. measurements at the Tevatron based on inclusive $H_b \to J/\psi X$ reconstruction, where the J/ψ is fully reconstructed.

The measurements of the first set are generally considered as estimates of τ_b, although the efficiency to reconstruct a secondary vertex most probably depends, in an analysis-specific way, on the number of tracks coming from the vertex, thereby depending on the type of the H_b. Even though these efficiency variations can in principle be accounted for using Monte Carlo simulations (which inevitably contain assumptions on branching fractions), the H_b mixture in

[5] In principle such a quantity could be slightly different in Z decays and a the Tevatron, in case the fractions of b-hadron species are not exactly the same; see the discussion in Sec. 3.1.3.

Table 5: Measurements of average b-hadron lifetimes.

Experiment	Method	Data set	τ_b (ps)	Ref.
ALEPH	Dipole	91	$1.511 \pm 0.022 \pm 0.078$	[38]
DELPHI	All track i.p. (2D)	91–92	$1.542 \pm 0.021 \pm 0.045$	[39][a]
DELPHI	Sec. vtx	91–93	$1.582 \pm 0.011 \pm 0.027$	[40][a]
DELPHI	Sec. vtx	94–95	$1.570 \pm 0.005 \pm 0.008$	[41]
L3	Sec. vtx + i.p.	91–94	$1.556 \pm 0.010 \pm 0.017$	[42][b]
OPAL	Sec. vtx	91–94	$1.611 \pm 0.010 \pm 0.027$	[43]
SLD	Sec. vtx	93	$1.564 \pm 0.030 \pm 0.036$	[44]
Average set 1 (b vertex)			1.572 ± 0.009	
ALEPH	Lepton i.p. (3D)	91–93	$1.533 \pm 0.013 \pm 0.022$	[45]
L3	Lepton i.p. (2D)	91–94	$1.544 \pm 0.016 \pm 0.021$	[42][b]
OPAL	Lepton i.p. (2D)	90–91	$1.523 \pm 0.034 \pm 0.038$	[46]
Average set 2 ($b \to \ell$)			1.537 ± 0.020	
CDF1	J/ψ vtx	92–95	$1.533 \pm 0.015^{+0.035}_{-0.031}$	[47]
Average of all above			1.568 ± 0.009	

[a] The combined DELPHI result quoted in [40] is $1.575 \pm 0.010 \pm 0.026$ ps.
[b] The combined L3 result quoted in [42] is $1.549 \pm 0.009 \pm 0.015$ ps.

that case can remain somewhat ill-defined and could be slightly different among analyses in this set.

On the contrary, the mixtures corresponding to the other two sets of measurements are better defined in the limit where the reconstruction and selection efficiency of a lepton or a J/ψ from an H_b does not depend on the decaying hadron type. These mixtures are given by the production fractions and the inclusive branching fractions for each H_b species to give a lepton or a J/ψ. In particular, under the assumption that all b hadrons have the same semileptonic decay width, the analyses of the second set should measure $\tau(b \to \ell) = (\sum_i f_i \tau_i^2)/(\sum_i f_i \tau_i)$ which is necessarily larger than τ_b if lifetime differences exist. Given the present knowledge on τ_i and f_i, $\tau(b \to \ell) - \tau_b$ is expected to be of the order of 0.01 ps.

Measurements by SLC and LEP experiments are subject to a number of common systematic uncertainties, such as those due to (lack of knowledge of) b and c fragmentation, b and c decay models, $\mathcal{B}(B \to \ell)$, $\mathcal{B}(B \to c \to \ell)$, $\mathcal{B}(c \to \ell)$, τ_c, and H_b decay multiplicity. In the averaging, these systematic uncertainties are assumed to be 100% correlated. The averages for the sets defined above (also given in Table 5) are

$$\tau(b \text{ vertex}) = 1.572 \pm 0.009 \text{ ps}, \quad (25)$$

$$\tau(b \to \ell) = 1.537 \pm 0.020 \text{ ps}, \quad (26)$$

$$\tau(b \to J/\psi) = 1.533^{+0.038}_{-0.034} \text{ ps}, \quad (27)$$

whereas an average of all measurements, ignoring mixture differences, yields 1.568 ± 0.009 ps.

Table 6: Measurements of the B^0 lifetime.

Experiment	Method	Data set	$\tau(B^0)$ (ps)	Ref.
ALEPH	$D^{(*)}\ell$	91–95	$1.518 \pm 0.053 \pm 0.034$	[48]
ALEPH	Exclusive	91–94	$1.25^{+0.15}_{-0.13} \pm 0.05$	[49]
ALEPH	Partial rec. $\pi^+\pi^-$	91–94	$1.49^{+0.17+0.08}_{-0.15-0.06}$	[49]
DELPHI	$D^{(*)}\ell$	91–93	$1.61^{+0.14}_{-0.13} \pm 0.08$	[50]
DELPHI	Charge sec. vtx	91–93	$1.63 \pm 0.14 \pm 0.13$	[51]
DELPHI	Inclusive $D^*\ell$	91–93	$1.532 \pm 0.041 \pm 0.040$	[52]
DELPHI	Charge sec. vtx	94–95	$1.531 \pm 0.021 \pm 0.031$	[41]
L3	Charge sec. vtx	94–95	$1.52 \pm 0.06 \pm 0.04$	[53]
OPAL	$D^{(*)}\ell$	91–93	$1.53 \pm 0.12 \pm 0.08$	[54]
OPAL	Charge sec. vtx	93–95	$1.523 \pm 0.057 \pm 0.053$	[55]
OPAL	Inclusive $D^*\ell$	91–00	$1.541 \pm 0.028 \pm 0.023$	[56]
SLD	Charge sec. vtx ℓ	93–95	$1.56^{+0.14}_{-0.13} \pm 0.10$	[57][a]
SLD	Charge sec. vtx	93–95	$1.66 \pm 0.08 \pm 0.08$	[57][a]
CDF1	$D^{(*)}\ell$	92–95	$1.474 \pm 0.039^{+0.052}_{-0.051}$	[58]
CDF1	Excl. $J/\psi K^{*0}$	92–95	$1.497 \pm 0.073 \pm 0.032$	[59]
CDF2	Excl. $J/\psi K^{*0}$	02–04	$1.541 \pm 0.050 \pm 0.020$	[60]
CDF2	Incl. $D^{(*)}\ell$	02–04	$1.473 \pm 0.036 \pm 0.054$	[61][p]
CDF2	Excl. $D^-(3)\pi$	02–04	$1.511 \pm 0.023 \pm 0.013$	[62][p]
CDF2	Excl. $J/\psi K_S$	02–06	$1.524 \pm 0.030 \pm 0.016$	[63]
DØ	Excl. $J/\psi K^{*0}$	02–05	$1.530 \pm 0.043 \pm 0.023$	[64, 65]
DØ	Excl. $J/\psi K_S$	02–06	$1.492 \pm 0.075 \pm 0.047$	[66][p]
BABAR	Exclusive	99–00	$1.546 \pm 0.032 \pm 0.022$	[67]
BABAR	Inclusive $D^*\ell$	99–01	$1.529 \pm 0.012 \pm 0.029$	[68]
BABAR	Exclusive $D^*\ell$	99–02	$1.523^{+0.024}_{-0.023} \pm 0.022$	[69]
BABAR	Incl. $D^*\pi$, $D^*\rho$	99–01	$1.533 \pm 0.034 \pm 0.038$	[70]
BABAR	Inclusive $D^*\ell$	99–04	$1.504 \pm 0.013^{+0.018}_{-0.013}$	[71]
Belle	Exclusive	00–03	$1.534 \pm 0.008 \pm 0.010$	[72]
Average			1.527 ± 0.008	

[a] The combined SLD result quoted in [57] is $1.64 \pm 0.08 \pm 0.08$ ps.
[p] Preliminary.

3.2.3 B^0 and B^+ lifetimes and their ratio

After a number of years of dominating these averages the LEP experiments yielded the scene to the asymmetric B factories and the Tevatron experiments. The B factories have been very successful in utilizing their potential – in only a few years of running, *BABAR* and, to a greater extent, Belle, have struck a balance between the statistical and the systematic uncertainties, with both being close to (or even better than) the impressive 1%. In the meanwhile, CDF and DØ have emerged as significant contributors to the field as the Tevatron Run II data flowed in. Both appear to enjoy relatively small systematic effects, and while current statistical uncertainties of their measurements are factors of 2 to 4 larger than those of their B-factory counterparts, both Tevatron experiments stand to increase their samples by almost an order of

Table 7: Measurements of the B^+ lifetime.

Experiment	Method	Data set	$\tau(B^+)$ (ps)	Ref.
ALEPH	$D^{(*)}\ell$	91–95	$1.648 \pm 0.049 \pm 0.035$	[48]
ALEPH	Exclusive	91–94	$1.58^{+0.21+0.04}_{-0.18-0.03}$	[49]
DELPHI	$D^{(*)}\ell$	91–93	$1.61 \pm 0.16 \pm 0.12$	[50]^a
DELPHI	Charge sec. vtx	91–93	$1.72 \pm 0.08 \pm 0.06$	[51]^a
DELPHI	Charge sec. vtx	94–95	$1.624 \pm 0.014 \pm 0.018$	[41]
L3	Charge sec. vtx	94–95	$1.66 \pm 0.06 \pm 0.03$	[53]
OPAL	$D^{(*)}\ell$	91–93	$1.52 \pm 0.14 \pm 0.09$	[54]
OPAL	Charge sec. vtx	93–95	$1.643 \pm 0.037 \pm 0.025$	[55]
SLD	Charge sec. vtx ℓ	93–95	$1.61^{+0.13}_{-0.12} \pm 0.07$	[57]^b
SLD	Charge sec. vtx	93–95	$1.67 \pm 0.07 \pm 0.06$	[57]^b
CDF1	$D^{(*)}\ell$	92–95	$1.637 \pm 0.058^{+0.045}_{-0.043}$	[58]
CDF1	Excl. $J/\psi K$	92–95	$1.636 \pm 0.058 \pm 0.025$	[59]
CDF2	Excl. $J/\psi K$	02–04	$1.662 \pm 0.033 \pm 0.008$	[73]^p
CDF2	Incl. $D^0\ell$	02–04	$1.653 \pm 0.029^{+0.033}_{-0.031}$	[61]^p
CDF2	Excl. $D^0\pi$	02–04	$1.661 \pm 0.027 \pm 0.013$	[62]^p
BABAR	Exclusive	99–00	$1.673 \pm 0.032 \pm 0.023$	[67]
Belle	Exclusive	00–03	$1.635 \pm 0.011 \pm 0.011$	[72]
Average			1.643 ± 0.010	

^{a} The combined DELPHI result quoted in [51] is 1.70 ± 0.09 ps.
^{b} The combined SLD result quoted in [57] is $1.66 \pm 0.06 \pm 0.05$ ps.
^{p} Preliminary.

magnitude.

At present time we are in an interesting position of having three sets of measurements (from LEP/SLC, B factories and the Tevatron) that originate from different environments, obtained using substantially different techniques and are precise enough for incisive comparison.

The averaging of $\tau(B^+)$, $\tau(B^0)$ and $\tau(B^+)/\tau(B^0)$ measurements is summarized in Tables 6, 7, and 8. For $\tau(B^+)/\tau(B^0)$ we averaged only the measurements of this quantity provided by experiments rather than using all available knowledge, which would have included, for example, $\tau(B^+)$ and $\tau(B^0)$ measurements which did not contribute to any of the ratio measurements.

The following sources of correlated (within experiment/machine) systematic uncertainties have been considered:

- for SLC/LEP measurements – D^{**} branching ratio uncertainties [2], momentum estimation of b mesons from Z^0 decays (b-quark fragmentation parameter $\langle X_E \rangle = 0.702 \pm 0.008$ [2]), B_s^0 and b baryon lifetimes (see Secs. 3.2.4 and 3.2.6), and b-hadron fractions at high energy (see Table 4);

- for *BABAR* measurements – alignment, z scale, PEP-II boost, sample composition (where applicable);

- for DØ and CDF Run II measurements – alignment (separately within each experiment).

Table 8: Measurements of the ratio $\tau(B^+)/\tau(B^0)$.

Experiment	Method	Data set	Ratio $\tau(B^+)/\tau(B^0)$	Ref.
ALEPH	$D^{(*)}\ell$	91–95	$1.085 \pm 0.059 \pm 0.018$	[48]
ALEPH	Exclusive	91–94	$1.27^{+0.23+0.03}_{-0.19-0.02}$	[49]
DELPHI	$D^{(*)}\ell$	91–93	$1.00^{+0.17}_{-0.15} \pm 0.10$	[50]
DELPHI	Charge sec. vtx	91–93	$1.06^{+0.13}_{-0.11} \pm 0.10$	[51]
DELPHI	Charge sec. vtx	94–95	$1.060 \pm 0.021 \pm 0.024$	[41]
L3	Charge sec. vtx	94–95	$1.09 \pm 0.07 \pm 0.03$	[53]
OPAL	$D^{(*)}\ell$	91–93	$0.99 \pm 0.14^{+0.05}_{-0.04}$	[54]
OPAL	Charge sec. vtx	93–95	$1.079 \pm 0.064 \pm 0.041$	[55]
SLD	Charge sec. vtx ℓ	93–95	$1.03^{+0.16}_{-0.14} \pm 0.09$	[57][a]
SLD	Charge sec. vtx	93–95	$1.01^{+0.09}_{-0.08} \pm 0.05$	[57][a]
CDF1	$D^{(*)}\ell$	92–95	$1.110 \pm 0.056^{+0.033}_{-0.030}$	[58]
CDF1	Excl. $J/\psi K$	92–95	$1.093 \pm 0.066 \pm 0.028$	[59]
CDF2	Excl. $J/\psi K$	02–04	1.080 ± 0.042	[73][p]
CDF2	Incl. $D\ell$	02–04	$1.123 \pm 0.040^{+0.041}_{-0.039}$	[61][p]
CDF2	Excl. $D\pi$	02–04	$1.10 \pm 0.02 \pm 0.01$	[62][p]
DØ	$D^{*+}\mu$ $D^0\mu$ ratio	02–04	$1.080 \pm 0.016 \pm 0.014$	[74]
BABAR	Exclusive	99–00	$1.082 \pm 0.026 \pm 0.012$	[67]
Belle	Exclusive	00–03	$1.066 \pm 0.008 \pm 0.008$	[72]
Average			1.076 ± 0.008	

[a] The combined SLD result quoted in [57] is $1.01 \pm 0.07 \pm 0.06$.
[p] Preliminary.

The resultant averages are:

$$\tau(B^0) = 1.527 \pm 0.008 \text{ ps}, \quad (28)$$

$$\tau(B^+) = 1.643 \pm 0.010 \text{ ps}, \quad (29)$$

$$\tau(B^+)/\tau(B^0) = 1.076 \pm 0.008. \quad (30)$$

3.2.4 B_s^0 lifetime

Similar to the kaon system, neutral B mesons contain short- and long-lived components, since the light (L) and heavy (H) eigenstates, $B_{\rm L}$ and $B_{\rm H}$, differ not only in their masses, but also in their widths with $\Delta\Gamma = \Gamma_{\rm L} - \Gamma_{\rm H}$. In the case of the B_s^0 system, $\Delta\Gamma_s$ can be particularly large. The current theoretical prediction in the Standard Model for the fractional width difference is $\Delta\Gamma_s = 0.096 \pm 0.039$ [75], where $\Gamma_s = (\Gamma_{\rm L} + \Gamma_{\rm H})/2$. Specific measurements of $\Delta\Gamma_s$ and Γ_s are explained in Sec. 3.3.2, but the result for Γ_s is quoted here.

Neglecting *CP* violation in $B_s^0 - \overline{B}_s^0$ mixing, which is expected to be small [75], the B_s^0 mass eigenstates are also *CP* eigenstates. In the Standard Model assuming no *CP* violation in the B_s^0 system, $\Gamma_{\rm L}$ is the width of the *CP*-even state and $\Gamma_{\rm H}$ the width of the *CP*-odd state. Final states can be decomposed into *CP*-even and *CP*-odd components, each with a different lifetime.

In view of a possibly substantial width difference, and the fact that various decay channels

will have different proportions of the $B_{\rm L}$ and $B_{\rm H}$ eigenstates, the straight average of all available B_s^0 lifetime measurements is rather ill-defined. Therefore, the B_s^0 lifetime measurements are broken down into four categories and averaged separately.

- ***Flavor-specific decays***, such as semileptonic $B_s \to D_s \ell \nu$ or $B_s \to D_s \pi$, will have equal fractions of $B_{\rm L}$ and $B_{\rm H}$ at time zero, where $\tau_{\rm L} = 1/\Gamma_{\rm L}$ is expected to be the shorter-lived component and $\tau_{\rm H} = 1/\Gamma_{\rm H}$ expected to be the longer-lived component. A superposition of two exponentials thus results with decay widths $\Gamma_s \pm \Delta\Gamma_s/2$. Fitting to a single exponential one obtains a measure of the flavor-specific lifetime [76]:

$$\tau(B_s^0)_{\rm fs} = \frac{1}{\Gamma_s} \frac{1 + \left(\frac{\Delta\Gamma_s}{2\Gamma_s}\right)^2}{1 - \left(\frac{\Delta\Gamma_s}{2\Gamma_s}\right)^2}. \tag{31}$$

  As given in Table 9, the flavor-specific B_s^0 lifetime world average is:

$$\tau(B_s^0)_{\rm fs} = 1.440 \pm 0.036 \text{ ps}. \tag{32}$$

  This world average will be used later in Sec. 3.3.2 in combination with other measurements to find $\overline{\tau}(B_s^0) = 1/\Gamma_s$ and $\Delta\Gamma_s$.

  The following correlated systematic errors were considered: average B lifetime used in backgrounds, B_s^0 decay multiplicity, and branching ratios used to determine backgrounds (*e.g.* $\mathcal{B}(B \to D_s D)$). A knowledge of the multiplicity of B_s^0 decays is important for measurements that partially reconstruct the final state such as $B \to D_s X$ (where X is not a lepton). The boost deduced from Monte Carlo simulation depends on the multiplicity used. Since this is not well known, the multiplicity in the simulation is varied and this range of values observed is taken to be a systematic. Similarly not all the branching ratios for the potential background processes are measured. Where they are available, the PDG values are used for the error estimate. Where no measurements are available estimates can usually be made by using measured branching ratios of related processes and using some reasonable extrapolation.

- ***$B_s^0 \to D_s^+ X$ decays***. Included in Table 9 are measurements of lifetimes using samples of B_s^0 decays to D_s plus hadrons, and hence into a less known mixture of *CP*-states. A lifetime weighted this way can still be a useful input for analyses examining such an inclusive sample. These are separated in Table 9 and combined with the semileptonic lifetime to obtain:

$$\tau(B_s^0)_{D_s{\rm X}} = 1.444 \pm 0.036 \text{ ps}. \tag{33}$$

- ***Fully exclusive $B_s^0 \to J/\psi\phi$ decays*** are expected to be dominated by the *CP*-even state and its lifetime. First measurements of the *CP* mix for this decay mode are outlined in Sec. 3.3.2. CDF and DØ measurements from this particular mode $B_s^0 \to J/\psi\phi$ are combined into an average given in Table 9. There are no correlations between the measurements for this fully exclusive channel, and the world average for this specific decay is:

$$\tau(B_s^0)_{J/\psi\phi} = 1.404 \pm 0.066 \text{ ps}. \tag{34}$$

Table 9: Measurements of the B_s^0 lifetime.

Experiment	Method	Data set	$\tau(B_s^0)$ (ps)	Ref.
ALEPH	$D_s\ell$	91–95	$1.54^{+0.14}_{-0.13} \pm 0.04$	[77]
CDF1	$D_s\ell$	92–96	$1.36 \pm 0.09^{+0.06}_{-0.05}$	[78]
DELPHI	$D_s\ell$	91–95	$1.42^{+0.14}_{-0.13} \pm 0.03$	[79]
OPAL	$D_s\ell$	90–95	$1.50^{+0.16}_{-0.15} \pm 0.04$	[80]
DØ	$D_s\mu$	02–04	$1.398 \pm 0.044^{+0.028}_{-0.025}$	[81]
CDF2	$D_s\pi, D_s\pi\pi\pi$	02–04	$1.60 \pm 0.10 \pm 0.02$	[82]^p
CDF2	$D_s\ell$	02–04	$1.381 \pm 0.055^{+0.052}_{-0.046}$	[83]^p
Average of flavor-specific measurements			1.440 ± 0.036	
ALEPH	D_sh	91–95	$1.47 \pm 0.14 \pm 0.08$	[84]
DELPHI	D_sh	91–95	$1.53^{+0.16}_{-0.15} \pm 0.07$	[85]
OPAL	D_s incl.	90–95	$1.72^{+0.20+0.18}_{-0.19-0.17}$	[86]
Average of all above D_s measurements			1.444 ± 0.036	
CDF1	$J/\psi\phi$	92–95	$1.34^{+0.23}_{-0.19} \pm 0.05$	[47]
CDF2	$J/\psi\phi$	02–04	$1.369 \pm 0.100^{+0.008}_{-0.010}$	[73]^p
DØ	$J/\psi\phi$	02–04	$1.444^{+0.098}_{-0.090} \pm 0.02$	[65]
Average of $J/\psi\phi$ measurements			1.404 ± 0.066	

^{p} Preliminary.

A caveat is that different experimental acceptances will likely lead to different admixtures of the *CP*-even and *CP*-odd states, and fits to a single exponential may result in inherently different measurements of these quantities.

- ***Fully exclusive $B_s^0 \to K^+K^-$ decays*** are expected to be *CP* even to within 5%, and hence measures the lifetime of the "light" mass eigenstate $\tau_L = 1/\Gamma_L$. The measurement of this lifetime from CDF in Run II [87] is:

$$\tau(B_s^0)_{K^+K^-} = 1.53 \pm 0.18 \pm 0.02\,\mathrm{ps}, \tag{35}$$

and will be used as an input in Sec. 3.3.2 for the average described below.

Finally, as will be shown in Sec. 3.3.2, measurements of $\Delta\Gamma_s$, including separation into *CP*-even and *CP*-odd components, give

$$\overline{\tau}(B_s^0) = 1/\Gamma_s = 1.494^{+0.055}_{-0.054}\ \mathrm{ps}\,, \tag{36}$$

and when combined with the flavor-specific lifetime measurements:

$$\overline{\tau}(B_s^0) = 1/\Gamma_s = 1.451^{+0.029}_{-0.028}\ \mathrm{ps}\,. \tag{37}$$

3.2.5 B_c^+ lifetime

There are currently three measurements of the lifetime of the B_c^+ meson from CDF [88,89] and DØ [90] using the semileptonic decay mode $B_c^+ \to J/\psi\ell$ and fitting simultaneously to the mass

Table 10: Measurements of the B_c^+ lifetime.

Experiment	Method	Data set	$\tau(B_c^+)$ (ps)	Ref.
CDF1	$J/\psi\ell$	92–95	$0.46^{+0.18}_{-0.16} \pm 0.03$	[88]
CDF2	$J/\psi e$	02–04	$0.463^{+0.073}_{-0.065} \pm 0.036$	[89]
DØ	$J/\psi\mu$	02–04	$0.448^{+0.123}_{-0.096} \pm 0.121$	[90]^p
Average			0.460 ± 0.066	

^{p} Preliminary.

and lifetime using the vertex formed with the leptons from the decay of the J/ψ and the third lepton. Correction factors to estimate the boost due to the missing neutrino are used. Mass values of $6.40 \pm 0.39 \pm 0.13$ GeV/c^2 for the CDF Run I result [88] and $5.95^{+0.14}_{-0.13} \pm 0.34$ GeV/c^2 for the DØ Run II result [90] are found by fitting to the tri-lepton invariant mass spectrum. In the CDF Run II result [89], the mass is fixed to 6.271 GeV/c^2, but then varied between 6.2 and 6.4 GeV/c^2 to assess the systematic error on the lifetime due to the B_c^+ mass value. These mass measurements are consistent within uncertainties, and also consistent with the precision mass measurement from CDF of $6285.7 \pm 5.3 \pm 1.2$ MeV/c^2 [91]. Correlated systematic errors include the impact of the uncertainty of the B_c^+ p_T spectrum on the correction factors, the level of feed-down from $\psi(2S)$, MC modeling of the decay model varying from phase space to the ISGW model, and mass variations. Values of the B_c^+ lifetime are given in Table 10 and the world average is determined to be:

$$\tau(B_c^+) = 0.460 \pm 0.066 \text{ ps}. \tag{38}$$

3.2.6 Λ_b^0 and b-baryon lifetimes

The most precise measurements of the b-baryon lifetime originate from two classes of partially reconstructed decays. In the first class, decays with an exclusively reconstructed Λ_c^+ baryon and a lepton of opposite charge are used. These products are more likely to occur in the decay of Λ_b^0 baryons. In the second class, more inclusive final states with a baryon (p, $\overline{p}$, Λ, or $\overline{\Lambda}$) and a lepton have been used, and these final states can generally arise from any b baryon.

The following sources of correlated systematic uncertainties have been considered: experimental time resolution within a given experiment, b-quark fragmentation distribution into weakly decaying b baryons, Λ_b^0 polarization, decay model, and evaluation of the b-baryon purity in the selected event samples. In computing the averages the central values of the masses are scaled to $M(\Lambda_b^0) = 5620 \pm 2$ MeV/c^2 [92] and $M(b\text{-baryon}) = 5670 \pm 100$ MeV/c^2.

The meaning of decay model and the correlations are not always clear. Uncertainties related to the decay model are dominated by assumptions on the fraction of n-body decays. To be conservative it is assumed that it is correlated whenever given as an error. DELPHI varies the fraction of 4-body decays from 0.0 to 0.3. In computing the average, the DELPHI result is corrected for 0.2 ± 0.2.

Furthermore, in computing the average, the semileptonic decay results from LEP are corrected for a polarization of $-0.45^{+0.19}_{-0.17}$ [2] and a Λ_b^0 fragmentation parameter $\langle X_E \rangle = 0.70 \pm 0.03$ [93].

Table 11: Measurements of the b-baryon lifetimes.

Experiment	Method	Data set	Lifetime (ps)	Ref.
ALEPH	$\Lambda_c^+\ell$	91–95	$1.18^{+0.13}_{-0.12} \pm 0.03$	[20][a]
ALEPH	$\Lambda\ell^-\ell^+$	91–95	$1.30^{+0.26}_{-0.21} \pm 0.04$	[20][a]
CDF1	$\Lambda_c^+\ell$	91–95	$1.32 \pm 0.15 \pm 0.07$	[94]
CDF2	$J/\psi\Lambda$	02–06	$1.593^{+0.083}_{-0.078} \pm 0.033$	[63]
DØ	$J/\psi\Lambda$	02–06	$1.298 \pm 0.137 \pm 0.050$	[66][p]
DØ	$\Lambda_c^+\mu$	02–06	$1.28^{+0.12}_{-0.11} \pm 0.09$	[95][p]
DELPHI	$\Lambda_c^+\ell$	91–94	$1.11^{+0.19}_{-0.18} \pm 0.05$	[96][b]
OPAL	$\Lambda_c^+\ell$, $\Lambda\ell^-\ell^+$	90–95	$1.29^{+0.24}_{-0.22} \pm 0.06$	[80]
Average of above 8 (Λ_b^0 lifetime)			1.393 ± 0.049	
ALEPH	$\Lambda\ell$	91–95	$1.20 \pm 0.08 \pm 0.06$	[20]
DELPHI	$\Lambda\ell\pi$ vtx	91–94	$1.16 \pm 0.20 \pm 0.08$	[96][b]
DELPHI	$\Lambda\mu$ i.p.	91–94	$1.10^{+0.19}_{-0.17} \pm 0.09$	[97][b]
DELPHI	$p\ell$	91–94	$1.19 \pm 0.14 \pm 0.07$	[96][b]
OPAL	$\Lambda\ell$ i.p.	90–94	$1.21^{+0.15}_{-0.13} \pm 0.10$	[98][c]
OPAL	$\Lambda\ell$ vtx	90–94	$1.15 \pm 0.12 \pm 0.06$	[98][c]
Average of above 14 (b-baryon lifetime)			1.325 ± 0.039	
ALEPH	$\Xi\ell$	90–95	$1.35^{+0.37+0.15}_{-0.28-0.17}$	[21]
DELPHI	$\Xi\ell$	91–93	$1.5^{+0.7}_{-0.4} \pm 0.3$	[23][d]
DELPHI	$\Xi\ell$	92–95	$1.45^{+0.55}_{-0.43} \pm 0.13$	[22][d]
Average of above 3 (Ξ_b lifetime)			$1.42^{+0.28}_{-0.24}$	

[a] The combined ALEPH result quoted in [20] is 1.21 ± 0.11 ps.
[b] The combined DELPHI result quoted in [96] is $1.14 \pm 0.08 \pm 0.04$ ps.
[c] The combined OPAL result quoted in [98] is $1.16 \pm 0.11 \pm 0.06$ ps.
[d] The combined DELPHI result quoted in [22] is $1.48^{+0.40}_{-0.31} \pm 0.12$ ps.
[p] Preliminary.

Inputs to the averages are given in Table 11. Note that before averaging, the CDF input of Λ_b lifetime measured exclusively in the decay mode $J/\psi\Lambda$ [63] is 3.1σ larger than the world average. It is combined with the rest without adjustment of input errors. The world average lifetime of b baryons is then:

$$\langle\tau(b\text{-baryon})\rangle = 1.325 \pm 0.039 \text{ ps}\,. \tag{39}$$

Keeping only $\Lambda_c^\pm\ell^\mp$, $\Lambda\ell^-\ell^+$, and fully exclusive final states, as representative of the Λ_b^0 baryon, the following lifetime is obtained:

$$\tau(\Lambda_b^0) = 1.393 \pm 0.049 \text{ ps}\,. \tag{40}$$

Averaging the measurements based on the $\Xi^\mp\ell^\mp$ final states [21–23] gives a lifetime value for a sample of events containing Ξ_b^0 and Ξ_b^- baryons:

$$\langle\tau(\Xi_b)\rangle = 1.42^{+0.28}_{-0.24} \text{ ps}\,. \tag{41}$$

Table 12: Summary of lifetimes of different b-hadron species.

b-hadron species	Measured lifetime
B^+	1.643 ± 0.010 ps
B^0	1.527 ± 0.008 ps
B_s^0 ($\rightarrow$ flavor specific)	1.440 ± 0.036 ps
B_s^0 ($\rightarrow J/\psi\phi$)	1.404 ± 0.066 ps
B_s^0 ($1/\Gamma_s$)	$1.451^{+0.029}_{-0.028}$ ps
B_c^+	0.460 ± 0.066 ps
Λ_b^0	1.393 ± 0.049 ps
Ξ_b mixture	$1.42^{+0.28}_{-0.24}$ ps
b-baryon mixture	1.325 ± 0.039 ps
b-hadron mixture	1.568 ± 0.009 ps

Table 13: Measured ratios of b-hadron lifetimes relative to the B^0 lifetime and ranges predicted by theory [35, 36].

Lifetime ratio	Measured value	Predicted range
$\tau(B^+)/\tau(B^0)$	1.076 ± 0.008	1.04 – 1.08
$\overline{\tau}(B_s^0)/\tau(B^0)^a$	0.950 ± 0.019	0.99 – 1.01
$\tau(\Lambda_b^0)/\tau(B^0)$	0.912 ± 0.032	0.86 – 0.95
$\tau(b\text{-baryon})/\tau(B^0)$	0.867 ± 0.026	0.86 – 0.95

[a] Using $\overline{\tau}(B_s^0) = 1/\Gamma_s = 2/(\Gamma_{\rm L} + \Gamma_{\rm H})$.

3.2.7 Summary and comparison with theoretical predictions

Averages of lifetimes of specific b-hadron species are collected in Table 12. As described in Sec. 3.2, Heavy Quark Effective Theory can be employed to explain the hierarchy of $\tau(B_c^+) \ll \tau(\Lambda_b^0) < \overline{\tau}(B_s^0) \approx \tau(B^0) < \tau(B^+)$, and used to predict the ratios between lifetimes. Typical predictions are compared to the measured lifetime ratios in Table 13. A recent prediction of the ratio between the B^+ and B^0 lifetimes, is 1.06 ± 0.02 [35], in good agreement with experiment.

The total widths of the B_s^0 and B^0 mesons are expected to be very close and differ by at most 1% [36, 99]. However, the experimental ratio $\overline{\tau}(B_s^0)/\tau(B^0)$, where $\overline{\tau}(B_s^0) = 1/\Gamma_s$ is obtained from $\Delta\Gamma_s$ and flavour-specific lifetime measurements, appears to be smaller than 1 by $(5.0 \pm 1.9)\%$, at deviation with respect to the prediction.

The ratio $\tau(\Lambda_b^0)/\tau(B^0)$ has particularly been the source of theoretical scrutiny since earlier calculations [32,100] predicted a value greater than 0.90, almost two sigma higher than the world average at the time. Many predictions cluster around a most likely central value of 0.94 [101]. More recent calculations of this ratio that include higher-order effects predict a lower ratio between the Λ_b^0 and B^0 lifetimes [35, 36] and reduce this difference. References [35, 36] present probability density functions of their predictions with variation of theoretical inputs, and the indicated ranges in Table 13 are the RMS of the distributions from the most probable values. Again, the CDF measurement of the Λ_b lifetime in the exclusive decay mode $J/\psi\Lambda$ [63] is significantly higher than the world average before inclusion, with a ratio to the $\tau(B^0)$ world

average of $\tau(\Lambda_b^0)/\tau(B^0) = 1.042 \pm 0.057$, resulting in continued interest in lifetimes of b baryons.

3.3 Neutral B-meson mixing

The $B^0 - \overline{B}^0$ and $B_s^0 - \overline{B}_s^0$ systems both exhibit the phenomenon of particle-antiparticle mixing. For each of them, there are two mass eigenstates which are linear combinations of the two flavour states, B and $\overline{B}$. The heaviest (lightest) of the these mass states is denoted $B_{\rm H}$ ($B_{\rm L}$), with mass $m_{\rm H}$ ($m_{\rm L}$) and total decay width $\Gamma_{\rm H}$ ($\Gamma_{\rm L}$). We define

$$\Delta m = m_{\rm H} - m_{\rm L} \,, \tag{42}$$

$$\Delta\Gamma = \Gamma_{\rm L} - \Gamma_{\rm H} \,, \tag{43}$$

where Δm is positive by definition, and $\Delta\Gamma$ is expected to be positive within the Standard Model.[6]

There are four different time-dependent probabilities describing the case of a neutral B meson produced as a flavour state and decaying to a flavour-specific final state. If CPT is conserved (which will be assumed throughout), they can be written as

$$\begin{cases} \mathcal{P}(B \to B) = \frac{e^{-\Gamma t}}{2}\left[\cosh\left(\frac{\Delta\Gamma}{2}t\right) + \cos(\Delta m t)\right] \\ \mathcal{P}(B \to \overline{B}) = \frac{e^{-\Gamma t}}{2}\left[\cosh\left(\frac{\Delta\Gamma}{2}t\right) - \cos(\Delta m t)\right]\left|\frac{q}{p}\right|^2 \\ \mathcal{P}(\overline{B} \to B) = \frac{e^{-\Gamma t}}{2}\left[\cosh\left(\frac{\Delta\Gamma}{2}t\right) - \cos(\Delta m t)\right]\left|\frac{p}{q}\right|^2 \\ \mathcal{P}(\overline{B} \to \overline{B}) = \frac{e^{-\Gamma t}}{2}\left[\cosh\left(\frac{\Delta\Gamma}{2}t\right) + \cos(\Delta m t)\right] \end{cases} , \tag{44}$$

where t is the proper time of the system (*i.e.* the time interval between the production and the decay in the rest frame of the B meson) and $\Gamma = (\Gamma_{\rm H} + \Gamma_{\rm L})/2 = 1/\overline{\tau}(B)$ is the average decay width. At the B factories, only the proper-time difference Δt between the decays of the two neutral B mesons from the $\Upsilon(4S)$ can be determined, but, because the two B mesons evolve coherently (keeping opposite flavours as long as none of them has decayed), the above formulae remain valid if t is replaced with Δt and the production flavour is replaced by the flavour at the time of the decay of the accompanying B meson in a flavour-specific state. As can be seen in the above expressions, the mixing probabilities depend on three mixing observables: Δm, $\Delta\Gamma$, and $|q/p|^2$ which signals CP violation in the mixing if $|q/p|^2 \neq 1$.

In the next sections we review in turn the experimental knowledge on these three parameters, separately for the B^0 meson (Δm_d, $\Delta\Gamma_d$, $|q/p|_d$) and the B_s^0 meson (Δm_s, $\Delta\Gamma_s$, $|q/p|_s$).

3.3.1 B^0 mixing parameters

CP violation parameter $|q/p|_d$

Evidence for CP violation in B^0 mixing has been searched for, both with flavor-specific and inclusive B^0 decays, in samples where the initial flavor state is tagged. In the case of

[6]For reason of symmetry in Eqs. (42) and (43), $\Delta\Gamma$ is sometimes defined with the opposite sign. The definition adopted here, *i.e.* Eq. (43), is the one used by most experimentalists and many phenomenologists in B physics.

semileptonic (or other flavor-specific) decays, where the final state tag is also available, the following asymmetry

$$\mathcal{A}^d_{\rm SL} = \frac{N(\overline{B}^0(t) \to \ell^+\nu_\ell X) - N(B^0(t) \to \ell^-\overline{\nu}_\ell X)}{N(\overline{B}^0(t) \to \ell^+\nu_\ell X) + N(B^0(t) \to \ell^-\overline{\nu}_\ell X)} = \frac{|p/q|^2_d - |q/p|^2_d}{|p/q|^2_d + |q/p|^2_d} \tag{45}$$

has been measured, either in time-integrated analyses at CLEO [102–104], CDF [105] and DØ [31], or in time-dependent analyses at OPAL [106], ALEPH [107], *BABAR* [108–111] and Belle [112]. In the inclusive case, also investigated and published at ALEPH [107] and OPAL [113], no final state tag is used, and the asymmetry [114]

$$\frac{N(B^0(t) \to \text{all}) - N(\overline{B}^0(t) \to \text{all})}{N(B^0(t) \to \text{all}) + N(\overline{B}^0(t) \to \text{all})} \simeq \mathcal{A}^d_{\rm SL}\left[\frac{\Delta m_d}{2\Gamma_d}\sin(\Delta m_d\, t) - \sin^2\left(\frac{\Delta m_d\, t}{2}\right)\right] \tag{46}$$

must be measured as a function of the proper time to extract information on *CP* violation. In all cases asymmetries compatible with zero have been found, with a precision limited by the available statistics.

A simple average of all measurements performed at B factories [103,104,108,110–112] yields

$$\mathcal{A}^d_{\rm SL} = -0.0047 \pm 0.0046 \tag{47}$$

or, equivalently through Eq. (45),

$$|q/p|_d = 1.0024 \pm 0.0023\,. \tag{48}$$

Analyses performed at higher energy, either at LEP or at the Tevatron, can't separate the contributions from the B^0 and B^0_s mesons. Under the assumption of no *CP* violation in B^0_s mixing, a number of these analyses [31,106,107,113] quote a measurement of $\mathcal{A}^d_{\rm SL}$ or $|q/p|_d$ for the B^0 meson. Combining these results with the above B factory averages lead to

$$\left.\begin{array}{l}\mathcal{A}^d_{\rm SL} = -0.0064 \pm 0.0034 \\ |q/p|_d = 1.0033 \pm 0.0017\end{array}\right\} \text{ if } \mathcal{A}^s_{\rm SL} = 0,\ |q/p|_s = 1. \tag{49}$$

These results[7], summarized in Table 14, are compatible with no *CP* violation in the B^0 mixing, an assumption we make for the rest of this section.

Mass and decay width differences Δm_d and $\Delta\Gamma_d$

Many time-dependent B^0–$\overline{B}^0$ oscillation analyses have been performed by the ALEPH, *BABAR*, Belle, CDF, DØ, DELPHI, L3 and OPAL collaborations. The corresponding measurements of Δm_d are summarized in Table 15, where only the most recent results are listed (*i.e.* measurements superseded by more recent ones have been omitted). Although a variety of different techniques have been used, the individual Δm_d results obtained at high-energy colliders have remarkably similar precision. Their average is compatible with the recent and more precise measurements from the asymmetric B factories. The systematic uncertainties

[7]Early analyses and (perhaps hence) the PDG use the complex parameter $\epsilon_B = (p-q)/(p+q)$; if *CP* violation in the mixing in small, $\mathcal{A}^d_{\rm SL} \cong 4{\rm Re}(\epsilon_B)/(1+|\epsilon_B|^2)$ and our current averages are ${\rm Re}(\epsilon_B)/(1+|\epsilon_B|^2) = -0.0012 \pm 0.0011$ (B factory measurements only) and -0.0016 ± 0.0009 (all measurements).

Table 14: Measurements of CP violation in B^0 mixing and their average in terms of both $\mathcal{A}^d_{\rm SL}$ and $|q/p|_d$. The individual results are listed as quoted in the original publications, or converted[7] to an $\mathcal{A}^d_{\rm SL}$ value. When two errors are quoted, the first one is statistical and the second one systematic. The second group of measurements, performed at high-energy colliders, assume no CP violation in B^0_s mixing, *i.e.* $|q/p|_s = 1$.

Exp. & Ref.	Method	Measured $\mathcal{A}^d_{\rm SL}$	Measured $\lvert q/p\rvert_d$
CLEO [103]	partial hadronic rec.	$+0.017 \pm 0.070 \pm 0.014$	
CLEO [104]	dileptons	$+0.013 \pm 0.050 \pm 0.005$	
CLEO [104]	average of above two	$+0.014 \pm 0.041 \pm 0.006$	
BABAR [108]	full hadronic rec.		$1.029 \pm 0.013 \pm 0.011$
BABAR [110]	dileptons		$0.9992 \pm 0.0027 \pm 0.0019$
BABAR [111][p]	part. rec. $D^*\ell\nu$	$-0.0130 \pm 0.0068 \pm 0.0040$	$1.0065 \pm 0.0034 \pm 0.0020$
Belle [112]	dileptons	$-0.0011 \pm 0.0079 \pm 0.0085$	$1.0005 \pm 0.0040 \pm 0.0043$
	Average of 6 above	-0.0047 ± 0.0046 (tot)	1.0024 ± 0.0023 (tot)
OPAL [106]	leptons	$+0.008 \pm 0.028 \pm 0.012$	
OPAL [113]	inclusive (Eq. (46))	$+0.005 \pm 0.055 \pm 0.013$	
ALEPH [107]	leptons	$-0.037 \pm 0.032 \pm 0.007$	
ALEPH [107]	inclusive (Eq. (46))	$+0.016 \pm 0.034 \pm 0.009$	
ALEPH [107]	average of above two	-0.013 ± 0.026 (tot)	
DØ [31]	dimuons	$-0.0092 \pm 0.0044 \pm 0.0032$	
	Average of 11 above	-0.0064 ± 0.0034 (tot)	1.0033 ± 0.0017 (tot)

[p] Preliminary.

are not negligible; they are often dominated by sample composition, mistag probability, or b-hadron lifetime contributions. Before being combined, the measurements are adjusted on the basis of a common set of input values, including the averages of the b-hadron fractions and lifetimes given in this report (see Secs. 3.1 and 3.2). Some measurements are statistically correlated. Systematic correlations arise both from common physics sources (fractions, lifetimes, branching ratios of b hadrons), and from purely experimental or algorithmic effects (efficiency, resolution, flavour tagging, background description). Combining all published measurements listed in Table 15 and accounting for all identified correlations as described in [2] yields $\Delta m_d = 0.508 \pm 0.003 \pm 0.003$ ps^{-1}.

On the other hand, ARGUS and CLEO have published measurements of the time-integrated mixing probability χ_d [102,103,133], which average to $\chi_d = 0.182 \pm 0.015$. Following Ref. [103], the width difference $\Delta\Gamma_d$ could in principle be extracted from the measured value of $\Gamma_d = 1/\tau(B^0)$ and the above averages for Δm_d and χ_d (provided that $\Delta\Gamma_d$ has a negligible impact on the $\Delta m_d\ \tau(B^0)$ analyses that have assumed $\Delta\Gamma_d = 0$), using the relation

$$\chi_d = \frac{x_d^2 + y_d^2}{2(x_d^2+1)} \quad \text{with} \quad x_d = \frac{\Delta m_d}{\Gamma_d} \quad \text{and} \quad y_d = \frac{\Delta\Gamma_d}{2\Gamma_d}\,. \tag{50}$$

However, direct time-dependent studies provide much stronger constraints: $|\Delta\Gamma_d|/\Gamma_d < 18\%$ at 95% CL from DELPHI [117], and $-6.8\% < \text{sign}(\text{Re}\lambda_{CP})\Delta\Gamma_d/\Gamma_d < 8.4\%$ at 90% CL from *BABAR* [108], where $\lambda_{CP} = (q/p)_d(\overline{A}_{CP}/A_{CP})$ is defined for a CP-even final state (the sensitivity

Table 15: Time-dependent measurements included in the Δm_d average. The results obtained from multi-dimensional fits involving also the B^0 (and B^+) lifetimes as free parameter(s) [69, 71, 72] have been converted into one-dimensional measurements of Δm_d. All the measurements have then been adjusted to a common set of physics parameters before being combined. The CDF results from Run II are preliminary.

Experiment and Ref.	Method rec.	Method tag	Δm_d in ps^{-1} before adjustment	Δm_d in ps^{-1} after adjustment
ALEPH [115]	ℓ	$Q_{\rm jet}$	0.404±0.045±0.027	
ALEPH [115]	ℓ	ℓ	0.452±0.039±0.044	
ALEPH [115]	above two combined		0.422±0.032±0.026	0.441±0.032±0.020
ALEPH [115]	D^*	$\ell, Q_{\rm jet}$	0.482±0.044±0.024	0.482±0.044±0.024
DELPHI [116]	ℓ	$Q_{\rm jet}$	0.493±0.042±0.027	0.502±0.042±0.024
DELPHI [116]	$\pi^*\ell$	$Q_{\rm jet}$	0.499±0.053±0.015	0.501±0.053±0.015
DELPHI [116]	ℓ	ℓ	0.480±0.040±0.051	$0.498\pm0.040\ ^{+0.042}_{-0.041}$
DELPHI [116]	D^*	$Q_{\rm jet}$	0.523±0.072±0.043	0.518±0.072±0.043
DELPHI [117]	vtx	comb	0.531±0.025±0.007	0.528±0.025±0.006
L3 [118]	ℓ	ℓ	0.458±0.046±0.032	0.465±0.046±0.028
L3 [118]	ℓ	$Q_{\rm jet}$	0.427±0.044±0.044	0.438±0.044±0.042
L3 [118]	ℓ	ℓ(IP)	0.462±0.063±0.053	$0.472\pm0.063\ ^{+0.045}_{-0.044}$
OPAL [119]	ℓ	ℓ	$0.430\pm0.043\ ^{+0.028}_{-0.030}$	$0.463\pm0.043\ ^{+0.018}_{-0.016}$
OPAL [120]	ℓ	$Q_{\rm jet}$	$0.444\pm0.029\ ^{+0.020}_{-0.017}$	$0.471\pm0.029\ ^{+0.014}_{-0.013}$
OPAL [121]	$D^*\ell$	$Q_{\rm jet}$	0.539±0.060±0.024	0.544±0.060±0.023
OPAL [121]	D^*	ℓ	$0.567\pm0.089\ ^{+0.029}_{-0.023}$	$0.571\pm0.089\ ^{+0.028}_{-0.022}$
OPAL [122]	$\pi^*\ell$	$Q_{\rm jet}$	0.497±0.024±0.025	0.495±0.024±0.025
CDF1 [123]	$D\ell$	SST	$0.471\ ^{+0.078}_{-0.068}\ ^{+0.033}_{-0.034}$	$0.470\ ^{+0.078}_{-0.068}\ ^{+0.033}_{-0.034}$
CDF1 [124]	μ	μ	0.503±0.064±0.071	0.515±0.064±0.070
CDF1 [125]	ℓ	$\ell, Q_{\rm jet}$	0.500±0.052±0.043	0.541±0.052±0.036
CDF1 [126]	$D^*\ell$	ℓ	$0.516\pm0.099\ ^{+0.029}_{-0.035}$	$0.523\pm0.099\ ^{+0.028}_{-0.035}$
CDF2 [127]	$D^{(*)}\ell$	OST	0.509±0.010±0.016	0.509±0.010±0.016
CDF2 [128]	B^0	comb	0.536±0.028±0.006	0.536±0.028±0.006
DØ [129]	$D^{(*)}\mu$	OST	0.506±0.020±0.016	0.506±0.020±0.016
BABAR [130]	B^0	ℓ, K, NN	0.516±0.016±0.010	0.520±0.016±0.008
BABAR [131]	ℓ	ℓ	0.493±0.012±0.009	0.489±0.012±0.006
BABAR [71]	$D^*\ell\nu$(part)	ℓ	0.511±0.007±0.007	0.512±0.007±0.007
BABAR [69]	$D^*\ell\nu$	ℓ, K, NN	0.492±0.018±0.014	0.491±0.018±0.013
Belle [132]	$D^*\pi$(part)	ℓ	0.509±0.017±0.020	0.512±0.017±0.019
Belle [8]	ℓ	ℓ	0.503±0.008±0.010	0.506±0.008±0.009
Belle [72]	$B^0, D^*\ell\nu$	comb	0.511±0.005±0.006	0.512±0.005±0.006
World average (all above measurements included):				0.508±0.003±0.003
– ALEPH, DELPHI, L3, OPAL and CDF1 only:				0.496±0.010±0.009
– Above measurements of *BABAR* and Belle only:				0.508±0.003±0.003

Table 16: Simultaneous measurements of Δm_d and $\tau(B^0)$, and their average. The Belle analysis also measures $\tau(B^+)$ at the same time, but it is converted here into a two-dimensional measurement of Δm_d and $\tau(B^0)$, for an assumed value of $\tau(B^+)$. The first quoted error on the measurements is statistical and the second one systematic; in the case of adjusted measurements, the latter includes a contribution obtained from the variation of $\tau(B^+)$ or $\tau(B^+)/\tau(B^0)$ in the indicated range. Units are ps^{-1} for Δm_d and ps for lifetimes. The three different values of $\rho(\Delta m_d, \tau(B^0))$ correspond to the statistical, systematic and total correlation coefficients between the adjusted measurements of Δm_d and $\tau(B^0)$.

Exp. & Ref.	Measured Δm_d	Measured $\tau(B^0)$	Measured $\tau(B^+)$	Assumed $\tau(B^+)$
BABAR [69]	0.492±0.018±0.013	1.523±0.024±0.022	—	$(1.083 \pm 0.017)\tau(B^0)$
BABAR [71]	0.511±0.007 $^{+0.007}_{-0.006}$	1.504±0.013 $^{+0.018}_{-0.013}$	—	1.671 ± 0.018
Belle [72]	0.511±0.005±0.006	1.534±0.008±0.010	1.635 ±0.011±0.011	—
	Adjusted Δm_d	Adjusted $\tau(B^0)$	$\rho(\Delta m_d, B^0)$	Assumed $\tau(B^+)$
BABAR [69]	0.492±0.018±0.013	1.524±0.025±0.022	−0.22 +0.74 +0.16	(1.076±0.008)$\tau(B^0)$
BABAR [71]	0.512±0.007±0.007	1.506±0.013±0.018	+0.01 −0.85 −0.48	1.643±0.010
Belle [72]	0.510±0.007±0.005	1.535±0.009±0.009	−0.27 −0.08 −0.19	1.643±0.010
Average	0.509±0.005±0.003	1.527±0.007±0.007	−0.19 −0.29 −0.23	1.643±0.010

to the overall sign of sign(Reλ_{CP})$\Delta\Gamma_d/\Gamma_d$ comes from the use of B^0 decays to *CP* final states). Combining these two results after adjustment to $1/\Gamma_d = \tau(B^0) = 1.527 \pm 0.008$ ps yields

$$\mathrm{sign}(\mathrm{Re}\lambda_{CP})\Delta\Gamma_d/\Gamma_d = 0.009 \pm 0.037\,. \tag{51}$$

The sign of Reλ_{CP} is not measured, but expected to be positive from the global fits of the Unitarity Triangle within the Standard Model.

Assuming $\Delta\Gamma_d = 0$ and using $1/\Gamma_d = \tau(B^0) = 1.527 \pm 0.008$ ps, the Δm_d and χ_d results are combined through Eq. (50) to yield the world average

$$\Delta m_d = 0.507 \pm 0.004 \text{ ps}^{-1}\,, \tag{52}$$

or, equivalently,

$$x_d = 0.775 \pm 0.008 \quad \text{and} \quad \chi_d = 0.1877 \pm 0.0024\,. \tag{53}$$

Figure 4 compares the Δm_d values obtained by the different experiments.

The B^0 mixing averages given in Eqs. (52) and (53) and the *b*-hadron fractions of Table 4 have been obtained in a fully consistent way, taking into account the fact that the fractions are computed using the χ_d value of Eq. (53) and that many individual measurements of Δm_d at high energy depend on the assumed values for the *b*-hadron fractions. Furthermore, this set of averages is consistent with the lifetime averages of Sec. 3.2.

It should be noted that the most recent (and precise) analyses at the asymmetric *B* factories measure Δm_d as a result of a multi-dimensional fit. Two *BABAR* analyses [69,71], based on fully and partially reconstructed $B^0 \to D^*\ell\nu$ decays respectively, extract simultaneously Δm_d and $\tau(B^0)$ while the latest Belle analysis [72], based on fully reconstructed hadronic B^0 decays and $B^0 \to D^*\ell\nu$ decays, extracts simultaneously Δm_d, $\tau(B^0)$ and $\tau(B^+)$. The measurements of Δm_d and $\tau(B^0)$ of these three analyses are displayed in Table 16 and in Fig. 5. Their

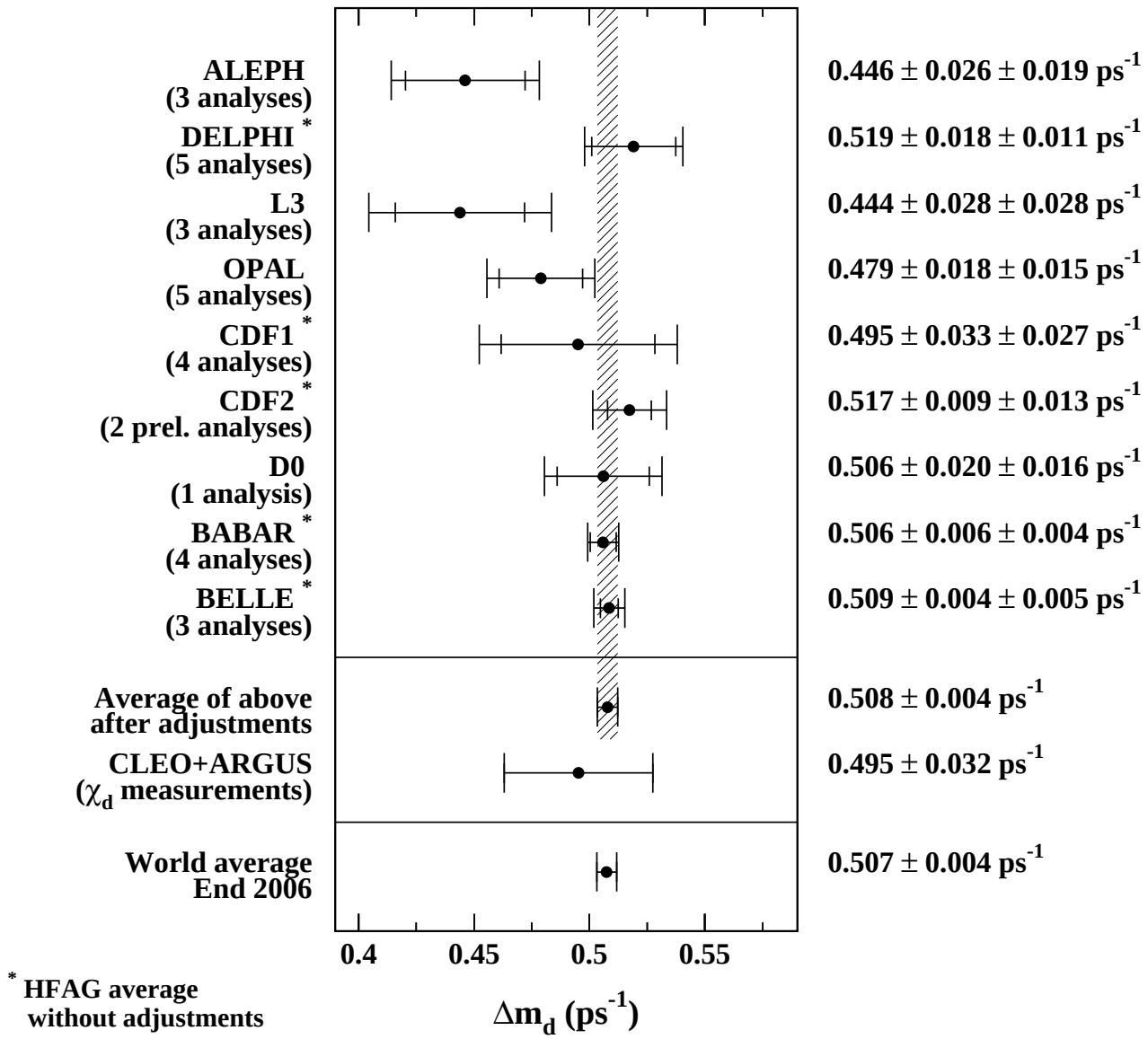

Figure 4: The B^0–$\overline{B}^0$ oscillation frequency Δm_d as measured by the different experiments. The averages quoted for ALEPH, L3 and OPAL are taken from the original publications, while the ones for DELPHI, CDF, *BABAR*, and Belle have been computed from the individual results listed in Table 15 without performing any adjustments. The time-integrated measurements of χ_d from the symmetric B factory experiments ARGUS and CLEO have been converted to a Δm_d value using $\tau(B^0) = 1.527 \pm 0.008$ ps. The two global averages have been obtained after adjustments of all the individual Δm_d results of Table 15 (see text).

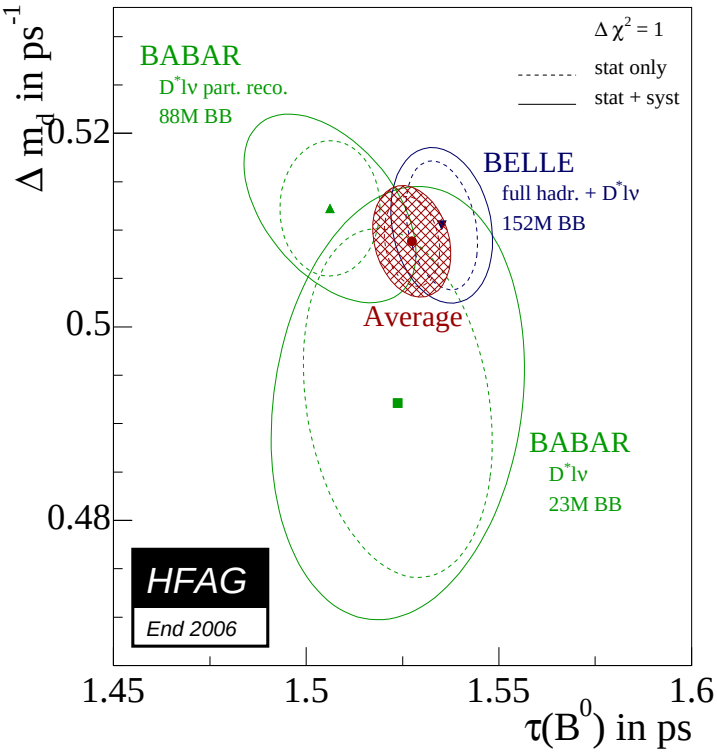

Figure 5: Simultaneous measurements of Δm_d and $\tau(B^0)$ [69, 71, 72], after adjustment to a common set of parameters (see text). Statistical and total uncertainties are represented as dashed and solid contours respectively. The average of the three measurements is indicated by a hatched ellipse.

two-dimensional average, taking into account all statistical and systematic correlations, and expressed at $\tau(B^+) = 1.643 \pm 0.010$ ps, is

$$\left.\begin{array}{r} \Delta m_d = 0.509 \pm 0.006 \text{ ps}^{-1} \\ \tau(B^0) = 1.527 \pm 0.010 \text{ ps} \end{array}\right\} \text{ with a total correlation of } -0.23. \tag{54}$$

3.3.2 B_s^0 mixing parameters

CP violation parameter $|q/p|_s$

Constraints on a combination of $|q/p|_d$ and $|q/p|_s$ have been explicitly quoted by the Tevatron experiments, using inclusive semileptonic decays of b hadrons:

$$f'_d\,\chi_d(1-|q/p|_d^2) + f'_s\,\chi_s(1-|q/p|_s^2) = +0.006 \pm 0.017 \qquad \text{CDF [105]}\,, \tag{55}$$

$$\frac{1}{4}\left(\mathcal{A}_{\rm SL}^d + \mathcal{A}_{\rm SL}^s \frac{f'_s\chi_s}{f'_d\chi_d}\right) = -0.0023 \pm 0.0011(\text{stat}) \pm 0.0008(\text{syst}) \qquad \text{DØ [31]}\,. \tag{56}$$

A first direct measurement of $\mathcal{A}_{\rm SL}^s$ and hence $|q/p|_s$ has been made by DØ by measuring the

charge asymmetry of $B_s^0 \to D_s\mu\nu$ decays [134]:

$$\mathcal{A}_{\rm SL}^s = +0.0245 \pm 0.0193({\rm stat}) \pm 0.0035({\rm syst})\,. \tag{57}$$

Given the average $\mathcal{A}_{\rm SL}^d = -0.0047 \pm 0.0046$ of Eq. (47), obtained from results at B factories, as well as other averages presented in this chapter for the quantities appearing in Eqs. (55) and (56), these three results are combined to yield

$$\mathcal{A}_{\rm SL}^s = +0.0003 \pm 0.0093 \tag{58}$$

or, equivalently through Eq. (45),

$$|q/p|_s = 0.9998 \pm 0.0046\,. \tag{59}$$

This result is compatible with no *CP* violation in B_s^0 mixing, an assumption made in almost all of the results described below.

Decay width difference $\Delta\Gamma_s$

Definitions and an introduction to $\Delta\Gamma_s$ can also be found in Sec. 3.2.4. Neglecting *CP* violation, the mass eigenstates are also *CP* eigenstates, with the short-lived state being *CP*-even and the long-lived one being *CP*-odd. Information on $\Delta\Gamma_s$ can be obtained by studying the proper time distribution of untagged data samples enriched in B_s^0 mesons [76]. In the case of an inclusive B_s^0 selection [53] or a semileptonic B_s^0 decay selection [78,79,81], both the short- and long-lived components are present, and the proper time distribution is a superposition of two exponentials with decay constants $\Gamma_s \pm \Delta\Gamma_s/2$. In principle, this provides sensitivity to both Γ_s and $(\Delta\Gamma_s/\Gamma_s)^2$. Ignoring $\Delta\Gamma_s$ and fitting for a single exponential leads to an estimate of Γ_s with a relative bias proportional to $(\Delta\Gamma_s/\Gamma_s)^2$. An alternative approach, which is directly sensitive to first order in $\Delta\Gamma_s/\Gamma_s$, is to determine the lifetime of B_s^0 candidates decaying to *CP* eigenstates; measurements exist for $B_s^0 \to J/\psi\phi$ [47,65,73] and $B_s^0 \to D_s^{(*)+}D_s^{(*)-}$, discussed later, which are mostly *CP*-even states [135]. However, more recent time-dependent angular analyses of $B_s^0 \to J/\psi\phi$ allow the simultaneous extraction of $\Delta\Gamma_s/\Gamma_s$ and the *CP*-even and *CP*-odd amplitudes [60,136].

Measurements quoting $\Delta\Gamma_s$ results from lifetime analyses are listed in Table 17 under the hypothesis of no *CP* violation. There is significant correlation between $\Delta\Gamma_s$ and $1/\Gamma_s$. In order to combine these measurements, the two-dimensional log-likelihood for each measurement in the $(1/\Gamma_s,\, \Delta\Gamma_s)$ plane is summed and the total normalized with respect to its minimum. The one-sigma contour (corresponding to 0.5 units of log-likelihood greater than the minimum) and 95% contour are found. Inputs as indicated in Table 17 were used in the combination, with the exception of the L3 [53] result since the likelihood in this case was not available.

Results of the combination are shown as the one-sigma contour labeled "Direct" in both plots of Fig. 6. Transformation of variables from $(1/\Gamma_s,\, \Delta\Gamma_s)$ space to other pairs of variables such as $(1/\Gamma_s,\, \Delta\Gamma_s/\Gamma_s)$ and $(\tau_{\rm L} = 1/\Gamma_{\rm L},\, \tau_{\rm H} = 1/\Gamma_{\rm H})$ are also made. The resulting one-sigma contour for the latter is shown in Fig. 6(b).

Table 17: Experimental constraints on $\Delta\Gamma_s/\Gamma_s$ from lifetime analyses, assuming no *CP* violation. The upper limits, which have been obtained by the working group, are quoted at the 95% CL.

Experiment	Method	$\Delta\Gamma_s/\Gamma_s$	Ref.
L3	lifetime of inclusive b-sample	< 0.67	[53]
DELPHI	$\overline{B}_s \to D_s^+ \ell^- \overline{\nu_\ell} X$, lifetime	< 0.46	[79]
DELPHI	$\overline{B}_s \to D_s^+$ hadron, lifetime	< 0.69	[85]
CDF1	$B_s^0 \to J/\psi\phi$, lifetime	$0.33^{+0.45}_{-0.42}$	[47]
CDF2	$B_s^0 \to J/\psi\phi$, time-dependent angular analysis	$0.65^{+0.25}_{-0.33} \pm 0.01$	[60]
		$\Delta\Gamma_s$	
DØ	$B_s^0 \to J/\psi\phi$, time-dependent angular analysis	$0.12^{+0.08}_{-0.10} \pm 0.02$	[136]

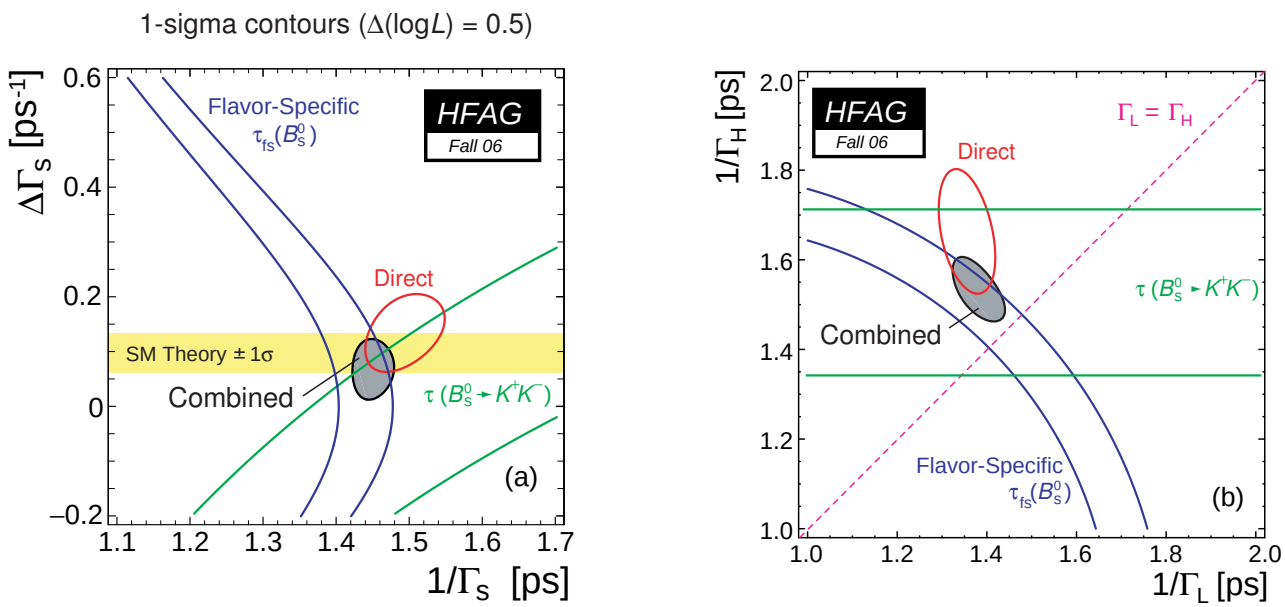

Figure 6: $\Delta\Gamma_s$ combination results with one-sigma contours ($\Delta \log \mathcal{L} = 0.5$) shown for (a) $\Delta\Gamma_s$ versus $\overline{\tau}(B_s^0) = 1/\Gamma_s$ and (b) $\tau_{\rm H} = 1/\Gamma_{\rm H}$ versus $\tau_{\rm L} = 1/\Gamma_{\rm L}$. The red contours labeled "Direct" are the result of the combination of most measurements of Table 17, the blue bands are the one-sigma contours due to the world average of flavor-specific measurements, the green bands are the one-sigma contour of the $B_s^0 \to K^+K-$ lifetime measurement, and the shaded region the combination of all three. In (b), the diagonal dashed line indicates $\Gamma_{\rm L} = \Gamma_{\rm H}$, *i.e.*, where $\Delta\Gamma_s = 0$.

Numerical results of the combination of the described inputs of Table 17 are:

$$\begin{aligned}
\Delta\Gamma_s/\Gamma_s &\in [-0.01, +0.51] \text{ at } 95\% \text{ CL}\,, && (60)\\
\Delta\Gamma_s/\Gamma_s &= +0.206^{+0.106}_{-0.111}\,, && (61)\\
\Delta\Gamma_s &= +0.138^{+0.068}_{-0.074}\ \text{ps}^{-1}\,, && (62)\\
\overline{\tau}(B_s^0) = 1/\Gamma_s &= 1.494^{+0.055}_{-0.054}\ \text{ps}\,, && (63)\\
\rho(\Delta\Gamma_s/\Gamma_s, 1/\Delta\Gamma_s) &= +0.39\,, && (64)\\
1/\Gamma_{\rm L} = \tau_{\rm short} &= 1.354^{+0.065}_{-0.062}\ \text{ps}\,, && (65)\\
1/\Gamma_{\rm H} = \tau_{\rm long} &= 1.665^{+0.143}_{+0.137}\ \text{ps}\,. && (66)
\end{aligned}$$

Flavor-specific lifetime measurements are of an equal mix of *CP*-even and *CP*-odd states at time zero, and if a single exponential function is used in the likelihood lifetime fit of such a sample [76],

$$\tau(B_s^0)_{\rm fs} = \frac{1}{\Gamma_s}\frac{1+\left(\frac{\Delta\Gamma_s}{2\Gamma_s}\right)^2}{1-\left(\frac{\Delta\Gamma_s}{2\Gamma_s}\right)^2}\,. \qquad (67)$$

Using the world average flavor-specific lifetime[8] of Sec. 3.2.4 the one-sigma blue bands shown in Fig. 6 are obtained. Higher-order corrections were checked to be negligible in the combination.

As described earlier, $B_s^0 \to K^+K^-$ decays can be used to measure the lifetime of the "light" mass eigenstate $\tau_L = 1/\Gamma_L = \tau(B_s^0)_{K^+K^-} = 1.53 \pm 0.18 \pm 0.02\,\text{ps}$ [87], and this additional constraint is shown by the green bands in Fig. 6.

When the flavor-specific lifetime measurements and τ_L measurements are combined with the measurements of Table 17, the shaded regions of Fig. 6 are obtained, with numerical results:

$$\begin{aligned}
\Delta\Gamma_s/\Gamma_s &\in [-0.07, +0.25] \text{ at } 95\% \text{ CL}\,, && (68)\\
\Delta\Gamma_s/\Gamma_s &= +0.104^{+0.076}_{-0.084}\,, && (69)\\
\Delta\Gamma_s &= 0.071^{+0.053}_{-0.057}\ \text{ps}^{-1}\,, && (70)\\
\overline{\tau}(B_s^0) = 1/\Gamma_s &= 1.451^{+0.029}_{-0.028}\ \text{ps}\,, && (71)\\
\rho(\Delta\Gamma_s/\Gamma_s, 1/\Delta\Gamma_s) &= +0.08\,, && (72)\\
1/\Gamma_{\rm L} = \tau_{\rm short} &= 1.380^{+0.060}_{-0.057}\ \text{ps}\,, && (73)\\
1/\Gamma_{\rm H} = \tau_{\rm long} &= 1.531^{+0.075}_{+0.069}\ \text{ps}\,. && (74)
\end{aligned}$$

These results can be compared with the theoretical prediction of $\Delta\Gamma_s/\Gamma_s = 0.096 \pm 0.039$ (or $\Delta\Gamma_s/\Gamma_s = 0.088 \pm 0.017$ if there is no new physics in Δm_s) [75].

Measurements of $\mathcal{B}(B_s^0 \to D_s^{(*)+} D_s^{(*)-})$ can also be sensitive to $\Delta\Gamma_s$. The decay $B_s^0 \to D_s^+ D_s^-$ is into a final state that is purely *CP* even. Under various theoretical assumptions [135], the inclusive decay into this plus the excited states $B_s^0 \to D_s^{(*)+} D_s^{(*)-}$ is also *CP* even to within 5%, and $B_s^0 \to D_s^{(*)+} D_s^{(*)-}$ saturates $\Gamma_s^{CP\,\text{even}}$. Under these assumptions, for no *CP* violation, we have:

$$\Delta\Gamma_s/\Gamma_s \approx \frac{2\mathcal{B}(B_s^0 \to D_s^{(*)+} D_s^{(*)-})}{1-\mathcal{B}(B_s^0 \to D_s^{(*)+} D_s^{(*)-})}\,. \qquad (75)$$

[8]The world average of all B_s^0 lifetime measurements using flavour-specific final states is 1.440 ± 0.036 ps; however, for the purpose of the $\Delta\Gamma_s$ extraction, we remove from this average one DELPHI analysis [79] that is already included in the set of "direct measurements" and obtain 1.441 ± 0.037 ps, shown as the blue bands on the two plots of Fig. 6.

Table 18: Measurements of $\mathcal{B}(B_s^0 \to D_s^{(*)+} D_s^{(*)-})$.

Experiment	Method	Value	Ref.
Belle	B_s^0-pair production at $\Upsilon(5S)$	< 0.257 at 90% CL	[17][a]
ALEPH	ϕ-ϕ correlations	$0.077 \pm 0.034^{+0.038}_{-0.026}$	[138][b]
DØ	$D_s \to \phi\pi$, $D_s \to \phi\mu\nu$	$0.039^{+0.019+0.016}_{-0.017-0.015}$	[139]
Average		0.046 ± 0.022	

[a] This limit is for $B_s^0 \to D_s^{*+} D_s^{*-}$.
[b] Recalculated using the PDG 2006 value of $\mathcal{B}(D_s \to \phi\pi)$.

However, there are concerns [137] that the assumptions needed for the above are overly restrictive and that the inclusive branching ratio may be *CP* even to only 30%. Due to this uncertainty, extracted values of $\Delta\Gamma_s/\Gamma_s$ from this branching ratio are not included in the overall combination but are only extracted here to compare with the world average result.

Measurements for the branching fraction for this decay channel are shown in Table 18. Using their average value of 0.046 ± 0.022 with Eq. (75) yields

$$\Delta\Gamma_s/\Gamma_s = +0.096 \pm 0.048\,, \tag{76}$$

consistent with the value given in Eq. (69), but with the above caveat. CDF has also measured the ratio of exclusive modes $\mathcal{B}(B_s^0 \to D_s^+ D_s^-)/\mathcal{B}(B_s^0 \to D_s^+ D^-)$ [140], and they continue work to use this ratio to extract $\Delta\Gamma_s$.

Again, note that the above combination and average was found assuming no *CP* violation in B_s^0 mixing, *i.e.*, that the *CP*-violating phase ϕ_s is zero:

$$\phi_s = \arg\left(-\frac{M_{12}}{\Gamma_{12}}\right) = 0\,. \tag{77}$$

Under the assumption of non-zero ϕ_s, in addition to the result listed in Table 17, the DØ collaboration [136] has also made simultaneous fits allowing ϕ_s to float finding:

$$\Delta\Gamma_s = +0.17 \pm 0.09 \pm 0.03 \text{ ps}^{-1}\,, \tag{78}$$

$$\overline{\tau}(B_s^0) = 1/\Gamma_s = 1.49 \pm 0.08^{+0.01}_{-0.03} \text{ ps}\,, \tag{79}$$

$$\phi_s = -0.79 \pm 0.56 \pm 0.01\,. \tag{80}$$

The *average* B_s^0 and B^0 lifetimes are predicted to be equal within 1% [36, 99] and in the past, an additional constraint was applied by setting $\Gamma_s = \Gamma_d$, *i.e.*, $1/\Gamma_s = \tau(B^0)$, where $\tau(B^0) = 1.527 \pm 0.008$ ps is the world average of experimental results, including a relative 1% theoretical uncertainty added in quadrature with the indicated experimental error. However, with the increased inconsistency of the measured values of $1/\Gamma_s = \overline{\tau}(B_s^0)$ and $\tau(B^0)$ at the level of $2.6\,\sigma$, this constraint is no longer applied.

Mass difference Δm_s

Without doubt, the most striking B_s^0 physics result in 2006 is the first observation of B_s^0 oscillations by the CDF collaboration [141], based on large samples of flavour-tagged hadronic

and semileptonic B_s^0 decays (in flavour-specific final states), partially or fully reconstructed in 1 fb^{-1} of data collected during Tevatron's Run II. From the proper-time dependence of these B_s^0 candidates, CDF observe B_s^0 oscillations with a significance of at least 5σ and measure [141]

$$\Delta m_s = 17.77 \pm 0.10 \pm 0.07 \text{ ps}^{-1} . \tag{81}$$

Multiplying this result with the mean B_s^0 lifetime of Eq. (71), $1/\Gamma_s = 1.451^{+0.029}_{-0.028}$ ps, yields

$$x_s = \frac{\Delta m_s}{\Gamma_s} = 25.8 \pm 0.5 . \tag{82}$$

With $2y_s = \Delta\Gamma_s/\Gamma_s = +0.104^{+0.076}_{-0.084}$ (see Eqs. (69) and (72)) and under the assumption of no CP violation in B_s^0 mixing, this corresponds to

$$\chi_s = \frac{x_s^2 + y_s^2}{2(x_s^2 + 1)} = 0.49925 \pm 0.00003 . \tag{83}$$

The ratio of the B^0 and B_s^0 oscillation frequencies, obtained from Eqs. (52) and (81),

$$\frac{\Delta m_d}{\Delta m_s} = 0.0286 \pm 0.0003 , \tag{84}$$

can be used to extract the following ratio of CKM matrix elements,

$$\left|\frac{V_{td}}{V_{ts}}\right| = \xi \sqrt{\frac{\Delta m_d}{\Delta m_s} \frac{m(B_s^0)}{m(B^0)}} = 0.2062 \pm 0.0011^{+0.0080}_{-0.0060} , \tag{85}$$

where the first quoted error is from experimental uncertainties (with the masses $m(B_s^0)$ and $m(B^0)$ taken from [4]), and where the second quoted error is from theoretical uncertainties in the estimation of the SU(3) flavor-symmetry breaking factor $\xi = 1.210^{+0.047}_{-0.035}$ obtained from lattice QCD calculations [142].

B_s^0 mesons were known to mix since many years. Indeed the time-integrated measurements of $\overline{\chi}$ (see Sec. 3.1.3), when compared to our knowledge of χ_d and the b-hadron fractions, indicated that B_s^0 mixing was large, with a value of χ_s close to its maximal possible value of 1/2. However, the time dependence of this mixing could not be observed until recently, mainly because of lack of proper-time resolution to resolve the small period of the B_s^0 oscillations.

The statistical significance $\mathcal{S}$ of a B_s^0 oscillation signal can be approximated as [143]

$$\mathcal{S} \approx \sqrt{\frac{N}{2}}\, f_{\text{sig}}\, (1 - 2w)\, \exp\left(-\left(\Delta m_s \sigma_t\right)^2 / 2\right) , \tag{86}$$

where N is the number of selected and tagged B_s^0 candidates, f_{sig} is the fraction of B_s^0 signal in the selected and tagged sample, w is the total mistag probability, and σ_t is the resolution on proper time. As can be seen, the quantity $\mathcal{S}$ decreases very quickly as Δm_s increases: this dependence is controlled by σ_t, which is therefore the most critical parameter for Δm_s analyses. The method widely used for B_s^0 oscillation searches consists of measuring a B_s^0 oscillation amplitude $\mathcal{A}$ at several different test values of Δm_s, using a maximum likelihood fit based on the functions of Eq. (44) where the cosine terms have been multiplied by $\mathcal{A}$. One expects $\mathcal{A} = 1$ at the true value of Δm_s and $\mathcal{A} = 0$ at a test value of Δm_s (far) below the true value. To a

good approximation, the statistical uncertainty on $\mathcal{A}$ is Gaussian and equal to $1/\mathcal{S}$ [143]. In any analysis, a particular value of Δm_s can be excluded at 95% CL if $\mathcal{A} + 1.645\,\sigma_{\mathcal{A}} < 1$, where $\sigma_{\mathcal{A}}$ is the total uncertainty on $\mathcal{A}$. Because of the proper time resolution, the quantity $\sigma_{\mathcal{A}}(\Delta m_s)$ is an increasing function of Δm_s (see Eq. (86) which merely models $1/\sigma_{\mathcal{A}}(\Delta m_s)$ in an analysis limited by the available statistics). Therefore, if the true value of Δm_s were infinitely large, one expects to be able to exclude all values of Δm_s up to $\Delta m_s^{\rm sens}$, where $\Delta m_s^{\rm sens}$, called here the sensitivity of the analysis, is defined by $1.645\,\sigma_{\mathcal{A}}(\Delta m_s^{\rm sens}) = 1$.

A large number of B_s^0 oscillation searches, all based on the amplitude method, have been performed over the years by ALEPH [144], CDF [141,145], DØ [146,147], DELPHI [79,85,117,148], OPAL [149,150] and SLD [151–153] (we omit references to searches that have been superseded by more recent ones). They have been combined by averaging the measured amplitudes $\mathcal{A}$ at each test value of Δm_s. The individual results have been adjusted to common physics inputs, and all known correlations have been accounted for; in the case of the inclusive (lepton) analyses, performed at LEP and SLC, the sensitivities (*i.e.* the statistical uncertainties on $\mathcal{A}$), which depend directly through Eq. (86) on the assumed fraction $f_{\rm sig} \sim f_s$ of B_s^0 mesons in an unbiased sample of weakly-decaying b hadrons, have also been rescaled to the LEP average $f_s = 0.104 \pm 0.009$.

The combined amplitude spectra for the individual experiments are displayed in Fig. 7, and the world average spectrum is displayed in Fig. 8. The appearance of the B_s^0 oscillation signal in 2006, which can clearly be seen by comparing the last two plots on Fig. 8, has been made possible by the latest analysis of the CDF data [141], which is, by far, the most sensitive one. It is interesting to note that a hint of a signal in the region 15–20 ps^{-1} has been around since many years at $e^+e^- \to Z$ experiments, and more recently at the DØ experiment as well.

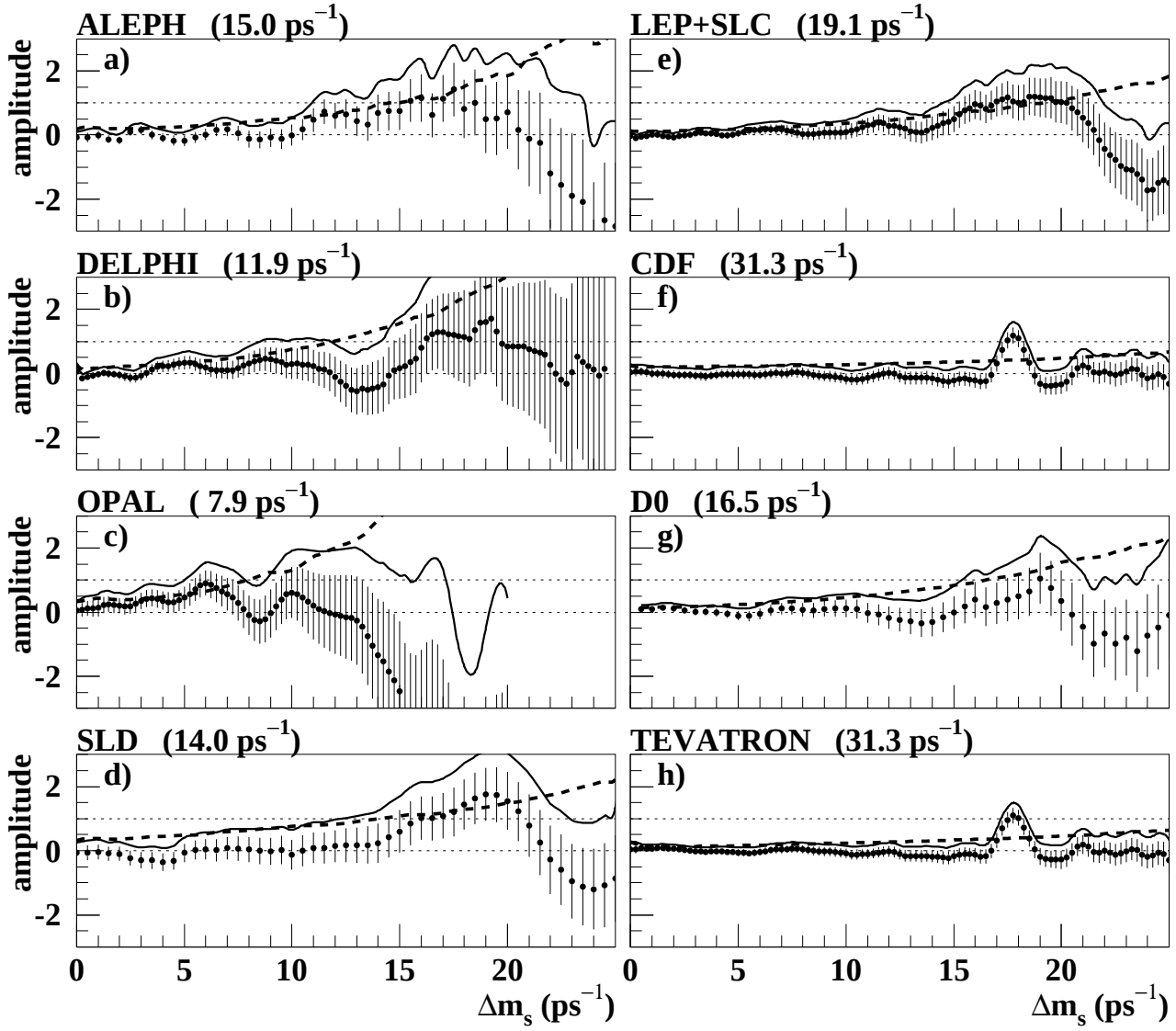

Figure 7: Combined B_s^0-oscillation amplitude spectra, displayed separately for each experiment. The points and error bars represent the measured amplitude $\mathcal{A}$ and its total uncertainty $\sigma_{\mathcal{A}}$, adjusted to a set of physics parameters common to all analyses (including $f_s = 0.104 \pm 0.009$ for LEP and SLC analyses). Values of Δm_s for which the solid curve ($\mathcal{A} + 1.645\,\sigma_{\mathcal{A}}$) is below 1 are excluded at 95% CL. The dashed curve shows $1.645\,\sigma_{\mathcal{A}}$; the number in parenthesis indicates where this curve is equal to 1, and is a measure of the sensitivity for 95% CL exclusion.
a) ALEPH [144], b) DELPHI [79, 85, 117, 148], c) OPAL [149, 150], d) SLD [151–153],
e) ALEPH, DELPHI, OPAL and SLD combined, f) CDF [141, 145], g) DØ [146, 147], h) CDF and DØ combined.

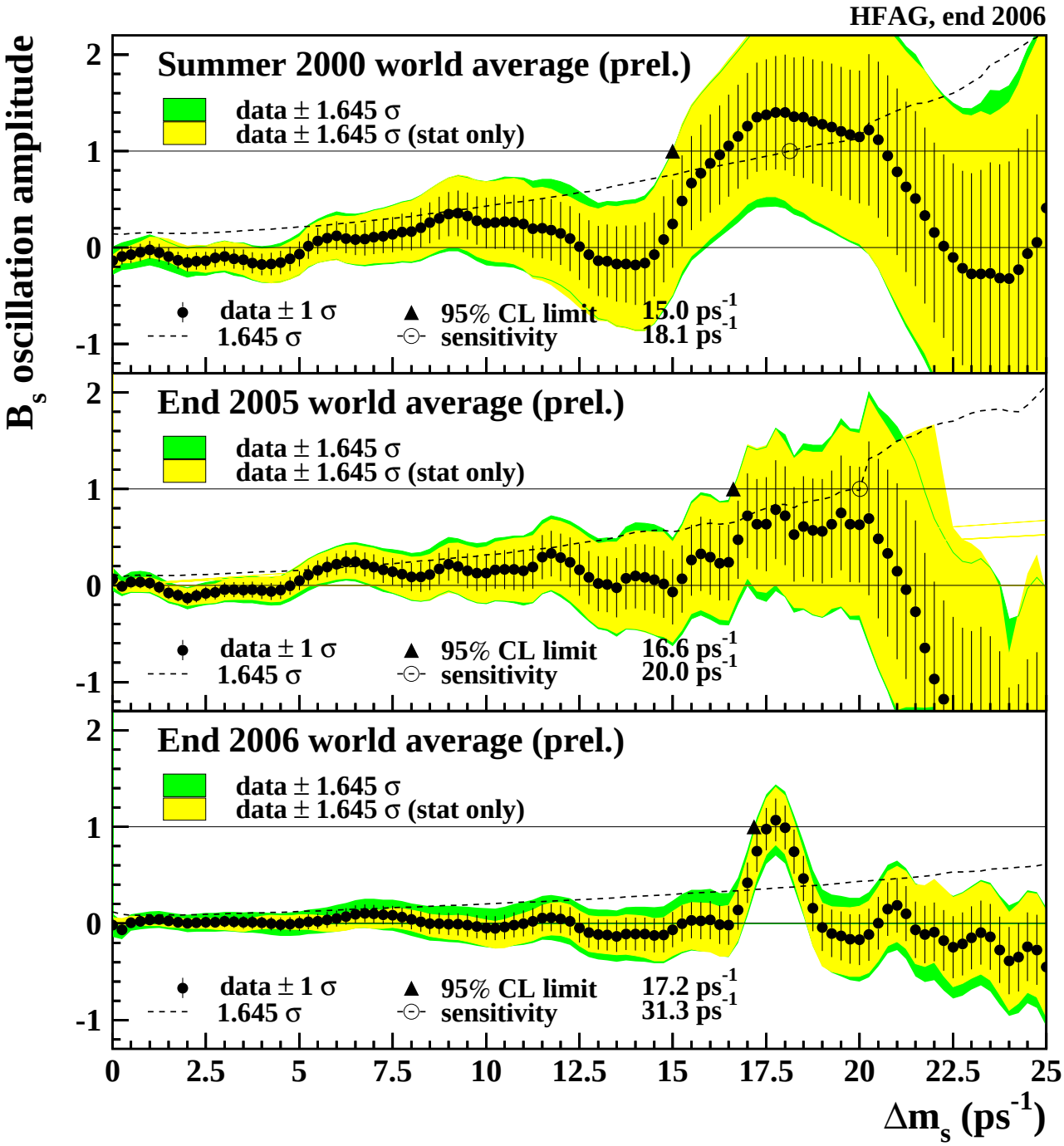

Figure 8: World averages of all measurements of the B_s^0 oscillation amplitude as a function of Δm_s. Top: situation in Summer 2000 [2]. Middle: situation at the end of 2005 [3]. Bottom: situation at the end of 2006, combining all published results [79, 85, 117, 141, 144–146, 148–152] as well as all recent preliminary results from Tevatron Run II [147]. The new results from CDF [141] and DØ [146, 147], which became available in 2006, supersede all previous analyses of Run II data [154, 155]. Statistical uncertainties dominate. Neighboring points are statistically correlated.

4 Measurements related to Unitarity Triangle angles

The charge of the "$CP(t)$ and Unitarity Triangle angles" group is to provide averages of measurements from time-dependent asymmetry analyses, and other quantities that are related to the angles of the Unitarity Triangle (UT). In cases where considerable theoretical input is required to extract the fundamental quantities, no attempt is made to do so at this stage. However, straightforward interpretations of the averages are given, where possible.

In Sec. 4.1 a brief introduction to the relevant phenomenology is given. In Sec. 4.2 an attempt is made to clarify the various different notations in use. In Sec. 4.3 the common inputs to which experimental results are rescaled in the averaging procedure are listed. We also briefly introduce the treatment of experimental errors. In the remainder of this section, the experimental results and their averages are given, divided into subsections based on the underlying quark-level decays.

4.1 Introduction

The Standard Model Cabibbo-Kobayashi-Maskawa (CKM) quark mixing matrix V must be unitary. A 3×3 unitary matrix has four free parameters,[9] and these are conventionally written by the product of three (complex) rotation matrices [156], where the rotations are characterized by the Euler angles θ_{12}, θ_{13} and θ_{23}, which are the mixing angles between the generations, and one overall phase δ,

$$V = \begin{pmatrix} V_{ud} & V_{us} & V_{ub} \\ V_{cd} & V_{cs} & V_{cb} \\ V_{td} & V_{ts} & V_{tb} \end{pmatrix} = \begin{pmatrix} c_{12}c_{13} & s_{12}c_{13} & s_{13}e^{-i\delta} \\ -s_{12}c_{23} - c_{12}s_{23}s_{13}e^{i\delta} & c_{12}c_{23} - s_{12}s_{23}s_{13}e^{i\delta} & s_{23}c_{13} \\ s_{12}s_{23} - c_{12}c_{23}s_{13}e^{i\delta} & -c_{12}s_{23} - s_{12}c_{23}s_{13}e^{i\delta} & c_{23}c_{13} \end{pmatrix} \quad (87)$$

where $c_{ij} = \cos\theta_{ij}$, $s_{ij} = \sin\theta_{ij}$ for $i < j = 1, 2, 3$.

Following the observation of a hierarchy between the different matrix elements, the Wolfenstein parameterization [157] is an expansion of V in terms of the four real parameters λ (the expansion parameter), A, ρ and η. Defining to all orders in λ [158]

$$\begin{aligned} s_{12} &\equiv \lambda, \\ s_{23} &\equiv A\lambda^2, \\ s_{13}e^{-i\delta} &\equiv A\lambda^3(\rho - i\eta), \end{aligned} \quad (88)$$

and inserting these into the representation of Eq. (87), unitarity of the CKM matrix is achieved to all orders. A Taylor expansion of V leads to the familiar approximation

$$V = \begin{pmatrix} 1 - \lambda^2/2 & \lambda & A\lambda^3(\rho - i\eta) \\ -\lambda & 1 - \lambda^2/2 & A\lambda^2 \\ A\lambda^3(1 - \rho - i\eta) & -A\lambda^2 & 1 \end{pmatrix} + \mathcal{O}\left(\lambda^4\right) . \quad (89)$$

At order λ^5, the obtained CKM matrix in this extended Wolfenstein parametrization is:

$$V = \begin{pmatrix} 1 - \frac{1}{2}\lambda^2 - \frac{1}{8}\lambda^4 & \lambda & A\lambda^3(\rho - i\eta) \\ -\lambda + \frac{1}{2}A^2\lambda^5\left[1 - 2(\rho + i\eta)\right] & 1 - \frac{1}{2}\lambda^2 - \frac{1}{8}\lambda^4(1 + 4A^2) & A\lambda^2 \\ A\lambda^3\left[1 - (1 - \frac{1}{2}\lambda^2)(\rho + i\eta)\right] & -A\lambda^2 + \frac{1}{2}A\lambda^4\left[1 - 2(\rho + i\eta)\right] & 1 - \frac{1}{2}A^2\lambda^4 \end{pmatrix} + \mathcal{O}\left(\lambda^6\right) . \quad (90)$$

[9] In the general case there are nine free parameters, but five of these are absorbed into unobservable quark phases.

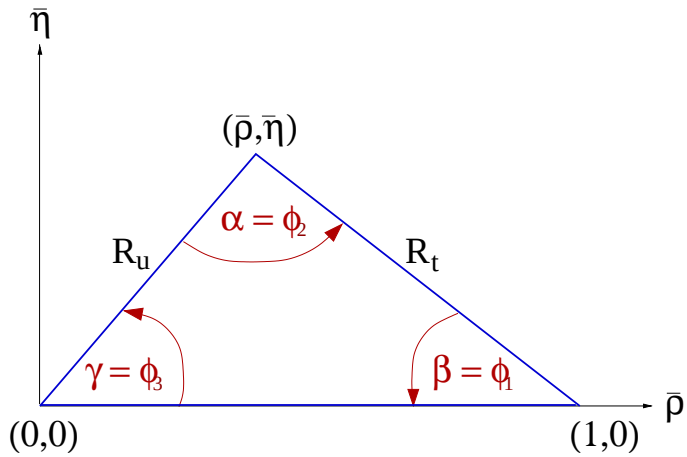

Figure 9: The Unitarity Triangle.

The non-zero imaginary part of the CKM matrix, which is the origin of *CP* violation in the Standard Model, is encapsulated in a non-zero value of η.

The unitarity relation $V^\dagger V = 1$ results in a total of nine expressions, that can be written as $\sum_{i=u,c,t} V_{ij}^* V_{ik} = \delta_{jk}$, where δ_{jk} is the Kronecker symbol. Of the off-diagonal expressions ($j \neq k$), three can be trivially transformed into the other three (under $j \leftrightarrow k$), leaving six relations, in which three complex numbers sum to zero, which therefore can be expressed as triangles in the complex plane.

One of these,

$$V_{ud}V_{ub}^* + V_{cd}V_{cb}^* + V_{td}V_{tb}^* = 0, \tag{91}$$

is specifically related to B decays. The three terms in Eq. (91) are of the same order ($\mathcal{O}(\lambda^3)$), and this relation is commonly known as the Unitarity Triangle. For presentational purposes, it is convenient to rescale the triangle by $(V_{cd}V_{cb}^*)^{-1}$, as shown in Fig. 9.

Two popular naming conventions for the UT angles exist in the literature:

$$\alpha \equiv \phi_2 = \arg\left[-\frac{V_{td}V_{tb}^*}{V_{ud}V_{ub}^*}\right], \quad \beta \equiv \phi_1 = \arg\left[-\frac{V_{cd}V_{cb}^*}{V_{td}V_{tb}^*}\right], \quad \gamma \equiv \phi_3 = \arg\left[-\frac{V_{ud}V_{ub}^*}{V_{cd}V_{cb}^*}\right]. \tag{92}$$

In this document the (α, β, γ) set is used. The sides R_u and R_t of the Unitarity Triangle (the third side being normalized to unity) are given by

$$R_u = \left|\frac{V_{ud}V_{ub}^*}{V_{cd}V_{cb}^*}\right| = \sqrt{\overline{\rho}^2 + \overline{\eta}^2}, \quad R_t = \left|\frac{V_{td}V_{tb}^*}{V_{cd}V_{cb}^*}\right| = \sqrt{(1-\overline{\rho})^2 + \overline{\eta}^2}. \tag{93}$$

where $\overline{\rho}$ and $\overline{\eta}$ define the apex of the Unitarity Triangle [158]

$$\overline{\rho} + i\overline{\eta} \equiv -\frac{V_{ud}V_{ub}^*}{V_{cd}V_{cb}^*} \equiv 1 + \frac{V_{td}V_{tb}^*}{V_{cd}V_{cb}^*} = \frac{\sqrt{1-\lambda^2}\,(\rho + i\eta)}{\sqrt{1-A^2\lambda^4} + \sqrt{1-\lambda^2}A^2\lambda^4(\rho + i\eta)} \tag{94}$$

The exact relation between (ρ, η) and $(\overline{\rho}, \overline{\eta})$ is

$$\rho + i\eta \;=\; \frac{\sqrt{1-A^2\lambda^4}(\overline{\rho} + i\overline{\eta})}{\sqrt{1-\lambda^2}\,[1 - A^2\lambda^4(\overline{\rho} + i\overline{\eta})]}\,. \tag{95}$$

By expanding in powers of λ, several useful approximate expressions can be obtained, including

$$\overline{\rho} = \rho(1 - \frac{1}{2}\lambda^2) + \mathcal{O}(\lambda^4)\,, \quad \overline{\eta} = \eta(1 - \frac{1}{2}\lambda^2) + \mathcal{O}(\lambda^4)\,, \quad V_{td} = A\lambda^3(1 - \overline{\rho} - i\overline{\eta}) + \mathcal{O}(\lambda^6)\,. \quad (96)$$

4.2 Notations

Several different notations for CP violation parameters are commonly used. This section reviews those found in the experimental literature, in the hope of reducing the potential for confusion, and to define the frame that is used for the averages.

In some cases, when B mesons decay into multibody final states via broad resonances (ρ, K^*, *etc.*), the experimental analyses ignore the effects of interference between the overlapping structures. This is referred to as the quasi-two-body (Q2B) approximation in the following.

4.2.1 *CP* asymmetries

The CP asymmetry is defined as the difference between the rate involving a b quark and that involving a $\overline{b}$ quark, divided by the sum. For example, the partial rate (or charge) asymmetry for a charged B decay would be given as

$$\mathcal{A}_f \;\equiv\; \frac{\Gamma(B^- \to f) - \Gamma(B^+ \to \overline{f})}{\Gamma(B^- \to f) + \Gamma(B^+ \to \overline{f})}. \quad (97)$$

4.2.2 Time-dependent *CP* asymmetries in decays to *CP* eigenstates

If the amplitudes for B^0 and $\overline{B}^0$ to decay to a final state f, which is a CP eigenstate with eigenvalue η_f, are given by A_f and $\overline{A}_f$, respectively, then the decay distributions for neutral B mesons, with known flavour at time $\Delta t = 0$, are given by

$$\Gamma_{\overline{B}^0\to f}(\Delta t) \;=\; \frac{e^{-|\Delta t|/\tau(B^0)}}{4\tau(B^0)}\left[1 + \frac{2\,\mathrm{Im}(\lambda_f)}{1+|\lambda_f|^2}\sin(\Delta m\Delta t) - \frac{1-|\lambda_f|^2}{1+|\lambda_f|^2}\cos(\Delta m\Delta t)\right], \quad (98)$$

$$\Gamma_{B^0\to f}(\Delta t) \;=\; \frac{e^{-|\Delta t|/\tau(B^0)}}{4\tau(B^0)}\left[1 - \frac{2\,\mathrm{Im}(\lambda_f)}{1+|\lambda_f|^2}\sin(\Delta m\Delta t) + \frac{1-|\lambda_f|^2}{1+|\lambda_f|^2}\cos(\Delta m\Delta t)\right]. \quad (99)$$

Here $\lambda_f = \frac{q}{p}\frac{\overline{A}_f}{A_f}$ contains terms related to B^0–$\overline{B}^0$ mixing and to the decay amplitude (the eigenstates of the effective Hamiltonian in the $B^0\overline{B}^0$ system are $|B_\pm\rangle = p\,|B^0\rangle \pm q\,|\overline{B}^0\rangle$). This formulation assumes CPT invariance, and neglects possible lifetime differences (between the eigenstates of the effective Hamiltonian; see Section 3.3 where the mass difference Δm is also defined) in the neutral B meson system. The case where non-zero lifetime differences are taken into account is discussed in Section 4.2.6. The time-dependent CP asymmetry, again defined as the difference between the rate involving a b quark and that involving a $\overline{b}$ quark, is then given by

$$\mathcal{A}_f\,(\Delta t) \;\equiv\; \frac{\Gamma_{\overline{B}^0\to f}(\Delta t) - \Gamma_{B^0\to f}(\Delta t)}{\Gamma_{\overline{B}^0\to f}(\Delta t) + \Gamma_{B^0\to f}(\Delta t)} \;=\; \frac{2\,\mathrm{Im}(\lambda_f)}{1+|\lambda_f|^2}\sin(\Delta m\Delta t) - \frac{1-|\lambda_f|^2}{1+|\lambda_f|^2}\cos(\Delta m\Delta t). \quad (100)$$

While the coefficient of the $\sin(\Delta m \Delta t)$ term in Eq. (100) is everywhere[10] denoted S_f:

$$S_f \equiv \frac{2\,\mathrm{Im}(\lambda_f)}{1+|\lambda_f|^2}, \tag{101}$$

different notations are in use for the coefficient of the $\cos(\Delta m \Delta t)$ term:

$$C_f \equiv -A_f \equiv \frac{1-|\lambda_f|^2}{1+|\lambda_f|^2}. \tag{102}$$

The C notation is used by the *BABAR* collaboration (see *e.g.* [160]), and also in this document. The A notation is used by the Belle collaboration (see *e.g.* [161]).

Neglecting effects due to *CP* violation in mixing (by taking $|q/p| = 1$), if the decay amplitude contains terms with a single weak (*i.e.*, *CP* violating) phase then $|\lambda_f| = 1$ and one finds $S_f = -\eta_f \sin(\phi_{\rm mix} + \phi_{\rm dec})$, $C_f = 0$, where $\phi_{\rm mix} = \arg(q/p)$ and $\phi_{\rm dec} = \arg(\overline{A}_f/A_f)$. Note that the B^0–$\overline{B}^0$ mixing phase $\phi_{\rm mix} \approx 2\beta$ in the Standard Model (in the usual phase convention).

If amplitudes with different weak phases contribute to the decay, no clean interpretation of S_f is possible. If the decay amplitudes have in addition different *CP* conserving strong phases, then $|\lambda_f| \neq 1$ and no clean interpretation is possible. The coefficient of the cosine term becomes non-zero, indicating direct *CP* violation. The sign of A_f as defined above is consistent with that of $\mathcal{A}_f$ in Eq. (97).

Frequently, we are interested in combining measurements governed by similar or identical short-distance physics, but with different final states (*e.g.*, $B^0 \to J/\psi K^0_S$ and $B^0 \to J/\psi K^0_L$). In this case, we remove the dependence on the *CP* eigenvalue of the final state by quoting $-\eta S_f$. In cases where the final state is not a *CP* eigenstate but has an effective *CP* content (see below), the reported $-\eta S$ is corrected by the effective *CP*.

4.2.3 Time-dependent *CP* asymmetries in decays to vector-vector final states

Consider B decays to states consisting of two spin-1 particles, such as $J/\psi K^{*0}(\to K^0_S \pi^0)$, $D^{*+}D^{*-}$ and $\rho^+\rho^-$, which are eigenstates of charge conjugation but not of parity.[11] In fact, for such a system, there are three possible final states; in the helicity basis these can be written h_{-1}, h_0, h_{+1}. The h_0 state is an eigenstate of parity, and hence of *CP*; however, *CP* transforms $h_{+1} \leftrightarrow h_{-1}$ (up to an unobservable phase). In the transversity basis, these states are transformed into $h_\parallel = (h_{+1}+h_{-1})/2$ and $h_\perp = (h_{+1}-h_{-1})/2$. In this basis all three states are *CP* eigenstates, and $h_\perp$ has the opposite *CP* to the others.

The amplitudes to these states are usually given by $A_{0,\perp,\parallel}$ (here we use a normalization such that $|A_0|^2 + |A_\perp|^2 + |A_\parallel|^2 = 1$). Then the effective *CP* of the vector-vector state is known if $|A_\perp|^2$ is measured. An alternative strategy is to measure just the longitudinally polarized component, $|A_0|^2$ (sometimes denoted by $f_{\rm long}$), which allows a limit to be set on the effective *CP* since $|A_\perp|^2 \leq |A_\perp|^2 + |A_\parallel|^2 = 1 - |A_0|^2$. The most complete treatment for neutral B decays to vector-vector final states is time-dependent angular analysis (also known as time-dependent transversity analysis). In such an analysis, the interference between the *CP* even and *CP* odd states provides additional sensitivity to the weak and strong phases involved.

[10] Occasionally one also finds Eq. (100) written as $\mathcal{A}_f(\Delta t) = \mathcal{A}_f^{\rm mix}\sin(\Delta m \Delta t) + \mathcal{A}_f^{\rm dir}\cos(\Delta m \Delta t)$, or similar.

[11] This is not true of all vector-vector final states, *e.g.*, $D^{*\pm}\rho^\mp$ is clearly not an eigenstate of charge conjugation.

4.2.4 Time-dependent asymmetries in decays to self-conjugate multiparticle final states

Amplitudes for neutral B decays into self-conjugate multiparticle final states such as $\pi^+\pi^-\pi^0$, $K^+K^-K^0_S$, $J/\psi\,\pi^+\pi^-$ or $D\pi^0$ with $D \to K^0_S\pi^+\pi^-$ may be written in terms of CP-even and CP-odd amplitudes. As above, the interference between these terms provides additional sensitivity to the weak and strong phases involved in the decay, and the time-dependence depends on both the sine and cosine of the weak phase difference. In order to perform unbinned maximum likelihood fits, and thereby extract as much information as possible from the distributions, it is necessary to select a model for the multiparticle decay, and therefore the results acquire some model dependence (binned, model independent methods are also possible, though are not as statistically powerful). The number of observables depends on the final state (and on the model used); the key feature is that as long as there are regions where both CP-even and CP-odd amplitudes contribute, the interference terms will be sensitive to the cosine of the weak phase difference. Therefore, these measurements allow distinction between multiple solutions for, *e.g.*, the four values of β from the measurement of $\sin(2\beta)$.

We now consider the various notations which have been used in experimental studies of time-dependent asymmetries in decays to self-conjugate multiparticle final states.

$B^0 \to D^{(*)}h^0$ with $D \to K^0_S\pi^+\pi^-$

The states $D\pi^0$, $D^*\pi^0$, $D\eta$, $D^*\eta$, $D\omega$ are collectively denoted $D^{(*)}h^0$. When the D decay model is fixed, fits to the time-dependent decay distributions can be performed to extract the weak phase difference. However, it is experimentally advantageous to use the sine and cosine of this phase as fit parameters, since these behave as essentially independent parameters, with low correlations and (potentially) rather different uncertainties. A parameter representing direct CP violation in the B decay can also be floated. For consistency with other analyses, this could be chosen to be C_f, but could equally well be $|\lambda_f|$, or other possibilities.

Belle performed an analysis of these channels with $\sin(2\phi_1)$ and $\cos(2\phi_1)$ as free parameters [182]. *BABAR* have performed an analysis floating also $|\lambda_f|$ [183] (and, of course, replacing $\phi_1 \Leftrightarrow \beta$).

$B^0 \to D^{*+}D^{*-}K^0_S$

The hadronic structure of the $B^0 \to D^{*+}D^{*-}K^0_S$ decay is not sufficiently well understood to perform a full time-dependent Dalitz plot analysis. Instead, following Browder *et al.* [175], *BABAR* [176] divide the Dalitz plane in two: $m(D^{*+}K^0_S)^2 > m(D^{*-}K^0_S)^2$ ($\eta_y = +1$) and $m(D^{*+}K^0_S)^2 < m(D^{*-}K^0_S)^2$ ($\eta_y = -1$); and then fit to a decay time distribution with asymmetry given by

$$\mathcal{A}_f\,(\Delta t) = \eta_y \frac{J_c}{J_0}\cos(\Delta m \Delta t) - \left[\frac{2J_{s1}}{J_0}\sin(2\beta) + \eta_y \frac{2J_{s2}}{J_0}\cos(2\beta)\right]\sin(\Delta m \Delta t)\,. \tag{103}$$

The measured values are $\frac{J_c}{J_0}$, $\frac{2J_{s1}}{J_0}\sin(2\beta)$ and $\frac{2J_{s2}}{J_0}\cos(2\beta)$, where the parameters J_0, J_c, J_{s1} and J_{s2} are the integrals over the half Dalitz plane $m(D^{*+}K^0_S)^2 < m(D^{*-}K^0_S)^2$ of the functions $|a|^2+|\overline{a}|^2$, $|a|^2-|\overline{a}|^2$, $\mathrm{Re}(\overline{a}a^*)$ and $\mathrm{Im}(\overline{a}a^*)$ respectively, where a and $\overline{a}$ are the decay amplitudes of $B^0 \to D^{*+}D^{*-}K^0_S$ and $\overline{B}^0 \to D^{*+}D^{*-}K^0_S$ respectively. The parameter J_{s2} (and hence J_{s2}/J_0) is predicted to be positive; with this assumption is it possible to determine the sign of $\cos(2\beta)$.

$B^0 \to K^+K^-K^0$

Studies of $B^0 \to K^+K^-K^0$ [195] and of the related decay $B^+ \to K^+K^-K^+$ [196,197], show that the decay is dominated by components from the intermediate K^+K^- resonances $\phi(1020)$, $f_0(980)$, a poorly understood scalar structure that peaks near $m(K^+K^-) \sim 1550$ MeV/c^2 and is denoted $X_0(1550)$, as well as a large nonresonant contribution. There is also a contribution from χ_{c0}.

The full time-dependent Dalitz plot analysis allows the complex amplitudes of each contributing term to be determined from data, including *CP* violation effects (*i.e.* allowing the complex amplitude for the B^0 decay to be independent from that for $\overline{B}^0$ decay), although one amplitude must be fixed to give a reference point. There are several choices for parametrization of the complex amplitudes (*e.g.* real and imaginary part, or magnitude and phase). Similarly, there are various approaches to include *CP* violation effects. Note that positive definite parameters such as magnitudes are disfavoured in certain circumstances (they inevitably lead to biases for small values). In order to compare results between analyses, it is useful for each experiment to present results in terms of the parameters that can be measured in a Q2B analysis (such as $\mathcal{A}_f$, S_f, C_f, $\sin(2\beta^{\rm eff})$, $\cos(2\beta^{\rm eff})$, *etc.*)

In the *BABAR* analysis of $B^0 \to K^+K^-K^0$ [195], the complex amplitude for each resonant contribution is written as

$$A_f = c_f(1+b_f)e^{i(\phi_f+\delta_f)} \ , \quad \overline{A}_f = c_f(1-b_f)e^{i(\phi_f-\delta_f)} \ , \tag{104}$$

where b_f and δ_f introduce *CP* violation in the magnitude and phase respectively. [The weak phase in B^0–$\overline{B}^0$ mixing (2β) also appears in the full formula for the time-dependent decay distribution.] The Q2B direct *CP* violation parameter is directly related to b_f

$$\mathcal{A}_f = \frac{-2b_f}{1+b_f^2} \, . \tag{105}$$

BABAR present results for c_f, ϕ_f, $\mathcal{A}_f$ and $\beta^{\rm eff}$ for each resonant contribution, as well as averaged values of $\mathcal{A}_f$ and $\beta^{\rm eff}$ for the entire $K^+K^-K^0$ Dalitz plot.

$B^0 \to \pi^+\pi^-\pi^0$

The $B^0 \to \pi^+\pi^-\pi^0$ decay is dominated by intermediate ρ resonances. Though it is possible, as above, to determine directly the complex amplitudes for each component, an alternative approach, suggested by Quinn and Silva [212], has been used by both *BABAR* [219] and Belle [220]. The amplitudes for B^0 and $\overline{B}^0$ to $\pi^+\pi^-\pi^0$ are written

$$A_{3\pi} = f_+A_+ + f_-A_- + f_0A_0 \ , \quad \overline{A}_{3\pi} = f_+\overline{A}_+ + f_-\overline{A}_- + f_0\overline{A}_0 \tag{106}$$

respectively. A_+, A_- and A_0 represent the complex decay amplitudes for $B^0 \to \rho^+\pi^-$, $B^0 \to \rho^-\pi^+$ and $B^0 \to \rho^0\pi^0$ while $\overline{A}_+$, $\overline{A}_-$ and $\overline{A}_0$ represent those for $\overline{B}^0 \to \rho^+\pi^-$, $\overline{B}^0 \to \rho^-\pi^+$ and $\overline{B}^0 \to \rho^0\pi^0$ respectively. f_+, f_- and f_0 incorporate kinematical and dynamical factors and depend on the Dalitz plot coordinates. The full time-dependent decay distribution can then be written in terms of 27 free parameters, one for each coefficient of the form factor bilinears, as listed in Table 19. These parameters are often referred to as "the Us and Is", and can be expressed in terms of A_+, A_-, A_0, $\overline{A}_+$, $\overline{A}_-$ and $\overline{A}_0$. If the full set of parameters is determined,

together with their correlations, other parameters, such as weak and strong phases, direct *CP* violation parameters, *etc.*, can be subsequently extracted. Note that one of the parameters (typically U_+^+) is often fixed to unity to provide a reference point; this does not affect the analysis.

Parameter	Description
U_+^+	Coefficient of $\lvert f_+\rvert^2$
U_0^+	Coefficient of $\lvert f_0\rvert^2$
U_-^+	Coefficient of $\lvert f_-\rvert^2$
U_0^-	Coefficient of $\lvert f_0\rvert^2 \cos(\Delta m \Delta t)$
U_-^-	Coefficient of $\lvert f_-\rvert^2 \cos(\Delta m \Delta t)$
U_+^-	Coefficient of $\lvert f_+\rvert^2 \cos(\Delta m \Delta t)$
I_0	Coefficient of $\lvert f_0\rvert^2 \sin(\Delta m \Delta t)$
I_-	Coefficient of $\lvert f_-\rvert^2 \sin(\Delta m \Delta t)$
I_+	Coefficient of $\lvert f_+\rvert^2 \sin(\Delta m \Delta t)$
$U_{+-}^{+,\mathrm{Im}}$	Coefficient of $\mathrm{Im}[f_+ f_-^*]$
$U_{+-}^{+,\mathrm{Re}}$	Coefficient of $\mathrm{Re}[f_+ f_-^*]$
$U_{+-}^{-,\mathrm{Im}}$	Coefficient of $\mathrm{Im}[f_+ f_-^*] \cos(\Delta m \Delta t)$
$U_{+-}^{-,\mathrm{Re}}$	Coefficient of $\mathrm{Re}[f_+ f_-^*] \cos(\Delta m \Delta t)$
I_{+-}^{Im}	Coefficient of $\mathrm{Im}[f_+ f_-^*] \sin(\Delta m \Delta t)$
I_{+-}^{Re}	Coefficient of $\mathrm{Re}[f_+ f_-^*] \sin(\Delta m \Delta t)$
$U_{+0}^{+,\mathrm{Im}}$	Coefficient of $\mathrm{Im}[f_+ f_0^*]$
$U_{+0}^{+,\mathrm{Re}}$	Coefficient of $\mathrm{Re}[f_+ f_0^*]$
$U_{+0}^{-,\mathrm{Im}}$	Coefficient of $\mathrm{Im}[f_+ f_0^*] \cos(\Delta m \Delta t)$
$U_{+0}^{-,\mathrm{Re}}$	Coefficient of $\mathrm{Re}[f_+ f_0^*] \cos(\Delta m \Delta t)$
I_{+0}^{Im}	Coefficient of $\mathrm{Im}[f_+ f_0^*] \sin(\Delta m \Delta t)$
I_{+0}^{Re}	Coefficient of $\mathrm{Re}[f_+ f_0^*] \sin(\Delta m \Delta t)$
$U_{-0}^{+,\mathrm{Im}}$	Coefficient of $\mathrm{Im}[f_- f_0^*]$
$U_{-0}^{+,\mathrm{Re}}$	Coefficient of $\mathrm{Re}[f_- f_0^*]$
$U_{-0}^{-,\mathrm{Im}}$	Coefficient of $\mathrm{Im}[f_- f_0^*] \cos(\Delta m \Delta t)$
$U_{-0}^{-,\mathrm{Re}}$	Coefficient of $\mathrm{Re}[f_- f_0^*] \cos(\Delta m \Delta t)$
I_{-0}^{Im}	Coefficient of $\mathrm{Im}[f_- f_0^*] \sin(\Delta m \Delta t)$
I_{-0}^{Re}	Coefficient of $\mathrm{Re}[f_- f_0^*] \sin(\Delta m \Delta t)$

Table 19: Definitions of the U and I coefficients. Modified from [219].

4.2.5 Time-dependent *CP* asymmetries in decays to non-*CP* eigenstates

Consider a non-*CP* eigenstate f, and its conjugate $\overline{f}$. For neutral B decays to these final states, there are four amplitudes to consider: those for B^0 to decay to f and $\overline{f}$ (A_f and $A_{\overline{f}}$, respectively), and the equivalents for $\overline{B}^0$ ($\overline{A}_f$ and $\overline{A}_{\overline{f}}$). If *CP* is conserved in the decay, then $A_f = \overline{A}_{\overline{f}}$ and $A_{\overline{f}} = \overline{A}_f$.

The time-dependent decay distributions can be written in many different ways. Here, we follow Sec. 4.2.2 and define $\lambda_f = \frac{q}{p}\frac{\overline{A}_f}{A_f}$ and $\lambda_{\overline{f}} = \frac{q}{p}\frac{\overline{A}_{\overline{f}}}{A_{\overline{f}}}$. The time-dependent CP asymmetries then follow Eq. (100):

$$\mathcal{A}_f(\Delta t) \equiv \frac{\Gamma_{\overline{B}^0\to f}(\Delta t) - \Gamma_{B^0\to f}(\Delta t)}{\Gamma_{\overline{B}^0\to f}(\Delta t) + \Gamma_{B^0\to f}(\Delta t)} = S_f \sin(\Delta m \Delta t) - C_f \cos(\Delta m \Delta t), \tag{107}$$

$$\mathcal{A}_{\overline{f}}(\Delta t) \equiv \frac{\Gamma_{\overline{B}^0\to \overline{f}}(\Delta t) - \Gamma_{B^0\to \overline{f}}(\Delta t)}{\Gamma_{\overline{B}^0\to \overline{f}}(\Delta t) + \Gamma_{B^0\to \overline{f}}(\Delta t)} = S_{\overline{f}} \sin(\Delta m \Delta t) - C_{\overline{f}} \cos(\Delta m \Delta t), \tag{108}$$

with the definitions of the parameters C_f, S_f, $C_{\overline{f}}$ and $S_{\overline{f}}$, following Eqs. (101) and (102).

The time-dependent decay rates are given by

$$\Gamma_{\overline{B}^0\to f}(\Delta t) = \frac{e^{-|\Delta t|/\tau(B^0)}}{8\tau(B^0)}(1 + \langle \mathcal{A}_{f\overline{f}}\rangle)\left\{1 + S_f \sin(\Delta m \Delta t) - C_f \cos(\Delta m \Delta t)\right\}, \tag{109}$$

$$\Gamma_{B^0\to f}(\Delta t) = \frac{e^{-|\Delta t|/\tau(B^0)}}{8\tau(B^0)}(1 + \langle \mathcal{A}_{f\overline{f}}\rangle)\left\{1 - S_f \sin(\Delta m \Delta t) + C_f \cos(\Delta m \Delta t)\right\}, \tag{110}$$

$$\Gamma_{\overline{B}^0\to \overline{f}}(\Delta t) = \frac{e^{-|\Delta t|/\tau(B^0)}}{8\tau(B^0)}(1 - \langle \mathcal{A}_{f\overline{f}}\rangle)\left\{1 + S_{\overline{f}} \sin(\Delta m \Delta t) - C_{\overline{f}} \cos(\Delta m \Delta t)\right\}, \tag{111}$$

$$\Gamma_{B^0\to \overline{f}}(\Delta t) = \frac{e^{-|\Delta t|/\tau(B^0)}}{8\tau(B^0)}(1 - \langle \mathcal{A}_{f\overline{f}}\rangle)\left\{1 - S_{\overline{f}} \sin(\Delta m \Delta t) + C_{\overline{f}} \cos(\Delta m \Delta t)\right\}, \tag{112}$$

where the time-independent parameter $\langle \mathcal{A}_{f\overline{f}}\rangle$ represents an overall asymmetry in the production of the f and $\overline{f}$ final states,[12]

$$\langle \mathcal{A}_{f\overline{f}}\rangle = \frac{\left(|A_f|^2 + |\overline{A}_f|^2\right) - \left(|A_{\overline{f}}|^2 + |\overline{A}_{\overline{f}}|^2\right)}{\left(|A_f|^2 + |\overline{A}_f|^2\right) + \left(|A_{\overline{f}}|^2 + |\overline{A}_{\overline{f}}|^2\right)}. \tag{113}$$

Assuming $|q/p| = 1$, the parameters C_f and $C_{\overline{f}}$ can also be written in terms of the decay amplitudes as follows:

$$C_f = \frac{|A_f|^2 - |\overline{A}_f|^2}{|A_f|^2 + |\overline{A}_f|^2} \quad \text{and} \quad C_{\overline{f}} = \frac{|A_{\overline{f}}|^2 - |\overline{A}_{\overline{f}}|^2}{|A_{\overline{f}}|^2 + |\overline{A}_{\overline{f}}|^2}, \tag{114}$$

giving asymmetries in the decay amplitudes of B^0 and $\overline{B}^0$ to the final states f and $\overline{f}$ respectively. In this notation, the direct CP invariance conditions are $\langle \mathcal{A}_{f\overline{f}}\rangle = 0$ and $C_f = -C_{\overline{f}}$. Note that C_f and $C_{\overline{f}}$ are typically non-zero; *e.g.*, for a flavour-specific final state, $\overline{A}_f = A_{\overline{f}} = 0$ ($A_f = \overline{A}_{\overline{f}} = 0$), they take the values $C_f = -C_{\overline{f}} = 1$ ($C_f = -C_{\overline{f}} = -1$).

The coefficients of the sine terms contain information about the weak phase. In the case that each decay amplitude contains only a single weak phase (*i.e.*, no direct CP violation), these terms can be written

$$S_f = \frac{-2\,|A_f|\,|\overline{A}_f|\sin(\phi_{\rm mix} + \phi_{\rm dec} - \delta_f)}{|A_f|^2 + |\overline{A}_f|^2} \quad \text{and} \quad S_{\overline{f}} = \frac{-2\,|A_{\overline{f}}|\,|\overline{A}_{\overline{f}}|\sin(\phi_{\rm mix} + \phi_{\rm dec} + \delta_f)}{|A_{\overline{f}}|^2 + |\overline{A}_{\overline{f}}|^2}, \tag{115}$$

[12] This parameter is often denoted $\mathcal{A}_f$ (or $\mathcal{A}_{CP}$), but here we avoid this notation to prevent confusion with the time-dependent CP asymmetry.

where δ_f is the strong phase difference between the decay amplitudes. If there is no *CP* violation, the condition $S_f = -S_{\overline{f}}$ holds. If decay amplitudes with different weak and strong phases contribute, no clean interpretation of S_f and $S_{\overline{f}}$ is possible.

Since two of the *CP* invariance conditions are $C_f = -C_{\overline{f}}$ and $S_f = -S_{\overline{f}}$, there is motivation for a rotation of the parameters:

$$S_{f\overline{f}} = \frac{S_f + S_{\overline{f}}}{2}, \quad \Delta S_{f\overline{f}} = \frac{S_f - S_{\overline{f}}}{2}, \quad C_{f\overline{f}} = \frac{C_f + C_{\overline{f}}}{2}, \quad \Delta C_{f\overline{f}} = \frac{C_f - C_{\overline{f}}}{2}. \tag{116}$$

With these parameters, the *CP* invariance conditions become $S_{f\overline{f}} = 0$ and $C_{f\overline{f}} = 0$. The parameter $\Delta C_{f\overline{f}}$ gives a measure of the "flavour-specificity" of the decay: $\Delta C_{f\overline{f}} = \pm 1$ corresponds to a completely flavour-specific decay, in which no interference between decays with and without mixing can occur, while $\Delta C_{f\overline{f}} = 0$ results in maximum sensitivity to mixing-induced *CP* violation. The parameter $\Delta S_{f\overline{f}}$ is related to the strong phase difference between the decay amplitudes of B^0 to f and to $\overline{f}$. We note that the observables of Eq. (116) exhibit experimental correlations (typically of $\sim 20\%$, depending on the tagging purity, and other effects) between $S_{f\overline{f}}$ and $\Delta S_{f\overline{f}}$, and between $C_{f\overline{f}}$ and $\Delta C_{f\overline{f}}$. On the other hand, the final state specific observables of Eq. (107) tend to have low correlations.

Alternatively, if we recall that the *CP* invariance conditions at the decay amplitude level are $A_f = \overline{A}_{\overline{f}}$ and $A_{\overline{f}} = \overline{A}_f$, we are led to consider the parameters [169]

$$\mathcal{A}_{f\overline{f}} = \frac{\left|\overline{A}_{\overline{f}}\right|^2 - \left|A_f\right|^2}{\left|\overline{A}_{\overline{f}}\right|^2 + \left|A_f\right|^2} \quad \text{and} \quad \mathcal{A}_{\overline{f}f} = \frac{\left|\overline{A}_f\right|^2 - \left|A_{\overline{f}}\right|^2}{\left|\overline{A}_f\right|^2 + \left|A_{\overline{f}}\right|^2}. \tag{117}$$

These are sometimes considered more physically intuitive parameters since they characterize direct *CP* violation in decays with particular topologies. For example, in the case of $B^0 \to \rho^\pm\pi^\mp$ (choosing $f = \rho^+\pi^-$ and $\overline{f} = \rho^-\pi^+$), $\mathcal{A}_{f\overline{f}}$ (also denoted $\mathcal{A}_{\rho\pi}^{+-}$) parameterizes direct *CP* violation in decays in which the produced ρ meson does not contain the spectator quark, while $\mathcal{A}_{\overline{f}f}$ (also denoted $\mathcal{A}_{\rho\pi}^{-+}$) parameterizes direct *CP* violation in decays in which it does. Note that we have again followed the sign convention that the asymmetry is the difference between the rate involving a b quark and that involving a $\overline{b}$ quark, *cf.* Eq. (97). Of course, these parameters are not independent of the other sets of parameters given above, and can be written

$$\mathcal{A}_{f\overline{f}} = -\frac{\langle\mathcal{A}_{f\overline{f}}\rangle + C_{f\overline{f}} + \langle\mathcal{A}_{f\overline{f}}\rangle\Delta C_{f\overline{f}}}{1 + \Delta C_{f\overline{f}} + \langle\mathcal{A}_{f\overline{f}}\rangle C_{f\overline{f}}} \quad \text{and} \quad \mathcal{A}_{\overline{f}f} = \frac{-\langle\mathcal{A}_{f\overline{f}}\rangle + C_{f\overline{f}} + \langle\mathcal{A}_{f\overline{f}}\rangle\Delta C_{f\overline{f}}}{-1 + \Delta C_{f\overline{f}} + \langle\mathcal{A}_{f\overline{f}}\rangle C_{f\overline{f}}}. \tag{118}$$

They usually exhibit strong correlations.

We now consider the various notations which have been used in experimental studies of time-dependent *CP* asymmetries in decays to non-*CP* eigenstates.

$B^0 \to D^{*\pm}D^\mp$

The above set of parameters ($\langle\mathcal{A}_{f\overline{f}}\rangle$, C_f, S_f, $C_{\overline{f}}$, $S_{\overline{f}}$), has been used by both *BABAR* [200] and Belle [204] in the $D^{*\pm}D^\mp$ system ($f = D^{*+}D^-$, $\overline{f} = D^{*-}D^+$). However, slightly different names for the parameters are used: *BABAR* uses ($\mathcal{A}$, C_{+-}, S_{+-}, C_{-+}, S_{-+}); Belle uses ($\mathcal{A}$, C_+, S_+, C_-, S_-). In this document, we follow the notation used by *BABAR*.

$B^0 \to \rho^\pm\pi^\mp$

In the $\rho^\pm\pi^\mp$ system, the ($\langle\mathcal{A}_{f\overline{f}}\rangle$, $C_{f\overline{f}}$, $S_{f\overline{f}}$, $\Delta C_{f\overline{f}}$, $\Delta S_{f\overline{f}}$) set of parameters has been used originally by *BABAR* [217] and Belle [218], in the Q2B approximation; the exact names[13] used in this case are ($\mathcal{A}_{CP}^{\rho\pi}, C_{\rho\pi}, S_{\rho\pi}, \Delta C_{\rho\pi}, \Delta S_{\rho\pi}$), and these names are also used in this document.

Since $\rho^\pm\pi^\mp$ is reconstructed in the final state $\pi^+\pi^-\pi^0$, the interference between the ρ resonances can provide additional information about the phases (see Sec. 4.2.4). Both *BABAR* [219] and Belle [220] have performed time-dependent Dalitz plot analyses, from which the weak phase α is directly extracted. In such an analysis, the measured Q2B parameters are also naturally corrected for interference effects. See Sec. 4.2.4.

$B^0 \to D^\pm\pi^\mp, D^{*\pm}\pi^\mp, D^\pm\rho^\mp$

Time-dependent *CP* analyses have also been performed for the final states $D^\pm\pi^\mp$, $D^{*\pm}\pi^\mp$ and $D^\pm\rho^\mp$. In these theoretically clean cases, no penguin contributions are possible, so there is no direct *CP* violation. Furthermore, due to the smallness of the ratio of the magnitudes of the suppressed ($b \to u$) and favoured ($b \to c$) amplitudes (denoted R_f), to a very good approximation, $C_f = -C_{\overline{f}} = 1$ (using $f = D^{(*)-}h^+$, $\overline{f} = D^{(*)+}h^-$ $h = \pi, \rho$), and the coefficients of the sine terms are given by

$$S_f = -2R_f \sin(\phi_{\rm mix} + \phi_{\rm dec} - \delta_f) \quad \text{and} \quad S_{\overline{f}} = -2R_f \sin(\phi_{\rm mix} + \phi_{\rm dec} + \delta_f). \tag{119}$$

Thus weak phase information can be cleanly obtained from measurements of S_f and $S_{\overline{f}}$, although external information on at least one of R_f or δ_f is necessary. (Note that $\phi_{\rm mix} + \phi_{\rm dec} = 2\beta + \gamma$ for all the decay modes in question, while R_f and δ_f depend on the decay mode.)

Again, different notations have been used in the literature. *BABAR* [226, 228] defines the time-dependent probability function by

$$f^\pm(\eta, \Delta t) = \frac{e^{-|\Delta t|/\tau}}{4\tau}\left[1 \mp S_\zeta \sin(\Delta m \Delta t) \mp \eta C_\zeta \cos(\Delta m \Delta t)\right], \tag{120}$$

where the upper (lower) sign corresponds to the tagging meson being a B^0 ($\overline{B}^0$). [Note here that a tagging B^0 ($\overline{B}^0$) corresponds to $-S_\xi$ ($+S_\xi$).] The parameters η and ζ take the values $+1$ and $+$ (-1 and $-$) when the final state is, *e.g.*, $D^-\pi^+$ ($D^+\pi^-$). However, in the fit, the substitutions $C_\zeta = 1$ and $S_\zeta = a \mp \eta b_i - \eta c_i$ are made.[14] [Note that, neglecting b terms, $S_+ = a - c$ and $S_- = a + c$, so that $a = (S_+ + S_-)/2$, $c = (S_- - S_+)/2$, in analogy to the parameters of Eq. (116).] The subscript i denotes the tagging category. These are motivated by the possibility of *CP* violation on the tag side [230], which is absent for semileptonic B decays (mostly lepton tags). The parameter a is not affected by tag side *CP* violation. The parameter b only depends on tag side *CP* violation parameters and is not directly useful for determining UT angles. A clean interpretation of the c parameter is only possible for lepton-tagged events, so the *BABAR* measurements report c measured with those events only.

The parameters used by Belle in the analysis using partially reconstructed B decays [229], are similar to the S_ζ parameters defined above. However, in the Belle convention, a tagging B^0 corresponds to a $+$ sign in front of the sine coefficient; furthermore the correspondence between the super/subscript and the final state is opposite, so that $S_\pm$ (*BABAR*) $= -S^\mp$ (Belle). In this analysis, only lepton tags are used, so there is no effect from tag side *CP* violation. In the

[13] *BABAR* has used the notations $A_{CP}^{\rho\pi}$ [217] and $\mathcal{A}_{\rho\pi}$ [219] in place of $\mathcal{A}_{CP}^{\rho\pi}$.
[14] The subscript i denotes tagging category.

Table 20: Conversion between the various notations used for *CP* violation parameters in the $D^{\pm}\pi^{\mp}$, $D^{*\pm}\pi^{\mp}$ and $D^{\pm}\rho^{\mp}$ systems. The b_i terms used by *BABAR* have been neglected. Recall that $(\alpha, \beta, \gamma) = (\phi_2, \phi_1, \phi_3)$.

	BABAR	Belle partial rec.	Belle full rec.
$S_{D^+\pi^-}$	$-S_- = -(a + c_i)$	N/A	$2R_{D\pi}\sin(2\phi_1 + \phi_3 + \delta_{D\pi})$
$S_{D^-\pi^+}$	$-S_+ = -(a - c_i)$	N/A	$2R_{D\pi}\sin(2\phi_1 + \phi_3 - \delta_{D\pi})$
$S_{D^{*+}\pi^-}$	$-S_- = -(a + c_i)$	S^+	$-2R_{D^*\pi}\sin(2\phi_1 + \phi_3 + \delta_{D^*\pi})$
$S_{D^{*-}\pi^+}$	$-S_+ = -(a - c_i)$	S^-	$-2R_{D^*\pi}\sin(2\phi_1 + \phi_3 - \delta_{D^*\pi})$
$S_{D^+\rho^-}$	$-S_- = -(a + c_i)$	N/A	N/A
$S_{D^-\rho^+}$	$-S_+ = -(a - c_i)$	N/A	N/A

Table 21: Translations used to convert the parameters measured by Belle to the parameters used for averaging in this document. The angular momentum factor L is -1 for $D^*\pi$ and $+1$ for $D\pi$. Recall that $(\alpha, \beta, \gamma) = (\phi_2, \phi_1, \phi_3)$.

	$D^*\pi$ partial rec.	$D^{(*)}\pi$ full rec.
a	$-(S^+ + S^-)$	$\frac{1}{2}(-1)^{L+1}\left(2R_{D^{(*)}\pi}\sin(2\phi_1 + \phi_3 + \delta_{D^{(*)}\pi}) + 2R_{D^{(*)}\pi}\sin(2\phi_1 + \phi_3 - \delta_{D^{(*)}\pi})\right)$
c	$-(S^+ - S^-)$	$\frac{1}{2}(-1)^{L+1}\left(2R_{D^{(*)}\pi}\sin(2\phi_1 + \phi_3 + \delta_{D^{(*)}\pi}) - 2R_{D^{(*)}\pi}\sin(2\phi_1 + \phi_3 - \delta_{D^{(*)}\pi})\right)$

Belle analysis using fully reconstructed B decays [227], this effect is measured and taken into account using $D^*l\nu$ decays; in neither Belle analysis are the a, b and c parameters used. In the latter case, the measured parameters are $2R_{D^{(*)}\pi}\sin(2\phi_1 + \phi_3 \pm \delta_{D^{(*)}\pi})$; the definition is such that $S^{\pm}$ (Belle) $= -2R_{D^*\pi}\sin(2\phi_1 + \phi_3 \pm \delta_{D^*\pi})$. However, the definition includes an angular momentum factor $(-1)^L$ [231], and so for the results in the $D\pi$ system, there is an additional factor of -1 in the conversion.

Explicitly, the conversion then reads as given in Table 20, where we have neglected the b_i terms used by *BABAR* (which are zero in the absence of tag side *CP* violation). For the averages in this document, we use the a and c parameters, and give the explicit translations used in Table 21. It is to be fervently hoped that the experiments will converge on a common notation in future.

Time-dependent asymmetries in radiative B decays

As a special case of decays to non-*CP* eigenstates, let us consider radiative B decays. Here, the emitted photon has a distinct helicity, which is in principle observable, but in practice is not usually measured. Thus the measured time-dependent decay rates are given by [206, 207]

$$\begin{aligned}\Gamma_{\overline{B}^0\to X\gamma}(\Delta t) &= \Gamma_{\overline{B}^0\to X\gamma_L}(\Delta t) + \Gamma_{\overline{B}^0\to X\gamma_R}(\Delta t) \qquad (121)\\ &= \frac{e^{-|\Delta t|/\tau(B^0)}}{4\tau(B^0)}\left\{1 + (S_L + S_R)\sin(\Delta m\Delta t) - (C_L + C_R)\cos(\Delta m\Delta t)\right\},\\ \Gamma_{B^0\to X\gamma}(\Delta t) &= \Gamma_{B^0\to X\gamma_L}(\Delta t) + \Gamma_{B^0\to X\gamma_R}(\Delta t) \qquad (122)\\ &= \frac{e^{-|\Delta t|/\tau(B^0)}}{4\tau(B^0)}\left\{1 - (S_L + S_R)\sin(\Delta m\Delta t) + (C_L + C_R)\cos(\Delta m\Delta t)\right\},\end{aligned}$$

where in place of the subscripts f and $\overline{f}$ we have used L and R to indicate the photon helicity. In order for interference between decays with and without B^0-$\overline{B}^0$ mixing to occur, the X system must not be flavour-specific, *e.g.*, in case of $B^0 \to K^{*0}\gamma$, the final state must be $K_S^0\pi^0\gamma$. The sign of the sine term depends on the C eigenvalue of the X system. At leading order, the photons from $b \to q\gamma$ ($\overline{b} \to \overline{q}\gamma$) are predominantly left (right) polarized, with corrections of order of m_q/m_b, thus interference effects are suppressed. Higher order effects can lead to corrections of order $\Lambda_{\rm QCD}/m_b$ [208]. The predicted smallness of the S terms in the Standard Model results in sensitivity to new physics contributions.

4.2.6 Time-dependent *CP* asymmetries in the B_s System

A complete analysis of the time-dependent decay rates of neutral B mesons must also take into account the lifetime difference between the eigenstates of the effective Hamiltonian, denoted by $\Delta\Gamma$. This is particularly important in the B_s system, since non-negligible values of $\Delta\Gamma_s$ are expected (see Section 3.3 for the latest experimental constraints). Neglecting *CP* violation in mixing, the relevant replacements for Eqs. 98 & 99 are [177]

$$\Gamma_{\overline{B}_s\to f}(\Delta t) = \mathcal{N}\frac{e^{-|\Delta t|/\tau(B_s^0)}}{4\tau(B_s^0)}\Big[\cosh(\tfrac{\Delta\Gamma\Delta t}{2}) + \frac{2\,\mathrm{Im}(\lambda_f)}{1+|\lambda_f|^2}\sin(\Delta m\Delta t) - \frac{1-|\lambda_f|^2}{1+|\lambda_f|^2}\cos(\Delta m\Delta t) - \frac{2\,\mathrm{Re}(\lambda_f)}{1+|\lambda_f|^2}\sinh(\tfrac{\Delta\Gamma\Delta t}{2})\Big], \tag{123}$$

and

$$\Gamma_{B_s^0\to f}(\Delta t) = \mathcal{N}\frac{e^{-|\Delta t|/\tau(B_s^0)}}{4\tau(B_s^0)}\Big[\cosh(\tfrac{\Delta\Gamma\Delta t}{2}) - \frac{2\,\mathrm{Im}(\lambda_f)}{1+|\lambda_f|^2}\sin(\Delta m\Delta t) + \frac{1-|\lambda_f|^2}{1+|\lambda_f|^2}\cos(\Delta m\Delta t) - \frac{2\,\mathrm{Re}(\lambda_f)}{1+|\lambda_f|^2}\sinh(\tfrac{\Delta\Gamma\Delta t}{2})\Big]. \tag{124}$$

The *untagged* time-dependent decay rate is given by

$$\Gamma_{\overline{B}_s\to f}(\Delta t) + \Gamma_{B_s^0\to f}(\Delta t) = \mathcal{N}\frac{e^{-|\Delta t|/\tau(B_s^0)}}{2\tau(B_s^0)}\Big[\cosh(\frac{\Delta\Gamma\Delta t}{2}) - \frac{2\,\mathrm{Re}(\lambda_f)}{1+|\lambda_f|^2}\sinh(\frac{\Delta\Gamma\Delta t}{2})\Big]. \tag{125}$$

With the requirement $\int_{-\infty}^{+\infty}\Gamma_{\overline{B}_s\to f}(\Delta t) + \Gamma_{B_s^0\to f}(\Delta t)d(\Delta t) = 1$, the normalization factor $\mathcal{N}$ is fixed to $1-(\frac{\Delta\Gamma}{2\Gamma})^2$. Note that an untagged time-dependent analysis can probe λ_f, through $\mathrm{Re}(\lambda_f)$, when $\Delta\Gamma \neq 0$. The tagged analysis is, of course, more sensitive.

To be consistent with our earlier notation,[15] we write here the coefficient of the sinh term as

$$A_f^{\Delta\Gamma} = -\frac{2\,\mathrm{Re}(\lambda_f)}{1+|\lambda_f|^2}\,. \tag{126}$$

Note that

$$(S_f)^2 + (C_f)^2 + \left(A_f^{\Delta\Gamma}\right)^2 = 1\,. \tag{127}$$

Other expressions can be similarly modified to take into account non-zero lifetime differences. Note that when the final state contains a mixture of *CP* even and *CP* odd states (as, for example, for vector-vector or multibody self-conjugate states), that $\mathrm{Re}(\lambda_f)$ contains terms proportional to both the sine and cosine of the weak phase difference, albeit with rather different sensitivities.

[15] As ever, alternative and conflicting notations appear in the literature. One popular alternative notation for this parameter is $\mathcal{A}_{\Delta\Gamma}$. Particular care must be taken over the signs.

4.2.7 Asymmetries in $B \to D^{(*)}K^{(*)}$ decays

CP asymmetries in $B \to D^{(*)}K^{(*)}$ decays are sensitive to γ. The neutral $D^{(*)}$ meson produced is an admixture of $D^{(*)0}$ (produced by a $b \to c$ transition) and $\overline{D}^{(*)0}$ (produced by a colour-suppressed $b \to u$ transition) states. If the final state is chosen so that both $D^{(*)0}$ and $\overline{D}^{(*)0}$ can contribute, the two amplitudes interfere, and the resulting observables are sensitive to γ, the relative weak phase between the two B decay amplitudes [232]. Various methods have been proposed to exploit this interference, including those where the neutral D meson is reconstructed as a *CP* eigenstate (GLW) [233], in a suppressed final state (ADS) [234], or in a self-conjugate three-body final state, such as $K_S^0\pi^+\pi^-$ (Dalitz) [235]. It should be emphasised that while each method differs in the choice of D decay, they are all sensitive to the same parameters of the B decay, and can be considered as variations of the same technique.

Consider the case of $B^\mp \to DK^\mp$, with D decaying to a final state f, which is accessible to both D^0 and $\overline{D}^0$. We can write the decay rates for B^- and B^+ ($\Gamma_\mp$), the charge averaged rate ($\Gamma = (\Gamma_- + \Gamma_+)/2$) and the charge asymmetry ($\mathcal{A} = (\Gamma_- - \Gamma_+)/(\Gamma_- + \Gamma_+)$, see Eq. (97)) as

$$\Gamma_\mp \propto r_B^2 + r_D^2 + 2r_B r_D \cos(\delta_B + \delta_D \mp \gamma), \tag{128}$$

$$\Gamma \propto r_B^2 + r_D^2 + 2r_B r_D \cos(\delta_B + \delta_D)\cos(\gamma), \tag{129}$$

$$\mathcal{A} = \frac{2r_B r_D \sin(\delta_B + \delta_D)\sin(\gamma)}{r_B^2 + r_D^2 + 2r_B r_D \cos(\delta_B + \delta_D)\cos(\gamma)}, \tag{130}$$

where the ratio of B decay amplitudes[16] is usually defined to be less than one,

$$r_B = \frac{\left|A\left(B^- \to \overline{D}^0 K^-\right)\right|}{\left|A\left(B^- \to D^0 K^-\right)\right|}, \tag{131}$$

and the ratio of D decay amplitudes is correspondingly defined by

$$r_D = \frac{\left|A\left(D^0 \to f\right)\right|}{\left|A\left(\overline{D}^0 \to f\right)\right|}. \tag{132}$$

The strong phase differences between the B and D decay amplitudes are given by δ_B and δ_D, respectively. The values of r_D and δ_D depend on the final state f: for the GLW analysis, $r_D = 1$ and δ_D is trivial (either zero or π), in the Dalitz plot analysis r_D and δ_D vary across the Dalitz plot, and depend on the D decay model used, for the ADS analysis, the values of r_D and δ_D are not trivial.

Note that, for given values of r_B and r_D, the maximum size of $\mathcal{A}$ (at $\sin(\delta_B + \delta_D) = 1$) is $2r_B r_D \sin(\gamma) / (r_B^2 + r_D^2)$. Thus even for D decay modes with small r_D, large asymmetries, and hence sensitivity to γ, may occur for B decay modes with similar values of r_B. For this reason, the ADS analysis of the decay $B^\mp \to D\pi^\mp$ is also of interest.

In the GLW analysis, the measured quantities are the partial rate asymmetry, and the charge averaged rate, which are measured both for *CP* even and *CP* odd D decays. For the latter, it is experimentally convenient to measure a double ratio,

$$R_{CP} = \frac{\Gamma\left(B^- \to D_{CP}K^-\right) / \Gamma\left(B^- \to D^0 K^-\right)}{\Gamma\left(B^- \to D_{CP}\pi^-\right) / \Gamma\left(B^- \to D^0 \pi^-\right)} \tag{133}$$

[16] Note that here we use the notation r_B to denote the ratio of B decay amplitudes, whereas in Sec. 4.2.5 we used, *e.g.*, $R_{D\pi}$, for a rather similar quantity. The reason is that here we need to be concerned also with D decay amplitudes, and so it is convenient to use the subscript to denote the decaying particle. Hopefully, using r in place of R will help reduce potential confusion.

Table 22: Summary of relations between measured and physical parameters in GLW, ADS and Dalitz analyses of $B \to D^{(*)}K^{(*)}$.

	GLW analysis
$R_{CP\pm}$	$1 + r_B^2 \pm 2r_B \cos(\delta_B)\cos(\gamma)$
$A_{CP\pm}$	$\pm 2r_B \sin(\delta_B)\sin(\gamma)/R_{CP\pm}$
	ADS analysis
$R_{\rm ADS}$	$r_B^2 + r_D^2 + 2r_B r_D \cos(\delta_B + \delta_D)\cos(\gamma)$
$A_{\rm ADS}$	$2r_B r_D \sin(\delta_B + \delta_D)\sin(\gamma)/R_{\rm ADS}$
	Dalitz analysis
$x_\pm$	$r_B \cos(\delta_B \pm \gamma)$
$y_\pm$	$r_B \sin(\delta_B \pm \gamma)$

that is normalized both to the rate for the favoured $D^0 \to K^-\pi^+$ decay, and to the equivalent quantities for $B^- \to D\pi^-$ decays (charge conjugate modes are implicitly included in Eq. (133)). In this way the constant of proportionality drops out of Eq. (129).

For the ADS analysis, using a suppressed $D \to f$ decay, the measured quantities are again the partial rate asymmetry, and the charge averaged rate. In this case it is sufficient to measure the rate in a single ratio (normalized to the favoured $D \to \overline{f}$ decay) since detection systematics cancel naturally; the observed quantity is then

$$R_{\rm ADS} = \frac{\Gamma\left(B^- \to [f]_D K^-\right)}{\Gamma\left(B^- \to \left[\overline{f}\right]_D K^-\right)}. \tag{134}$$

In the ADS analysis, there are an additional two unknowns (r_D and δ_D) compared to the GLW case. However, the value of r_D can be measured using decays of D mesons of known flavour.

In the Dalitz plot analysis, once a model is assumed for the D decay, which gives the values of r_D and δ_D across the Dalitz plot, it is possible to perform a simultaneous fit to the B^+ and B^- samples and directly extract γ, r_B and δ_B. However, the uncertainties on the phases depend inversely on r_B. Furthermore, r_B is positive definite (and small), and therefore tends to be overestimated, which can lead to an underestimation of the uncertainty. Some statistical treatment is necessary to correct for this bias. An alternative approach is to extract from the data the "Cartesian" variables

$$(x_\pm, y_\pm) = \left(\mathrm{Re}(r_B e^{i(\delta_B \pm \gamma)}), \mathrm{Im}(r_B e^{i(\delta_B \pm \gamma)})\right) = (r_B \cos(\delta_B \pm \gamma), r_B \sin(\delta_B \pm \gamma)). \tag{135}$$

These are (a) approximately statistically uncorrelated and (b) almost Gaussian. Use of these variables makes the combination of results much simpler.

The relations between the measured quantities and the underlying parameters are summarized in Table 22. Note carefully that the hadronic factors r_B and δ_B are different, in general, for each B decay mode.

4.3 Common inputs and error treatment

The common inputs used for rescaling are listed in Table 23. The B^0 lifetime ($\tau(B^0)$) and mixing parameter (Δm_d) averages are provided by the HFAG Lifetimes and Oscillations subgroup

Table 23: Common inputs used in calculating the averages.

$\tau(B^0)$ (ps)	1.527 ± 0.008
Δm_d (ps^{-1})	0.508 ± 0.004
$\lvert A_\perp \rvert^2$ ($J/\psi K^*$)	0.219 ± 0.009

(Sec. 3). The fraction of the perpendicularly polarized component ($|A_\perp|^2$) in $B \to J/\psi K^*(892)$ decays, which determines the *CP* composition, is averaged from results by *BABAR* [162] and Belle [163]. See also HFAG B to Charm Decay Parameters subgroup (Sec. 7).

At present, we only rescale to a common set of input parameters for modes with reasonably small statistical errors ($b \to c\bar{c}s$ transitions). Correlated systematic errors are taken into account in these modes as well. For all other modes, the effect of such a procedure is currently negligible.

As explained in Sec. 1, we do not apply a rescaling factor on the error of an average that has $\chi^2/\text{dof} > 1$ (unlike the procedure currently used by the PDG [4]). We provide a confidence level of the fit so that one can know the consistency of the measurements included in the average, and attach comments in case some care needs to be taken in the interpretation. Note that, in general, results obtained from data samples with low statistics will exhibit some non-Gaussian behaviour. We average measurements with asymmetric errors using the PDG [4] prescription. In cases where several measurements are correlated (*e.g.* S_f and C_f in measurements of time-dependent *CP* violation in B decays to a particular *CP* eigenstate) we take these into account in the averaging procedure if the uncertainties are sufficiently Gaussian. For measurements where one error is given, it represents the total error, where statistical and systematic uncertainties have been added in quadrature. If two errors are given, the first is statistical and the second systematic. If more than two errors are given, the origin of the additional uncertainty will be explained in the text.

4.4 Time-dependent asymmetries in $b \to c\bar{c}s$ transitions

4.4.1 Time-dependent *CP* asymmetries in $b \to c\bar{c}s$ decays to *CP* eigenstates

In the Standard Model, the time-dependent parameters for $b \to c\bar{c}s$ transitions are predicted to be: $S_{b\to c\bar{c}s} = -\eta \sin(2\beta)$, $C_{b\to c\bar{c}s} = 0$ to very good accuracy. The averages for $-\eta S_{b\to c\bar{c}s}$ and $C_{b\to c\bar{c}s}$ are provided in Table 24. The averages for $-\eta S_{b\to c\bar{c}s}$ are shown in Fig. 10.

Both *BABAR* and Belle have used the $\eta = -1$ modes $J/\psi K^0_S$, $\psi(2S)K^0_S$, $\chi_{c1}K^0_S$ and $\eta_c K^0_S$, as well as $J/\psi K^0_L$, which has $\eta = +1$ and $J/\psi K^{*0}(892)$, which is found to have η close to $+1$ based on the measurement of $|A_\perp|$ (see Sec. 4.3). ALEPH, OPAL and CDF use only the $J/\psi K^0_S$ final state. In the latest result from Belle, only $J/\psi K^0_S$ and $J/\psi K^0_L$ are used. In future updates, it is hoped to perform separate averages for each charmonium-kaon final state.

It should be noted that, while the uncertainty in the average for $-\eta S_{b\to c\bar{c}s}$ is still limited by statistics, that for $C_{b\to c\bar{c}s}$ is close to being dominated by systematics. This occurs due to the possible effect of tag side interference on the $C_{b\to c\bar{c}s}$ measurement, an effect which is correlated between the different experiments. Understanding of this effect may continue to improve in future, allowing the uncertainty to reduce.

Table 24: $S_{b\to c\bar{c}s}$ and $C_{b\to c\bar{c}s}$.

Experiment		$-\eta S_{b\to c\bar{c}s}$	$C_{b\to c\bar{c}s}$
BABAR	[164]	$0.710 \pm 0.034 \pm 0.019$	$0.070 \pm 0.028 \pm 0.018$
Belle	[165]	$0.642 \pm 0.031 \pm 0.017$	$-0.018 \pm 0.021 \pm 0.014$
***B* factory average**		0.674 ± 0.026	0.012 ± 0.022
Confidence level		0.18	0.02
ALEPH	[166]	$0.84\,^{+0.82}_{-1.04} \pm 0.16$	
OPAL	[167]	$3.2\,^{+1.8}_{-2.0} \pm 0.5$	
CDF	[168]	$0.79\,^{+0.41}_{-0.44}$	
Average		0.675 ± 0.026	0.012 ± 0.022

From the average for $-\eta S_{b\to c\bar{c}s}$ above, we obtain the following solutions for β (in $[0, \pi]$):

$$\beta = (21.2 \pm 1.0)^\circ \quad \text{or} \quad \beta = (68.8 \pm 1.0)^\circ \tag{136}$$

In radians, these values are $\beta = (0.37 \pm 0.02)$, $\beta = (1.20 \pm 0.02)$.

This result gives a precise constraint on the $(\overline{\rho}, \overline{\eta})$ plane, as shown in Fig. 10. The measurement is in remarkable agreement with other constraints from *CP* conserving quantities, and with *CP* violation in the kaon system, in the form of the parameter ϵ_K. Such comparisons have been performed by various phenomenological groups, such as CKMfitter [169] and UTFit [170].

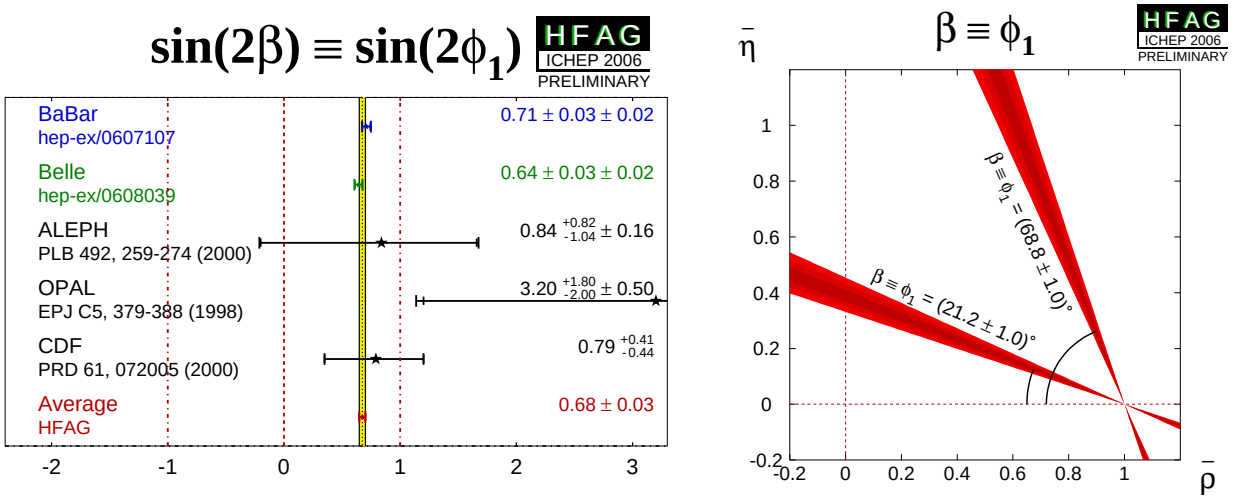

Figure 10: (Left) Average of measurements of $S_{b\to c\bar{c}s}$. (Right) Constraints on the $(\overline{\rho}, \overline{\eta})$ plane, obtained from the average of $-\eta S_{b\to c\bar{c}s}$ and Eq. 136.

4.4.2 Time-dependent transversity analysis of $B^0 \to J/\psi K^{*0}$

B meson decays to the vector-vector final state $J/\psi K^{*0}$ are also mediated by the $b \to c\bar{c}s$ transition. When a final state which is not flavour-specific ($K^{*0} \to K^0_S \pi^0$) is used, a time-dependent transversity analysis can be performed allowing sensitivity to both $\sin(2\beta)$ and

$\cos(2\beta)$ [171]. Such analyses have been performed by both B factory experiments. In principle, the strong phases between the transversity amplitudes are not uniquely determined by such an analysis, leading to a discrete ambiguity in the sign of $\cos(2\beta)$. The *BABAR* collaboration resolves this ambiguity using the known variation [172] of the P-wave phase (fast) relative to the S-wave phase (slow) with the invariant mass of the $K\pi$ system in the vicinity of the $K^*(892)$ resonance. The result is in agreement with the prediction from s quark helicity conservation, and corresponds to Solution II defined by Suzuki [173]. We use this phase convention for the averages given in Table 25.

Table 25: Averages from $B^0 \to J/\psi K^{*0}$ transversity analyses.

Experiment		$N(B\overline{B})$	$\sin 2\beta$	$\cos 2\beta$	Correlation
BABAR	[174]	88M	$-0.10 \pm 0.57 \pm 0.14$	$3.32^{+0.76}_{-0.96} \pm 0.27$	-0.37
Belle	[163]	275M	$0.24 \pm 0.31 \pm 0.05$	$0.56 \pm 0.79 \pm 0.11$	0.22
Average			0.16 ± 0.28	1.64 ± 0.62	-
Confidence level			0.61 (0.5σ)	0.03 (2.2σ)	

At present the results are dominated by large and non-Gaussian statistical errors, and exhibit significant correlations. We perform uncorrelated averages, the interpretation of which has to be done with the greatest care. Nonetheless, it is clear that $\cos(2\beta) > 0$ is preferred by the experimental data in $J/\psi K^*$. [*BABAR* [174] find a confidence level for $\cos(2\beta) > 0$ of 89%.]

4.4.3 Time-dependent *CP* asymmetries in $B^0 \to D^{*+}D^{*-}K^0_S$ decays

BABAR [176] have performed a time-dependent analysis of the $B^0 \to D^{*+}D^{*-}K^0_S$ decay, to obtain information on the sign of $\cos(2\beta)$. More information can be found in Sec. 4.2.4. The results are shown in Table 26.

Table 26: Results from time-dependent analysis of $B^0 \to D^{*+}D^{*-}K^0_S$.

Experiment		$N(B\overline{B})$	$\frac{J_c}{J_0}$	$\frac{2J_{s1}}{J_0}\sin(2\beta)$	$\frac{2J_{s2}}{J_0}\cos(2\beta)$
BABAR	[176]	230M	$0.76 \pm 0.18 \pm 0.07$	$0.10 \pm 0.24 \pm 0.06$	$0.38 \pm 0.24 \pm 0.05$

From the above result and the assumption that $J_{s2} > 0$, *BABAR* infer that $\cos(2\beta) > 0$ at the 94% confidence level.

4.4.4 Time-dependent analysis of $B^0_s \to J/\psi\phi$

As described in Sec. 4.2.6, an untagged time-dependent analysis of $B^0_s \to J/\psi\phi$ can probe the *CP* violating phase of B^0_s–$\overline{B}_s$ oscillations, ϕ_s. Within the Standard Model, this parameter is predicted to be small.

DØ [136] have performed such an analysis. They simultaneously measure the average B^0_s lifetime $\tau(B^0_s)$, $\Delta\Gamma$, ϕ_s, the magnitude of the perpendicularly polarized component $A_\perp$, the difference in the fractions of the two CP-even components $|A_0|^2 - |A|^2_\parallel$, and the strong phases

associated with the two CP-even components δ_0 and $\delta_\parallel$. The results are given in Table 27 below. See also Section 3.3.2.

Table 27: Results from time-dependent analysis of $B_s^0 \to J/\psi\phi$.

Experiment		$\tau(B_s^0)$	$\Delta\Gamma$	ϕ_s
DØ	[136]	$1.49 \pm 0.08\,^{+0.01}_{-0.03}$	$0.17 \pm 0.09 \pm 0.03$	$-0.79 \pm 0.56\,^{+0.14}_{-0.01}$

Experiment		$A_\perp$	$\lvert A_0\rvert^2 - \lvert A\rvert^2_\parallel$	$\delta_\parallel$	δ_0
DØ	[136]	$0.46 \pm 0.06 \pm 0.01$	$0.37 \pm 0.06 \pm 0.01$	$3.30 \pm 1.10 \pm 0.00$	$0.70 \pm 1.00 \pm 0.00$

Note the implicit convention above is that $|A_\perp|^2 + |A_0|^2 + |A_\parallel|^2 = 1$, and the strong phases are measured relative to that of the $A_\perp$ component (which is set to zero). The polarization components are defined at time $t = 0$, *i.e.* at the production (primary) vertex of the B_s^0. Note also that there is an ambiguity in the result for ϕ_s.

DØ [178] have combined the contour in the $(\phi_s, \Delta\Gamma)$ plane obtained above with a constraint obtained from the charge asymmetry in B_s^0–$\overline{B}_s$ oscillations (see also HFAG Lifetimes and Oscillations, Sec. 3) to obtain the result $\phi_s = -0.70\,^{+0.47}_{-0.39}$.

4.5 Time-dependent *CP* asymmetries in colour-suppressed $b \to c\overline{u}d$ transitions

Decays of B mesons to final states such as $D\pi^0$ are governed by $b \to c\overline{u}d$ transitions. If the final state is a CP eigenstate, *e.g.* $D_{CP}\pi^0$, the usual time-dependence formulae are recovered, with the sine coefficient sensitive to $\sin(2\beta)$. Since there is no penguin contribution to these decays, there is even less associated theoretical uncertainty than for $b \to c\overline{c}s$ decays like $B \to J/\psi\, K_S^0$. Such measurements therefore allow to test the Standard Model prediction that the CP violation parameters in $b \to c\overline{u}d$ transitions are the same as those in $b \to c\overline{c}s$ [179].

Note that there is an additional contribution from CKM suppressed $b \to u\overline{c}d$ decays. The effect of this contribution is small, and can be taken into account in the analysis [180].

When multibody D decays, such as $D \to K_S^0\pi^+\pi^-$ are used, a time-dependent analysis of the Dalitz plot of the neutral D decay allows a direct determination of the weak phase: 2β. (Equivalently, both $\sin(2\beta)$ and $\cos(2\beta)$ can be measured.) This information allows to resolve the ambiguity in the measurement of 2β from $\sin(2\beta)$ [181].

Results of such analyses are available from both Belle [182] and *BABAR* [183]. The decays $B \to D\pi^0$, $B \to D\eta$, $B \to D\omega$, $B \to D^*\pi^0$ and $B \to D^*\eta$ are used. [This collection of states is denoted by $D^{(*)}h^0$.] The daughter decays are $D^* \to D\pi^0$ and $D \to K_S^0\pi^+\pi^-$. The results are shown in Table 28, and Fig. 11. Note that *BABAR* quote uncertainties due to the D decay model separately from other systematic errors, while Belle do not.

Again, it is clear that the data prefer $\cos(2\beta) > 0$. Indeed, Belle [182] determine the sign of $\cos(2\phi_1)$ to be positive at 98.3% confidence level, while *BABAR* [183] favour the solution of β with $\cos(2\beta) > 0$ at 87% confidence level. Note, however, that the Belle measurement has strongly non-Gaussian behaviour. Therefore, we perform uncorrelated averages, from which any interpretation has to be done with the greatest care.

Table 28: Averages from $B^0 \to D^{(*)}h^0$ analyses.

Experiment	$N(B\overline{B})$	$\sin(2\beta)$	$\cos(2\beta)$	$\lvert\lambda\rvert$
BABAR [183]	311M	$0.45 \pm 0.36 \pm 0.05 \pm 0.07$	$0.54 \pm 0.54 \pm 0.08 \pm 0.18$	$0.975\,^{+0.093}_{-0.085} \pm 0.012 \pm 0.002$
Belle [182]	386M	$0.78 \pm 0.44 \pm 0.22$	$1.87\,^{+0.40}_{-0.53}\,^{+0.22}_{-0.32}$	
Average		0.57 ± 0.30	1.16 ± 0.42	
Confidence level		0.59 (0.5σ)	0.12 (1.6σ)	

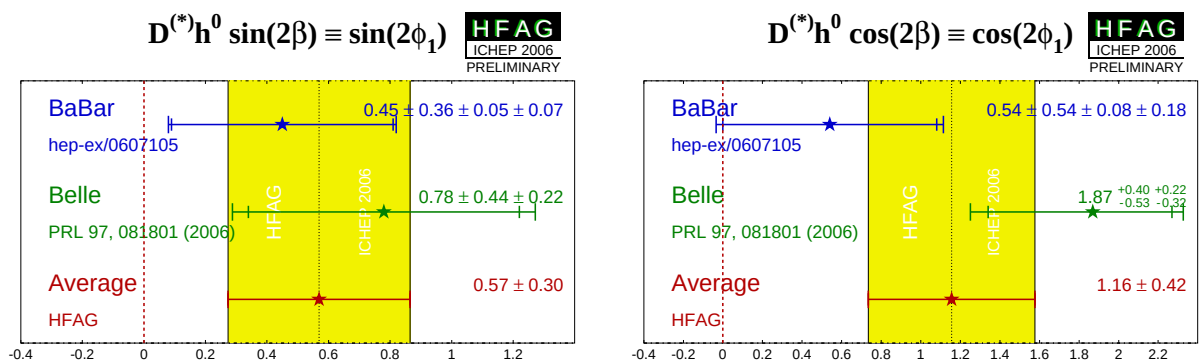

Figure 11: Averages of (left) $\sin(2\beta)$ and (right) $\cos(2\beta)$ measured in colour-suppressed $b \to c\overline{u}d$ transitions.

4.6 Time-dependent *CP* asymmetries in charmless $b \to q\overline{q}s$ transitions

The flavour changing neutral current $b \to s$ penguin can be mediated by any up-type quark in the loop, and hence the amplitude can be written as

$$\begin{aligned} A_{b\to s} &= F_u V_{ub} V_{us}^* + F_c V_{cb} V_{cs}^* + F_t V_{tb} V_{ts}^* \\ &= (F_u - F_c) V_{ub} V_{us}^* \quad + \quad (F_t - F_c) V_{tb} V_{ts}^* \\ &= \mathcal{O}(\lambda^4) \quad + \quad \mathcal{O}(\lambda^2) \end{aligned} \tag{137}$$

using the unitarity of the CKM matrix. Therefore, in the Standard Model, this amplitude is dominated by $V_{tb}V_{ts}^*$, and to within a few degrees ($\delta\beta \lesssim 2^\circ$ for $\beta \approx 20^\circ$) the time-dependent parameters can be written[17] $S_{b\to q\overline{q}s} \approx -\eta \sin(2\beta)$, $C_{b\to q\overline{q}s} \approx 0$, assuming $b \to s$ penguin contributions only ($q = u, d, s$).

Due to the large virtual mass scales occurring in the penguin loops, additional diagrams from physics beyond the Standard Model, with heavy particles in the loops, may contribute. In general, these contributions will affect the values of $S_{b\to q\overline{q}s}$ and $C_{b\to q\overline{q}s}$. A discrepancy between the values of $S_{b\to c\overline{c}s}$ and $S_{b\to q\overline{q}s}$ can therefore provide a clean indication of new physics.

[17] The presence of a small ($\mathcal{O}(\lambda^2)$) weak phase in the dominant amplitude of the s penguin decays introduces a phase shift given by $S_{b\to q\overline{q}s} = -\eta \sin(2\beta) \cdot (1 + \Delta)$. Using the CKMfitter results for the Wolfenstein parameters [169], one finds: $\Delta \simeq 0.033$, which corresponds to a shift of 2β of $+2.1$ degrees. Nonperturbative contributions can alter this result.

However, there is an additional consideration to take into account. The above argument assumes only the $b \to s$ penguin contributes to the $b \to q\overline{q}s$ transition. For $q = s$ this is a good assumption, which neglects only rescattering effects. However, for $q = u$ there is a colour-suppressed $b \to u$ tree diagram (of order $\mathcal{O}(\lambda^4)$), which has a different weak (and possibly strong) phase. In the case $q = d$, any light neutral meson that is formed from $d\overline{d}$ also has a $u\overline{u}$ component, and so again there is "tree pollution". The B^0 decays to $\pi^0 K^0_S$ and ωK^0_S belong to this category. The mesons f_0 and η' are expected to have predominant $s\overline{s}$ parts, which reduces the possible tree pollution. If the inclusive decay $B^0 \to K^+K^-K^0$ (excluding ϕK^0) is dominated by a non-resonant three-body transition, an OZI-rule suppressed tree-level diagram can occur through insertion of an $s\overline{s}$ pair. The corresponding penguin-type transition proceeds via insertion of a $u\overline{u}$ pair, which is expected to be favored over the $s\overline{s}$ insertion by fragmentation models. Neglecting rescattering, the final state $K^0\overline{K}^0K^0$ (reconstructed as $K^0_S K^0_S K^0_S$) has no tree pollution. Various estimates, using different theoretical approaches, of the values of $\Delta S = S_{b\to q\overline{q}s} - S_{b\to c\overline{c}s}$ exist in the literature [184]. In general, there is agreement that the modes ϕK^0, $\eta' K^0$ and $K^0\overline{K}^0K^0$ are the cleanest, with values of $|\Delta S|$ at or below the few percent level (ΔS is usually positive).

4.6.1 Time-dependent *CP* asymmetries in charmless $b \to q\overline{q}s$ decays to *CP* eigenstates

The averages for $-\eta S_{b\to q\overline{q}s}$ and $C_{b\to q\overline{q}s}$ can be found in Table 29, and are shown in Fig. 12 and Fig. 13. Results from both *BABAR* and Belle are averaged for the modes ϕK^0, $\eta' K^0$, $f_0 K^0$ and $K^+K^-K^0$ (K^0 indicates that both K^0_S and K^0_L are used, although Belle use neither $f_0 K^0_L$ nor $K^+K^-K^0_L$), $\pi^0 K^0_S$, ωK^0_S and $K^0_S K^0_S K^0_S$. *BABAR* also has results using $\pi^0\pi^0 K^0_S$ and $\rho^0 K^0_S$. Of these modes, ϕK^0_S, $\eta' K^0_S$, $\pi^0 K^0_S$, ωK^0_S and $\rho^0 K^0_S$ have *CP* eigenvalue $\eta = -1$, while ϕK^0_L, $\eta' K^0_L$, $f_0 K^0_S$, $\pi^0\pi^0 K^0_S$ and $K^0_S K^0_S K^0_S$ have $\eta = +1$.

The final state $K^+K^-K^0$ (contributions from ϕK^0 are implicitly excluded) is not a *CP* eigenstate. However, the *CP* composition can be determined using either an isospin argument (used by Belle to determine a *CP* even fraction of $0.93 \pm 0.09 \pm 0.05$ [189]) or a moments analysis (used by *BABAR* to find *CP* even fractions of $0.89 \pm 0.08 \pm 0.06$ in $K^+K^-K^0_S$ [185] and $0.92 \pm 0.07 \pm 0.06$ in $K^+K^-K^0_L$ [194]). The uncertainty in the *CP* even fraction leads to an asymmetric error on $S_{b\to q\overline{q}s}$, which is taken to be correlated among the experiments. To combine, we rescale the results to the average *CP* even fraction of 0.91 ± 0.07.

BABAR have performed a time-dependent Dalitz plot analysis of $B^0 \to K^+K^-K^0$ (see subsection 4.6.2). Their results for ϕK^0 are determined from that analysis. Their results for $f^0 K^0$ are a combination of results from the Dalitz plot analysis ($-\eta S_{b\to q\overline{q}s} = 0.31 \pm 0.32 \pm 0.07$, $C_{b\to q\overline{q}s} = -0.45 \pm 0.28 \pm 0.10$ [195]), with those from the quasi-two-body analysis of $B^0 \to f^0 K^0_S$, $f^0 \to \pi^+\pi^-$ ($-\eta S_{b\to q\overline{q}s} = 0.95\,^{+0.23}_{-0.32} \pm 0.10$, $C_{b\to q\overline{q}s} = -0.24 \pm 0.31 \pm 0.15$ [192]). The *BABAR* results for $K^+K^-K^0$ are taken from their previous quasi-two-body analysis [194]. Note that for both *BABAR* and Belle results for $K^+K^-K^0$, uncertainty in the *CP* composition of the final state leads to a third source of uncertainty on the results for $-\eta S_{K^+K^-K^0}$.

As explained above, each of the modes listed in Table 29 has different uncertainties within the Standard Model, and so each may have a different value of $-\eta S_{b\to q\overline{q}s}$. Therefore, there is no strong motivation to make a combined average over the different modes. We refer to such an average as a "naïve s-penguin average." It is naïve not only because of the neglect of the theoretical uncertainty, but also since possible correlations of systematic effects between

Table 29: Averages of $-\eta S_{b\to q\bar{q}s}$ and $C_{b\to q\bar{q}s}$.

Experiment		$N(B\overline{B})$	$-\eta S_{b\to q\bar{q}s}$	$C_{b\to q\bar{q}s}$	Correlation
			ϕK^0		
BABAR	[195]	347M	$0.12 \pm 0.31 \pm 0.10$	$0.18 \pm 0.20 \pm 0.10$	-
Belle	[165]	535M	$0.50 \pm 0.21 \pm 0.06$	$-0.07 \pm 0.15 \pm 0.05$	0.05
Average			0.39 ± 0.18	0.01 ± 0.13	0.03
Confidence level			$\chi^2 = 1.8/2$ dof (CL=0.41 $\to 0.8\sigma$)		
			$\eta' K^0$		
BABAR	[186]	384M	$0.58 \pm 0.10 \pm 0.03$	$-0.16 \pm 0.07 \pm 0.03$	0.03
Belle	[165]	535M	$0.64 \pm 0.10 \pm 0.04$	$0.01 \pm 0.07 \pm 0.05$	0.09
Average			0.61 ± 0.07	-0.09 ± 0.06	0.04
Confidence level			$\chi^2 = 2.3/2$ dof (CL=0.32 $\to 1.0\sigma$)		
			$K^0_S K^0_S K^0_S$		
BABAR	[187]	347M	$0.66 \pm 0.26 \pm 0.08$	$-0.14 \pm 0.22 \pm 0.05$	0.09
Belle	[165]	535M	$0.30 \pm 0.32 \pm 0.08$	$-0.31 \pm 0.20 \pm 0.07$	-
Average			0.51 ± 0.21	-0.23 ± 0.15	0.04
Confidence level			$\chi^2 = 1.0/2$ dof (CL=0.61 $\to 0.5\sigma$)		
			$\pi^0 K^0_S$		
BABAR	[188]	348M	$0.33 \pm 0.26 \pm 0.04$	$0.20 \pm 0.16 \pm 0.03$	-0.06
Belle	[189]	532M	$0.33 \pm 0.35 \pm 0.08$	$0.05 \pm 0.14 \pm 0.05$	-0.08
Average			0.33 ± 0.21	0.12 ± 0.11	-0.06
Confidence level			$\chi^2 = 0.5/2$ dof (CL=0.79 $\to 0.3\sigma$)		
			$\rho^0 K^0_S$		
BABAR	[190]	227M	$0.20 \pm 0.52 \pm 0.24$	$0.64 \pm 0.41 \pm 0.20$	-
Average			0.20 ± 0.57	0.64 ± 0.46	-
			ωK^0_S		
BABAR	[191]	347M	$0.62^{+0.25}_{-0.30} \pm 0.02$	$-0.43^{+0.25}_{-0.23} \pm 0.03$	-
Belle	[189]	532M	$0.11 \pm 0.46 \pm 0.07$	$0.09 \pm 0.29 \pm 0.06$	-0.04
Average			0.48 ± 0.24	-0.21 ± 0.19	-
Confidence level			$\chi^2 = 0.9$ (CL=0.35 $\to 0.9\sigma$)	$\chi^2 = 1.8$ (CL=0.18 $\to 1.3\sigma$)	
			$f_0 K^0$		
BABAR	[192, 195]	–	0.62 ± 0.23	-0.36 ± 0.23	-
Belle	[189]	532M	$0.18 \pm 0.23 \pm 0.11$	$0.15 \pm 0.15 \pm 0.07$	-0.01
Average			0.42 ± 0.17	-0.02 ± 0.13	-0.00
Confidence level			$\chi^2 = 4.9/2$ dof (CL=0.09 $\to 1.7\sigma$)		
			$\pi^0\pi^0 K^0_S$		
BABAR	[193]	227M	$-0.84 \pm 0.71 \pm 0.08$	$0.27 \pm 0.52 \pm 0.13$	-
Average			-0.84 ± 0.71	0.27 ± 0.54	-
			$K^+K^-K^0$		
BABAR Q2B	[194]	227M	$0.41 \pm 0.18 \pm 0.07 \pm 0.11$	$0.23 \pm 0.12 \pm 0.07$	-
Belle	[189]	532M	$0.68 \pm 0.15 \pm 0.03^{+0.21}_{-0.13}$	$0.09 \pm 0.10 \pm 0.05$	-0.00
Average			0.58 ± 0.13	0.15 ± 0.09	-
Confidence level			$\chi^2 = 1.6$ (CL=0.21)	$\chi^2 = 0.6$ (CL=0.43)	

different modes are neglected. In spite of these caveats, there remains substantial interest in the value of this quantity, and therefore it is given here: $\langle -\eta S_{b\to q\overline{q}s}\rangle = 0.53 \pm 0.05$, with confidence level 0.59 (0.5σ). Again treating the uncertainties as Gaussian and neglecting correlations, this value is found to be 2.6σ below the average $-\eta S_{b\to c\overline{c}s}$ given in Sec. 4.4.1. (The average for $C_{b\to q\overline{q}s}$ is $\langle C_{b\to q\overline{q}s}\rangle = -0.01 \pm 0.04$ with confidence level 0.13 (1.5σ)). However, we do not advocate the use of these averages, and we emphasise that the values should be treated with *extreme caution*, if at all. What is unambiguous (although only qualitative) is that there is a trend that the values of $-\eta S_{b\to q\overline{q}s}$ in different modes are below the average for $-\eta S_{b\to c\overline{c}s}$.

From Table 29 it may be noted that the average for $-\eta S_{b\to q\overline{q}s}$ in $\eta' K^0$ (0.61 ± 0.07), is now more than 5σ away from zero, so that *CP* violation in this mode is well established. Amongst other modes, *CP* violation in both $f_0 K^0_S$ and $K^+K^-K^0$ is near the 3σ level, although due to possible non-Gaussian errors in these results it may be prudent to defer any strong conclusion on these modes. There is no evidence (above 2σ) for direct *CP* violation in any $b \to q\overline{q}s$ mode.

4.6.2 Time-dependent Dalitz plot analysis of $B^0 \to K^+K^-K^0$ decays

As mentioned in Sec. 4.2.4, *BABAR* have performed a time-dependent Dalitz plot analysis of the $B^0 \to K^+K^-K^0$ decay [195]. The results are summarized in Tab. 30. They are presented in terms of the effective weak phase (from mixing and decay) difference $\beta^{\rm eff}$ and the direct *CP* violation parameter $\mathcal{A}$ ($\mathcal{A} = -C$) for each of the resonant contributions ϕK^0 and $f_0 K^0$, together with averaged values of those parameters (taking *CP* properties into account) over the entire Dalitz plot.

Table 30: Results from time-dependent Dalitz plot analysis of the $B^0 \to K^+K^-K^0$ decay.

Experiment	$N(B\overline{B})$	ϕK^0		$f_0 K^0$	
		$\beta^{\rm eff}$	$\mathcal{A}$	$\beta^{\rm eff}$	$\mathcal{A}$
BABAR [195]	347M	$0.06 \pm 0.16 \pm 0.05$	$-0.18 \pm 0.20 \pm 0.10$	$0.18 \pm 0.19 \pm 0.04$	$0.45 \pm 0.28 \pm 0.10$

Experiment	$N(B\overline{B})$	$K^+K^-K^0$	
		$\beta^{\rm eff}$	$\mathcal{A}$
BABAR [195]	347M	$0.361 \pm 0.079 \pm 0.037$	$-0.034 \pm 0.079 \pm 0.025$

From the above results *BABAR* infer that the trigonometric reflection at $\pi/2 - \beta^{\rm eff}$, which is inconsistent with the Standard Model expectation, is disfavoured at 4.6σ.

4.7 Time-dependent *CP* asymmetries in $b \to c\overline{c}d$ transitions

The transition $b \to c\overline{c}d$ can occur via either a $b \to c$ tree or a $b \to d$ penguin amplitude. Similarly to Eq. (137), the amplitude for the $b \to d$ penguin can be written

$$\begin{aligned} A_{b\to d} &= F_u V_{ub} V_{ud}^* + F_c V_{cb} V_{cd}^* + F_t V_{tb} V_{td}^* \\ &= (F_u - F_c) V_{ub} V_{ud}^* \;+\; (F_t - F_c) V_{tb} V_{td}^* \\ &= \mathcal{O}(\lambda^3) \;+\; \mathcal{O}(\lambda^3). \end{aligned} \tag{138}$$

From this it can be seen that the $b \to d$ penguin amplitude contains terms with different weak phases at the same order of CKM suppression.

In the above, we have followed Eq. (137) by eliminating the F_c term using unitarity. However, we could equally well write

$$\begin{aligned} A_{b\to d} &= (F_u - F_t)V_{ub}V_{ud}^* + (F_c - F_t)V_{cb}V_{cd}^*, \\ &= (F_c - F_u)V_{cb}V_{cd}^* + (F_t - F_u)V_{tb}V_{td}^*. \end{aligned} \tag{139}$$

Since the $b \to c\bar{c}d$ tree amplitude has the weak phase of $V_{cb}V_{cd}^*$, either of the above expressions allow the penguin to be decomposed into parts with weak phases the same and different to the tree amplitude (the relative weak phase can be chosen to be either β or γ). However, if the tree amplitude dominates, there is little sensitivity to any phase other than that from B^0–$\overline{B}^0$ mixing.

The $b \to c\bar{c}d$ transitions can be investigated with studies of various different final states. Results are available from both *BABAR* and Belle using the final states $J/\psi\pi^0$, D^+D^-, $D^{*+}D^{*-}$ and $D^{*\pm}D^{\mp}$, the averages of these results are given in Table 31. The results using the *CP* eigenstate ($\eta = +1$) modes $J/\psi\pi^0$ and D^+D^- are shown in Fig. 14 and Fig. 15 respectively.

The vector-vector mode $D^{*+}D^{*-}$ is found to be dominated by the *CP* even longitudinally polarized component; *BABAR* measures a *CP* odd fraction of $0.125 \pm 0.044 \pm 0.007$ [202] while Belle measures a *CP* odd fraction of $0.19 \pm 0.08 \pm 0.01$ [203] (here we do not average these fractions and rescale the inputs, however the average is almost independent of the treatment). We treat the uncertainty due to the error in the *CP*-odd fractions (quoted as a third uncertainty) as a correlated systematic error. Results using $D^{*+}D^{*-}$ are shown in Fig. 16.

For the non-*CP* eigenstate mode $D^{*\pm}D^{\mp}$ *BABAR* uses fully reconstructed events while Belle combines both fully and partially reconstructed samples. The most recent results from *BABAR* do not include a measurement of the overall asymmetry $\mathcal{A}$. At present we perform uncorrelated averages of the parameters in the $D^{*\pm}D^{\mp}$ system, using only the information from Belle on $\mathcal{A}$.

In the absence of the penguin contribution (tree dominance), the time-dependent parameters would be given by $S_{b\to c\bar{c}d} = -\eta\sin(2\beta)$, $C_{b\to c\bar{c}d} = 0$, $S_{+-} = \sin(2\beta + \delta)$, $S_{-+} = \sin(2\beta - \delta)$, $C_{+-} = -C_{-+}$ and $\mathcal{A} = 0$, where δ is the strong phase difference between the $D^{*+}D^-$ and $D^{*-}D^+$ decay amplitudes. In the presence of the penguin contribution, there is no clean interpretation in terms of CKM parameters, however direct *CP* violation may be observed as any of $C_{b\to c\bar{c}d} \neq 0$, $C_{+-} \neq -C_{-+}$ or $A_{+-} \neq 0$.

The averages for the $b \to c\bar{c}d$ modes are shown in Fig. 17. Results are consistent with tree dominance, and with the Standard Model, though the Belle results in $B^0 \to D^+D^-$ [201] show an indication of direct *CP* violation, and hence a non-zero penguin contribution. The average of $S_{b\to c\bar{c}d}$ in the $D^{*+}D^{*-}$ final state is about 3σ from zero; however, due to the large uncertainty and possible non-Gaussian effects, any strong conclusion should be deferred.

4.8 Time-dependent *CP* asymmetries in $b \to q\bar{q}d$ transitions

Decays such as $B^0 \to K_S^0K_S^0$ are pure $b \to q\bar{q}d$ penguin transitions. As shown in Eq. 138, this diagram has different contributing weak phases, and therefore the observables are sensitive to the difference (which can be chosen to be either β or γ). Note that if the contribution with the top quark in the loop dominates, the weak phase from the decay amplitudes should cancel that from mixing, so that no *CP* violation (neither mixing-induced nor direct) occurs. Non-zero contributions from loops with intermediate up and charm quarks can result in both types of effect (as usual, a strong phase difference is required for direct *CP* violation to occur).

Table 31: Averages for the $b \to c\bar{c}d$ modes, $B^0 \to J/\psi\pi^0$, D^+D^-, $D^{*+}D^{*-}$ and $D^{*\pm}D^{\mp}$.

Experiment	$N(B\overline{B})$	S_{CP}	C_{CP}	Correlation
		$J/\psi\pi^0$		
BABAR [198]	232M	$-0.68 \pm 0.30 \pm 0.04$	$-0.21 \pm 0.26 \pm 0.06$	0.08
Belle [199]	152M	$-0.72 \pm 0.42 \pm 0.09$	$0.01 \pm 0.29 \pm 0.03$	-0.12
Average		-0.68 ± 0.25	-0.11 ± 0.20	0.00
Confidence level		$\chi^2 = 0.3/2$ dof (CL=0.86 $\to 0.2\sigma$)		
		D^+D^-		
BABAR [200]	232M	$-0.29 \pm 0.63 \pm 0.06$	$0.11 \pm 0.35 \pm 0.06$	-
Belle [201]	535M	$-1.12 \pm 0.37 \pm 0.09$	$-0.92 \pm 0.23 \pm 0.05$	0.04
Average		-0.89 ± 0.33	-0.60 ± 0.20	0.03
Confidence level		$\chi^2 = 7.1/2$ dof (CL=0.03 $\to 2.2\sigma$)		
		$D^{*+}D^{*-}$		
BABAR [202]	227M	$-0.75 \pm 0.25 \pm 0.03$	$0.06 \pm 0.17 \pm 0.03$	0.04
Belle [203]	152M	$-0.75 \pm 0.56 \pm 0.10 \pm 0.06$	$0.26 \pm 0.26 \pm 0.05 \pm 0.01$	-
Average		-0.75 ± 0.23	0.12 ± 0.14	0.03
Confidence level		$\chi^2 = 0.4/2$ dof (CL=0.82 $\to 0.2\sigma$)		

Experiment	$N(B\overline{B})$	S_{+-}	C_{+-}	S_{-+}	C_{-+}	$\mathcal{A}$
			$D^{*\pm}D^{\mp}$			
BABAR [200]	232M	$-0.54 \pm 0.35 \pm 0.07$	$0.09 \pm 0.25 \pm 0.06$	$-0.29 \pm 0.33 \pm 0.07$	$0.17 \pm 0.24 \pm 0.04$	
Belle [204]	152M	$-0.55 \pm 0.39 \pm 0.12$	$-0.37 \pm 0.22 \pm 0.06$	$-0.96 \pm 0.43 \pm 0.12$	$0.23 \pm 0.25 \pm 0.06$	$0.07 \pm 0.08 \pm 0.04$
Average		-0.54 ± 0.27	-0.17 ± 0.17	-0.53 ± 0.27	0.20 ± 0.18	0.07 ± 0.09
Confidence level		CL=0.99 (0.0σ)	CL=0.18 (1.3σ)	CL=0.23 (1.2σ)	CL=0.87 (0.2σ)	

Table 32: Results for $B^0 \to K^0_S K^0_S$.

Experiment	$N(B\overline{B})$	S_{CP}	C_{CP}	Correlation
BABAR [205]	350M	$-1.28\,^{+0.80}_{-0.73}\,^{+0.11}_{-0.16}$	$-0.40 \pm 0.41 \pm 0.06$	-0.32

BABAR [205] have performed a time-dependent analysis of $B^0 \to K^0_S K^0_S$. The results are shown in Table 32.

4.9 Time-dependent asymmetries in $b \to s\gamma$ transitions

The radiative decays $b \to s\gamma$ produce photons which are highly polarized in the Standard Model. The decays $B^0 \to F\gamma$ and $\overline{B}^0 \to F\gamma$ produce photons with opposite helicities, and since the polarization is, in principle, observable, these final states cannot interfere. The finite mass of the s quark introduces small corrections to the limit of maximum polarization, but any large mixing induced *CP* violation would be a signal for new physics. Since a single weak phase dominates the $b \to s\gamma$ transition in the Standard Model, the cosine term is also expected to be small.

Atwood *et al.* [207] have shown that an inclusive analysis with respect to $K^0_S\pi^0\gamma$ can be performed, since the properties of the decay amplitudes are independent of the angular mo-

Table 33: Averages for $b \to s\gamma$ modes.

Experiment		$N(B\overline{B})$	$S_{CP}(b \to s\gamma)$	$C_{CP}(b \to s\gamma)$	Correlation
			$K^*(892)\gamma$		
BABAR	[209]	232M	$-0.21 \pm 0.40 \pm 0.05$	$-0.40 \pm 0.23 \pm 0.04$	0.07
Belle	[210]	532M	$-0.32^{+0.36}_{-0.33} \pm 0.05$	$0.20 \pm 0.24 \pm 0.05$	0.08
Average			-0.28 ± 0.26	-0.11 ± 0.17	0.07
Confidence level			$\chi^2 = 3.2/2$ dof (CL=0.20 $\to 1.3\sigma$)		
			$K^0_S\pi^0\gamma$ (including $K^*(892)\gamma$)		
BABAR	[209]	232M	-0.06 ± 0.37	-0.48 ± 0.22	0.05
Belle	[210]	532M	$-0.10 \pm 0.31 \pm 0.07$	$0.20 \pm 0.20 \pm 0.06$	0.08
Average			-0.09 ± 0.24	-0.12 ± 0.15	0.06
Confidence level			$\chi^2 = 5.1/2$ dof (CL=0.08 $\to 1.8\sigma$)		

mentum of the $K^0_S\pi^0$ system. However, if non-dipole operators contribute significantly to the amplitudes, then the Standard Model mixing-induced *CP* violation could be larger than the naïve expectation $S \simeq -2(m_s/m_b)\sin(2\beta)$ [208]. In this case, the *CP* parameters may vary over the $K^0_S\pi^0\gamma$ Dalitz plot, for example as a function of the $K^0_S\pi^0$ invariant mass.

With the above in mind, we quote two averages: one for $K^*(892)$ candidates only, and the other one for the inclusive $K^0_S\pi^0\gamma$ decay (including the $K^*(892)$). If the Standard Model dipole operator is dominant, both should give the same quantities (the latter naturally with smaller statistical error). If not, care needs to be taken in interpretation of the inclusive parameters, while the results on the $K^*(892)$ resonance remain relatively clean. Results from *BABAR* and Belle are used for both averages; both experiments use the invariant mass range $0.60\ \mathrm{GeV}/c^2 < M_{K^0_S\pi^0} < 1.80\ \mathrm{GeV}/c^2$ in the inclusive analysis.

The results are shown in Table 33, and in Fig. 18. No significant *CP* violation results are seen; the results are consistent with the Standard Model and with other measurements in the $b \to s\gamma$ system (see Sec. 6).

4.10 Time-dependent *CP* asymmetries in $b \to u\overline{u}d$ transitions

The $b \to u\overline{u}d$ transition can be mediated by either a $b \to u$ tree amplitude or a $b \to d$ penguin amplitude. These transitions can be investigated using the time dependence of B^0 decays to final states containing light mesons. Results are available from both *BABAR* and Belle for the *CP* eigenstate ($\eta = +1$) $\pi^+\pi^-$ final state and for the vector-vector final state $\rho^+\rho^-$, which is found to be dominated by the *CP* even longitudinally polarized component (*BABAR* measure $f_{\rm long} = 0.977 \pm 0.024\,^{+0.015}_{-0.013}$ [215] while Belle measure $f_{\rm long} = 0.941\,^{+0.034}_{-0.040} \pm 0.030$ [216]). *BABAR* have also performed a time-dependent analysis of the $B^0 \to a_1^\pm\pi^\mp$ decay [221]. These results, and averages, are listed in Table 34. The averages for $\pi^+\pi^-$ are shown in Fig. 19, and those for $\rho^+\rho^-$ are shown in Fig. 20.

If the penguin contribution is negligible, the time-dependent parameters for $B^0 \to \pi^+\pi^-$ and $B^0 \to \rho^+\rho^-$ are given by $S_{b\to u\overline{u}d} = \eta\sin(2\alpha)$ and $C_{b\to u\overline{u}d} = 0$. In the presence of the penguin contribution, direct *CP* violation may arise, and there is no straightforward interpretation of $S_{b\to u\overline{u}d}$ and $C_{b\to u\overline{u}d}$. An isospin analysis [224] can be used to disentangle the contributions and extract α.

Table 34: Averages for $b \to u\overline{u}d$ modes.

Experiment		$N(B\overline{B})$	S_{CP}	C_{CP}	Correlation
			$\pi^+\pi^-$		
BABAR	[213]	350M	$-0.53 \pm 0.14 \pm 0.02$	$-0.16 \pm 0.11 \pm 0.03$	-0.08
Belle	[214]	532M	$-0.61 \pm 0.10 \pm 0.04$	$-0.55 \pm 0.08 \pm 0.05$	-0.15
Average			-0.59 ± 0.09	-0.39 ± 0.07	-0.10
Confidence level			$\chi^2 = 7.4/2$ dof (CL=0.02 $\to 2.3\sigma$)		
			$\rho^+\rho^-$		
BABAR	[215]	350M	$-0.19 \pm 0.21^{+0.05}_{-0.07}$	$-0.07 \pm 0.15 \pm 0.06$	-0.06
Belle	[216]	535M	$0.19 \pm 0.30 \pm 0.07$	$-0.16 \pm 0.21 \pm 0.07$	0.10
Average			-0.06 ± 0.18	-0.11 ± 0.13	-0.00
Confidence level			$\chi^2 = 1.2/2$ dof (CL=0.56 $\to 0.6\sigma$)		

Experiment		$N(B\overline{B})$	A_{CP}	C	S	ΔC	ΔS
				$a_1^\pm\pi^\mp$			
BABAR	[221]	384M	$-0.07 \pm 0.07 \pm 0.02$	$-0.10 \pm 0.15 \pm 0.09$	$0.37 \pm 0.21 \pm 0.07$	$0.26 \pm 0.15 \pm 0.07$	$-0.14 \pm 0.21 \pm 0.06$

Table 35: Averages of quasi-two-body parameters extracted from time-dependent Dalitz plot analysis of $B^0 \to \pi^+\pi^-\pi^0$.

Experiment		$N(B\overline{B})$	$\mathcal{A}_{CP}^{\rho\pi}$	$C_{\rho\pi}$	$S_{\rho\pi}$	$\Delta C_{\rho\pi}$	$\Delta S_{\rho\pi}$
BABAR	[219]	347M	$-0.14 \pm 0.04 \pm 0.01$	$0.15 \pm 0.09 \pm 0.04$	$0.01 \pm 0.12 \pm 0.03$	$0.38 \pm 0.09 \pm 0.02$	$0.06 \pm 0.13 \pm 0.03$
Belle	[220]	447M	$-0.12 \pm 0.05 \pm 0.03$	$-0.13 \pm 0.09 \pm 0.06$	$0.06 \pm 0.13 \pm 0.07$	$0.35 \pm 0.10 \pm 0.06$	$-0.12 \pm 0.14 \pm 0.07$
Average			-0.13 ± 0.03	0.03 ± 0.07	0.03 ± 0.09	0.36 ± 0.07	-0.02 ± 0.10
Confidence level			$\chi^2 = 4.7/5$ dof (CL=0.45 $\to 0.8\sigma$)				

Experiment		$N(B\overline{B})$	$\mathcal{A}_{\rho\pi}^{-+}$	$\mathcal{A}_{\rho\pi}^{+-}$	Correlation
BABAR	[219]	347M	$-0.38^{+0.15}_{-0.16} \pm 0.07$	$0.03 \pm 0.07 \pm 0.03$	0.62
Belle	[220]	447M	$0.08 \pm 0.17 \pm 0.12$	$0.22 \pm 0.08 \pm 0.05$	0.53
Average			-0.19 ± 0.13	0.11 ± 0.06	0.46
Confidence level			$\chi^2 = 3.8/2$ dof (CL=0.15 $\to 1.4\sigma$)		

Experiment		$N(B\overline{B})$	$C_{\rho^0\pi^0}$	$S_{\rho^0\pi^0}$	Correlation
Belle	[220]	447M	$0.45 \pm 0.35 \pm 0.32$	$0.15 \pm 0.57 \pm 0.43$	0.07

For the non-*CP* eigenstate $\rho^\pm\pi^\mp$, both *BABAR* [219] and Belle [220] have performed time-dependent Dalitz plot (DP) analyses of the $\pi^+\pi^-\pi^0$ final state [211]; such analyses allow direct measurements of the phases. Both experiments have measured the U and I parameters discussed in Sec. 4.2.4 and defined in Table 19. We have performed a full correlated average of these parameters, the results of which are summarized in Fig. 21.

Both experiments have also extracted the Q2B parameters. We have performed a full correlated average of these parameters, which is equivalent to determining the values from the averaged U and I parameters. The results are shown in Table. 35. Note that only Belle has extracted the Q2B *CP* violation parameters for $B^0 \to \rho^0\pi^0$.

With the notation described in Sec. 4.2 (Eq. (116)), the time-dependent parameters for the Q2B $B^0 \to \rho^\pm\pi^\mp$ analysis are, neglecting penguin contributions, given by

$$S_{\rho\pi} = \sqrt{1-\left(\frac{\Delta C}{2}\right)^2}\sin(2\alpha)\cos(\delta)\ , \quad \Delta S_{\rho\pi} = \sqrt{1-\left(\frac{\Delta C}{2}\right)^2}\cos(2\alpha)\sin(\delta) \tag{140}$$

and $C_{\rho\pi} = \mathcal{A}_{CP}^{\rho\pi} = 0$, where $\delta = \arg(A_{-+}A_{+-}^*)$ is the strong phase difference between the $\rho^-\pi^+$ and $\rho^+\pi^-$ decay amplitudes. In the presence of the penguin contribution, there is no straightforward interpretation of the Q2B observables in the $B^0 \to \rho^\pm\pi^\mp$ system in terms of CKM parameters. However direct *CP* violation may arise, resulting in either or both of $C_{\rho\pi} \neq 0$ and $\mathcal{A}_{CP}^{\rho\pi} \neq 0$. Equivalently, direct *CP* violation may be seen by either of the decay-type-specific observables $\mathcal{A}_{\rho\pi}^{+-}$ and $\mathcal{A}_{\rho\pi}^{-+}$, defined in Eq. (117), deviating from zero. Results and averages for these parameters are also given in Table 35. Averages of the direct *CP* violation effect in $B^0 \to \rho^\pm\pi^\mp$ are shown in Fig. 22, both in $\mathcal{A}_{CP}^{\rho\pi}$ *vs.* $C_{\rho\pi}$ space and in $\mathcal{A}_{\rho\pi}^{-+}$ *vs.* $\mathcal{A}_{\rho\pi}^{+-}$ space.

Some difference is seen between the *BABAR* and Belle measurements in the $\pi^+\pi^-$ system. The confidence level of the average is 0.024, which corresponds to a 2.3σ discrepancy. Since there is no evidence of systematic problems in either analysis, we do not rescale the errors of the averages. The averages for $S_{b\to u\overline{u}d}$ and $C_{b\to u\overline{u}d}$ in $B^0 \to \pi^+\pi^-$ are both more than 5σ away from zero, suggesting that both mixing-induced and direct *CP* violation are well-established in this channel. Nonetheless, due to the possible discrepancy mentioned above, only a cautious interpretation should be made on the significance of direct *CP* violation.

In $B^0 \to \rho^\pm\pi^\mp$, however, both experiments see an indication of direct *CP* violation in the $\mathcal{A}_{CP}^{\rho\pi}$ parameter (as seen in Fig. 22). The average is more than 3σ from zero, providing evidence of direct *CP* violation in this channel.

Constraints on α

The precision of the measured *CP* violation parameters in $b \to u\overline{u}d$ transitions allows constraints to be set on the UT angle α. In addition to the value of α from the *BABAR* time-dependent DP analysis, given in Table 34, constraints have been obtained with various methods:

- Both *BABAR* [213] and Belle [214] have performed isospin analyses in the $\pi\pi$ system. Belle exclude $9^\circ < \phi_2 < 81^\circ$ at the 95.4% C.L. while *BABAR* give a confidence level interpretation for α. In both cases, only solutions in 0°–180° are considered.

- Both experiments have also performed isospin analyses in the $\rho\rho$ system. *BABAR* [215] find $\alpha \in [74, 117]^\circ$ at 68% C.L. while Belle [216] obtain $\phi_2 = (88 \pm 17)^\circ$ or $59^\circ < \phi_2 < 117^\circ$ at 90% confidence level. The largest contribution to the uncertainty is due to the possible penguin contribution, limited by the knowledge of the $B^0 \to \rho^0\rho^0$ branching fraction [223], and is correlated between the measurements.

- The time-dependent Dalitz plot analysis of the $B^0 \to \pi^+\pi^-\pi^0$ decay allows a determination of α without input from any other channels. *BABAR* [219] obtain the constraint $75^\circ < \alpha < 152^\circ$ at 68% C.L. Belle [220] have performed a similar analysis, and in addition have included information from the SU(2) partners of $B \to \rho\pi$, which can be used to constrain α via an isospin pentagon relation [225]. With this analysis, Belle obtain the tighter constraint $\phi_2 = (83\,^{+12}_{-23})^\circ$ (where the errors correspond to 1σ, *i.e.* 68.3% confidence level.

- Each experiment has obtained a value of α from combining its results in the different $b \to u\overline{u}d$ modes (with some input also from HFAG). These values have appeared in talks, but not in publications, and are not listed here.

- The CKMfitter [169] and UTFit [170] groups use the measurements from Belle and *BABAR* given above with other branching fractions and *CP* asymmetries in $B \to \pi\pi$, $\rho\pi$ and $\rho\rho$ modes, to perform isospin analyses for each system, and to make combined constraints on α.

Note that methods based on isospin symmetry make extensive use of measurements of branching fractions and direct *CP* asymmetries, as averaged by the HFAG Rare Decays subgroup (Sec. 6). Note also that each method suffers from discrete ambiguities in the solutions. The model assumption in the $B^0 \to \pi^+\pi^-\pi^0$ analysis allows to resolve some of the multiple solutions, and results in a single preferred value for α in $[0, \pi]$. All the above measurements correspond to the choice that is in agreement with the global CKM fit.

At present we make no attempt to provide an HFAG average for α. More details on procedures to calculate a best fit value for α can be found in Refs. [169, 170].

4.11 Time-dependent *CP* asymmetries in $b \to c\overline{u}d/u\overline{c}d$ transitions

Non-*CP* eigenstates such as $D^{\pm}\pi^{\mp}$, $D^{*\pm}\pi^{\mp}$ and $D^{\pm}\rho^{\mp}$ can be produced in decays of B^0 mesons either via Cabibbo favoured ($b \to c$) or doubly Cabibbo suppressed ($b \to u$) tree amplitudes. Since no penguin contribution is possible, these modes are theoretically clean. The ratio of the magnitudes of the suppressed and favoured amplitudes, R, is sufficiently small (predicted to be about 0.02), that terms of $\mathcal{O}(R^2)$ can be neglected, and the sine terms give sensitivity to the combination of UT angles $2\beta + \gamma$.

As described in Sec. 4.2.5, the averages are given in terms of parameters a and c. *CP* violation would appear as $a \neq 0$. Results are available from both *BABAR* and Belle in the modes $D^{\pm}\pi^{\mp}$ and $D^{*\pm}\pi^{\mp}$; for the latter mode both experiments have used both full and partial reconstruction techniques. (*BABAR* have provided separate results with each technique, while Belle have in addition provided a combined result.) Results are also available from *BABAR* using $D^{\pm}\rho^{\mp}$. These results, and their averages, are listed in Table 36, and are shown in Fig. 23. The constraints in c *vs.* a space for the $D\pi$ and $D^*\pi$ modes are shown in Fig. 24. It is notable that the average value of a from $D^*\pi$ is more than 3σ from zero, providing evidence of *CP* violation in this channel.

For each of $D\pi$, $D^*\pi$ and $D\rho$, there are two measurements (a and c, or S^+ and S^-) which depend on three unknowns (R, δ and $2\beta + \gamma$), of which two are different for each decay mode. Therefore, there is not enough information to solve directly for $2\beta + \gamma$. However, for each choice of R and $2\beta + \gamma$, one can find the value of δ that allows a and c to be closest to their measured values, and calculate the distance in terms of numbers of standard deviations. (We currently neglect experimental correlations in this analysis.) These values of $N(\sigma)_{\rm min}$ can then be plotted as a function of R and $2\beta + \gamma$ (and can trivially be converted to confidence levels). These plots are given for the $D\pi$ and $D^*\pi$ modes in Figure 24; the uncertainties in the $D\rho$ mode are currently too large to give any meaningful constraint.

The constraints can be tightened if one is willing to use theoretical input on the values of R and/or δ. One popular choice is the use of SU(3) symmetry to obtain R by relating

Table 36: Averages for $b \to c\overline{u}d/u\overline{c}d$ modes. Note that the "Belle (combined)" result for $D^{*\pm}\pi^{\mp}$ is a combination of the "Belle (full rec.)" and "Belle (partial rec.)" results.

Experiment		$N(B\overline{B})$	a	c
			$D^{*\pm}\pi^{\mp}$	
BABAR (full rec.)	[226]	232M	$-0.040 \pm 0.023 \pm 0.010$	$0.049 \pm 0.042 \pm 0.015$
BABAR (partial rec.)	[228]	232M	$-0.034 \pm 0.014 \pm 0.009$	$-0.019 \pm 0.022 \pm 0.013$
Belle (full rec.)	[227]	386M	$-0.039 \pm 0.020 \pm 0.013$	$-0.011 \pm 0.020 \pm 0.013$
Belle (partial rec.)	[227]	386M	$-0.041 \pm 0.019 \pm 0.017$	$-0.007 \pm 0.019 \pm 0.017$
Belle (combined)	[227]	386M	$-0.040 \pm 0.014 \pm 0.011$	$-0.009 \pm 0.014 \pm 0.011$
Average			-0.037 ± 0.011	-0.006 ± 0.014
Confidence level			0.96 (0.0σ)	0.41 (0.8σ)
			$D^{\pm}\pi^{\mp}$	
BABAR (full rec.)	[226]	232M	$-0.010 \pm 0.023 \pm 0.007$	$-0.033 \pm 0.042 \pm 0.012$
Belle (full rec.)	[227]	386M	$-0.050 \pm 0.021 \pm 0.012$	$-0.019 \pm 0.021 \pm 0.012$
Average			-0.030 ± 0.017	-0.022 ± 0.021
Confidence level			0.24 (1.2σ)	0.78 (0.3σ)
			$D^{\pm}\rho^{\mp}$	
BABAR (full rec.)	[226]	232M	$-0.024 \pm 0.031 \pm 0.009$	$-0.098 \pm 0.055 \pm 0.018$
Average			-0.024 ± 0.033	-0.098 ± 0.058

the suppressed decay mode to B decays involving D_s mesons. More details can be found in Refs. [169, 170].

4.12 Rates and asymmetries in $B^{\mp} \to D^{(*)}K^{(*)\mp}$ decays

As explained in Sec. 4.2.7, rates and asymmetries in $B^{\mp} \to D^{(*)}K^{(*)\mp}$ decays are sensitive to γ. Various methods using different $D^{(*)}$ final states exist.

4.12.1 D decays to CP eigenstates

Results are available from both *BABAR* and Belle on GLW analyses in the decay modes $B^{\mp} \to DK^{\mp}$, $B^{\mp} \to D^*K^{\mp}$ and $B^{\mp} \to DK^{*\mp}$. Both experiments use the CP even D decay final states K^+K^- and $\pi^+\pi^-$ in all three modes; both experiments also use only the $D^* \to D\pi^0$ decay, which gives $CP(D^*) = CP(D)$. For CP odd D decay final states, Belle uses $K^0_S\pi^0$, $K^0_S\eta$ and $K^0_S\phi$ in all three analyses, and also use $K^0_S\omega$ in $DK^{\mp}$ and $D^*K^{\mp}$ analyses. *BABAR* uses $K^0_S\pi^0$ only for $DK^{\mp}$ analysis; for $DK^{*\mp}$ analysis they also use $K^0_S\phi$ and $K^0_S\omega$ (and assign an asymmetric systematic error due to CP even pollution in these CP odd channels [239]). The results and averages are given in Table 37 and shown in Fig. 25.

4.12.2 D decays to suppressed final states

For ADS analysis, both *BABAR* and Belle have studied the mode $B^{\mp} \to DK^{\mp}$; Belle has also studied $B^{\mp} \to D\pi^{\mp}$ and *BABAR* has also analyzed the $B^{\mp} \to D^*K^{\mp}$ and $B^{\mp} \to DK^{*\mp}$ modes ($D^* \to D\pi^0$ and $D^* \to D\gamma$ are studied separately; $K^{*\mp}$ is reconstructed as $K^0_S\pi^{\mp}$). In all cases

Table 37: Averages from GLW analyses of $b \to c\overline{u}s/u\overline{c}s$ modes.

Experiment	$N(B\overline{B})$	A_{CP+}	A_{CP-}	R_{CP+}	R_{CP-}
			$D_{CP}K^-$		
BABAR [237]	232M	$0.35 \pm 0.13 \pm 0.04$	$-0.06 \pm 0.13 \pm 0.04$	$0.90 \pm 0.12 \pm 0.04$	$0.86 \pm 0.10 \pm 0.05$
Belle [238]	275M	$0.06 \pm 0.14 \pm 0.05$	$-0.12 \pm 0.14 \pm 0.05$	$1.13 \pm 0.16 \pm 0.08$	$1.17 \pm 0.14 \pm 0.14$
Average		0.22 ± 0.10	-0.09 ± 0.10	0.98 ± 0.10	0.94 ± 0.10
			$D^*_{CP}K^-$		
BABAR [239]	123M	$-0.10 \pm 0.23\,^{+0.03}_{-0.04}$		$1.06 \pm 0.26\,^{+0.10}_{-0.09}$	
Belle [238]	275M	$-0.20 \pm 0.22 \pm 0.04$	$0.13 \pm 0.30 \pm 0.08$	$1.41 \pm 0.25 \pm 0.06$	$1.15 \pm 0.31 \pm 0.12$
Average		-0.15 ± 0.16	0.13 ± 0.31	1.25 ± 0.19	1.15 ± 0.33
			$D_{CP}K^{*-}$		
BABAR [240]	232M	$-0.08 \pm 0.19 \pm 0.08$	$-0.26 \pm 0.40 \pm 0.12$	$1.96 \pm 0.40 \pm 0.11$	$0.65 \pm 0.26 \pm 0.08$

Table 38: Averages from ADS analyses of $b \to c\overline{u}s/u\overline{c}s$ and $b \to c\overline{u}d/u\overline{c}d$ modes.

Experiment		$N(B\overline{B})$	$A_{\rm ADS}$	$R_{\rm ADS}$
			DK^-, $D \to K^+\pi^-$	
BABAR	[241]	232M		$0.013\,^{+0.011}_{-0.009}$
Belle	[242]	386M		$0.000 \pm 0.008 \pm 0.001$
Average				0.006 ± 0.006
			D^*K^-, $D^* \to D\pi^0$, $D \to K^+\pi^-$	
BABAR	[241]	232M		$-0.002\,^{+0.010}_{-0.006}$
			D^*K^-, $D^* \to D\gamma$, $D \to K^+\pi^-$	
BABAR	[241]	232M		$0.011\,^{+0.018}_{-0.013}$
			DK^{*-}, $D \to K^+\pi^-$, $K^{*-} \to K^0_S\pi^-$	
BABAR	[243]	232M	$-0.22 \pm 0.61 \pm 0.17$	$0.046 \pm 0.031 \pm 0.008$
			DK^-, $D \to K^+\pi^-\pi^0$	
BABAR	[244]	226M		$0.012 \pm 0.012 \pm 0.009$
			$D\pi^-$, $D \to K^+\pi^-$	
Belle	[242]	386M	$0.10 \pm 0.22 \pm 0.06$	$0.0035\,^{+0.0008}_{-0.0007} \pm 0.0003$

the suppressed decay $D \to K^+\pi^-$ has been used. *BABAR* also has results using $B^\mp \to DK^\mp$ with $D \to K^+\pi^-\pi^0$. The results and averages are given in Table 38 and shown in Fig. 26. Note that although no clear signals for these modes have yet been seen, the central values are given. In $B^- \to D^*K^-$ decays there is an effective shift of π in the strong phase difference between the cases that the D^* is reconstructed as $D\pi^0$ and $D\gamma$ [236]. As a consequence, the different D^* decay modes are treated separately.

4.12.3 *D* decays to multiparticle self-conjugate final states

For the Dalitz plot analysis, both *BABAR* [246] and Belle [247] have studied the modes $B^\mp \to DK^\mp$, $B^\mp \to D^*K^\mp$ and $B^\mp \to DK^{*\mp}$. For $B^\mp \to D^*K^\mp$, Belle has used only $D^* \to D\pi^0$, while *BABAR* has used both D^* decay modes and taken the effective shift in the strong phase

difference into account. In all cases the decay $D \to K_S^0\pi^+\pi^-$ has been used. Results and averages are given in Table 39. The third error on each measurement is due to D decay model uncertainty.

The parameters measured in the analyses are explained in Sec. 4.2.7. Both *BABAR* and Belle have measured the "Cartesian" $(x_\pm, y_\pm)$ variables, and perform frequentist statistical procedures, to convert these into measurements of γ, r_B and δ_B.

Both experiments reconstruct $K^{*\mp}$ as $K_S^0\pi^\mp$, but the treatment of possible nonresonant $K_S^0\pi^\mp$ differs: Belle assign an additional model uncertainty, while *BABAR* use a reparametrization suggested by Gronau [245]. The parameters r_B and δ_B are replaced with effective parameters κr_s and δ_s; no attempt is made to extract the true hadronic parameters of the $B^\mp \to DK^{*\mp}$ decay.

We perform averages using the following procedure, which is based on a set of reasonable, though imperfect, assumptions.

- It is assumed that both experiments use the same D decay model. Therefore, we do not rescale the results to a common model.
- It is further assumed that the model uncertainty is 100% correlated between experiments, and therefore this source of error is not used in the averaging procedure.
- We include in the average the effect of correlations within each experiments set of measurements.
- At present it is unclear how to assign an average model uncertainty. We have not attempted to do so. Our average includes only statistical and systematic error. An unknown amount of model uncertainty should be added to the final error.
- We follow the suggestion of Gronau [245] in making the DK^* averages. Explicitly, we assume that the selection of $K^{*\pm} \to K_S^0\pi^\pm$ is the same in both experiments (so that κ, r_s and δ_s are the same), and drop the additional source of model uncertainty assigned by Belle due to possible nonresonant decays.
- We do not consider common systematic errors, other than the D decay model.

Constraints on γ

The measurements of $(x_\pm, y_\pm)$ can be used to obtain constraints on γ, as well as the hadronic parameters r_B and δ_B. Both *BABAR* [246] and Belle [247] have done so using a frequentist procedure (there are some differences in the details of the techniques used).

- *BABAR* obtain $\gamma = (92 \pm 41 \pm 11 \pm 12)^\circ$ from $DK^\pm$ and $D^*K^\pm$
- Belle obtain $\phi_3 = (53\,^{+15}_{-18} \pm 3 \pm 9)^\circ$ from $DK^\pm$, $D^*K^\pm$ and $DK^{*\pm}$
- The experiments also obtain values for the hadronic parameters.
  In $DK^\pm$
  BABAR obtain $r_B(DK^\pm) < 0.140(1\sigma)$ and $\delta_B(DK^\pm) = (118 \pm 63 \pm 19 \pm 36)^\circ$
  Belle obtain $r_B(DK^\pm) = 0.16 \pm 0.05 \pm 0.01 \pm 0.05$ and $\delta_B(DK^\pm) = (146\,^{+19}_{-20} \pm 3 \pm 23)^\circ$.
  In $D^*K^\pm$
  BABAR obtain $0.017 < r_B(D^*K^\pm) < 0.203$ and $\delta_B(D^*K^\pm) = (298 \pm 59 \pm 18 \pm 10)^\circ$

Table 39: Averages from Dalitz plot analyses of $b \to c\overline{u}s/u\overline{c}s$ modes. Note that the uncertainities assigned to the averages do not include model errors.

Experiment	$N(B\overline{B})$	x_+	y_+	x_-	y_-
			DK^-, $D \to K^0_S\pi^+\pi^-$		
BABAR [246]	347M	$-0.072 \pm 0.056 \pm 0.014 \pm 0.029$	$-0.033 \pm 0.066 \pm 0.007 \pm 0.018$	$0.041 \pm 0.059 \pm 0.018 \pm 0.011$	$0.056 \pm 0.071 \pm 0.007 \pm 0.023$
Belle [247]	386M	$-0.135^{+0.069}_{-0.070} \pm 0.017 \pm 0.051$	$-0.085^{+0.090}_{-0.086} \pm 0.009 \pm 0.066$	$0.025^{+0.072}_{-0.080} \pm 0.013 \pm 0.068$	$0.170^{+0.093}_{-0.117} \pm 0.016 \pm 0.049$
Average		-0.097 ± 0.045	-0.051 ± 0.053	0.045 ± 0.047	0.093 ± 0.058
Confidence level			$\chi^2 = 1.5/4$ dof (CL=0.83 $\to 0.2\sigma$)		
			D^*K^-, $D^* \to D\pi^0$ or $D\gamma$, $D \to K^0_S\pi^+\pi^-$		
BABAR [246]	347M	$0.084 \pm 0.088 \pm 0.015 \pm 0.018$	$0.096 \pm 0.111 \pm 0.032 \pm 0.017$	$-0.106 \pm 0.091 \pm 0.020 \pm 0.009$	$-0.019 \pm 0.096 \pm 0.022 \pm 0.016$
Belle [247]	386M	$0.032^{+0.120}_{-0.116} \pm 0.004 \pm 0.049$	$0.008^{+0.137}_{-0.136} \pm 0.011 \pm 0.074$	$-0.128^{+0.167}_{-0.146} \pm 0.023 \pm 0.071$	$-0.339^{+0.172}_{-0.158} \pm 0.027 \pm 0.053$
Average		0.067 ± 0.071	0.061 ± 0.088	-0.110 ± 0.080	-0.101 ± 0.085
Confidence level			$\chi^2 = 3.2/4$ dof (CL=0.52 $\to 0.6\sigma$)		
			DK^{*-}, $D \to K^0_S\pi^+\pi^-$		
BABAR [248]	227M	$-0.070 \pm 0.230 \pm 0.130 \pm 0.030$	$-0.010 \pm 0.320 \pm 0.180 \pm 0.050$	$-0.200 \pm 0.200 \pm 0.110 \pm 0.030$	$0.260 \pm 0.300 \pm 0.160 \pm 0.030$
Belle [247]	386M	$-0.105^{+0.177}_{-0.167} \pm 0.006 \pm 0.088$	$-0.004^{+0.164}_{-0.156} \pm 0.013 \pm 0.095$	$-0.784^{+0.249}_{-0.295} \pm 0.029 \pm 0.097$	$-0.281^{+0.440}_{-0.335} \pm 0.046 \pm 0.086$
Average		-0.094 ± 0.144	-0.007 ± 0.146	-0.480 ± 0.173	-0.056 ± 0.253
Confidence level			$\chi^2 = 4.6/4$ dof (CL=0.33 $\to 1.0\sigma$)		

Belle obtain $r_B(D^*K^\pm) = 0.18\,^{+0.11}_{-0.10} \pm 0.01 \pm 0.05$ and $\delta_B(D^*K^\pm) = (302\,^{+34}_{-35} \pm 6 \pm 23)^\circ$. In $DK^{*\pm}$
Belle obtain $r_B(DK^{*\pm}) = 0.56\,^{+0.22}_{-0.16} \pm 0.04 \pm 0.08$ and $\delta_B(DK^{*\pm}) = (243\,^{+20}_{-23} \pm 3 \pm 50)^\circ$. *BABAR* do not obtain a constraint on the hadronic parameters in $DK^{*\pm}$ due to the reparametrization described above.

- Improved constraints can be achieved combining the information from $B^\pm \to DK^\pm$ analysis with different D decay modes. The experiments have not yet published such results, and none are listed here.
- The CKMfitter [169] and UTFit [170] groups use the measurements from Belle and *BABAR* given above to make combined constraints on γ.

At present we make no attempt to provide an HFAG average for γ. More details on procedures to calculate a best fit value for γ can be found in Refs. [169, 170].

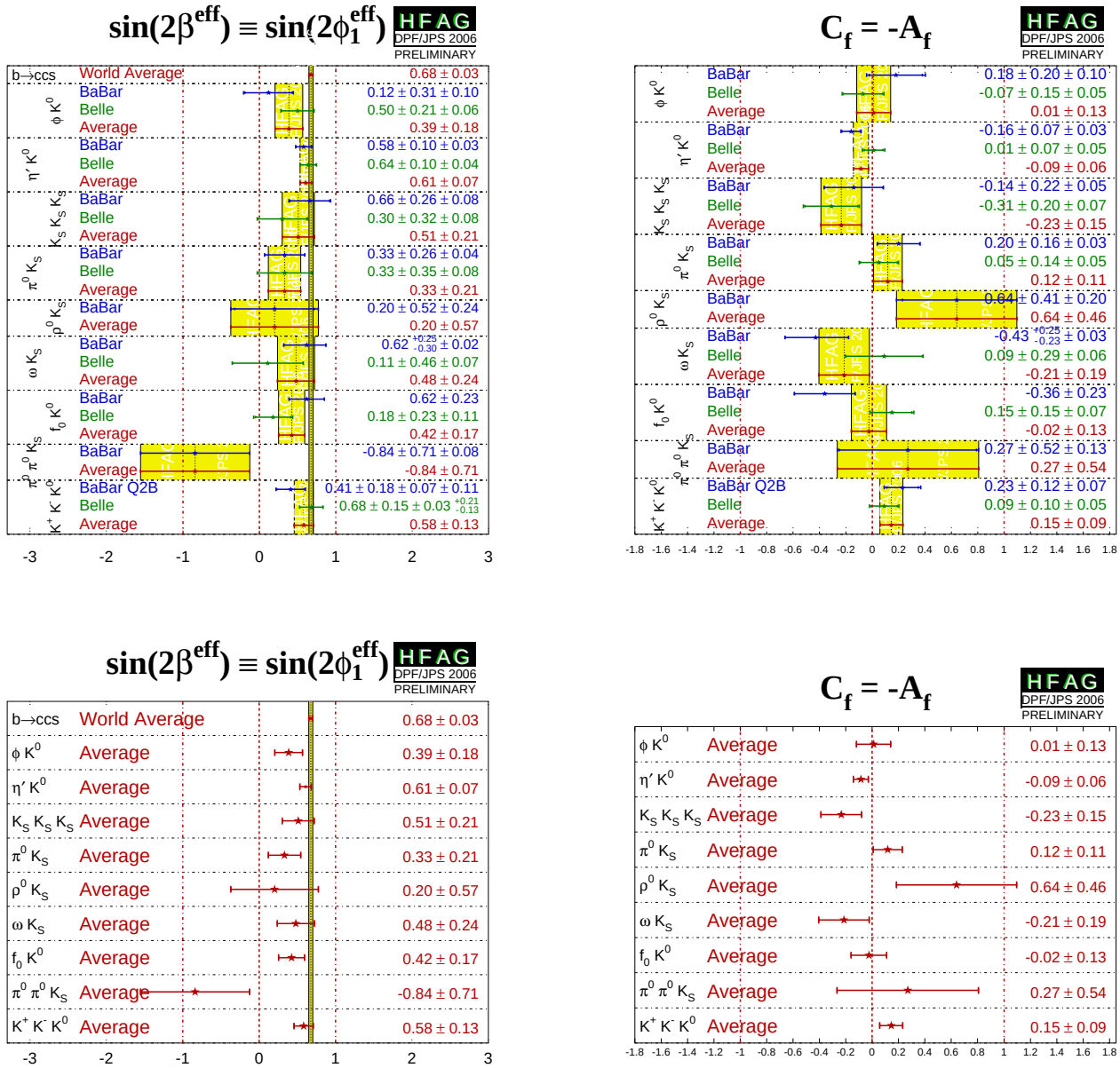

Figure 12: (Top) Averages of (left) $-\eta S_{b\to q\bar{q}s}$ and (right) $C_{b\to q\bar{q}s}$. The $-\eta S_{b\to q\bar{q}s}$ figure compares the results to the world average for $-\eta S_{b\to c\bar{c}s}$ (see Section 4.4.1). (Bottom) Same, but only averages for each mode are shown. More figures are available from the HFAG web pages.

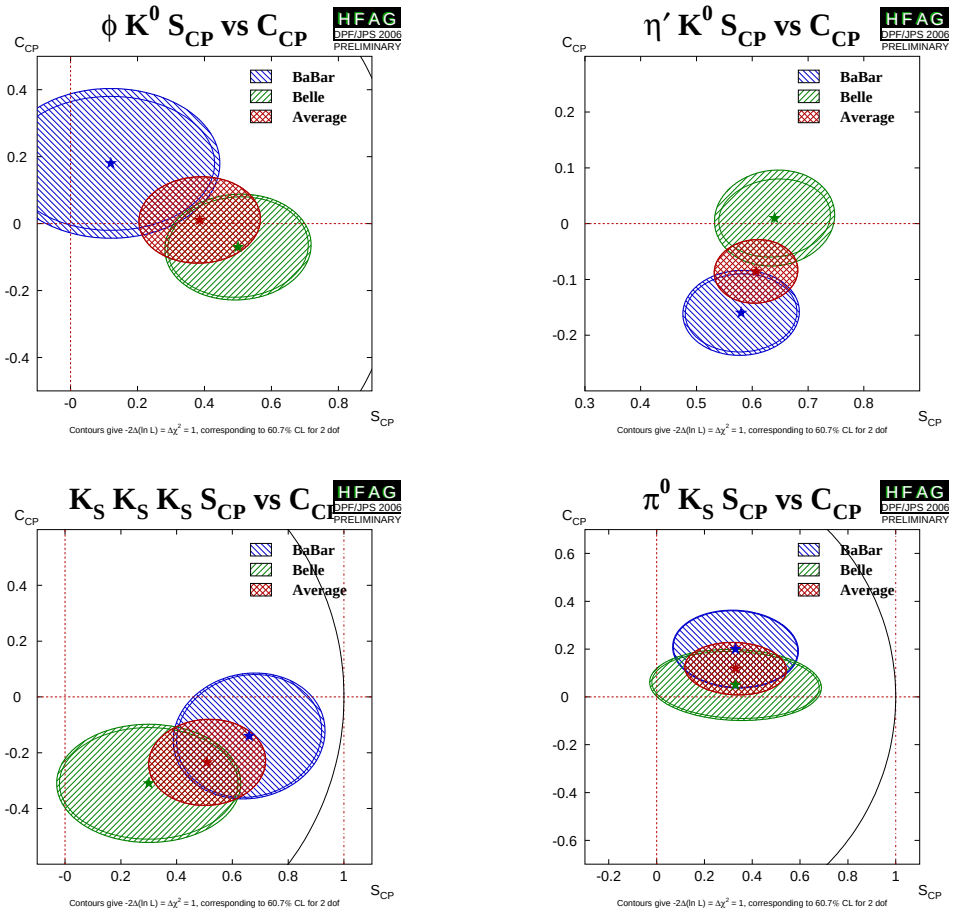

Figure 13: (Top) Averages of four $b \to q\overline{q}s$ dominated channels, for which correlated averages are performed, in the S_{CP} *vs.* C_{CP} plane, where S_{CP} has been corrected by the CP eigenvalue to give $\sin(2\beta^{\rm eff})$. (Top left) $B^0 \to \phi K^0$, (top right) $B^0 \to \eta' K^0$, (bottom left) $B^0 \to K^0_S K^0_S K^0_S$, (bottom right) $B^0 \to \pi^0 K^0_S$. More figures are available from the HFAG web pages.

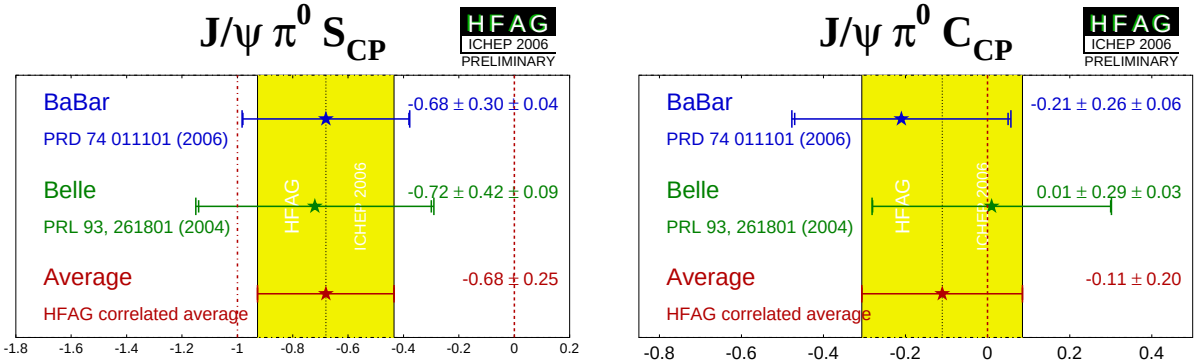

Figure 14: Averages of (left) $S_{b\to c\overline{c}d}$ and (right) $C_{b\to c\overline{c}d}$ for the mode $B^0 \to J/\psi\pi^0$.

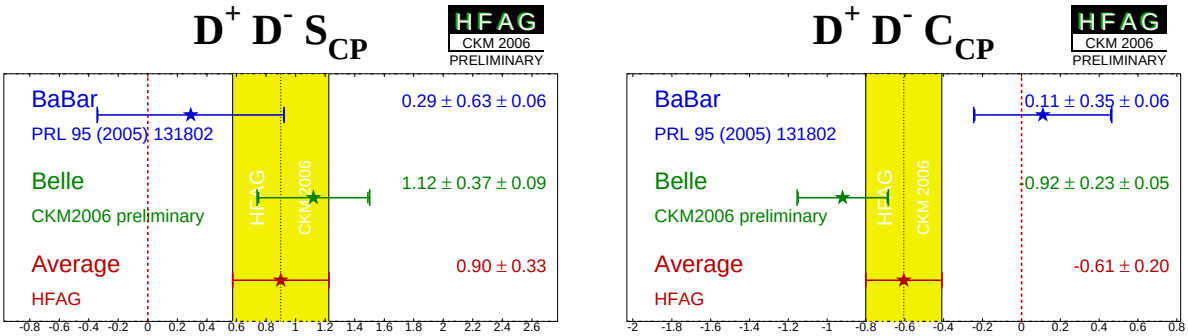

Figure 15: Averages of (left) $S_{b\to c\bar{c}d}$ and (right) $C_{b\to c\bar{c}d}$ for the mode $B^0 \to D^+D^-$.

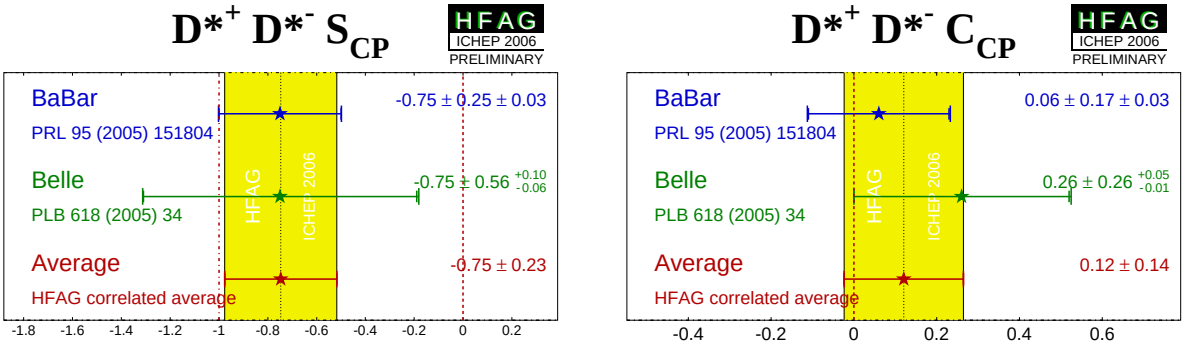

Figure 16: Averages of (left) $S_{b\to c\bar{c}d}$ and (right) $C_{b\to c\bar{c}d}$ for the mode $B^0 \to D^{*+}D^{*-}$.

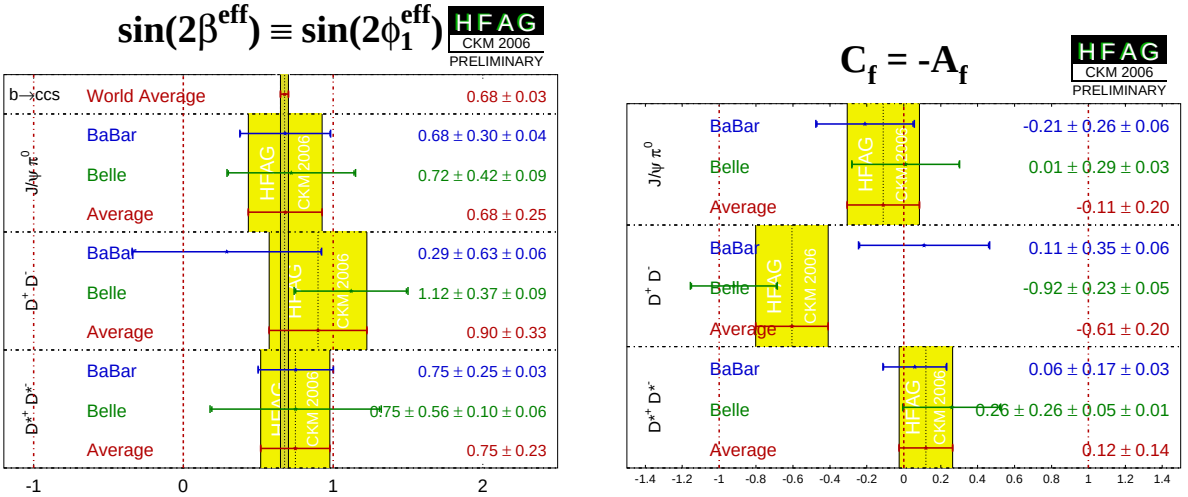

Figure 17: Averages of (left) $-\eta S_{b\to c\bar{c}d}$ and (right) $C_{b\to c\bar{c}d}$. The $-\eta S_{b\to q\bar{q}s}$ figure compares the results to the world average for $-\eta S_{b\to c\bar{c}s}$ (see Section 4.4.1).

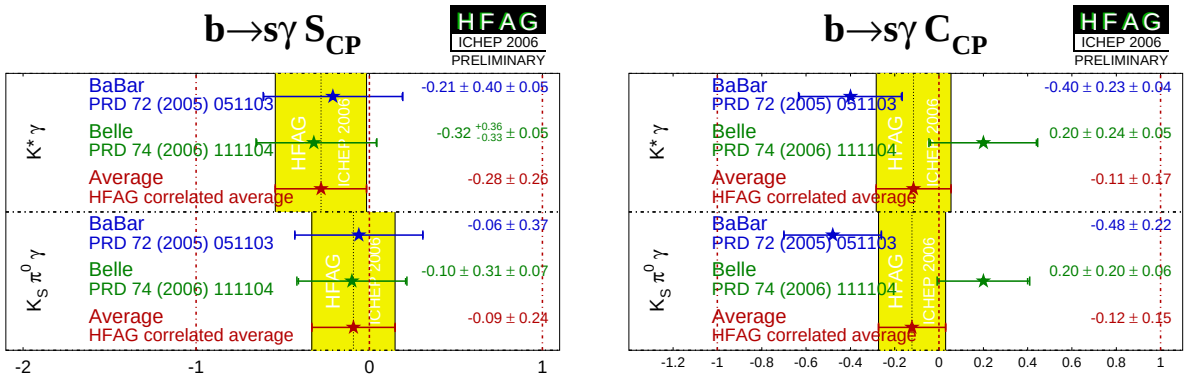

Figure 18: Averages of (left) $S_{b\to s\gamma}$ and (right) $C_{b\to s\gamma}$. Recall that the data for $K^*\gamma$ is a subset of that for $K^0_S\pi^0\gamma$.

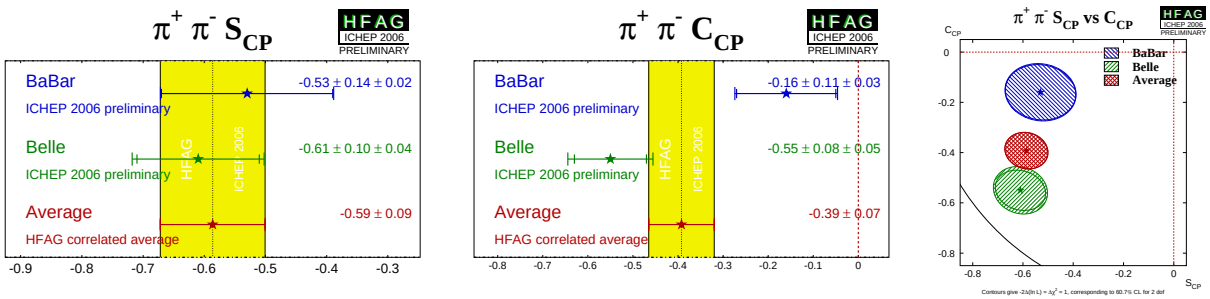

Figure 19: Averages of (left) $S_{b\to u\bar{u}d}$, (middle) $C_{b\to u\bar{u}d}$ and (right) $S_{b\to u\bar{u}d}$ *vs.* $C_{b\to u\bar{u}d}$ for the mode $B^0 \to \pi^+\pi^-$.

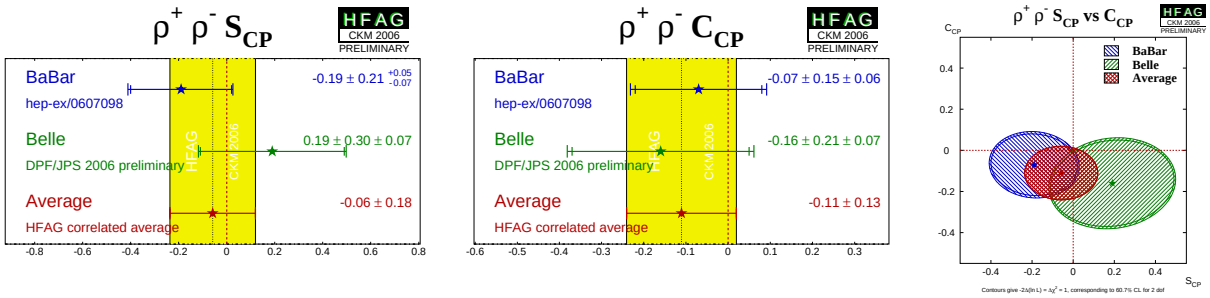

Figure 20: Averages of (left) $S_{b\to u\bar{u}d}$, (middle) $C_{b\to u\bar{u}d}$ and (right) $S_{b\to u\bar{u}d}$ *vs.* $C_{b\to u\bar{u}d}$ for the mode $B^0 \to \rho^+\rho^-$.

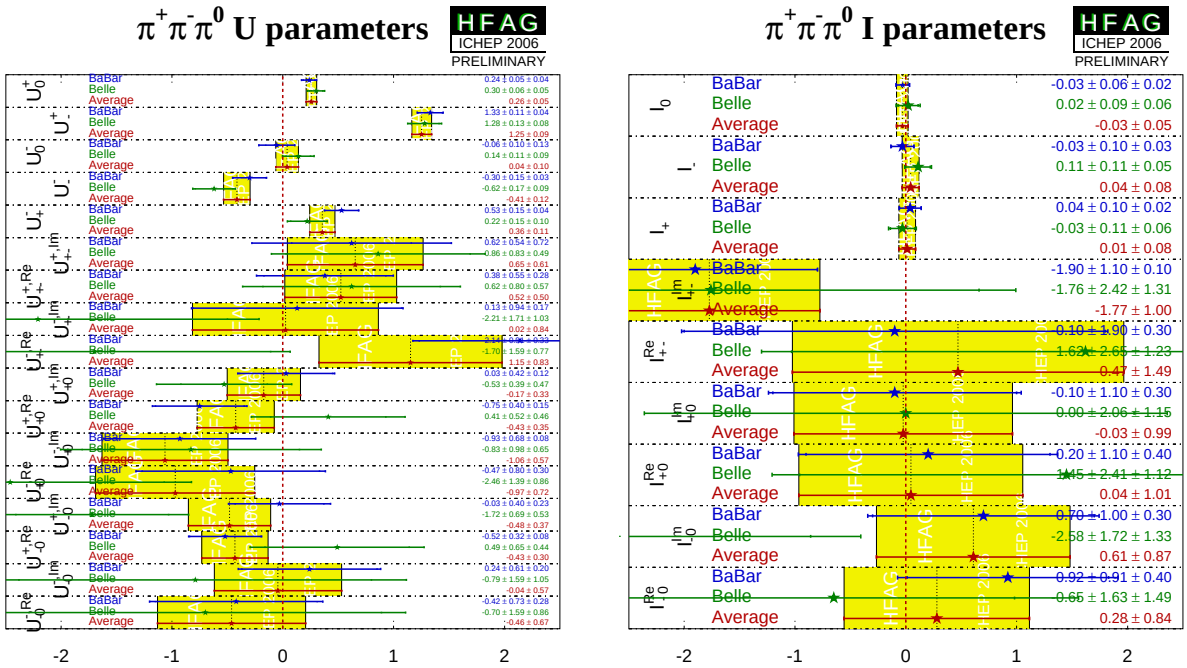

Figure 21: Summary of the U and I parameters measured in the time-dependent $B^0 \to \pi^+\pi^-\pi^0$ Dalitz plot analysis.

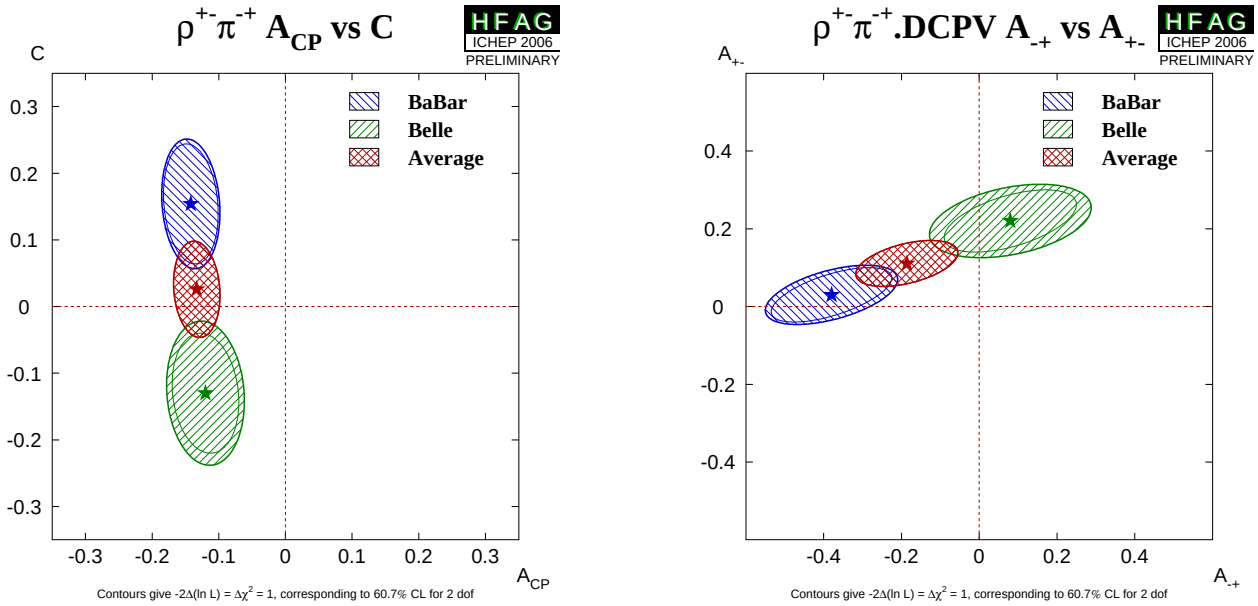

Figure 22: Direct CP violation in $B^0 \to \rho^\pm\pi^\mp$. (Left) $\mathcal{A}_{CP}^{\rho\pi}$ *vs.* $C_{\rho\pi}$ space, (right) $\mathcal{A}_{\rho\pi}^{-+}$ *vs.* $\mathcal{A}_{\rho\pi}^{+-}$ space.

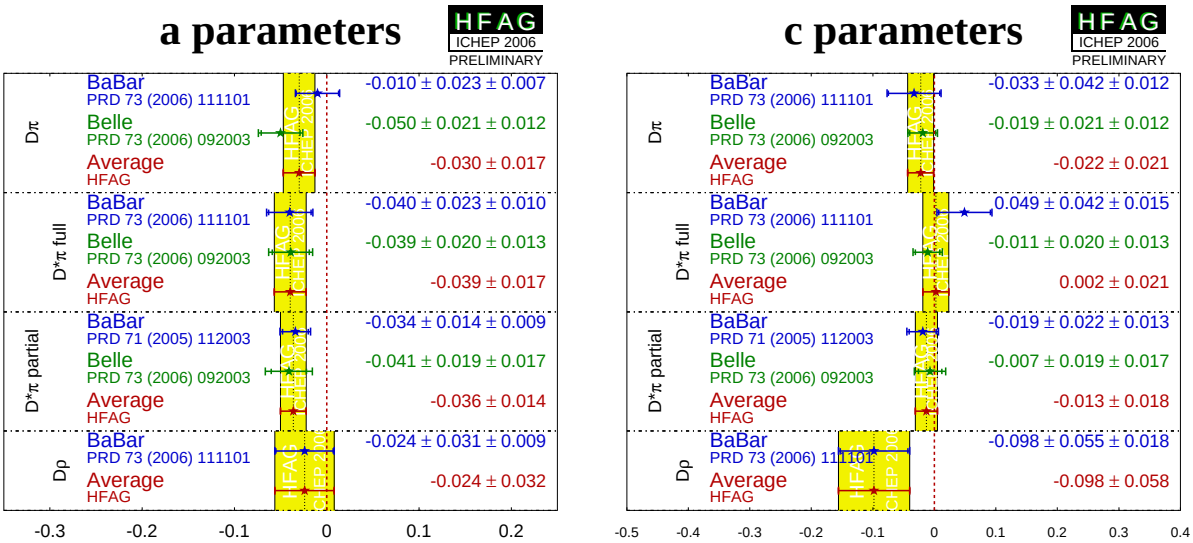

Figure 23: Averages for $b \to c\bar{u}d/u\bar{c}d$ modes.

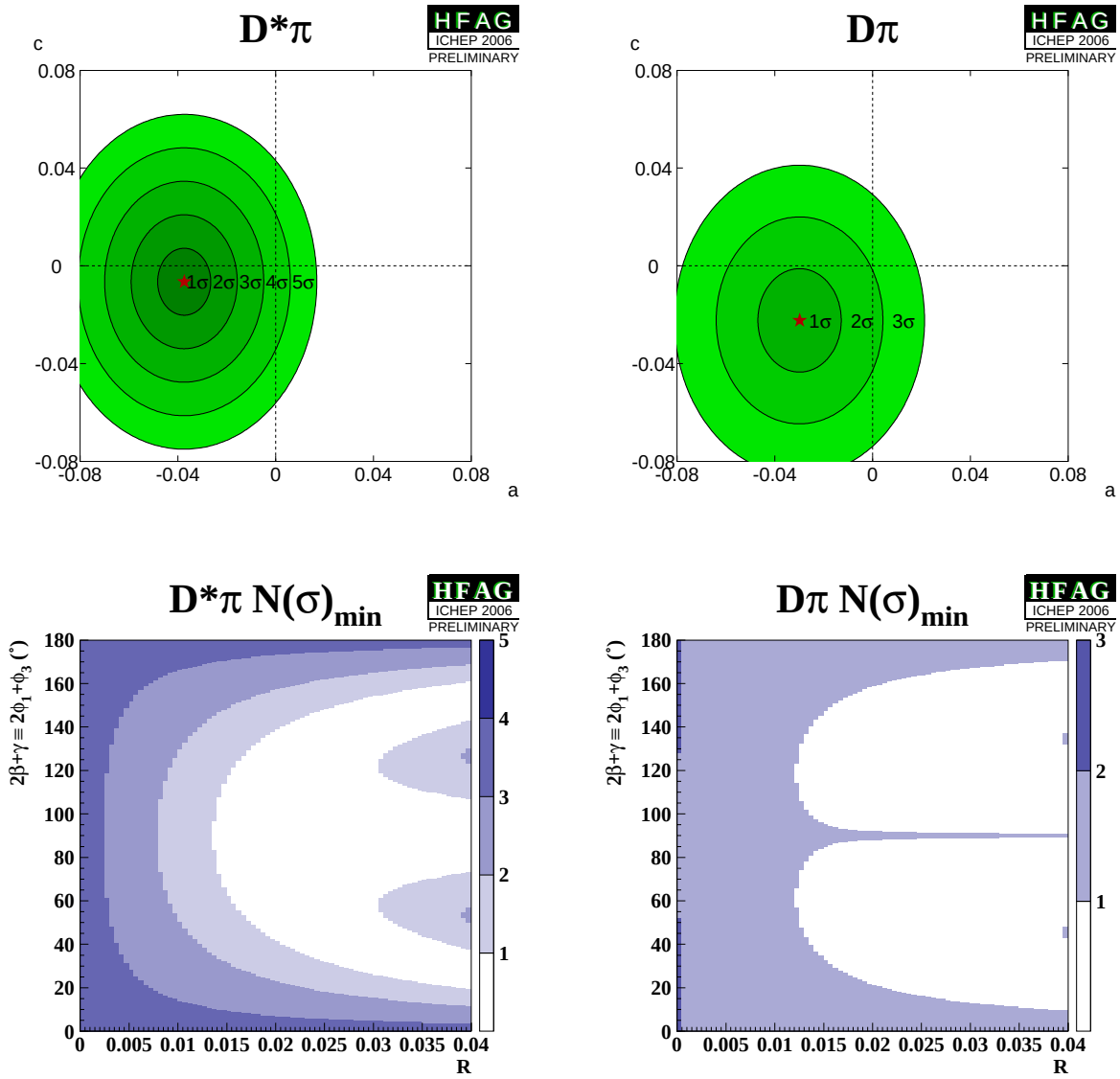

Figure 24: Results from $b \to c\bar{u}d/u\bar{c}d$ modes. (Top) Constraints in c *vs.* a space. (Bottom) Constraints in $2\beta + \gamma$ *vs.* R space. (Left) $D^*\pi$ and (right) $D\pi$ modes.

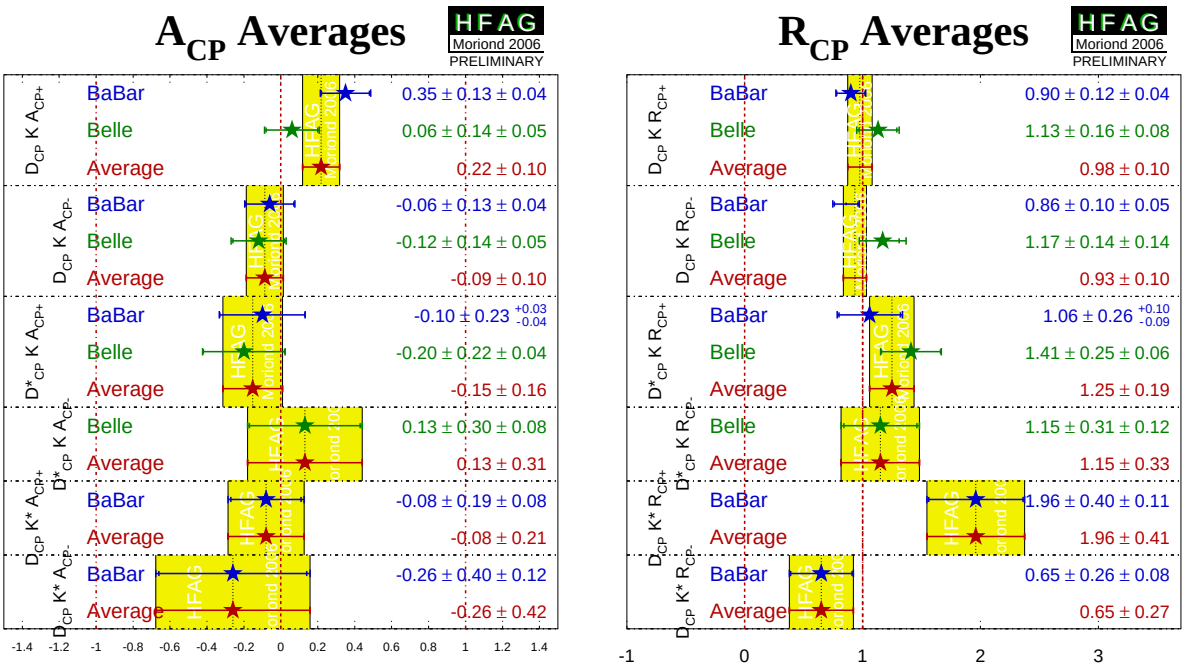

Figure 25: Averages of A_{CP} and R_{CP} from GLW analyses.

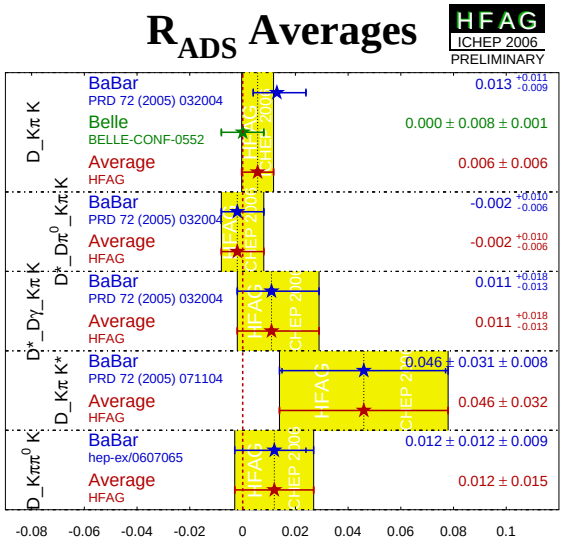

Figure 26: Averages of $R_{\rm ADS}$.

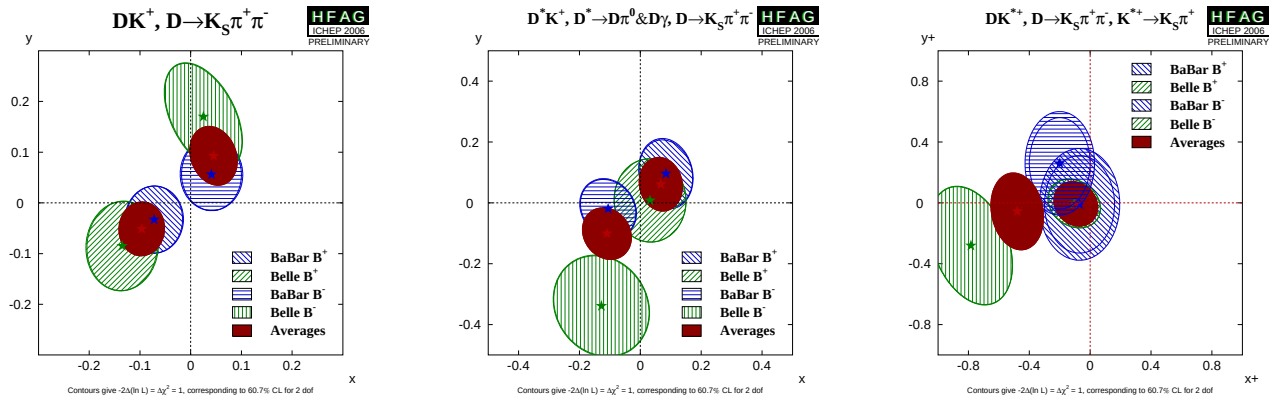

Figure 27: Contours in the $(x_\pm, y_\pm)$ from $B^\mp \to D^{(*)}K^{(*)\pm}$. (Left) $B^\mp \to DK^\mp$, (middle) $B^\mp \to D^*K^\mp$, (right) $B^\mp \to DK^{*\mp}$. Note that the uncertainities assigned to the averages given in these plots do not include model errors.

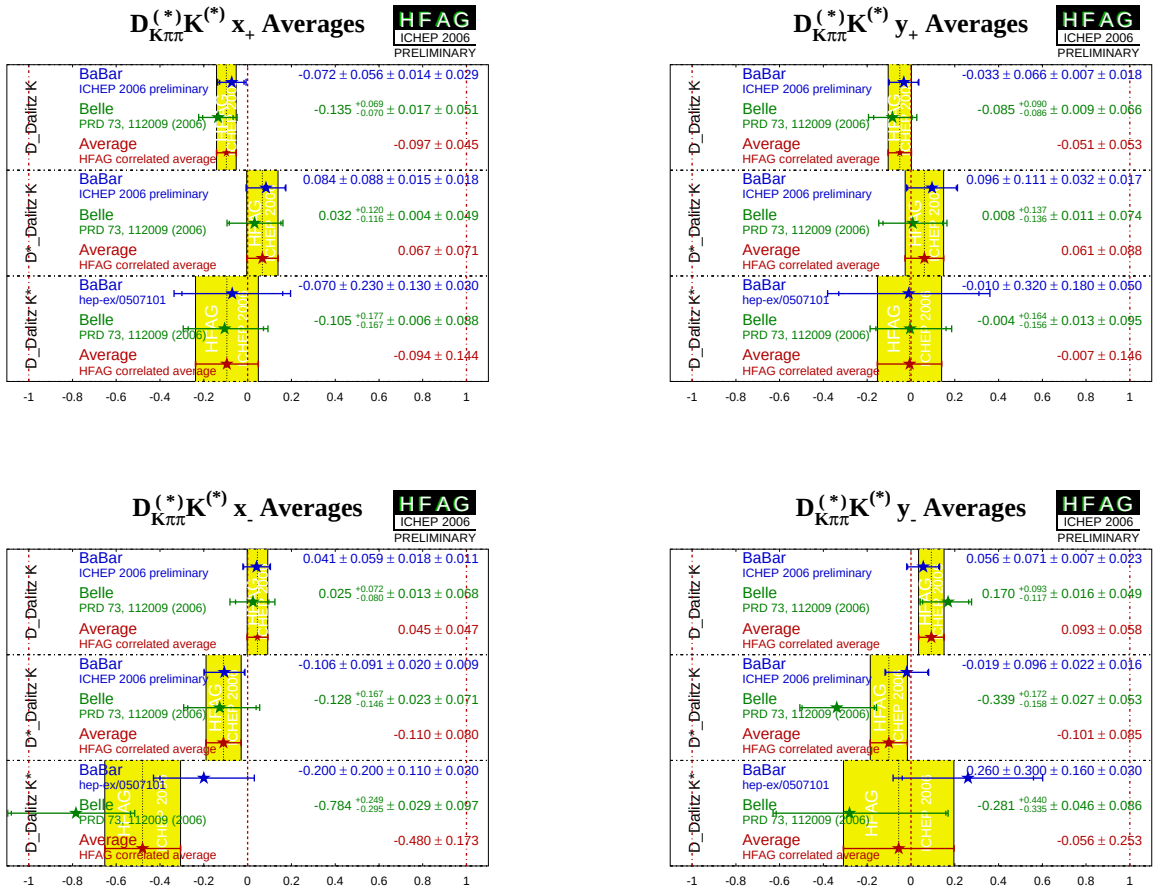

Figure 28: Averages of $(x_\pm, y_\pm)$ from $B^\mp \to D^{(*)}K^{(*)\pm}$. (Top left) x_+, (top right) y_+, (bottom left) x_-, (bottom right) y_-. Note that the uncertainities assigned to the averages given in these plots do not include model errors.

5 Semileptonic B decays

Measurements of semileptonic B-meson decays are essential to determining the magnitude of the CKM matrix elements $|V_{cb}|$ and $|V_{ub}|$. The ratio $|V_{ub}|/|V_{cb}|$ is an important ingredient in tests of the flavor sector of the Standard Model since it limits the precision with which one side-length of the Unitarity Triangle is known. That side-length and the precisely known angle ϕ_1 or β, opposite to it, provide a stringest test of the Kobayashi-Maskawa mechanism for CP violation.

In the following, we provide averages of exclusive and inclusive branching fractions, the product of $|V_{cb}|$ and the form factor normalisation $F(1)$ and $G(1)$ for $\overline{B}^0 \to D^{*+}\ell^-\overline{\nu}$ and $\overline{B}^0 \to D^+\ell^-\overline{\nu}$ decays respectively, and $|V_{ub}|$ as determined from inclusive and exclusive measurements of $B \to X_u\ell\nu_\ell$ decays. Brief descriptions of all parameters and analyses (published or preliminary) relevant for the determination of the combined results are given. The descriptions are based on the information available on the web page at

`http://www.slac.stanford.edu/xorg/hfag/semi/summer06/summer06.shtml`

A description of the technique employed for calculating averages can be found in section 2.

5.1 Common set of input parameters

In the combination of the published results, the central values and errors are rescaled to a common set of input parameters, summarized in Table 40 and provided in the file `common.param` (accessible from the web-page). All measurements with a dependence on any of these parameters are rescaled to the central values given in Table 40, and their error is recalculated based on the error provided in the column "Excursion". The detailed dependence for each measurement is contained in files (provided by the experiments) accessible from the web-page.

5.2 Exclusive CKM-favored decays

Averages are provided for the branching fractions $\mathcal{B}(\overline{B}^0 \to D^{*+}\ell^-\overline{\nu})$ and $\mathcal{B}(\overline{B}^0 \to D^+\ell^-\overline{\nu})$. In addition, averages are provided for $|V_{cb}|F(1)$ vs ρ^2, where $F(1)$ and ρ^2 are the normalization and slope of the form factor at zero recoil in $\overline{B}^0 \to D^{*+}\ell^-\overline{\nu}$ decays, and for the corresponding quantities $|V_{cb}|G(1)$ vs ρ^2 in $\overline{B}^0 \to D^+\ell^-\overline{\nu}$ decays.

5.2.1 $\overline{B}^0 \to D^{*+}\ell^-\overline{\nu}$

The measurements included in the average, shown in Table 41, are scaled to a consistent set of input parameters and their errors, see Section 5.1. Therefore some of the (older) measurements are subject to considerable adjustments. Advances have also been made in the determination of V_{cb} from exclusive $B \to D^* l\nu$ decays with substantially improved measurements of the form factor ratios R_1 and R_2. The measurements included in the average have been adjusted to take into account the new values.

In order to reduce the dependence on theoretical error estimates, the central values and errors for the form factors R_1 and R_2 are taken from the measurement by BABAR [249]. The original measurements by CLEO [250], $R_1 = 1.18 \pm 0.30 \pm 0.12$ and $R_2 = 0.71 \pm 0.22 \pm 0.07$ have been improved by BABAR, with results that are consistent with the earlier ones, but

Table 40: Common input parameters for the combination of semileptonic B decays. Most of the parameters are taken from Ref. [4]. This table is encoded in the file `common.param`. The units are picoseconds for lifetimes and percentage for branching fractions.

Parameter	Assumed Value	Excursion	Description
rb	21.629	± 0.066	R_b
bdst	1.27	± 0.021	$\mathcal{B}(\overline{B} \to D^* \tau \overline{\nu})$
bdsd	1.62	± 0.040	$\mathcal{B}(\overline{B} \to D^* D)$
bdst2	0.65	± 0.013	$\mathcal{B}(b \to D^* \tau)$ (OPAL incl)
bdsd2	4.2	± 1.5	$\mathcal{B}(b \to D^* D)$ (OPAL incl)
bdsd3	0.87	$^{+0.23}_{-0.19}$	$\mathcal{B}(b \to D^* D)$ (DELPHI incl)
xe	0.702	± 0.008	B fragmentation: $\langle E_B \rangle / E_{\rm beam}$
bdsi	17.3	± 2.0	$\mathcal{B}(b \to D^{*+}$ incl)
cdsi	22.6	± 1.4	$\mathcal{B}(c \to D^{*+}$ incl)
tb0	1.527	± 0.008	$\tau(B^0)$
tbplus	1.643	± 0.010	$\tau(B^+)$
tbps	1.440	± 0.036	$\tau(B_s^0)$
fbd	40.2	± 0.9	B^0 fraction at $\sqrt{s} = m_{Z^0}$
fbs	10.4	± 0.9	B_s^0 fraction at $\sqrt{s} = m_{Z^0}$
fbar	9.1	± 1.5	Baryon fraction at $\sqrt{s} = m_{Z^0}$
dst	67.7	± 0.5	$\mathcal{B}(D^{*+} \to D^0 \pi^+)$
dkpp	9.51	± 0.34	$\mathcal{B}(D^+ \to K^- \pi^+ \pi^+)$
dkp	3.80	± 0.07	$\mathcal{B}(D^0 \to K^- \pi^+)$
dkpzp	14.1	± 0.5	$\mathcal{B}(D^0 \to K^- \pi^+ \pi^0)$
dkppp	7.72	± 0.28	$\mathcal{B}(D^0 \to K^- \pi^+ \pi^+ \pi^-)$
dkzpp	2.90	± 0.19	$\mathcal{B}(D^0 \to K^0 \pi^+ \pi^-)$
dkln	6.7	± 0.19	$\mathcal{B}(D^0 \to K^- \ell^+ \nu)$
dkk	3.84	± 0.10	$\mathcal{B}(D^0 \to K^- K^+)$
dkx	1.100	± 0.025	$K^- \pi^+ X$ rates
dkox	0.42	± 0.05	$\mathcal{B}(D^0 \to K^0 X)$
dnlx	6.71	± 0.29	$\mathcal{B}(D^0 \to X \ell \overline{\nu})$
dkpcl	61.9	± 2.9	$\mathcal{B}(D^{*0} \to D^0 \pi^0)$
dssR	0.64	± 0.11	$\mathcal{B}(b \to D^{**} \ell \overline{\nu}) \times \mathcal{B}(D^{**} \to D^{*+} X)$
fb0	49.3	± 0.7	$f^{00} = \mathcal{B}(\Upsilon(4S) \to B^0 \overline{B}^0)$
chid	0.188	± 0.002	χ_d, time-integrated probability for B^0 mixing
chi	0.0925	± 0.0018	$\chi = \chi_d \times (f^{00}/100)$

considerably more precise, $R_1 = 1.417 \pm 0.061 \pm 0.044$ and $R_2 = 0.836 \pm 0.037 \pm 0.022$. All earlier measurements have been adjusted to these values of R_1 and R_2.

The average branching fraction $\mathcal{B}(\overline{B}^0 \to D^{*+} \ell^- \overline{\nu})$ is determined in a one-dimensional fit from the measurements provided in Table 41. At LEP, the measurements of $\overline{B}^0 \to D^{*+} \ell^- \overline{\nu}$ decays have been done both with inclusive and exclusive analyses based on a partial and full reconstruction of the $\overline{B}^0 \to D^{*+} \ell^- \overline{\nu}$ decay, respectively. Statistical correlations between

measurements from the same experiment have been taken into account. Figure 29(a) illustrates the measurements and the resulting average.

Table 41: Average branching fraction $\mathcal{B}(\overline{B}^0 \to D^{*+}\ell^-\overline{\nu})$ and individual results, where "excl" and "partial reco" refer to full and partial reconstruction of the $\overline{B}^0 \to D^{*+}\ell^-\overline{\nu}$ decay, respectively.

Experiment		$\mathcal{B}(\overline{B}^0 \to D^{*+}\ell^-\overline{\nu})[\%]$ (rescaled)	$\mathcal{B}(\overline{B}^0 \to D^{*+}\ell^-\overline{\nu})[\%]$ (published)
ALEPH (excl)	[251]	$5.72 \pm 0.27_{\rm stat} \pm 0.35_{\rm syst}$	$5.53 \pm 0.26_{\rm stat} \pm 0.52_{\rm syst}$
OPAL (excl)	[252]	$5.24 \pm 0.20_{\rm stat} \pm 0.37_{\rm syst}$	$5.11 \pm 0.20_{\rm stat} \pm 0.49_{\rm syst}$
OPAL (partial reco)	[252]	$6.17 \pm 0.28_{\rm stat} \pm 0.58_{\rm syst}$	$5.92 \pm 0.28_{\rm stat} \pm 0.68_{\rm syst}$
DELPHI (partial reco)	[253]	$5.00 \pm 0.14_{\rm stat} \pm 0.36_{\rm syst}$	$4.70 \pm 0.14_{\rm stat}\ ^{+0.36}_{-0.31}\ _{\rm syst}$
Belle (excl)	[254]	$4.73 \pm 0.24_{\rm stat} \pm 0.41_{\rm syst}$	$4.60 \pm 0.24_{\rm stat} \pm 0.42_{\rm syst}$
CLEO (excl)	[255]	$6.26 \pm 0.19_{\rm stat} \pm 0.38_{\rm syst}$	$6.09 \pm 0.19_{\rm stat} \pm 0.40_{\rm syst}$
DELPHI (excl)	[256]	$5.44 \pm 0.20_{\rm stat} \pm 0.43_{\rm syst}$	$5.90 \pm 0.20_{\rm stat} \pm 0.50_{\rm syst}$
BABAR (excl)	[249]	$4.77 \pm 0.04_{\rm stat} \pm 0.39_{\rm syst}$	$4.77 \pm 0.04_{\rm stat} \pm 0.39_{\rm syst}$
Average		$\mathbf{5.28 \pm 0.18}$	$\boldsymbol{\chi^2/\mathrm{dof} = 13/7}$ (CL=**6.8%**)

The average for $F(1)|V_{cb}|$ is determined by the two-dimensional combination of the results provided in Table 42. This allows the correlation between $F(1)|V_{cb}|$ and ρ^2 to be maintained. Figure 30(a) illustrates the average $F(1)|V_{cb}|$ and the measurements included in the average. Figure 30(b) provides a one-dimensional projection for illustrative purposes. The largest systematic errors correlated between measurements are owing to uncertainties on: R_b, the ratio of production cross-sections $\sigma_{b\overline{b}}/\sigma_{\rm had}$, the B^0 fraction at $\sqrt{s} = m_{Z^0}$, the branching fractions $\mathcal{B}(D^0 \to K^-\pi^+)$ and $\mathcal{B}(D^0 \to K^-\pi^+\pi^0)$, the correlated background from D^{**}, and the D^* form factor ratios R_1 and R_2. Together these uncertainties account for about two thirds of the systematic error. In all the measurements the total systematic errors are reduced with respect to the published values because the values and uncertainties assumed for parameters on which these measurements depend, for example R_1 and R_2, have since been better determined.

For a determination of $|V_{cb}|$, the form factor at zero recoil $F(1)$ needs to be computed. A possible choice is $F(1) = 0.919^{+0.030}_{-0.035}$ [257], which takes into account the QED correction(+0.7%), resulting in

$$|V_{cb}| = (39.2 \pm 0.7_{\rm exp} \pm 1.4_{\rm theo}) \times 10^{-3},$$

where the errors are from experiment and theory, respectively.

5.2.2 $\overline{B}^0 \to D^+\ell^-\overline{\nu}$

The average branching fraction $\mathcal{B}(\overline{B}^0 \to D^+\ell^-\overline{\nu})$ is determined by the combination of the results provided in Table 43. The error sources here are the same as discussed for $\mathcal{B}(\overline{B}^0 \to D^{*+}\ell^-\overline{\nu})$, but generally higher due to larger background levels, less stringent kinematic constraints, and larger kinematic suppression at the endpoint. Figure 29(b) illustrates the measurements and the resulting average.

Table 42: Average of $F(1)|V_{cb}|$ determined in the decay $\overline{B}^0 \to D^{*+}\ell^-\overline{\nu}$ and individual results, where "excl" and "partial reco" refer to full and partial reconstruction of the $\overline{B}^0 \to D^{*+}\ell^-\overline{\nu}$ decay, respectively. The fit for the average has $\chi^2/\mathrm{dof} = 31/14$ (CL=0.5%). The total correlation between the average $F(1)|V_{cb}|$ and ρ^2 is 0.46.

Experiment		$F(1)\lvert V_{cb}\rvert[10^{-3}]$ (rescaled) $F(1)\lvert V_{cb}\rvert[10^{-3}]$ (published)	ρ^2 (rescaled) ρ^2 (published)
ALEPH (excl)	[251]	$32.8 \pm 1.8_{\mathrm{stat}} \pm 1.3_{\mathrm{syst}}$ $31.9 \pm 1.8_{\mathrm{stat}} \pm 1.9_{\mathrm{syst}}$	$0.57 \pm 0.25_{\mathrm{stat}} \pm 0.12_{\mathrm{syst}}$ $0.37 \pm 0.26_{\mathrm{stat}} \pm 0.14_{\mathrm{syst}}$
OPAL (excl)	[252]	$37.2 \pm 1.6_{\mathrm{stat}} \pm 1.5_{\mathrm{syst}}$ $36.8 \pm 1.6_{\mathrm{stat}} \pm 2.0_{\mathrm{syst}}$	$1.28 \pm 0.21_{\mathrm{stat}} \pm 0.15_{\mathrm{syst}}$ $1.31 \pm 0.21_{\mathrm{stat}} \pm 0.16_{\mathrm{syst}}$
OPAL (partial reco)	[252]	$37.9 \pm 1.2_{\mathrm{stat}} \pm 2.4_{\mathrm{syst}}$ $37.5 \pm 1.2_{\mathrm{stat}} \pm 2.5_{\mathrm{syst}}$	$1.15 \pm 0.14_{\mathrm{stat}} \pm 0.30_{\mathrm{syst}}$ $1.12 \pm 0.14_{\mathrm{stat}} \pm 0.29_{\mathrm{syst}}$
DELPHI (partial reco)	[253]	$36.2 \pm 1.4_{\mathrm{stat}} \pm 2.3_{\mathrm{syst}}$ $35.5 \pm 1.4_{\mathrm{stat}}\ ^{+2.3}_{-2.4}{}_{\mathrm{syst}}$	$1.36 \pm 0.14_{\mathrm{stat}} \pm 0.27_{\mathrm{syst}}$ $1.34 \pm 0.14_{\mathrm{stat}}\ ^{+0.24}_{-0.22}{}_{\mathrm{syst}}$
Belle (excl)	[254]	$35.2 \pm 1.9_{\mathrm{stat}} \pm 1.7_{\mathrm{syst}}$ $35.8 \pm 1.9_{\mathrm{stat}} \pm 1.9_{\mathrm{syst}}$	$1.31 \pm 0.16_{\mathrm{stat}} \pm 0.11_{\mathrm{syst}}$ $1.45 \pm 0.16_{\mathrm{stat}} \pm 0.20_{\mathrm{syst}}$
CLEO (excl)	[255]	$42.7 \pm 1.3_{\mathrm{stat}} \pm 1.6_{\mathrm{syst}}$ $43.1 \pm 1.3_{\mathrm{stat}} \pm 1.8_{\mathrm{syst}}$	$1.47 \pm 0.09_{\mathrm{stat}} \pm 0.09_{\mathrm{syst}}$ $1.61 \pm 0.09_{\mathrm{stat}} \pm 0.21_{\mathrm{syst}}$
DELPHI (excl)	[256]	$37.2 \pm 1.8_{\mathrm{stat}} \pm 1.9_{\mathrm{syst}}$ $39.2 \pm 1.8_{\mathrm{stat}} \pm 2.3_{\mathrm{syst}}$	$1.13 \pm 0.15_{\mathrm{stat}} \pm 0.16_{\mathrm{syst}}$ $1.32 \pm 0.15_{\mathrm{stat}} \pm 0.33_{\mathrm{syst}}$
BABAR (excl)	[249]	$34.7 \pm 0.3_{\mathrm{stat}} \pm 1.1_{\mathrm{syst}}$ $34.7 \pm 0.3_{\mathrm{stat}} \pm 1.1_{\mathrm{syst}}$	$1.18 \pm 0.05_{\mathrm{stat}} \pm 0.03_{\mathrm{syst}}$ $1.18 \pm 0.05_{\mathrm{stat}} \pm 0.03_{\mathrm{syst}}$
Average		$\mathbf{36.0 \pm 0.6}$	$\mathbf{1.19 \pm 0.05}$

Table 43: Average of the branching fraction $\mathcal{B}(\overline{B}^0 \to D^+\ell^-\overline{\nu})$ and individual results.

Experiment		$\mathcal{B}(\overline{B}^0 \to D^+\ell^-\overline{\nu})[\%]$ (rescaled)	$\mathcal{B}(\overline{B}^0 \to D^+\ell^-\overline{\nu})[\%]$ (published)
ALEPH	[251]	$2.15 \pm 0.18_{\mathrm{stat}} \pm 0.37_{\mathrm{syst}}$	$2.35 \pm 0.18_{\mathrm{stat}} \pm 0.44_{\mathrm{syst}}$
CLEO	[258]	$2.07 \pm 0.13_{\mathrm{stat}} \pm 0.16_{\mathrm{syst}}$	$2.20 \pm 0.13_{\mathrm{stat}} \pm 0.18_{\mathrm{syst}}$
Belle	[259]	$2.13 \pm 0.12_{\mathrm{stat}} \pm 0.39_{\mathrm{syst}}$	$2.13 \pm 0.12_{\mathrm{stat}} \pm 0.41_{\mathrm{syst}}$
Average		$\mathbf{2.09 \pm 0.18}$	$\boldsymbol{\chi^2/\mathrm{dof} = 0.04/2}$ (CL=**98%**)

The average for $G(1)|V_{cb}|$ is determined by the two-dimensional combination of the results provided in Table 44. Figure 31 (a) provides a one-dimensional projection for illustrative purposes, (b) illustrates the average $G(1)|V_{cb}|$ and the measurements included in the average.

For a determination of $|V_{cb}|$, the form factor at zero recoil $G(1)$ needs to be computed. A possible choice is $G(1) = 1.04 \pm 0.01_{\mathrm{power}} \pm 0.01_{\mathrm{pert}}$ [260], which takes into account the QED correction(+0.7%), resulting in

$$|V_{cb}| = (40.8 \pm 4.3_{\mathrm{exp}} \pm 0.6_{\mathrm{theo}}) \times 10^{-3},$$

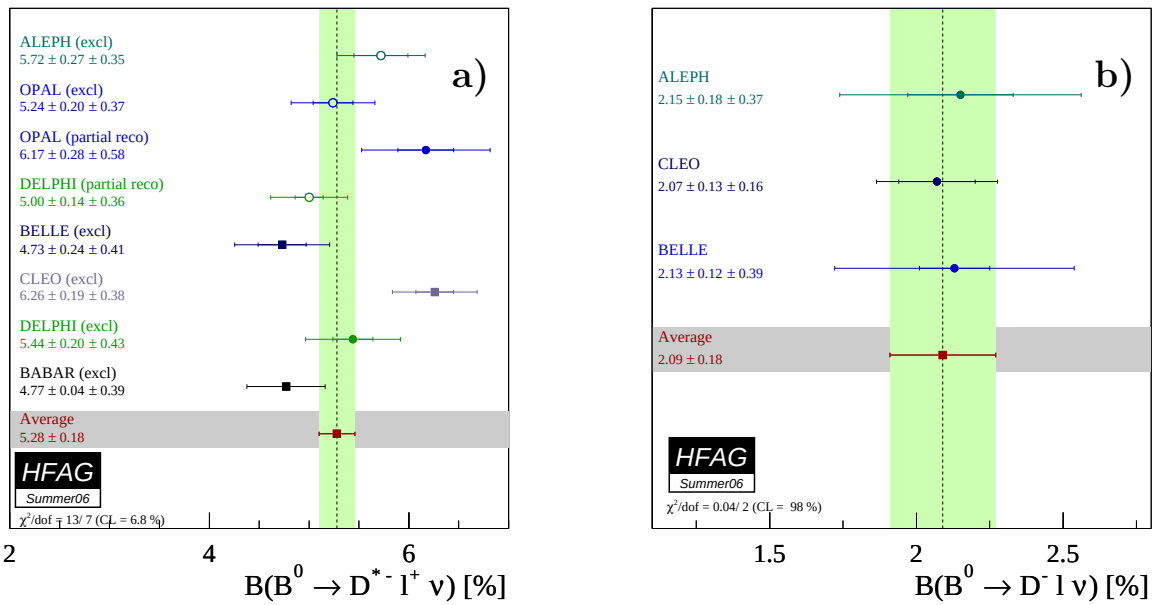

Figure 29: Average branching fraction of exclusive semileptonic B decays (a) $\overline{B}^0 \to D^{*+}\ell^-\overline{\nu}$ and (b) $\overline{B}^0 \to D^+\ell^-\overline{\nu}$ and individual results, where "excl" and "partial reco" refer to full and partial reconstruction of the $\overline{B}^0 \to D^{*+}\ell^-\overline{\nu}$ decay, respectively.

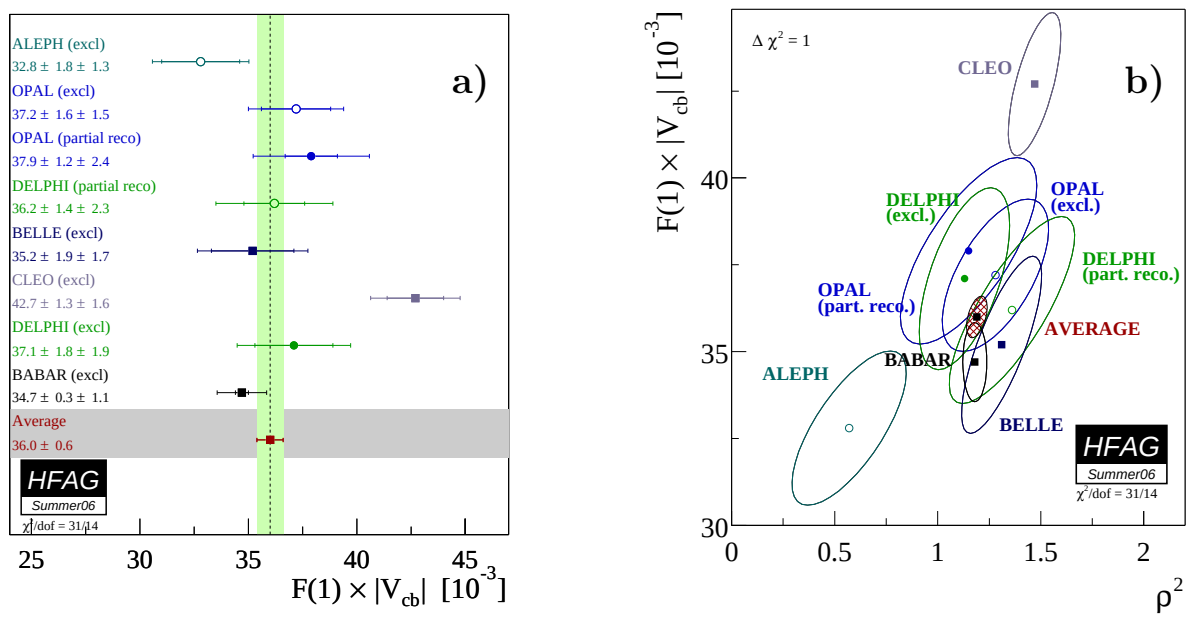

Figure 30: (a) Illustration of $F(1)|V_{cb}|$ vs. ρ^2. The error ellipses correspond to $\Delta\chi^2 = 1$ (CL=39%). (b) Illustration of the average $F(1)|V_{cb}|$ and rescaled measurements of exclusive $\overline{B}^0 \to D^{*+}\ell^-\overline{\nu}$ decays determined in a two-dimensional fit, where "excl" and "partial reco" refer to full and partial reconstruction.

where the errors are from experiment and theory, respectively.

Table 44: Average of $G(1)|V_{cb}|$ determined in the decay $\overline{B}^0 \to D^+\ell^-\overline{\nu}$ and individual results. The fit for the average has $\chi^2/\text{dof} = 0.3/4$. The total correlation between the average $G(1)|V_{cb}|$ and ρ^2 is 0.93.

Experiment	$G(1)\lvert V_{cb}\rvert[10^{-3}]$ (rescaled) $G(1)\lvert V_{cb}\rvert[10^{-3}]$ (published)	ρ^2 (rescaled) ρ^2 (published)
ALEPH [251]	$39.0 \pm 11.8_{\text{stat}} \pm 6.2_{\text{syst}}$ $31.1 \pm 9.9_{\text{stat}} \pm 8.6_{\text{syst}}$	$0.96 \pm 0.98_{\text{stat}} \pm 0.36_{\text{syst}}$ $0.20 \pm 0.98_{\text{stat}} \pm 0.50_{\text{syst}}$
CLEO [258]	$44.8 \pm 5.9_{\text{stat}} \pm 3.5_{\text{syst}}$ $44.8 \pm 6.1_{\text{stat}} \pm 3.7_{\text{syst}}$	$1.27 \pm 0.25_{\text{stat}} \pm 0.14_{\text{syst}}$ $1.30 \pm 0.27_{\text{stat}} \pm 0.14_{\text{syst}}$
Belle [259]	$41.1 \pm 4.4_{\text{stat}} \pm 5.2_{\text{syst}}$ $41.1 \pm 4.4_{\text{stat}} \pm 5.1_{\text{syst}}$	$1.12 \pm 0.22_{\text{stat}} \pm 0.14_{\text{syst}}$ $1.12 \pm 0.22_{\text{stat}} \pm 0.14_{\text{syst}}$
Average	$\mathbf{42.4 \pm 4.5}$	$\mathbf{1.17 \pm 0.18}$

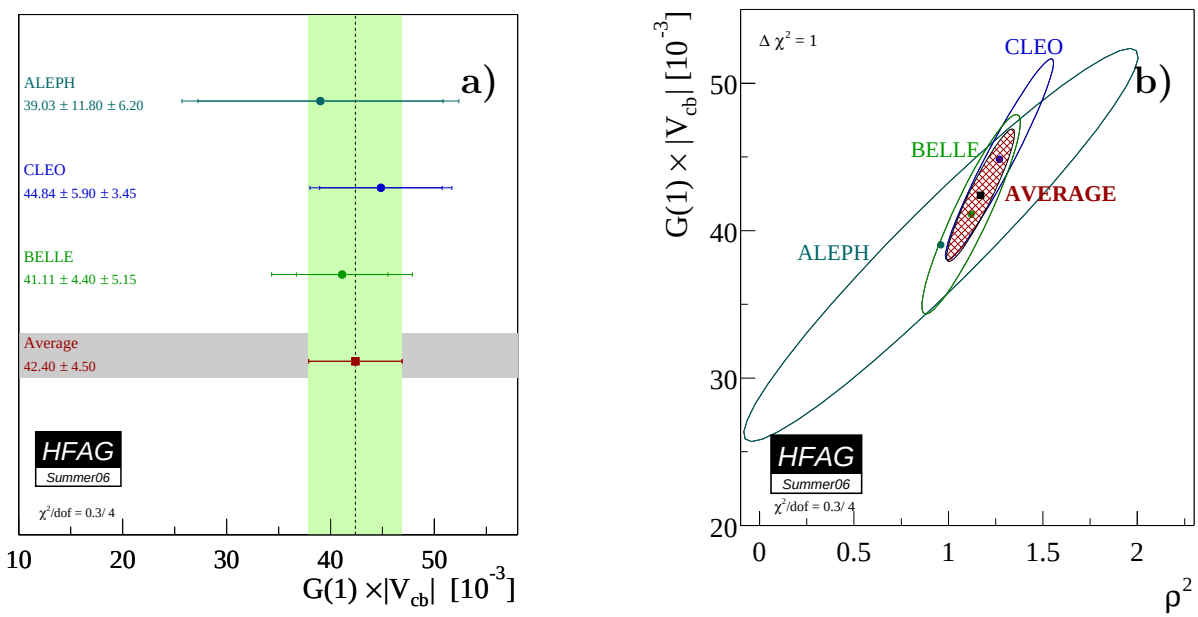

Figure 31: (a) Illustration of $G(1)|V_{cb}|$ vs. ρ^2. The error ellipses correspond to $\Delta\chi^2 = 1$. (b) Illustration of the average $G(1)|V_{cb}|$ and rescaled measurements of exclusive $\overline{B}^0 \to D^+\ell^-\overline{\nu}$ decays determined in a two-dimensional fit.

5.3 Inclusive CKM-favored decays

5.3.1 Inclusive Semileptonic Branching Fraction for $B^0/B^+ \to X\ell\nu_\ell$

The average of the inclusive semileptonic branching fraction has undergone revision. We have gone from averaging measurements of full branching fractions, which relied on various models, to averaging partial branching fractions, which are relatively model independent. The subsequent average of the partial branching fractions is extrapolated to the full phase space using a model-independent approach.

We use measurements that require the momentum of the prompt charged lepton ($p_{\rm cms}$) to be greater than 0.6 GeV/c, as measured in the rest frame of either the B-meson or $\Upsilon(4S)$ [18]. The measurements and average are given in Table 45 and plotted in Figure 32. We extrapolate from the partial to full branching fraction using a factor derived from a global fit [261] used to extract HQET parameters in the Kinetic Scheme [262]. That fit, which doesn't include any of the measurements used in our average, yielded the extrapolation factor $1.0495 \pm 0.0005 \pm 0.0010$. The first error includes experiment and theory uncertainties as got from the fit. The second error is assigned as an additional theoretical uncertainty for the ratio $\Gamma_{\rm sl}(0.6)/\Gamma_{\rm sl}(0.0)$ - for the total width ($\Gamma_{\rm sl}(0.0)$) this uncertainty is typically 1.5%, on the recommendation of the authors of the fit, for the ratio it is estimated to be 0.1%. Finally the full branching fraction is extracted as $\mathcal{B}(B^0/B^+ \to X\ell\nu_\ell) = (10.75 \pm 0.16)\%$.

Table 45: Average of the partial semileptonic branching fractions $\mathcal{B}(B^0/B^+ \to X\ell\nu_\ell)(p_{\rm cms} > 0.6\,{\rm GeV/c})$ and the full branching fraction extrapolated from the average. In parentheses we identify the type of analysis performed: ℓ-tag and e-tag refer to inclusive analyses where both electrons and muons or just electrons are reconstructed, respectively, and $B_{\rm reco}$-tag refers to analyses at the $\Upsilon(4S)$ where one of the B-mesons is fully reconstructed in a hadronic mode with the lepton reconstructed from the other B decay.

Experiment		$\mathcal{B}(B^0/B^+ \to X\ell\nu_\ell)[\%]$ (rescaled) ($p_{\rm cms} > 0.6\,{\rm GeV/c}$)
ARGUS (e-tag)	[263]	$9.17 \pm 0.50 \pm 0.33$
Belle (ℓ-tag)	[264]	$10.32 \pm 0.11 \pm 0.46$
CLEO (e-tag)	[265]	$10.24 \pm 0.08 \pm 0.22$
BABAR (e-tag)	[266]	$10.37 \pm 0.06 \pm 0.23$
BABAR (B_{reco}-tag)	[267]	$10.03 \pm 0.19 \pm 0.33$
Belle (B_{reco}-tag)	[268]	$10.28 \pm 0.18 \pm 0.24$
Average at ($p_{\rm cms} > 0.6\,{\rm GeV/c}$)		$\mathbf{10.24 \pm 0.15}$ $\boldsymbol{\chi^2}$**/dof = 4.2/5** (CL=**52%**)
$\mathcal{B}_{tot}(B^0/B^+ \to X\ell\nu_\ell)$ (%)		$\mathbf{10.75 \pm 0.16}$

5.3.2 Ratio of $\mathcal{B}(B^+ \to X\ell^+\nu_\ell)$ to $\mathcal{B}(B^0 \to X^-\ell^+\nu_\ell)$

The total width of semileptonic B-meson decays is expected to be the same for both neutral and charged channels. Therefore the ratio of the branching fractions, R_{+0}, should be equivalent to the ratio of the B-meson lifetimes τ_{B^+}/τ_{B^0}, where

$$R_{+0} = \frac{\mathcal{B}(B^+ \to X\ell^+\nu_\ell)}{\mathcal{B}(B^0 \to X^-\ell^+\nu_\ell)}.$$

Recently both Babar and Belle reported precise measurements of R_{+0}, using a "$B_{\rm reco}$"-tagged sample, for which we provide an average. The measurements and average are listed in Table 46 and plotted in Figure 32. The average, 1.076 ± 0.034 is in agreement with the ratio of lifetimes, 1.076 ± 0.008 [269].

[18] The difference in reference frames has a negligible impact.

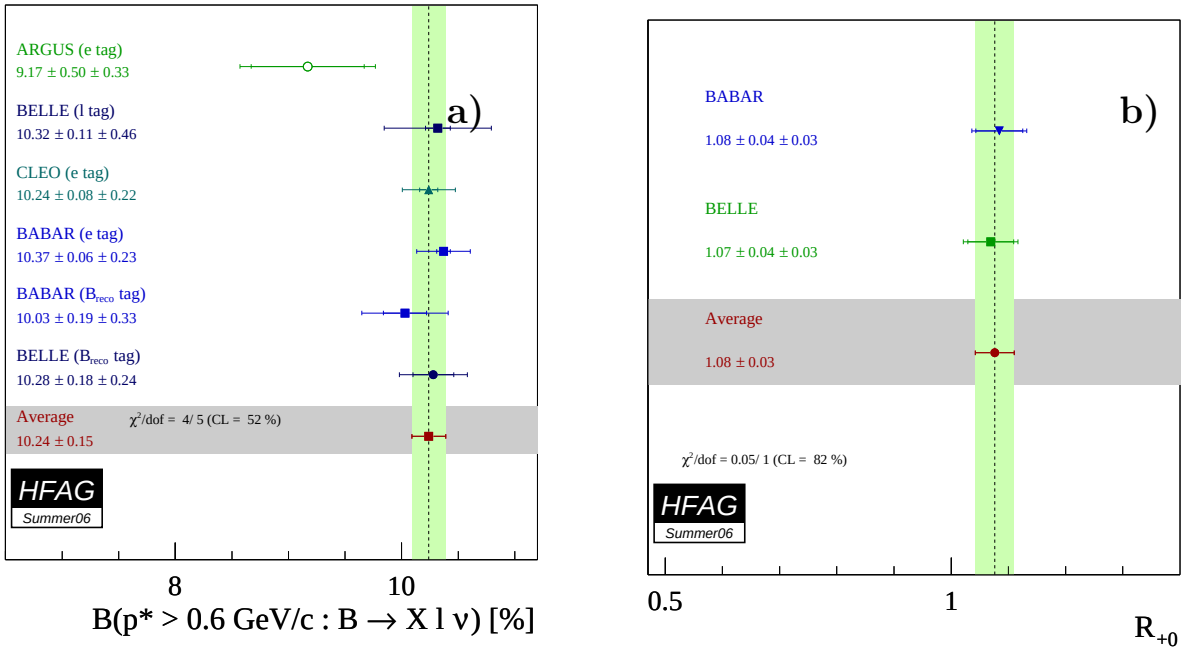

Figure 32: (a) Measurements of $\mathcal{B}(B^0/B^+ \to X\ell\nu_\ell)$ and their average. (b) Measurements of the ratio of the branching fractions R_{+0} and their average. In parenthesis we identify the type of analysis performed: l-tag and e-tag refer to inclusive analyses where both electrons and muons or just the former are reconstructed, respectively, and B_{reco}-tag refer to analyses at the $\Upsilon(4S)$ where one of the B-mesons is fully reconstructed in a hadronic mode with the lepton reconstructed from the other B decay.

Table 46: Individual measurements and average of the ratio of the branching fractions R_{+0}.

Experiment	R_{+0}
BABAR [267]	$1.084 \pm 0.041 \pm 0.025$
Belle [268]	$1.069 \pm 0.040 \pm 0.026$
Average	$\mathbf{1.076 \pm 0.034}$ $\boldsymbol{\chi^2/\text{dof} = 0.05/1}$ **CL=82%**

5.3.3 Branching Fractions for $B^+ \to X\ell^+\nu_\ell$ and $B^0 \to X^-\ell^+\nu_\ell$

For the first time we provide averages of the branching fractions of $B^+ \to X\ell^+\nu_\ell$ and $B^0 \to X^-\ell^+\nu_\ell$ separately, using the available measurements at the $\Upsilon(4S)$. We include the measurements listed in the Review of Particle Physics [4] and as well as the latest measurements made by Belle and Babar that utilise the full reconstruction B-meson tag [267, 268]. In contrast to the B admixture average, averages are made of the full branching fraction since the CLEO and ARGUS papers do not stipulate partial branching fractions. The measurements and averages are given in Tables 47 and 48 and plotted in Figure 33 for $B^+ \to X\ell^+\nu_\ell$ and $B^0 \to X^-l^+\nu_\ell$, respectively.

Table 47: Individual measurements and average of the total semileptonic branching fraction $\mathcal{B}(B^+ \to X\ell^+\nu_\ell)$. "$\ell$-tag" and "$B_{reco}$-tag" indicate analysis experimental technique.

Experiment	$\mathcal{B}_{tot}(B^+ \to X\ell^+\nu_\ell)[\%]$ (rescaled)
CLEO (ℓ-tag) [270]	$10.25 \pm 0.57 \pm 0.66$
BABAR (B_{reco}-tag) [267]	$10.90 \pm 0.27 \pm 0.39$
Belle (B_{reco}-tag) [268]	$11.17 \pm 0.25 \pm 0.28$
Average	$\mathbf{10.99 \pm 0.28}$ $\boldsymbol{\chi^2/\mathrm{dof} = 1.0/2}$ **CL=61%**

Table 48: Individual measurements and average of the total semileptonic branching fraction $\mathcal{B}(B^0 \to X^-\ell^+\nu)$. "partial-tag" and "$B_{reco}$-tag" indicate analysis experimental technique.

Experiment	$\mathcal{B}_{tot}(B^0 \to X^-\ell^+\nu)[\%]$ (rescaled)
CLEO (partial-tag) [271]	$9.9 \pm 3.0 \pm 0.9$
ARGUS (partial-tag) [272]	$9.3 \pm 1.1 \pm 1.5$
CLEO (partial-tag) [270]	$10.78 \pm 0.60 \pm 0.69$
BABAR (B_{reco}-tag) [267]	$10.14 \pm 0.28 \pm 0.33$
Belle (B_{reco}-tag) [268]	$10.46 \pm 0.30 \pm 0.23$
Average	$\mathbf{10.33 \pm 0.28}$ $\boldsymbol{\chi^2/\mathrm{dof} = 0.9/4}$ **CL= 92%**

5.3.4 $|V_{cb}|$ Determined from $B \to X\ell\overline{\nu}$

The magnitude of the CKM matrix $|V_{cb}|$ can be determined from the branching fraction of inclusive charmed semileptonic B-meson decays $\mathcal{B}(\overline{B} \to X_c\ell\overline{\nu})$ and with parameters that describe the motion of the b-quark in the B-meson. These parameters, within the framework of the Heavy Quark Expansion (HQE), include the b-quark mass, m_b. Phenomenology of these decays is reviewed in many papers [273]. In practice $|V_{cb}|$, m_b, and other parameters are determined simultaneously from a *global* fit to data of inclusive semileptonic and radiative B-meson decays. These data include rates and moments of energy and hadronic mass spectra measured as a function of cut-offs in those variables. HFAG has yet to quote an average value of $|V_{cb}|$ obtained from such fits. To date three types of global fits have been performed; these differ in the choice of scheme, either *pole*, "1S" or *kinetic*, used to define the b-quark mass m_b. T able 49 lists the results of global fits performed to date. We are working to determine $|V_{cb}|$ from global fits in both the "1S" and *kinetic* schemes. The fits will utilise a common set of measurements. Fits in the t pole scheme are disfavoured due to the poor convergence of series expansions in that scheme.

Updated values for the parameters m_b and μ_π^2 are taken from the Buchmüller and Flächer global fit and used below in the determination of $|V_{ub}|$ from inclusive decays. Their fit uses many different measurements: BABAR [279–283], Belle [284–286], CLEO [287–289] CDF [290], and

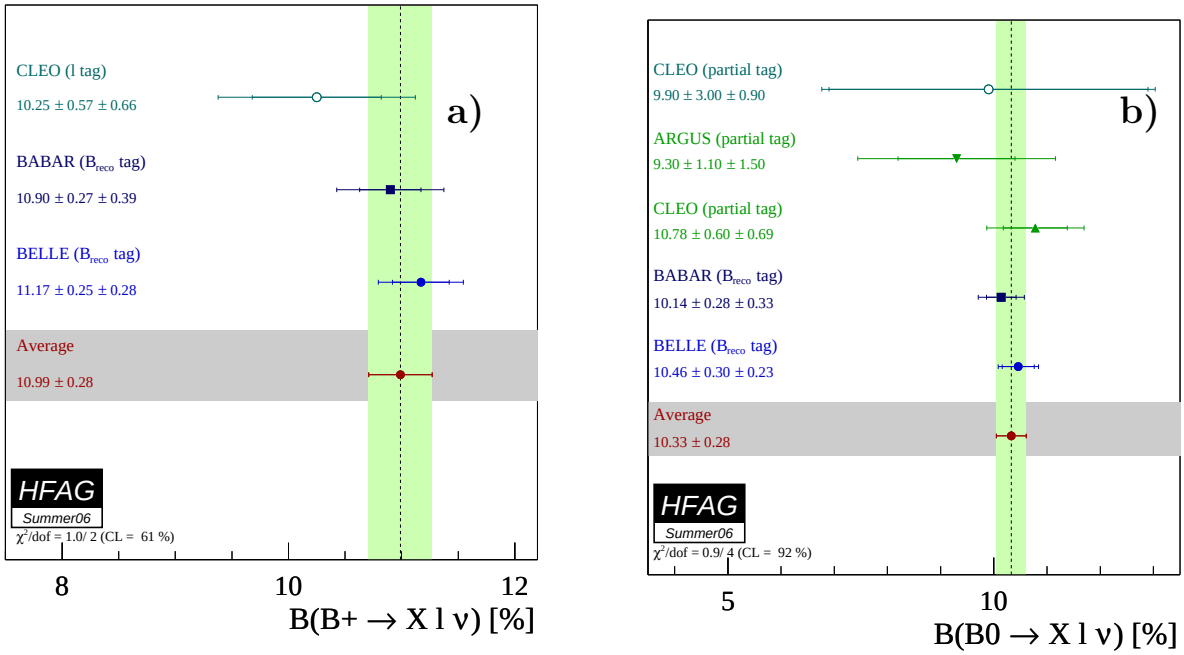

Figure 33: (a) Measurements of the total semileptonic branching fraction $\mathcal{B}(B^+ \to X\ell^+\nu_\ell)$ and their average. (b) Individual measurements and average of the total semileptonic branching fraction $\mathcal{B}(B^0 \to X^-\ell^+\nu)$. "$\ell$-tag", "partial-tag" and "B_{reco}-tag" indicate analysis experimental technique.

DELPHI [291]. We use their result since it uses most of the currently available measurements.

5.4 Exclusive CKM-suppressed decays

Several new measurements of the exclusive decay $\overline{B} \to \pi\ell\overline{\nu}$ were presented at the 2006 Summer conferences. Their precision is at a level that calls for improved calculations of the form factors and in particular their normalization.

Here we list results on exclusive semileptonic branching fractions and determinations of $|V_{ub}|$ based on $\overline{B} \to \pi\ell\overline{\nu}$ decays. The measurements are based on two different event selections: tagged events, in which case the second B meson in the event is fully reconstructed in either a hadronic decay ("B_{reco}") or in a CKM-favored semileptonic decay ("SL"); and untagged events, in which case the selection infers the momentum of the undetected neutrino based on measurements of the total momentum sum of detected particles and knowledge of the initial state. The results for the full and partial branching fraction are given in Table 50 and shown in Figure 34.

When averaging these results, systematic uncertainties due to external inputs, e.g., form factor shapes and background estimates from the modeling of $\overline{B} \to X_c\ell\overline{\nu}$ and $\overline{B} \to X_u\ell\overline{\nu}$ decays, are treated as fully correlated (in the sense of Eq. 10). Uncertainties due to experimental reconstruction effects are treated as fully correlated among measurements from a given experiment. Varying the assumed dependence of the quoted errors on the measured value (see Eq. 8) for error sources where the dependence was not obvious had no significant impact.

The determination of $|V_{ub}|$ from the $\overline{B} \to \pi\ell\overline{\nu}$ decays is shown in Table 51 and uses our average for the branching fraction given in Table 50. Two theoretical approaches are used:

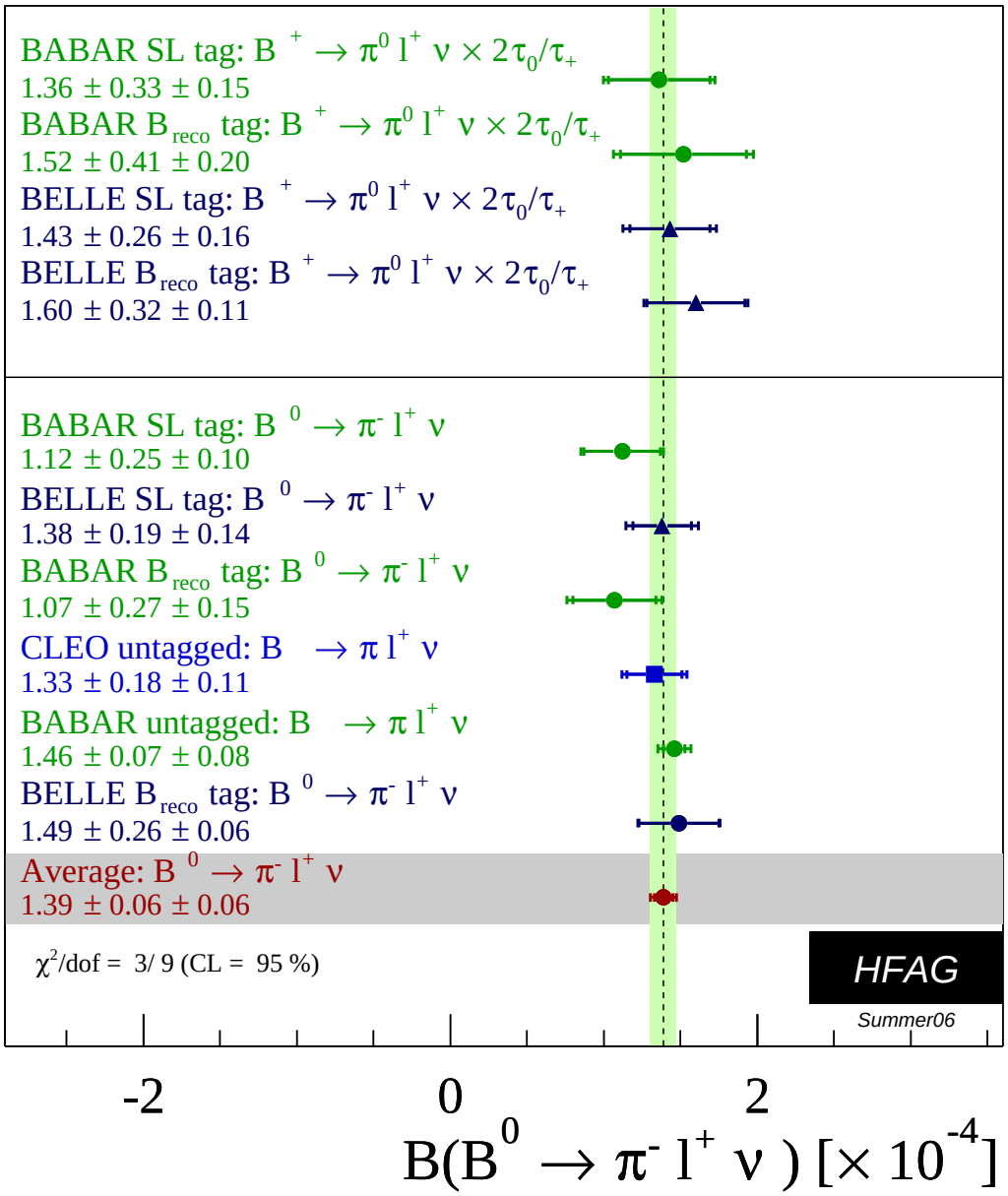

Figure 34: Summary of exclusive determinations of $\mathcal{B}(\overline{B} \to \pi \ell \overline{\nu})$ and their average. Measured branching fractions for $B \to \pi^0 l \nu$ have been multiplied by $2 \times \tau_{B^0}/\tau_{B^+}$ in accordance with isospin symmetry. The labels "B_{reco}" and "SL" refer to type of B decay tag used in a measurement. "untagged" refers to an untagged measurement.

Table 49: *Global fit* results for the *pole*, "1S" and *kinetic* schemes.

Source (Scheme)	Measurements
Battaglia *et al.* (Kinetic) [274]	$\lvert V_{cb}\rvert = (41.9 \pm 0.7_{meas} \pm 0.6_{fit} \pm 0.4_{pert}) \times 10^{-3}$ $m_b^{\rm kin} = 4.59 \pm 0.08_{fit} \pm 0.01_{syst.}\,{\rm GeV/c^2}$
Battaglia *et al.* (Pole) [274]	$\lvert V_{cb}\rvert = (41.3 \pm 0.7_{meas} \pm 0.7_{fit} \pm 0.2_{nl} \pm 0.9_{pert}) \times 10^{-3}$ $\overline{\Lambda} = 0.40 \pm 0.10_{fit} \pm 0.02_{syst.}\,{\rm GeV/c^2}$
CLEO (Pole) [275] (1S)	$\lvert V_{cb}\rvert = (40.8 \pm 0.5_{\Gamma_{\rm SL}} \pm 0.4_{\lambda_1,\overline{\Lambda}} \pm 0.9_{theory}) \times 10^{-3}$ $\overline{\Lambda} = 0.39 \pm 0.03_{stat} \pm 0.06_{syst.} \pm 0.12_{theory}\,{\rm GeV/c^2}$ $m_b^{\rm 1S} = 4.82 \pm 0.07_{exp} \pm 0.11_{theory}\,{\rm GeV/c^2}$
BABAR (Kinetic) [276]	$\lvert V_{cb}\rvert = (41.4 \pm 0.4_{exp} \pm 0.4_{HQE} \pm 0.6_{theory}) \times 10^{-3}$ $m_b^{\rm kin} = 4.61 \pm 0.05_{exp} \pm 0.04_{HQE} \pm 0.02_{theory}\,{\rm GeV/c^2}$
Bauer *et al.* (1S) [277]	$\lvert V_{cb}\rvert = (41.4 \pm 0.6 \pm 0.1_{\tau_B}) \times 10^{-3}$ $m_b^{\rm 1S} = 4.68 \pm 0.03\,{\rm GeV/c^2}$
Buchmüller & Flächer (Kinetic) [261]	$\lvert V_{cb}\rvert = (41.96 \pm 0.23_{exp} \pm 0.35_{HQE} \pm 0.59_{\Gamma_{\rm SL}}) \times 10^{-3}$ $m_b^{\rm kin} = 4.59 \pm 0.025_{exp} \pm 0.030_{HQE}\,{\rm GeV/c^2}$
Belle (Kinetic) [278]	$\lvert V_{cb}\rvert = (41.93 \pm 0.65_{fit} \pm 0.48_{\alpha_s} \pm 0.68_{theory}) \times 10^{-3}$ $m_b^{\rm kin} = 4.564 \pm 0.076\,{\rm GeV/c^2}$
Belle ($1S$) [278]	$\lvert V_{cb}\rvert = (41.5 \pm 0.5_{fit} \pm 0.2_{\tau_B}) \times 10^{-3}$ $m_b^{\rm 1S} = 4.73 \pm 0.05\,{\rm GeV/c^2}$

Lattice QCD (quenched and unquenched) and QCD sum rules. Lattice calculations of the Form Factors (FF) are limited to small hadron momenta, i.e. large q^2, while calculations based on light cone sum rules are restricted to small q^2. More precise calculations of the FF, in particular their normalization, are needed to reduce the overall uncertainties.

Branching fractions for other $\overline{B} \to X_u \ell \overline{\nu}$ decays are given in Table 52. At this time the determination of $|V_{ub}|$ from these other channels looks less promising than for $\overline{B} \to \pi \ell \overline{\nu}$.

5.5 Inclusive CKM-suppressed decays

Our last update [269] provided a best value of $|V_{ub}|$ that was the first to be based on common inputs in a consistent framework. In this update we use two theory prescriptions in addition to BLNP [306], namely DGE [307] and BLL [308]. We determine an average for $|V_{ub}|$ for each of BLNP, DGE, and BLL, and do not advocate the use of one method over another.

The large background from $\overline{B} \to X_c \ell \overline{\nu}$ decays is the chief experimental limitation in determinations of $|V_{ub}|$. Cuts designed to reject this background limit the acceptance for $\overline{B} \to X_u \ell \overline{\nu}$ decays. The calculation of partial rates for these restricted acceptances is more complicated and requires substantial theoretical machinery. BLNP and DGE authors have provided us codes that allows us to perform the calculation for all the limited regions of phase space covered by measurements. BLL provides calculations for measurements that cut on the dilepton mass squared and hadronic mass.

In the averages performed the systematic errors associated with the modeling of $\overline{B} \to X_c \ell \overline{\nu}$ and $\overline{B} \to X_u \ell \overline{\nu}$ decays and the theoretical uncertainties are taken as fully correlated

Table 50: Summary of exclusive determinations of $\mathcal{B}(\overline{B} \to \pi\ell\overline{\nu})$. The errors quoted correspond to statistical and systematic uncertainties, respectively. Measured branching fractions for $B \to \pi^0 l\nu$ have been multiplied by $2 \times \tau_{B^0}/\tau_{B^+}$ in accordance with isospin symmetry. The labels "B_{reco}" and "SL" tags refer to the type of B decay tag used in a measurement, and "untagged" refers to an untagged measurement.

	$\mathcal{B}[10^{-4}]$	$\mathcal{B}(q^2 > 16\,\mathrm{GeV}^2/c^2)[10^{-4}]$	$\mathcal{B}(q^2 < 16\,\mathrm{GeV}^2/c^2)[10^{-4}]$
CLEO π^+, π^0 [292]	$1.33 \pm 0.18 \pm 0.11$	$0.25 \pm 0.09 \pm 0.05$	$1.08 \pm 0.16 \pm 0.10$
BABAR π^+ [293]	$1.46 \pm 0.07 \pm 0.08$	$0.38 \pm 0.04 \pm 0.03$	$1.09 \pm 0.06 \pm 0.07$
Average of untagged	$\mathbf{1.43 \pm 0.07 \pm 0.09}$	$\mathbf{0.35 \pm 0.04 \pm 0.04}$	$\mathbf{1.09 \pm 0.06 \pm 0.07}$
BELLE SL π^+ [294]	$1.38 \pm 0.19 \pm 0.14$	$0.36 \pm 0.10 \pm 0.04$	$1.02 \pm 0.16 \pm 0.11$
BELLE SL π^0 [294]	$1.43 \pm 0.26 \pm 0.16$	$0.37 \pm 0.15 \pm 0.04$	$1.06 \pm 0.22 \pm 0.11$
BABAR SL π^+ [295]	$1.12 \pm 0.25 \pm 0.12$	$0.29 \pm 0.15 \pm 0.04$	$0.83 \pm 0.22 \pm 0.08$
BABAR SL π^0 [295]	$1.36 \pm 0.33 \pm 0.19$	$0.19 \pm 0.22 \pm 0.07$	$1.17 \pm 0.30 \pm 0.11$
BABAR B_{reco} π^+ [295]	$1.07 \pm 0.27 \pm 0.17$	$0.65 \pm 0.20 \pm 0.13$	$0.42 \pm 0.18 \pm 0.05$
BABAR B_{reco} π^0 [295]	$1.52 \pm 0.41 \pm 0.20$	$0.48 \pm 0.22 \pm 0.11$	$1.04 \pm 0.35 \pm 0.15$
BELLE B_{reco} π^+ [296]	$1.49 \pm 0.20 \pm 0.16$	n/a	n/a
BELLE B_{reco} π^0 [296]	$1.60 \pm 0.32 \pm 0.11$	n/a	n/a
Average of tagged	$\mathbf{1.35 \pm 0.10 \pm 0.07}$	$\mathbf{0.36 \pm 0.06 \pm 0.03}$	$\mathbf{0.83 \pm 0.09 \pm 0.06}$
Average	$\mathbf{1.39 \pm 0.06 \pm 0.06}$	$\mathbf{0.35 \pm 0.03 \pm 0.03}$	$\mathbf{0.97 \pm 0.05 \pm 0.05}$

among all measurements in the sense of Eq. 10. Reconstruction-related uncertainties are taken as fully correlated within a given experiment. From the three results quoted in Ref. [309], only one is used in the average, as they are all based on the same dataset and are highly correlated. Specifically we use the M_X analysis result for BLNP and DGE averages, and the M_X, q^2 analysis result for the BLL average. The other experimental results have negligible statistical correlations. The assumed dependence of the quoted error on the measured value was input for each source of error, as discussed in section 2. Measurements of partial decay rates for $\overline{B} \to X_u\ell\overline{\nu}$ transitions from $\Upsilon(4S)$ decays are given in Table 53.

Recently BABAR measured $|V_{ub}|$ using the prescription of Leibovich, Low, and Rothstein (LLR) [310]. LLR reduces model dependence by combining data of the hadronic mass spectrum from $B \to X_u\ell\overline{\nu}$ decays with that of the photon energy spectrum from $B \to X_s\gamma$ decays [311] thus eliminating the need for a model of the shape function, which is necessary, for example, in BLNP. However shape function model uncertainties are not altogether eliminated as they still enter via the signal models used for the determination of efficiency. In principle other measurements of spectra of $B \to X_u\ell\overline{\nu}$ could utilise the available BABAR measurement of the photon energy spectrum in the rest frame of the B-meson to extract $|V_{ub}|$ using LLR, we've considered this undertaking, however it is not yet practical. Later, for completeness, we provide a comparison of the LLR-based $|V_{ub}|$ with our BLNP, DGE and BLL averages.

5.5.1 BLNP

BLNP, which stands for Bosch, Lange, Neubert and Paz [306, 319–322], provides theoretical expressions for the triple differential $B \to X_u l^- \nu$ decay rate incorporating all known contri-

Table 51: Determinations of $|V_{ub}|$ based on the average total and partial $\overline{B} \to \pi\ell\overline{\nu}$ decay branching fraction stated in Table 50. The first uncertainty is experimental, and the second is from theory. The full or partial $\mathcal{B}$ are used as indicated.

Method	$\lvert V_{ub}\rvert[10^{-3}]$
LCSR, full q^2 [297]	$3.43 \pm 0.10^{+0.67}_{-0.42}$
LCSR, $q^2 < 16\,\mathrm{GeV}^2/c^2$ [297]	$3.41 \pm 0.13^{+0.56}_{-0.38}$
HPQCD, full q^2 [298]	$3.89 \pm 0.12^{+0.84}_{-0.51}$
HPQCD, $q^2 > 16\,\mathrm{GeV}^2/c^2$ [298]	$3.97 \pm 0.25^{+0.59}_{-0.41}$
FNAL, full q^2 [299]	$3.82 \pm 0.12^{+0.88}_{-0.52}$
FNAL, $q^2 > 16\,\mathrm{GeV}^2/c^2$ [299]	$3.55 \pm 0.22^{+0.61}_{-0.40}$
APE, full q^2 [300]	$3.61 \pm 0.11^{+1.11}_{-0.57}$
APE, $q^2 > 16\,\mathrm{GeV}^2/c^2$ [300]	$3.58 \pm 0.22^{+1.37}_{-0.63}$

Table 52: Summary of branching fractions to $\mathcal{B}(\overline{B} \to X\ell\overline{\nu})$ decays other than $\overline{B} \to \pi\ell\overline{\nu}$. The errors quoted correspond to statistical and systematic uncertainties, respectively. Where a third uncertainty is quoted, it corresponds to uncertainties from form factor shapes.

Experiment	Mode	$\mathcal{B}[10^{-4}]$
CLEO [301]	$B^0 \to \rho^-\ell\overline{\nu}$	$2.69 \pm 0.41\ ^{+\ 0.35}_{-\ 0.40}\ \pm 0.50$
BABAR [302]	$B^0 \to \rho^-\ell\overline{\nu}$	$2.57 \pm 0.52 \pm 0.59$
BABAR [303]	$B^0 \to \rho^-\ell\overline{\nu}$	$3.29 \pm 0.42 \pm 0.47 \pm 0.60$
BABAR [293]	$B^0 \to \rho^-\ell\overline{\nu}$	$2.14 \pm 0.21 \pm 0.51 \pm 0.28$
BELLE [294]	$B^0 \to \rho^-\ell\overline{\nu}$	$2.17 \pm 0.54 \pm 0.31 \pm 0.08$
BELLE [294]	$B^+ \to \rho^0\ell\overline{\nu}$	$1.33 \pm 0.23 \pm 0.17 \pm 0.03$
BELLE [304]	$B^+ \to \omega\ell\overline{\nu}$	$1.3\ \pm 0.4\ \pm 0.2\ \pm 0.3$
CLEO [292]	$B^+ \to \eta\ell\overline{\nu}$	$0.84 \pm 0.31 \pm 0.16 \pm 0.09$
BABAR [305]	$B^+ \to \eta\ell\overline{\nu}$	$0.84 \pm 0.27 \pm 0.21$
BABAR [305]	$B^+ \to \eta'\ell\overline{\nu}$	$0.33 \pm 0.60 \pm 0.30$

butions whilst smoothly interpolating between the "shape-function region" of large hadronic energy and small invariant mass, and the "OPE region" in which all hadronic kinematical variables scale with M_B. BLNP assign uncertainties for the b-quark mass which enters through the leading shape function, sub-leading shape function forms, possible weak annihilation contribution, and for matching scales. The extracted values of $|V_{ub}|$ for each measurement along with their average are given in Table 54 and illustrated in Figure 35. The breakdown of the uncertainty on the average is given in Table 55. The error on the b-quark mass is the source of the largest uncertainty while the uncertainty assigned for the matching scales is a close second.

5.5.2 DGE

DGE, which stands for Dressed Gluon Exponentiation [307], is a framework where the on-shell b-quark calculation, converted into hadronic variables, is directly used as an approximation to

Table 53: Summary of inclusive determinations of partial branching fractions for $B \to X_u l\nu$ decays. The errors quoted on $\Delta\mathcal{B}$ correspond to statistical and systematic uncertainties, respectively. The $s_{\rm h}^{\rm max}$ variable is described in Ref. [312]

Measurement	Accepted region	$\Delta\mathcal{B}[10^{-4}]$
CLEO [313]	$E_e > 2.1\,\mathrm{GeV}$	$3.3 \pm 0.2 \pm 0.7$
BABAR [314]	$E_e > 2.0\,\mathrm{GeV}$, $s_{\rm h}^{\rm max} < 3.5\,\mathrm{GeV}^2$	$4.4 \pm 0.4 \pm 0.4$
BABAR [315]	$E_e > 2.0\,\mathrm{GeV}$	$5.7 \pm 0.4 \pm 0.5$
BELLE [316]	$E_e > 1.9\,\mathrm{GeV}$	$8.5 \pm 0.4 \pm 1.5$
BABAR [317]	$M_X < 1.7\,\mathrm{GeV}/c^2, q^2 > 8\,\mathrm{GeV}^2/c^2$	$8.7 \pm 0.9 \pm 0.9$
BELLE [318]	$M_X < 1.7\,\mathrm{GeV}/c^2, q^2 > 8\,\mathrm{GeV}^2/c^2$	$7.4 \pm 0.9 \pm 1.3$
BELLE [309]	$M_X < 1.7\,\mathrm{GeV}/c^2, q^2 > 8\,\mathrm{GeV}^2/c^2$	$8.4 \pm 0.8 \pm 1.0$
BELLE [309]	$P_+ < 0.66\,\mathrm{GeV}$	$11.0 \pm 1.0 \pm 1.6$
BELLE [309]	$M_X < 1.7\,\mathrm{GeV}/c^2$	$12.4 \pm 1.1 \pm 1.2$

Table 54: Summary of inclusive determinations with the investigated acceptance region in the analysis and their determination of $|V_{ub}|$ in the BLNP prescription together with their average. The errors quoted on $|V_{ub}|$ correspond to experimental and theoretical uncertainties, respectively. The $s_{\rm h}^{\rm max}$ variable is described in Ref. [312].

	accepted region	f_u	$\lvert V_{ub}\rvert[10^{-3}]$
CLEO [313]	$E_e > 2.1\,\mathrm{GeV}$	0.13	$4.09 \pm 0.48 \pm 0.37$
BELLE [316]	$E_e > 1.9\,\mathrm{GeV}$	0.24	$4.82 \pm 0.45 \pm 0.30$
BABAR [315]	$E_e > 2.0\,\mathrm{GeV}$	0.19	$4.39 \pm 0.25 \pm 0.32$
BABAR [314]	$E_e > 2.0\,\mathrm{GeV}$, $s_{\rm h}^{\rm max} < 3.5\,\mathrm{GeV}^2$	0.13	$4.57 \pm 0.31 \pm 0.42$
BELLE [309]	$M_X < 1.7\,\mathrm{GeV}/c^2$	0.47	$4.06 \pm 0.27 \pm 0.24$
BELLE [318]	$M_X < 1.7\,\mathrm{GeV}/c^2, q^2 > 8\,\mathrm{GeV}^2/c^2$	0.24	$4.37 \pm 0.46 \pm 0.29$
BABAR [317]	$M_X < 1.7\,\mathrm{GeV}/c^2, q^2 > 8\,\mathrm{GeV}^2/c^2$	0.24	$4.75 \pm 0.35 \pm 0.31$
Average	$\boldsymbol{\chi^2 = 6/6}$, CL= **0.41**		$\mathbf{4.52 \pm 0.19 \pm 0.27}$

the meson decay spectrum without need of a leading-power non-perturbative function (or, in other words, a shape function). The on-shell mass of the b-quark within the B-meson (m_b) is required as an input. Theoretical uncertainties are assessed by varying the inputs of: the b-quark mass (m_b), the strong coupling constant (α_s), the number of light fermion flavours (N_F), and the method and scale of the matching scheme intrinsic to the approach. The extracted values of $|V_{ub}|$ for each measurement along with their average are given in Table 56 and illustrated in Figure 36. The breakdown of the uncertainty on the average is given in Table 57. The error in m_b contributes to the evalution of the total semileptonic width as well as to the spectral fraction, and is a leading source of uncertainty. The next largest uncertainty is from the matching scale and scheme.

Table 55: Summary of uncertainties on the $|V_{ub}|$ average in the BLNP prescription.

Source	Uncertainty(%)
Statistics	± 2.1
Detector	± 2.7
$B \to X_c l\nu$ model	± 2.1
$B \to X_u l\nu$ model	± 1.4
Heavy quark parameters m_b	± 4.1
Sub-leading shape functions	± 0.9
BLNP theory : Matching scales μ, μ_i, μ_h	± 3.8
Weak annihilation	± 2.1
Total	± 7.4

Table 56: Summary of inclusive determinations with the investigate acceptance region in the analysis and their determination of $|V_{ub}|$ in the DGE prescription together with their average. The errors quoted on $|V_{ub}|$ correspond to experimental and theoretical uncertainties, respectively. The $s_{\rm h}^{\rm max}$ variable is described in Ref. [312].

	accepted region	f_u	$\|V_{ub}\|[10^{-3}]$
CLEO [313]	$E_e > 2.1\,\mathrm{GeV}$	0.22	$3.85 \pm 0.45 \pm 0.22$
BELLE [316]	$E_e > 1.9\,\mathrm{GeV}$	0.37	$4.80 \pm 0.45 \pm 0.20$
BABAR [315]	$E_e > 2.0\,\mathrm{GeV}$	0.30	$4.29 \pm 0.29 \pm 0.21$
BABAR [314]	$E_e > 2.0\,\mathrm{GeV}$, $s_{\rm h}^{\rm max} < 3.5\,\mathrm{GeV}^2$	0.21	$4.42 \pm 0.30 \pm 0.24$
BELLE [309]	$M_X < 1.7\,\mathrm{GeV}/c^2$	0.64	$4.29 \pm 0.28 \pm 0.22$
BELLE [318]	$M_X < 1.7\,\mathrm{GeV}/c^2, q^2 > 8\,\mathrm{GeV}^2/c^2$	0.36	$4.42 \pm 0.47 \pm 0.19$
BABAR [317]	$M_X < 1.7\,\mathrm{GeV}/c^2, q^2 > 8\,\mathrm{GeV}^2/c^2$	0.36	$4.80 \pm 0.35 \pm 0.21$
Average	$\boldsymbol{\chi^2 = 10/6}$, CL= **0.12**		$\mathbf{4.46 \pm 0.20 \pm 0.20}$

Table 57: Summary of uncertainties on the $|V_{ub}|$ average in the DGE prescription.

Source	Uncertainty(%)
Statistics	± 1.8
Detector	± 2.5
$B \to X_c l\nu$ model	± 2.3
$B \to X_u l\nu$ model	± 2.3
Spectral fraction (m_b)	± 1.2
Strong coupling α_s	± 1.0
Total semileptonic width (m_b)	± 3.0
DGE theory : matching scales	± 2.9
Total	± 6.3

5.5.3 BLL

BLL, which stands for Bauer, Ligeti, and Luke [308], is a HQET-based prescription that advocates combined cuts on the dilepton invariant mass, q^2, and hadronic mass, m_X, to minimise the overall uncertainty on $|V_{ub}|$. In their reckoning a cut on m_X only, although most efficient at preserving phase space (80%), makes the calculation of the partial rate untenable owing to uncalculable corrections to the b-quark distribution function or shape function. These corrections are suppressed if a cut on q^2 is introduced. The cut combination used in measurements is $M_x < 1.7$ GeV/c^2 and $q^2 > 8$ GeV$^2/c^2$. The extracted values of $|V_{ub}|$ for each measurement along with their average are given in Table 58 and illustrated in Figure 37. The breakdown of the uncertainty on the average is given in Table 59. The leading uncertainties, both from theory, are due to residual shape function effects and third order terms in the OPE expansion. The leading experimental uncertainty is due to statistics.

Table 58: Summary of inclusive determinations of $|V_{ub}|$ in the BLL prescription. The errors quoted on $|V_{ub}|$ correspond to experimental and theoretical uncertainties, respectively.

	accepted region	f_u	$\|V_{ub}\|[10^{-3}]$
BELLE [318]	$M_X < 1.7\,\mathrm{GeV}/c^2, q^2 > 8\,\mathrm{GeV}^2/c^2$	0.26	$4.72 \pm 0.50 \pm 0.35$
BABAR [317]	$M_X < 1.7\,\mathrm{GeV}/c^2, q^2 > 8\,\mathrm{GeV}^2/c^2$	0.26	$5.12 \pm 0.38 \pm 0.38$
BELLE [309]	$M_X < 1.7\,\mathrm{GeV}/c^2, q^2 > 8\,\mathrm{GeV}^2/c^2$	0.26	$5.04 \pm 0.39 \pm 0.37$
Average	$\boldsymbol{\chi^2 = 0.5/2}$, CL= **0.77**		$\mathbf{5.02 \pm 0.26 \pm 0.37}$

Table 59: Summary of uncertainties on $|V_{ub}|$ in the BLL prescription.

Source	Uncertainty(%)
Statistics	± 3.2
Detector	± 2.9
$B \to X_c l\nu$ model	± 1.8
$B \to X_u l\nu$ model	± 2.4
Spectral fraction (m_b)	± 3.0
Perturbative : Strong coupling α_s	± 3.0
Residual shape function	± 4.5
Third order terms in the OPE	± 4.0
Total	± 9.1

5.5.4 Summary

We have performed averages of inclusive $|V_{ub}|$ measurements using the three frameworks of BLNP, DGE and BLL. Table 60 lists these averages, as well as additional extractions for m_X/q^2 measurements only and the LLR-based BABAR measurement. The values display a remarkable agreement. The uncertainties that dominate both BLNP and DGE averages arise from m_b and

matching scales, while for BLL they are due to residual shape function effects and higher order terms in the OPE. The overall uncertainties on $|V_{ub}|$ for BLNP, DGE and BLL averages are 7.4%, 6.3% and 9.15l4%. respectively. A value judgement based on a direct comparison should be avoided, experimental and theoretical uncertainties play out differently between the schemes. What is clear is that a better determination of m_b and further investigation of matching scale effects and shape functions will add to our understanding of $|V_{ub}|$ and hopefully improve the precision to which it is known. The overall uncertainty on the one measurement employing LLR is 12.0%, although it is larger than the others it is a first look at the measurements that we can expect to see more of from B-factories.

Table 60: Summary of inclusive determinations of $|V_{ub}|$. The errors quoted on $|V_{ub}|$ correspond to experimental and theoretical uncertainties, respectively.

Framework	$\|V_{ub}\|[10^{-3}]$
BLNP	$4.52 \pm 0.19 \pm 0.27$
DGE	$4.46 \pm 0.20 \pm 0.20$
LLR (BABAR)	$4.43 \pm 0.45 \pm 0.29$
BLL (m_X/q^2 only)	$5.02 \pm 0.26 \pm 0.37$
BLNP (m_X/q^2 only)	$4.65 \pm 0.25 \pm 0.31$
DGE (m_X/q^2 only)	$4.70 \pm 0.26 \pm 0.22$

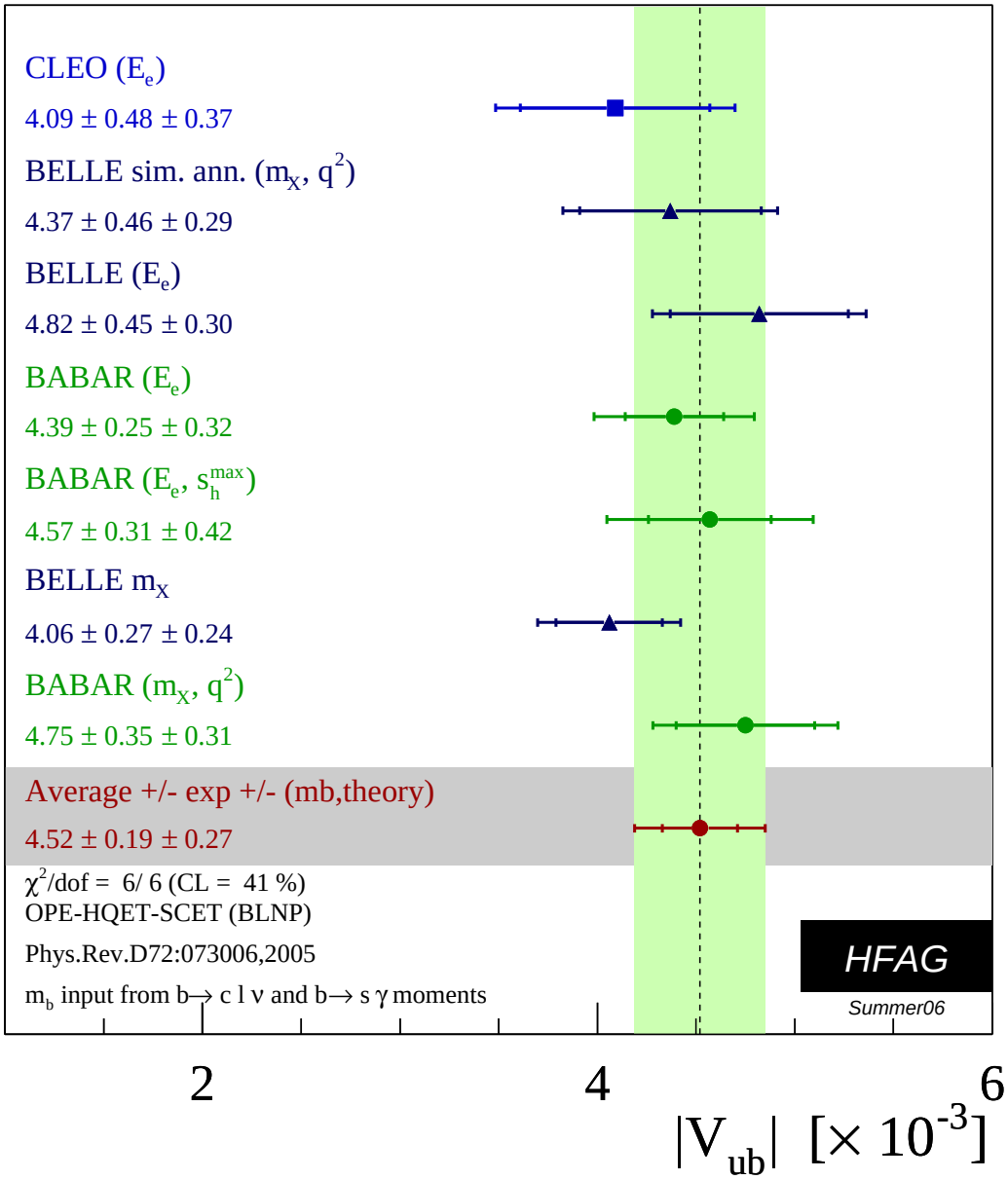

Figure 35: Measurements of $|V_{ub}|$ from inclusive semileptonic decays and their average in the BLNP description. "E_e", "M_X", "(M_X, q^2)" and "(E_e, s_h^{max})" indicate the analysis type.

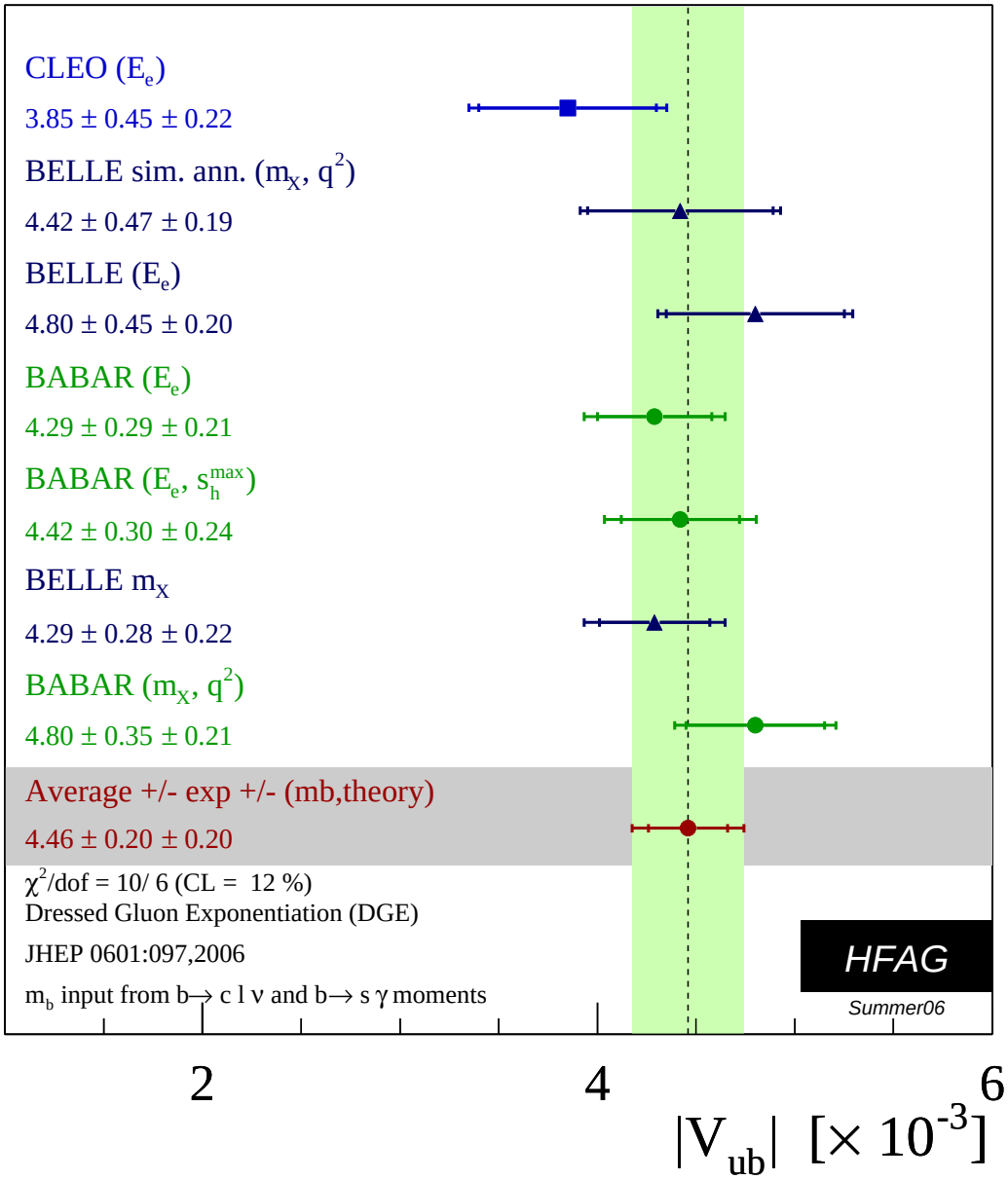

Figure 36: Measurements of $|V_{ub}|$ from inclusive semileptonic decays and their average in the DGE description. "E_e", "M_X", "(M_X, q^2)" and "(E_e, s_h^{max})" indicate the analysis type.

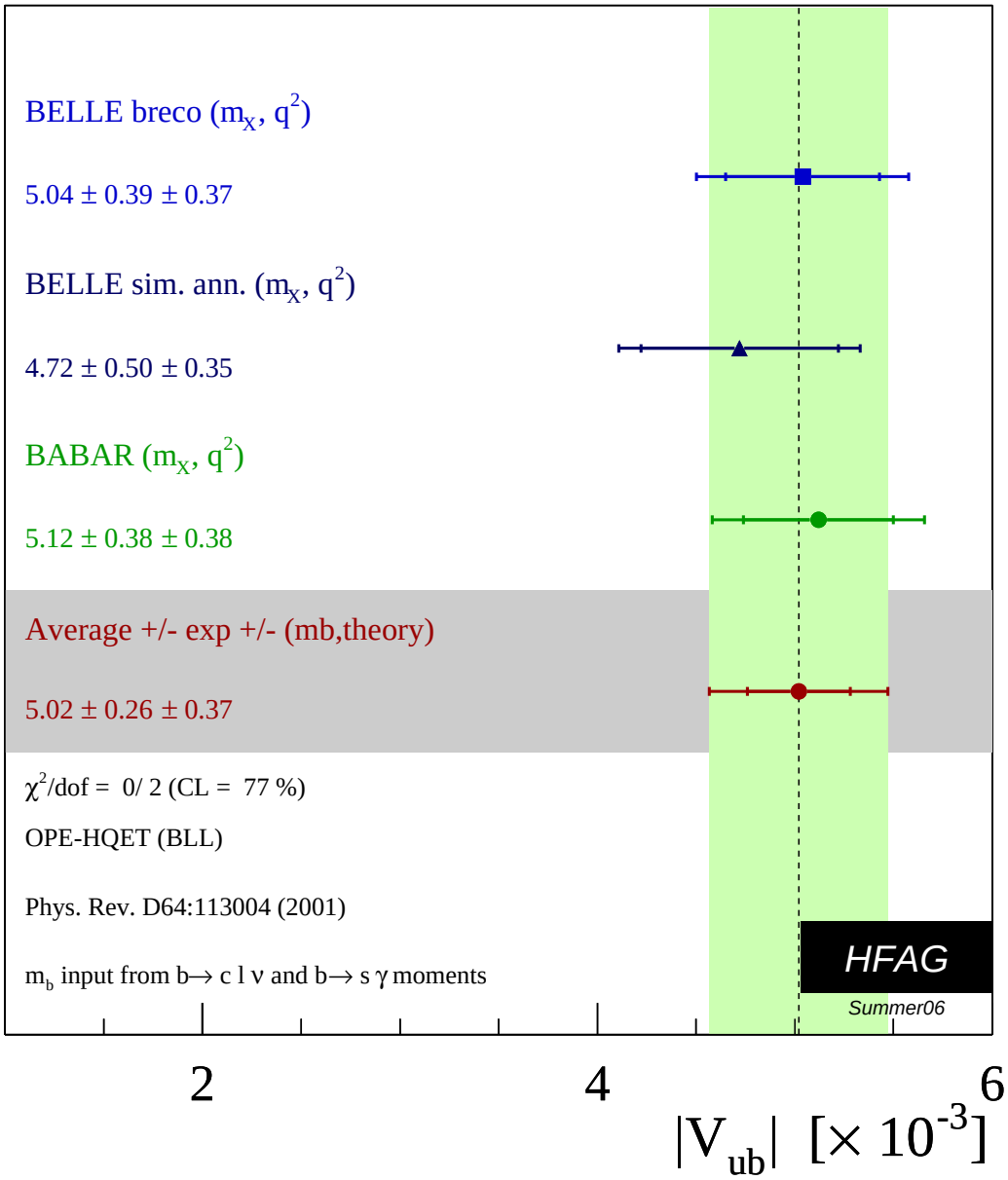

Figure 37: Measurements of $|V_{ub}|$ from inclusive semileptonic decays and their average in the BLL prescription. "(M_X, q^2)" indicates the analysis type.

6 Charmless B-decay branching fractions and their asymmetries

The aim of this section is to provide the branching fractions and the partial rate asymmetries (A_{CP}) of charmless B decays. The asymmetry is defined as $A_{CP} = \frac{N_{\overline{B}} - N_B}{N_{\overline{B}} + N_B}$, where $N_{\overline{B}}$ and N_B are respectively number of $\overline{B}^0/B^-$ and B^0/B^+ decaying into a specific final state. Four different B decay categories are considered: charmless mesonic, baryonic, radiative and leptonic. Measurements supported with written documents are accepted in the averages; written documents could be journal papers, conference contributed papers, preprints or conference proceedings. Results from A_{CP} measurements obtained from time dependent analyses are listed and described in Sec. 4. Measurements of charmful baryonic B decays, which were included in our previous averages [3], are now shown in Section 7, which deals with B decays to charm.

So far all branching fractions assume equal production of charged and neutral B pairs. The best measurements to date show that this is still a good approximation (see Sec. 3). For branching fractions, we provide either averages or the most stringent 90% confidence level upper limits. If one or more experiments have measurements with $>4\sigma$ for a decay channel, all available central values for that channel are used in the averaging. We also give central values and errors for cases where the significance of the average value is at least 3σ, even if no single measurement is above 4σ. Since a few decay modes are sensitive to the contribution of new physics and the current experimental upper limits are not far from the Standard Model expectation, we provide the combined upper limits or averages in these cases. Their upper limits can be estimated assuming that the errors are Gaussian. For A_{CP} we provide averages in all cases.

Our averaging is performed by maximizing the likelihood, $\mathcal{L} = \prod_i \mathcal{P}_i(x)$, where $\mathcal{P}_i$ is the probability density function (PDF) of the ith measurement, and x is the branching fraction or A_{CP}. The PDF is modeled by an asymmetric Gaussian function with the measured central value as its mean and the quadratic sum of the statistical and systematic errors as the standard deviations. The experimental uncertainties are considered to be uncorrelated with each other when the averaging is performed. No error scaling is applied when the fit χ^2 is greater than 1 since we believe that tends to overestimate the errors except in cases of extreme disagreement (we have no such cases). One exception to consider the correlated systematic errors is the inclusive $b \to s\gamma$ mode, which is sensitive to physics beyond the Standard Model. We tried to include as many measurements as possible and take the common systematic errors into account when performing the average. The detail is described in Sec. 6.3.

At present, we have measurements of more than 250 decay modes, reported in more than 150 papers. Because the number of references is so large, we do not include them with the tables shown here but the full set of references is available quickly from active gifs at the "Winter 2007" link on the rare web page: `http://www.slac.stanford.edu/xorg/hfag/rare/index.html`. Finally the inclusive measurements of $B \to KX$ branching fractions and full angular analysis on $B^0 \to \phi K_2^*(1430)^0$ are listed for the first time.

6.1 Mesonic charmless decays

Table 61: Branching fractions (BF) of charmless mesonic B^+ decays (in units of 10^{-6}). Upper limits are at 90% CL. Values in red (blue) are new published (preliminary) result since PDG2006 [as of March 15, 2007].

RPP#	Mode	PDG2006 Avg.	BABAR	Belle	CLEO	CDF	New Avg.
182	$K^0\pi^+$	24.1 ± 1.7	$23.9 \pm 1.1 \pm 1.0$	$22.8^{+0.8}_{-0.7} \pm 1.3$	$18.8^{+3.7+2.1}_{-3.3-1.8}$		23.1 ± 1.0
183	$K^+\pi^0$	12.1 ± 0.8	$13.3 \pm 0.6 \pm 0.6$	$12.4 \pm 0.5 \pm 0.6$	$12.9^{+2.4+1.2}_{-2.2-1.1}$		12.8 ± 0.6
184	$\eta' K^+$	70.5 ± 3.5	$68.9 \pm 2.0 \pm 3.2$	$69.2 \pm 2.2 \pm 3.7$	$80^{+10}_{-9} \pm 7$		$69.7^{+2.8}_{-2.7}$
185	$\eta' K^{*+}$	< 14	$4.9^{+1.9}_{-1.7} \pm 0.8$	< 2.8	$11.1^{+12.7}_{-8.0}$		$4.9^{+2.1}_{-1.9}$
186	ηK^+	2.6 ± 0.6	$3.3 \pm 0.6 \pm 0.3$	$1.9 \pm 0.3^{+0.2}_{-0.1}$	$2.2^{+2.8}_{-2.2}$		2.2 ± 0.3
187	ηK^{*+}	26 ± 4	$18.9 \pm 1.8 \pm 1.3$	$19.3^{+2.0}_{-1.9} \pm 1.5$	$26.4^{+9.6}_{-8.2} \pm 3.3$		19.3 ± 1.6
–	$\eta K_0^{*+}(1430)$	New	$15.8 \pm 2.2 \pm 2.2$				15.8 ± 3.1
–	$\eta K_2^{*+}(1430)$	New	$9.1 \pm 2.7 \pm 1.4$				9.1 ± 3.0
188	ωK^+	5.1 ± 0.7	$6.1 \pm 0.6 \pm 0.4$	$8.1 \pm 0.6 \pm 0.6$	$3.2^{+2.4}_{-1.9} \pm 0.8$		6.8 ± 0.5
189	ωK^{*+}	< 7.4	< 3.4		< 87		< 3.4
190	$a_0^+(980)K^0$ †	< 3.9	< 3.9				< 3.9
191	$a_0^0(980)K^+$ †	< 2.5	< 2.5				< 2.5
192	$K^{*0}\pi^+$	11.6 ± 1.9	$13.5 \pm 1.2^{+0.8}_{-0.9}$	$9.7 \pm 0.6^{+0.8}_{-0.9}$	$7.6^{+3.5}_{-3.0} \pm 1.6$		10.7 ± 0.8
193	$K^{*+}\pi^0$	6.9 ± 2.4	$6.9 \pm 2.0 \pm 1.3$		$7.1^{+11.4}_{-7.1} \pm 1.0$		6.9 ± 2.3
194	$K^+\pi^+\pi^-$	56 ± 9	$64.1 \pm 2.4 \pm 4.0$	$48.8 \pm 1.1 \pm 3.6$			54.8 ± 2.9
195	$K^+\pi^+\pi^-(NR)$	$3.1^{+1.0}_{-0.8}$	$2.9 \pm 0.6^{+0.8}_{-0.5}$		< 28		$2.9^{+1.0}_{-0.8}$
196	$K^+ f_0(980)$ †	8.9 ± 1.0	$9.5 \pm 1.0^{+0.6}_{-0.9}$	$8.8 \pm 0.8^{+0.9}_{-1.8}$			$9.2^{+0.8}_{-1.1}$
197	$f_2(1270)K^+$	< 2.3	< 16	$1.33 \pm 0.30^{+0.23}_{-0.34}$			$1.33^{+0.38}_{-0.45}$
198	$f_0(1370)K^+$ †	< 10.7	< 10.7				< 10.7
199	$\rho^0(1450)K^+$	< 11.7	< 11.7				< 11.7
200	$f_0(1500)K^+$ †	< 4.4	< 4.4				< 4.4
201	$f_2'(1525)K^+$ †	< 3.4	< 3.4	< 4.9			< 3.4
202	$K^+\rho^0$	$5.0^{+0.7}_{-0.8}$	$5.1 \pm 0.8^{+0.6}_{-0.9}$	$3.89 \pm 0.47^{+0.43}_{-0.41}$	$8.4^{+4.0}_{-3.4} \pm 1.8$		$4.25^{+0.55}_{-0.56}$
203	$K_0^*(1430)^0\pi^+$	38 ± 5	$44.4 \pm 2.2 \pm 5.3$	$51.6 \pm 1.7^{+7.0}_{-7.4}$			$47.1^{+4.5}_{-4.6}$
204	$K_2^*(1430)^0\pi^+$	< 6.9	< 23.1	< 6.9			< 6.9
205	$K^*(1410)^0\pi^+$	< 45		< 45			< 45
206	$K^*(1680)^0\pi^+$	< 12	< 15	< 12			< 12
207	$K^-\pi^+\pi^+$	< 1.8	< 1.8	< 4.5			< 1.8
210	$K^0\pi^+\pi^0$	< 66			< 66		< 66
211	$K^0\rho^+$	< 48	$8.0^{+1.4}_{-1.3} \pm 0.5$		< 48		$8.0^{+1.5}_{-1.4}$
213	$K^{*+}\rho^0$	11 ± 4	< 6.1		< 74		< 6.1
214	$K^{*0}\rho^+$	8.9 ± 2.1	$9.6 \pm 1.7 \pm 1.5$	$8.9 \pm 1.7 \pm 1.2$			9.2 ± 1.5
–	$K^{*+} f_0(980)$ †	New	$5.2 \pm 1.2 \pm 0.5$				5.2 ± 1.3
215	$K^{*+}\overline{K^{*0}}$	< 71			< 71		< 71
218	$K^+\overline{K^0}$	1.20 ± 0.32	$1.61 \pm 0.44 \pm 0.09$	$1.22^{+0.33+0.13}_{-0.28-0.16}$	< 3.3		$1.36^{+0.29}_{-0.27}$
219	$K^+\overline{K^0}\pi^0$	< 24			< 24		< 24
220	$K^+K_SK_S$	11.5 ± 1.3	$10.7 \pm 1.2 \pm 1.0$	$13.4 \pm 1.9 \pm 1.5$			11.5 ± 1.3
221	$K_SK_S\pi^+$	< 3.2		< 3.2			< 3.2
222	$K^+K^-\pi^+$	< 6.3	< 6.3	< 13			< 6.3
224	$K^+K^+\pi^-$	< 1.3	< 1.3	< 2.4			< 1.3
226	$\overline{K^{*0}}K^+$	< 5.3			< 5.3		< 5.3
228	$K^+K^-K^+$	30.1 ± 1.9	$35.2 \pm 0.9 \pm 1.6$	$30.6 \pm 1.2 \pm 2.3$			33.7 ± 1.5
229	ϕK^+	9.0 ± 0.8	$8.4 \pm 0.7 \pm 0.7$	$9.60 \pm 0.92^{+1.05}_{-0.84}$	$5.5^{+2.1}_{-1.8} \pm 0.6$	$7.6 \pm 1.3 \pm 0.6$	8.30 ± 0.65
231	a_2K^+†	< 1.1		< 1.1			< 1.1
233	$\phi(1680)K^+$†	< 0.8		< 0.8			< 0.8
235	$K^{*+}K^+K^-$	< 1600	$36.2 \pm 3.3 \pm 3.6$				36.2 ± 4.9
–	$K^{*+}\pi^+\pi^-$	New	$75.3 \pm 6.0 \pm 8.1$				75.3 ± 10.1
–	$K^{*+}\pi^+K^-$	New	< 11.8				< 11.8
–	$K^{*+}K^+\pi^-$	New	< 6.1				< 6.1
236	ϕK^{*+}	9.6 ± 3.0	$12.7^{+2.2}_{-2.0} \pm 1.1$	$6.7^{+2.1+0.7}_{-1.9-1.0}$	$10.6^{+6.4+1.8}_{-4.9-1.6}$		9.7 ± 1.5
239	$\phi\phi K^+$ §	$2.6^{+1.1}_{-0.9}$	$7.5 \pm 1.0 \pm 0.7$	$3.2^{+0.6}_{-0.5} \pm 0.3$			4.2 ± 0.6
–	$\eta'\eta' K^+$	New	< 25				< 25

†Product BF - daughter BF taken to be 100%; §$M_{\phi\phi} < 2.85$ GeV/c^2

Table 62: Branching fractions (BF) of charmless mesonic B^+ decays (part 2) (in units of 10^{-6}). Upper limits are at 90% CL. Values in red (blue) are new published (preliminary) result since PDG2006 [as of March 15, 2007].

RPP#	Mode	PDG2006 Avg.	BABAR	Belle	CLEO	CDF	New Avg.
254	$\pi^+\pi^0$	5.5 ± 0.6	$5.1 \pm 0.5 \pm 0.3$	$6.5 \pm 0.4^{+0.4}_{-0.5}$	$4.6^{+1.8+0.6}_{-1.6-0.7}$		5.7 ± 0.4
255	$\pi^+\pi^-\pi^+$	$16.2 \pm 1.2 \pm 0.9$	$16.2 \pm 1.2 \pm 0.9$				16.2 ± 1.5
256	$\rho^0\pi^+$	8.7 ± 1.1	$8.8 \pm 1.0^{+0.6}_{-0.9}$	$8.0^{+2.3}_{-2.0} \pm 0.7$	$10.4^{+3.3}_{-3.4} \pm 2.1$		$8.7^{+1.0}_{-1.1}$
257	$f_0(980)\pi^+$ †	< 3.0	< 3.0				< 3.0
258	$f_2(1270)\pi^+$	$8.2 \pm 2.1 \pm 1.4$	$8.2 \pm 2.1 \pm 1.4$				8.2 ± 2.5
259	$\rho^0(1450)\pi^+$	< 2.3	< 2.3				< 2.3
260	$f_0(1370)\pi^+$	< 3.0	< 3.0				< 3.0
261	$f_0(600)\pi^+$	< 4.1	< 4.1				< 4.1
262	$\pi^+\pi^-\pi^+(NR)$	< 4.6	< 4.6				< 4.6
264	$\rho^+\pi^0$	12.0 ± 1.9	$10.2 \pm 1.4 \pm 0.9$	$13.2 \pm 2.3^{+1.4}_{-1.9}$	< 43		$10.9^{+1.4}_{-1.5}$
266	$\rho^+\rho^0$	26 ± 6	$16.8 \pm 2.2 \pm 2.3$	$31.7 \pm 7.1^{+3.8}_{-6.7}$			18.2 ± 3.0
–	$\rho^+ f_0(980)$ †	New	< 1.9				< 1.9
269	$\omega\pi^+$	5.9 ± 1.0	$6.1 \pm 0.7 \pm 0.4$	$6.9 \pm 0.6 \pm 0.5$	$11.3^{+3.3}_{-2.9} \pm 1.4$		6.7 ± 0.6
270	$\omega\rho^+$	$12.6 \pm 3.7^{+3.3}_{-1.6}$	$10.6 \pm 2.1^{+1.6}_{-1.0}$		< 61		$10.6^{+2.6}_{-2.3}$
271	$\eta\pi^+$	4.9 ± 0.5	$5.1 \pm 0.6 \pm 0.3$	$4.2 \pm 0.4 \pm 0.2$	$1.2^{+2.8}_{-1.2}$		4.4 ± 0.4
272	$\eta'\pi^+$	4.0 ± 0.9	$4.0 \pm 0.8 \pm 0.4$	$1.8^{+0.7}_{-0.6} \pm 0.1$	$1.0^{+5.8}_{-1.0}$		$2.6^{+0.6}_{-0.5}$
273	$\eta'\rho^+$	< 22	$8.7^{+3.1+2.3}_{-2.8-1.3}$	< 4.7	$11.2^{+11.9}_{-7.0}$		$9.1^{+3.7}_{-2.8}$
274	$\eta\rho^+$	$8.4 \pm 1.9 \pm 1.1$	$8.4 \pm 1.9 \pm 1.1$	$4.1^{+1.4}_{-1.3} \pm 0.4$	$4.8^{+5.2}_{-3.8}$		5.4 ± 1.2
275	$\phi\pi^+$	< 0.41	< 0.24		< 5		< 0.24
276	$\phi\rho^+$	< 16			< 16		< 16
277	$a_0^0(980)\pi^+$ †	< 5.8	< 5.8				< 5.8
–	$a_0^+(980)\pi^0$ †	New	< 1.3				< 1.3

†Product BF - daughter BF taken to be 100%;

Table 63: Branching fractions of charmless mesonic B^0 decays (in units of 10^{-6}). Upper limits are at 90% CL. Values in red (blue) are new published (preliminary) result since PDG2006 [as of March 15, 2007].

RPP#	Mode	PDG2006 Avg.	BABAR	Belle	CLEO	CDF	New Avg.
168	$K^+\pi^-$	18.2 ± 0.8	$19.1 \pm 0.6 \pm 0.6$	$19.9 \pm 0.4 \pm 0.8$	$18.0^{+2.3+1.2}_{-2.1-0.9}$		19.4 ± 0.6
169	$K^0\pi^0$	11.5 ± 1.0	$10.5 \pm 0.7 \pm 0.5$	$9.2 \pm 0.7^{+0.6}_{-0.7}$	$12.8^{+4.0+1.7}_{-3.3-1.4}$		10.0 ± 0.6
170	$\eta' K^0$	68 ± 4	$67.4 \pm 3.3 \pm 3.2$	$58.9^{+3.6}_{-3.5} \pm 4.3$	$89^{+18}_{-16} \pm 9$		64.9 ± 3.5
171	$\eta' K^{*0}$	< 7.6	$3.8 \pm 1.1 \pm 0.5$	< 2.6	$7.8^{+7.7}_{-5.7}$		3.8 ± 1.2
172	ηK^{*0}	17.7 ± 2.3	$16.5 \pm 1.1 \pm 0.8$	$15.2 \pm 1.2 \pm 1.0$	$13.8^{+5.5}_{-4.6} \pm 1.6$		15.9 ± 1.0
–	$\eta K_0^{*0}(1430)$	New	$9.6 \pm 1.4 \pm 1.3$				9.6 ± 1.9
–	$\eta K_2^{*0}(1430)$	New	$9.6 \pm 1.8 \pm 1.1$				9.6 ± 2.1
173	ηK^0	< 2.0	< 2.9	< 1.9	< 9.3		< 1.9
–	$\eta K^+\pi^-$	New		$31.7 \pm 1.9^{+2.2}_{-2.6}$			$31.7^{+2.9}_{-3.2}$
174	ωK^0	$5.5^{+1.2}_{-1.0}$	$6.2 \pm 1.0 \pm 0.4$	$4.4^{+0.8}_{-0.7} \pm 0.4$	$10.0^{+5.4}_{-4.2} \pm 1.4$		5.2 ± 0.7
175	$a_0^0(980)K^0$ †	< 7.8	< 7.8				< 7.8
176	$a_0^-(980)K^+$ †	< 2.1	< 1.9	< 1.6			< 1.6
–	$a_0^-(1450)K^+$ †	New	< 3.1				< 3.1
178	ωK^{*0}	< 6.0	< 4.2		< 23		< 4.2
179	K^+K^-	< 0.37	$0.04 \pm 0.15 \pm 0.08$	$0.09^{+0.18}_{-0.13} \pm 0.01$	< 0.8	$0.39 \pm 0.16 \pm 0.12$ ‡	$0.15^{+0.11}_{-0.10}$
180	$K^0\overline{K^0}$	$1.13^{+0.38}_{-0.35}$	$1.08 \pm 0.28 \pm 0.11$	$0.87^{+0.25}_{-0.20} \pm 0.09$	< 3.3		$0.96^{+0.21}_{-0.19}$
181	$K_SK_SK_S$	$6.2^{+1.2}_{-1.1}$	$6.9^{+0.9}_{-0.8} \pm 0.6$	$4.2^{+1.6}_{-1.3} \pm 0.8$			6.2 ± 0.9
–	$K_SK_SK_L$	New	< 16[1]				< 16[1]
182	$K^+\pi^-\pi^0$	$36.6^{+4.2}_{-4.3} \pm 3.0$		$36.6^{+4.2}_{-4.3} \pm 3.0$	< 40		36.6 ± 5.2
183	$K^+\rho^-$	8.5 ± 2.8		$15.1^{+3.4+2.4}_{-3.3-2.6}$	$16^{+8}_{-6} \pm 3$		$15.3^{+3.7}_{-3.5}$
186	$K^0\pi^+\pi^-$	43.8 ± 2.9	$43.0 \pm 2.3 \pm 2.3$	$47.5 \pm 2.4 \pm 3.7$	$50^{+10}_{-9} \pm 7$		$44.8^{+2.6}_{-2.5}$
–	$f_2(1270)K^0$	New		< 2.5			< 2.5
–	$K^+\pi^-\pi^0(NR)$	New		< 9.4			< 9.4
–	$K^*(1410)^+\pi^-$	New		< 86			< 86
–	$K_0^*(1430)^+\pi^-$	New		$49.7 \pm 3.8^{+6.8}_{-8.2}$			$49.7^{+7.8}_{-9.0}$
187	$K^0\rho^0$	< 39	$4.9 \pm 0.8 \pm 0.9$	$6.1 \pm 1.0^{+1.1}_{-1.2}$	< 39		$5.4^{+0.9}_{-1.0}$
188	$K^0f_0(980)$ †	$5.5 \pm 0.7 \pm 0.6$	$5.5 \pm 0.7 \pm 0.6$	$7.6 \pm 1.7^{+0.9}_{-1.3}$			$5.8^{+0.8}_{-0.9}$
189	$K^{*+}\pi^-$	11.8 ± 1.5	$11.0 \pm 1.5 \pm 0.7$	$8.4 \pm 1.1^{+1.0}_{-0.9}$	$16^{+6}_{-5} \pm 2$		9.8 ± 1.1
191	$K^{*0}\pi^0$	< 3.5		$0.4^{+1.9}_{-1.7} \pm 0.1$	$0.0^{+1.3+0.5}_{-0.0-0.0}$		$0.0^{+1.3}_{-0.1}$
192	$K_2^*(1430)^+\pi^-$	< 18		< 6.3			< 6.3
–	$K^*(1680)^+\pi^-$	New		< 10.1			< 10.1
–	$K_1(1270)^+\pi^-$	New	< 25.2				< 25.2
–	$K_1(1400)^+\pi^-$	New	< 21.8				< 21.8
193	$K^0K^-\pi^+$	< 21		< 18	< 21		< 18
194	$K^+K^-\pi^0$	< 19			< 19		< 19
195	$K^+K^-K^0$	24.7 ± 2.3	$23.8 \pm 2.0 \pm 1.6$	$28.3 \pm 3.3 \pm 4.0$			24.7 ± 2.3
196	ϕK^0	$8.6^{+1.3}_{-1.1}$	$8.4^{+1.5}_{-1.3} \pm 0.5$	$9.0^{+2.2}_{-1.8} \pm 0.7$	$5.4^{+3.7}_{-2.7} \pm 0.7$		$8.3^{+1.2}_{-1.0}$
199	$K^{*0}\rho^0$	< 34	$5.6 \pm 0.9 \pm 1.3$		< 34		5.6 ± 1.6
200	$K^{*0}f_0(980)$ †	< 170	< 4.3				< 4.3
–	$K^{*+}\rho^-$	New	< 12				< 12
–	$K^{*0}\overline{K^0}$	New	< 1.9				< 1.9
204	ϕK^{*0}	9.5 ± 0.9	$9.2 \pm 0.7 \pm 0.6$	$10.0^{+1.6+0.7}_{-1.5-0.8}$	$11.5^{+4.5+1.8}_{-3.7-1.7}$		9.5 ± 0.8
–	$\phi K_0^*(1430)^0$	New	$4.6 \pm 0.7 \pm 0.6$				4.6 ± 0.9
–	$\phi K_2^*(1430)^0$	New	$7.8 \pm 1.1 \pm 0.6$				7.8 ± 1.3
–	$\phi\phi K^0$ §	New	$4.1^{+1.7}_{-1.4} \pm 0.4$	$2.3^{+1.0}_{-0.7} \pm 0.2$			$2.8^{+0.9}_{-0.7}$
205	$K^{*0}\overline{K^{*0}}$	< 22			< 22		< 22
207	$K^{*+}K^{*-}$	< 141			< 141		< 141
–	$\eta'\eta' K^0$	New	< 31				< 31

†Product BF - daughter BF taken to be 100%, ‡Relative BF converted to absolute BF §$M_{\phi\phi} < 2.85$ GeV/c^2 [1]Excludes $M(K_SK_S)$ regions [3.400,3.429] and [3.540,3.585] and $M(K_SK_L) < 1.049$ GeV/c^2

Table 64: Branching fractions of charmless mesonic B^0 decays (part 2) (in units of 10^{-6}). Upper limits are at 90% CL. Values in red (blue) are new published (preliminary) result since PDG2006 [as of March 15, 2007].

RPP#	Mode	PDG2006 Avg.	BABAR	Belle	CLEO	CDF	New Avg.
229	$\pi^+\pi^-$	4.6 ± 0.4	$5.5 \pm 0.4 \pm 0.3$	$5.1 \pm 0.2 \pm 0.2$	$4.5^{+1.4+0.5}_{-1.2-0.4}$	$5.10 \pm 0.33 \pm 0.36$ ‡	5.16 ± 0.22
230	$\pi^0\pi^0$	1.5 ± 0.5	$1.48 \pm 0.26 \pm 0.12$	$1.1 \pm 0.3 \pm 0.1$	< 4.4		1.31 ± 0.21
231	$\eta\pi^0$	< 2.5	< 1.3	< 2.5	< 2.9		< 1.3
232	$\eta\eta$	< 2.0	< 1.8	< 2.0	< 18		< 1.8
233	$\eta'\pi^0$	< 3.7	$0.8^{+0.8}_{-0.6} \pm 0.1$	$2.8 \pm 1.0 \pm 0.3$	$0.0^{+1.8}_{-0.0}$		$1.5^{+0.7}_{-0.6}$
234	$\eta'\eta'$	< 10	< 2.4	< 7.7	< 47		< 2.4
235	$\eta'\eta$	< 4.6	< 1.7	< 4.0	< 27		< 1.7
236	$\eta'\rho^0$	< 4.3	< 3.7	< 1.26	< 12		< 1.26
–	$\eta' f_0(980)$ †	New	< 1.5				< 1.5
–	$\eta\pi^+\pi^-$	New		$6.2^{+1.8+0.8}_{-1.6-0.6}$			$6.2^{+2.0}_{-1.7}$
237	$\eta\rho^0$	< 1.5	< 1.5	< 1.9	< 10		< 1.5
–	$\eta f_0(980)$ †	New	< 0.4				< 0.4
238	$\omega\eta$	< 1.9	< 1.9		< 12		< 1.9
239	$\omega\eta'$	< 2.8	< 2.8	< 2.2	< 60		< 2.2
240	$\omega\rho^0$	< 3.3	< 1.5		< 11		< 1.5
–	$\omega f_0(980)$ †	New	< 1.5				< 1.5
241	$\omega\omega$	< 19	< 4.0		< 19		< 4.0
242	$\phi\pi^0$	< 1	< 0.28		< 5		< 0.28
243	$\phi\eta$	< 1	< 0.6		< 9		< 0.6
244	$\phi\eta'$	< 4.5	< 1.0	< 0.5	< 31		< 0.5
245	$\phi\rho^0$	< 13			< 13		< 13
246	$\omega\phi$	< 21	< 1.2		< 21		< 1.2
247	$\phi\phi$	< 1.5	< 1.5		< 12		< 1.5
248	$a_0^{\mp}(980)\pi^{\pm}$ †	< 5.1	< 3.1	< 2.8			< 2.8
–	$a_0^{\mp}(1450)\pi^{\pm}$ †	New	< 2.3				< 2.3
250	$\rho^0\pi^0$	1.8 ± 0.8	$1.4 \pm 0.6 \pm 0.3$	$3.1^{+0.9+0.6}_{-0.8-0.8}$	$1.6^{+2.0}_{-1.4} \pm 0.8$		$1.8^{+0.6}_{-0.5}$
251	$\rho^{\mp}\pi^{\pm}$	22.8 ± 2.5	$22.6 \pm 1.8 \pm 2.2$	$29.1^{+5.0}_{-4.9} \pm 4.0$	$27.6^{+8.4}_{-7.4} \pm 4.2$		24.0 ± 2.5
253	$\rho^0\rho^0$	< 1.1	$1.07 \pm 0.33 \pm 0.19$		< 18		1.07 ± 0.38
–	$\rho^0 f_0(980)$ †	New	< 0.53				< 0.53
–	$f_0(980) f_0(980)$ †	New	< 0.16				< 0.16
254	$a_1^{\mp}\pi^{\pm}$	< 490	$33.2 \pm 3.8 \pm 3.0$	$48.6 \pm 4.1 \pm 3.9$			39.7 ± 3.7
257	$\rho^+\rho^-$	25 ± 4	$23.5 \pm 2.2 \pm 4.1$	$22.8 \pm 3.8^{+2.3}_{-2.6}$			$23.1^{+3.2}_{-3.3}$
259	$\omega\pi^0$	< 1.2	< 1.2	< 2.0	< 5.5		< 1.2
261	$a_1^{\pm}\rho^{\mp}$	< 3400	< 61				< 61

†Product BF - daughter BF taken to be 100%, ‡Relative BF converted to absolute BF

Table 65: Relative branching fractions of $B^0 \to K^+K^-, K^+\pi^-, \pi^+\pi^-$. Values in red (blue) are new published (preliminary) result since PDG2006 [as of March 15, 2007].

RPP#	Mode	PDG2006 Avg.	CDF	DØ	New Avg.
179	$\mathcal{B}(B^0 \to K^+K^-)/\mathcal{B}(B^0 \to K^+\pi^-)$		$0.020 \pm 0.008 \pm 0.006$		0.020 ± 0.010
229	$\mathcal{B}(B^0 \to \pi^+\pi^-)/\mathcal{B}(B^0 \to K^+\pi^-)$		$0.259 \pm 0.017 \pm 0.016$		0.259 ± 0.023

6.2 Radiative and leptonic decays

Table 66: Branching fractions of semileptonic and radiative B^+ decays (in units of 10^{-6}). Upper limits are at 90% CL. Values in red (blue) are new published (preliminary) result since PDG2006 [as of March 15, 2007].

RPP#	Mode	PDG2006 Avg.	BABAR	Belle	CLEO	CDF	New Avg.
240	$K^*(892)^+\gamma$	40.3 ± 2.6	$38.7 \pm 2.8 \pm 2.6$	$42.5 \pm 3.1 \pm 2.4$	$37.6^{+8.9}_{-8.3} \pm 2.8$		40.3 ± 2.6
241	$K_1(1270)^+\gamma$	$43 \pm 9 \pm 9$		$43 \pm 9 \pm 9$			43 ± 12
242	$K^+\eta\gamma$	$8.4^{+1.5}_{-1.2} \pm 0.9$	$10.0 \pm 1.3 \pm 0.5$	$8.4^{+1.5}_{-1.2} \pm 0.9$			9.4 ± 1.1
–	$K^+\eta'\gamma$	New	< 4.2				< 4.2
243	$K^+\phi\gamma$	$3.4 \pm 0.9 \pm 0.4$	$3.5 \pm 0.6 \pm 0.4$	$3.4 \pm 0.9 \pm 0.4$			3.5 ± 0.6
244	$K^+\pi^-\pi^+\gamma$ §	$25.0 \pm 1.8 \pm 2.2$	$29.5 \pm 1.3 \pm 1.9$	$25.0 \pm 1.8 \pm 2.2$			27.7 ± 1.8
–	$K^0\pi^+\pi^0\gamma$ §	New	$45.6 \pm 4.2 \pm 3.1$				45.6 ± 5.2
245	$K^{*0}\pi^+\gamma$ §	20^{+7}_{-6}		$20^{+7}_{-6} \pm 2$			20^{+7}_{-6}
245	$K^+\rho^0\gamma$ §	< 20		< 20			< 20
247	$K^+\pi^-\pi^+\gamma$ (N.R.) §	< 9.2		< 9.2			< 9.2
248	$K_1(1400)^+\gamma$	< 50		< 15			< 15
249	$K_2^*(1430)^+\gamma$	$14.5 \pm 4.0 \pm 1.5$	$14.5 \pm 4.0 \pm 1.5$				14.5 ± 4.3
251	$K_3^*(1780)^+\gamma$	< 39		< 39			< 39
253	$\rho^+\gamma$	< 1.8	$1.10^{+0.37}_{-0.33} \pm 0.09$	$0.55^{+0.42+0.09}_{-0.36-0.08}$	< 13		$0.88^{+0.28}_{-0.26}$
296	$p\overline{\Lambda}\gamma$	$2.16^{+0.58}_{-0.53} \pm 0.20$		$2.45^{+0.44}_{-0.38} \pm 0.22$			$2.16^{+0.61}_{-0.57}$
297	$p\overline{\Sigma^0}\gamma$	< 4.6		< 4.6			< 4.6
317	$\pi^+\nu\overline{\nu}$	< 100	< 100				< 100
318	$K^+e^+e^-$	$0.80^{+0.22}_{-0.19}$	$0.42^{+0.12}_{-0.11} \pm 0.02$	$0.63^{+0.19}_{-0.17} \pm 0.03$	< 2.4		0.49 ± 0.10
319	$K^+\mu^+\mu^-$	$0.34^{+0.19}_{-0.14}$	$0.31^{+0.15}_{-0.12} \pm 0.03$	$0.45^{+0.14}_{-0.12} \pm 0.03$	< 3.68	$0.60 \pm 0.15 \pm 0.04$	$0.45^{+0.09}_{-0.08}$
320	$K^+l^+l^-$	$0.53^{+0.11}_{-0.10} \pm 0.3$	$0.38^{+0.09}_{-0.08} \pm 0.02$				$0.38^{+0.09}_{-0.08}$
321	$K^+\nu\overline{\nu}$	< 52	< 52	< 36	< 240		< 36
322	$K^*(892)^+e^+e^-$	< 4.6	$0.75^{+0.76}_{-0.65} \pm 0.38$	$2.02^{+1.27+0.23}_{-1.01-0.24}$			$1.23^{+0.69}_{-0.62}$
323	$K^*(892)^+\mu^+\mu^-$	< 2.2	$0.97^{+0.94}_{-0.69} \pm 0.14$	$0.65^{+0.69+0.14}_{-0.53-0.15}$			$0.78^{+0.56}_{-0.44}$
324	$K^*(892)^+l^+l^-$	< 2.2	$0.73^{+0.50}_{-0.42} \pm 0.21$				$0.73^{+0.54}_{-0.47}$
327	$K^+e^+\mu^-$	< 0.8	< 0.09				< 0.09
328	$K^+e^-\mu^+$	< 6400	< 0.13				< 0.13
329	$K^{*+}e^\pm\mu^\mp$	< 7.9	< 1.4				< 1.4
330	$\pi^-e^+e^+$	< 1.6			< 1.6		< 1.6
331	$\pi^-\mu^+\mu^+$	< 1.4			< 1.4		< 1.4
332	$\pi^-e^+\mu^+$	< 1.3			< 1.3		< 1.3
333	$\rho^-e^+e^+$	< 2.6			< 2.6		< 2.6
334	$\rho^-\mu^+\mu^+$	< 5.0			< 5.0		< 5.0
335	$\rho^-e^+\mu^+$	< 3.3			< 3.3		< 3.3
336	$K^-e^+e^+$	< 1.0			< 1.0		< 1.0
337	$K^-\mu^+\mu^+$	< 1.8			< 1.8		< 1.8
338	$K^-e^+\mu^+$	< 2.0			< 2.0		< 2.0
339	$K^{*-}e^+e^+$	< 2.8			< 2.8		< 2.8
340	$K^{*-}\mu^+\mu^+$	< 8.3			< 8.3		< 8.3
341	$K^{*-}e^+\mu^+$	< 4.4			< 4.4		< 4.4
–	$\pi^+\ell^+\ell^-$	New	< 0.12				< 0.11

§ $M_{K\pi\pi} < 2.4$ GeV/c^2

Table 67: Branching fractions of semileptonic and radiative B^0 decays (in units of 10^{-6}). Upper limits are at 90% CL. Values in red (blue) are new published (preliminary) result since PDG2006 [as of March 15, 2007].

RPP#	Mode	PDG2006 Avg.	BABAR	Belle	CLEO	CDF	New Avg.
213	$K^*(892)^0\gamma$	40.1 ± 2.0	$39.2 \pm 2.0 \pm 2.4$	$40.1 \pm 2.1 \pm 1.7$	$45.5^{+7.2}_{-6.8} \pm 3.4$		40.1 ± 2.0
214	$K^0\eta\gamma$	$8.7^{+3.1+1.9}_{-2.7-1.6}$	$11.3^{+2.8}_{-2.6} \pm 0.6$	$8.7^{+3.1+1.9}_{-2.7-1.6}$			$10.3^{+2.3}_{-2.1}$
–	$K^0\eta'\gamma$	New	< 6.6				< 6.6
215	$K^0\phi\gamma$	< 8.3	< 2.7	< 8.3			< 2.7
216	$K^+\pi^-\gamma$ †	4.6 ± 1.4		$4.6^{+1.3+0.5}_{-1.2-0.7}$			4.6 ± 1.4
217	$K^*(1410)^0\gamma$	< 130		< 130			< 130
218	$K^+\pi^-\gamma$ (N.R.) †	< 2.6		< 2.6			< 2.6
219	$K^0\pi^+\pi^-\gamma$	$24 \pm 4 \pm 3$	$18.5 \pm 2.1 \pm 1.2$	$24 \pm 4 \pm 3$			19.5 ± 2.2
–	$K^+\pi^-\pi^0\gamma$	New	$40.7 \pm 2.2 \pm 3.1$				40.7 ± 3.8
220	$K_1(1270)^0\gamma$	< 58		< 58			< 58
221	$K_1(1400)^0\gamma$	< 15		< 15			< 15
222	$K_2^*(1430)^0\gamma$	12.4 ± 2.4	$12.2 \pm 2.5 \pm 1.0$	$13 \pm 5 \pm 1$			12.4 ± 2.4
224	$K_3^*(1780)^0\gamma$	< 83		< 83			< 83
226	$\rho^0\gamma$	< 0.4	$0.79^{+0.22}_{-0.20} \pm 0.06$	$1.25^{+0.37+0.07}_{-0.33-0.06}$	< 17		$0.93^{+0.19}_{-0.18}$
227	$\omega\gamma$	< 0.8	$0.40^{+0.24}_{-0.20} \pm 0.05$	$0.56^{+0.34+0.05}_{-0.27-0.10}$	< 9.2		$0.46^{+0.20}_{-0.17}$
228	$\phi\gamma$	< 0.85	< 0.85		< 3.3		< 0.85
293	$K^0e^+e^-$	< 0.54	$0.13^{+0.16}_{-0.11} \pm 0.02$	$0.00^{+0.20+0.02}_{-0.12-0.05}$	< 8.45		$0.09^{+0.12}_{-0.09}$
294	$K^0\mu^+\mu^-$	$0.20^{+0.13}_{-0.10}$	$0.59^{+0.33}_{-0.26} \pm 0.07$	$0.56^{+0.29}_{-0.23} \pm 0.05$	< 6.64		$0.57^{+0.22}_{-0.18}$
295	$K^0l^+l^-$	< 0.68	$0.29^{+0.16}_{-0.13} \pm 0.03$				$0.29^{+0.16}_{-0.13}$
296	$K^*(892)^0e^+e^-$	< 2.4	$1.04^{+0.33}_{-0.29} \pm 0.11$	$1.29^{+0.57+0.13}_{-0.49-0.10}$			$1.11^{+0.30}_{-0.26}$
297	$K^*(892)^0\mu^+\mu^-$	$1.22^{+0.38}_{-0.32}$	$0.87^{+0.38}_{-0.33} \pm 0.12$	$1.33^{+0.42}_{-0.37} \pm 0.11$		$0.82 \pm 0.31 \pm 0.10$	$0.98^{+0.22}_{-0.21}$
298	$K^*(892)^0\nu\overline{\nu}$	< 1000		< 360			< 360
299	$K^*(892)^0l^+l^-$	1.17 ± 0.30	$0.81^{+0.21}_{-0.19} \pm 0.09$				$0.81^{+0.23}_{-0.21}$
301	$K^0e^\pm\mu^\pm$	< 4.0	< 0.27				< 0.27
302	$K^(892)^0e^\pm\mu^\pm$	< 3.4	< 0.58				< 0.58
–	$\pi^0\ell^+\ell^-$	New	< 0.12				< 0.10

† $1.25\ \mathrm{GeV}/c^2 < M_{K\pi} < 1.6\ \mathrm{GeV}/c^2$

Table 68: Branching fractions of semileptonic and radiative B decays (in units of 10^{-6}). Upper limits are at 90% CL. Values in red (blue) are new published (preliminary) result since PDG2006 [as of March 15, 2007].

RPP#	Mode	PDG2006 Avg.	BABAR	Belle	CLEO	New Avg.
61	$K_2^*(1430)\gamma$	$1.7 \pm 0.6 \pm 0.1$			$1.7 \pm 0.6 \pm 0.1$	1.7 ± 0.6
63	$K_3^*(1780)\gamma$	< 37		< 2.8		< 2.8
70	$s\gamma$	343 ± 29	$327 \pm 18^{+55}_{-41}$	$355 \pm 32^{+30+11}_{-31-7}$	$321 \pm 43^{+32}_{-29}$	$355 \pm 24^{+9}_{-10} \pm 3$
–	$s\gamma$ with baryons	New			< 38 †	< 38 †
74	ρ/γ	< 1.9	$1.36^{+0.29}_{-0.27} \pm 0.10$		< 14	$1.36^{+0.31}_{-0.29}$
75	$\rho/\omega\gamma$	< 1.2	$1.25 \pm 0.25 \pm 0.09$	$1.32^{+0.34+0.10}_{-0.31-0.09}$	< 14	$1.28^{+0.21}_{-0.20}$
–	$K\eta\gamma$	New		$8.5^{+1.3}_{-1.2} \pm 0.9$		$8.5^{+1.6}_{-1.5}$
105	se^+e^- ‡	4.7 ± 1.3	$6.0 \pm 1.7 \pm 1.3$	$4.0 \pm 1.3^{+0.9}_{-0.8}$	< 57	4.7 ± 1.3
106	$s\mu^+\mu^-$	4.3 ± 1.2	$5.0 \pm 2.8 \pm 1.2$	$4.1 \pm 1.1^{+0.9}_{-0.8}$	< 58	$4.3^{+1.3}_{-1.2}$
107	$s\ell^+\ell^-$ ‡	4.5 ± 1.0	$5.6 \pm 1.5 \pm 1.3$	$4.11 \pm 0.83^{+0.85}_{-0.81}$	< 42	$4.50^{+1.03}_{-1.01}$
108	Ke^+e^-	$0.60^{+0.14}_{-0.12}$	$0.33^{+0.09}_{-0.08} \pm 0.02$	$0.48^{+0.15}_{-0.13} \pm 0.03$		$0.38^{+0.08}_{-0.07}$
109	$K^*(892)e^+e^-$	$1.24^{+0.37}_{-0.32}$	$0.97^{+0.30}_{-0.27} \pm 0.14$	$1.49^{+0.52+0.11}_{-0.46-0.13}$		$1.13^{+0.28}_{-0.26}$
110	$K\mu^+\mu^-$	$0.47^{+0.11}_{-0.10}$	$0.35^{+0.13}_{-0.11} \pm 0.03$	$0.48^{+0.13}_{-0.11} \pm 0.04$		$0.42^{+0.09}_{-0.08}$
111	$K^*(892)\mu^+\mu^-$	$1.19^{+0.34}_{-0.29}$	$0.88^{+0.35}_{-0.30} \pm 0.12$	$1.17^{+0.36}_{-0.31} \pm 0.10$		$1.03^{+0.26}_{-0.23}$
112	$K\ell^+\ell^-$	0.54 ± 0.08	$0.34 \pm 0.07 \pm 0.02$	$0.48^{+0.10}_{-0.09} \pm 0.03$	< 1.7	0.39 ± 0.06
113	$K^*(892)\ell^+\ell^-$	1.05 ± 0.20	$0.78^{+0.19}_{-0.17} \pm 0.11$	$1.15^{+0.26}_{-0.24} \pm 0.08$	< 3.3	$0.94^{+0.17}_{-0.16}$
115	$\pi e^\pm\mu^\mp$	< 1.6	< 0.092		< 1.6	< 1.6
116	$\rho e^\pm\mu^\mp$	< 3.2			< 3.2	< 3.2
117	$Ke^\pm\mu^\mp$	< 1.6	< 0.038		< 1.6	< 0.038
118	$K^*e^\pm\mu^\mp$	< 6.2	< 0.51		< 6.2	< 0.51
–	$\pi\ell^+\ell^-$	New	< 0.091			< 0.08

†$E_\gamma > 2.0$ GeV; ‡$M(\ell^+\ell^-) > 0.2$ GeV/c^2

Table 69: Branching fractions of inclusive B decays (in units of 10^{-6}). Values in red (blue) are new published (preliminary) result since PDG2006 [as of March 15, 2007].

RPP#	Mode	PDG2006 Avg.	BABAR	Belle	CLEO	New Avg.
–	K^+X	New	196^{+37+31}_{-34-30}			196^{+48}_{-45}
–	K^0X	New	154^{+55+55}_{-48-41}			154^{+77}_{-63}

† $p^* > 2.34$ GeV

Table 70: Branching fractions of leptonic B decays (in units of 10^{-6}). Upper limits are at 90% CL. Values in red (blue) are new published (preliminary) result since PDG2006 [as of March 15, 2007].

RPP#	Mode	PDG2006 Avg.	BABAR	Belle	CLEO	CDF	DØ	New Avg.
15	$e^+\nu$	< 15	< 7.9	< 1.0	< 15			< 1.0
16	$\mu^+\nu$	< 6.6	< 6.2	< 1.7	< 21			< 1.7
17	$\tau^+\nu$	< 260	$88 \pm 68 \pm 11$	179^{+56+46}_{-49-51}	< 840			132 ± 49
18	$e^+\nu_e\gamma$	< 200			< 200			< 200
19	$\mu^+\nu_\mu\gamma$	< 52			< 52			< 52
290	$\gamma\gamma$	< 0.62	< 1.7	< 0.62				< 0.62
291	e^+e^-	< 0.061	< 0.061	< 0.19	< 0.83			< 0.061
–	$e^+e^-\gamma$	New	< 0.07					< 0.07
292	$\mu^+\mu^-$	< 0.039	< 0.083	< 0.16	< 0.61	< 0.023		< 0.023
–	$\mu^+\mu^-\gamma$	New	< 0.34					< 0.34
–	$\tau^+\tau^-$	New	< 4100					< 4100
300	$e^\pm\mu^\mp$	< 0.17	< 0.18	< 0.17	< 1.5			< 0.17
303	$e^\pm\tau^\mp$	< 110			< 110			< 110
304	$\mu^\pm\tau^\mp$	< 38			< 38			< 38
305	$\nu\overline{\nu}$	< 220	< 220					< 220
306	$\nu\overline{\nu}\gamma$	< 47	< 47					< 47

6.3 $B \to s\gamma$

The decay $b \to s\gamma$ proceeds through a process of flavor changing neutral current. Since the charged Higgs or SUSY particles may contribute in the penguin loop, the branching fraction is sensitive to physics beyond the Standard Model. Experimentally, the branching fraction is measured using either a semi-inclusive or an inclusive approach. A minimum photon energy requirement is applied in the analysis and the branching fraction is corrected based on the theoretical model for the photon energy spectrum (shape function). Although there are several experimental results available, only one measurement each for *BABAR*, Belle and CLEO is used in the HFAG average to avoid dealing with correlated errors for results reported from the same experiment. Furthermore, the model uncertainties from the shape function should be highly correlated but no proper action was made in our previous averages. To perform the average with better precision and good accuracy, it is important to use as many experimental results as possible and to handle the shape function issue in a proper way. In this note, we report the updated average of $b \to s\gamma$ branching fraction by implementing a common shape function.

Several shape function schemes are commonly used. Usually one is chosen to obtain the extrapolation factor, defined as the ratio of the $b \to s\gamma$ branching fractions with minimum photon energies above and at 1.6 GeV, and the difference between various schemes are treated as the model uncertainty. Recently O. Buchmüller and H. Flächer have calculated the extrapolation factors [261]. Table 71 lists the extrapolation factors with various photon energy cuts for three different schemes and the average. The appropriate approach to average the experimental results is to first convert them according to the average extrapolation factors and then perform the average, assuming that the errors of the extrapolation factors are 100% correlated.

Table 71: Extrapolation factor in various scheme with various minimum photon energy requirement (in GeV).

Scheme	$E_\gamma < 1.7$	$E_\gamma < 1.8$	$E_\gamma < 1.9$	$E_\gamma < 2.0$	$E_\gamma < 2.242$
Kinetic	0.986 ± 0.001	0.968 ± 0.002	0.939 ± 0.005	0.903 ± 0.009	0.656 ± 0.031
Neubert SF	0.982 ± 0.002	0.962 ± 0.004	0.930 ± 0.008	0.888 ± 0.014	0.665 ± 0.035
Kagan-Neubert	0.988 ± 0.002	0.970 ± 0.005	0.940 ± 0.009	0.892 ± 0.014	0.643 ± 0.033
Average	0.985 ± 0.004	0.967 ± 0.006	0.936 ± 0.010	0.894 ± 0.016	0.655 ± 0.037

After surveying all available experimental results, the five shown in Table 72 are selected for the average. They have provided in their papers either the $b \to s\gamma$ branching fraction at a certain photon energy cut or the extrapolation factor used. Therefore we are able to convert them to the values at $E_{\rm min} = 1.6$ GeV using the information in Table 71. The errors are, in order, statistical, systematic and shape-function systematic, except for the *BABAR* inclusive where there is a second systematic error (third quoted error) due to theoretical uncertainties. Moreover, in the three inclusive analyses a possible $b \to d\gamma$ contamination has been considered according to the theoretical expectation of $(4.0 \pm 1.6)\%$. The uncertainty from the $b \to d\gamma$ fraction in the three inclusive measurements should not be considered independently. For those three measurements, a fourth uncertainty for the $b \to d\gamma$ fraction is included. We perform the average assuming that the systematic errors of the shape function and the $d\gamma$ fraction are correlated, and the other systematic errors and the statistical errors are Gaussian and uncorrelated. The obtained average is $\mathcal{B}(b \to s\gamma) = (355 \pm 24^{+9}_{-10} \pm 3) \times 10^{-6}$ with a χ^2/DOF$= 0.74/4$, where the errors are combined statistical and systematic, systematic due to

the shape function, and the $d\gamma$ fraction. The last two errors are estimated to be the difference of the average after simultaneously varying the central value of each experimental result by $\pm 1\sigma$. Although a small fraction of events was used in both the semi-inclusive and inclusive analyses in the same experiment, we neglect their statistical correlations. Some other correlated systematic errors, such as photon detection and the background suppression, are not considered in our new average. In the future it would be better if each collaboration would provide a single combined result so that the average can be performed more accurately and easily.

Table 72: Reported branching fraction, minimum photon energy, branching fraction at minimum photon energy and converted branching fraction for the decay $b \to s\gamma$. All the branching fractions are in units of 10^{-6}. See text for an explanation of the errors.

Mode	Reported $\mathcal{B}$	$E_{\rm min}$	$\mathcal{B}$ at $E_{\rm min}$	Modified $\mathcal{B}$ ($E_{\rm min} = 1.6$)
CLEO Inc. [327]	$321 \pm 43 \pm 27^{+18}_{-10}$	2.0	$306 \pm 41 \pm 26$	$329 \pm 44 \pm 28 \pm 6 \pm 6$
Belle Semi. [328]	$336 \pm 53 \pm 42^{+50}_{-54}$	2.24	–	$369 \pm 58 \pm 46^{+56}_{-60}$
Belle Inc. [329]	$355 \pm 32^{+30+11}_{-31-7}$	1.8	$351 \pm 32 \pm 29$	$350 \pm 32^{+30}_{-31} \pm 2 \pm 2$
BABAR Semi. [330]	$327 \pm 18^{+55+4}_{-40-9}$	1.9	$327 \pm 18^{+55+4}_{-40-9}$	$349 \pm 20^{+59+4}_{-46-3}$
BABAR Inc. [331]	–	1.9	$367 \pm 29 \pm 34 \pm 29$	$392 \pm 31 \pm 36 \pm 30 \pm 4 \pm 6$

6.4 Baryonic decays

Table 73: Branching fractions of baryonic B^+ decays (in units of 10^{-6}). Upper limits are at 90% CL. values in red (blue) are new published (preliminary) result since PDG2006 [as of March 15, 2007].

RPP#	Mode	PDG2006 Avg.	BABAR	Belle	CLEO	New Avg.
286	$p\overline{p}\pi^+$	$3.1^{+0.8}_{-0.7}$ §		$1.89^{+0.28}_{-0.24} \pm 0.14$ ‡	< 160	$3.06^{+0.82}_{-0.72}$
289	$p\overline{p}K^+$	5.6 ± 1.0 §	$6.7 \pm 0.5 \pm 0.4$ †	$5.98^{+0.29}_{-0.27} \pm 0.46$ ‡		6.10 ± 0.48
290	$\Theta^{++}\overline{p}$ *	< 0.091	< 0.09	< 0.091		< 0.09
291	$f_J(2221)K^+$ *	< 0.41		< 0.41		< 0.41
292	$p\overline{\Lambda}(1520)$	< 1.5	< 1.5			< 1.5
294	$p\overline{p}K^{*+}$	$10.3^{+3.6+1.3}_{-2.8-1.7}$ ‡		$10.3^{+3.6+1.3}_{-2.8-1.7}$ ‡		$10.3^{+3.8}_{-3.3}$
295	$p\overline{\Lambda}$	< 0.49		< 0.32	< 1.5	< 0.29
New	$p\overline{\Lambda}\pi^0$			$3.00^{+0.61}_{-0.53} \pm 0.33$		$3.00^{+0.69}_{-0.62}$
299	$\Lambda\overline{\Lambda}\pi^+$	< 2.8 ‡		< 2.8 ‡		< 2.8 ‡
300	$\Lambda\overline{\Lambda}K^+$	$2.9^{+0.9}_{-0.7} \pm 0.4$ ‡		$2.9^{+0.9}_{-0.7} \pm 0.4$ ‡		$2.9^{+1.0}_{-0.8}$
301	$\overline{\Delta}^0 p$	< 380		< 1.42	< 380	< 1.42
302	$\Delta^{++}\overline{p}$	< 150		< 0.14	< 150	< 0.14

† Charmonium decays to $p\overline{p}$ have been statistically subtracted.
‡ The charmonium mass region has been vetoed.
* Product BF - daughter BF taken to be 100%:
$\Theta(1540)^{++} \to K^+p$ (pentaquark candidate);
$\mathcal{G}(2220) \to p\overline{p}$ (glueball candidate).

Table 74: Branching fractions of baryonic B^0 decays (in units of 10^{-6}). Upper limits are at 90% CL. values in red (blue) are new published (preliminary) result since PDG2006 [as of March 15, 2007].

RPP#	Mode	PDG2006 Avg.	BABAR	Belle	CLEO	New Avg.
266	$p\overline{p}$	< 0.27	< 0.27	< 0.11	< 1.4	< 0.11
268	$p\overline{p}K^0$	$2.1^{+0.6}_{-0.4}$ §		$2.40^{+0.64}_{-0.44} \pm 0.28$ ‡		$2.40^{+0.70}_{-0.52}$
269	Θ^+K^0 †	< 0.23		< 0.23		< 0.23
270	$p\overline{p}K^{*0}$	< 7.6 ‡		< 7.6 ‡		< 7.6 ‡
271	$p\overline{\Lambda}\pi^-$	2.6 ± 0.5 §	$3.30 \pm 0.53 \pm 0.31$	$3.23^{+0.33}_{-0.29} \pm 0.33$	< 13	$3.29^{+0.47}_{-0.44}$
272	$p\overline{\Lambda}K^-$	< 0.82		< 0.82		< 0.82
273	$p\overline{\Sigma}^0\pi^-$	< 3.8		< 3.8		< 3.8
274	$\Lambda\overline{\Lambda}$	< 0.69		< 0.32	< 1.2	< 0.32

† Product BF - daughter BF taken to be 100%: ‡ The charmonium mass region has been vetoed. $\Theta(1540)^+ \to pK^0_S$ (pentaquark candidate).

6.5 B_s decays

Table 75: B_s branching fractions (in units of 10^{-6}). Upper limits are at 90% CL. Values in red (blue) are new published (preliminary) result since PDG2006 [as of March 15, 2007].

RPP#	Mode	PDG2006 Avg.	Belle	CDF	DØ	New Avg.
9	$\pi^+\pi^-$	< 170		$0.53 \pm 0.31 \pm 0.40$		0.53 ± 0.51
15	$\phi\phi$	14 ± 8		$14^{+6}_{-5} \pm 6$ †		14^{+8}_{-7}
16	π^+K^-	< 210		$5.0 \pm 0.75 \pm 1.0$		5.00 ± 1.25
17	K^+K^-	< 59	< 340	$24.4 \pm 1.4 \pm 4.6$		24.4 ± 4.8
22	$\gamma\gamma$	< 148	< 56			< 56
23	$\phi\gamma$	< 120	< 410			< 410
24	$\mu^+\mu^-$	< 0.15		< 0.080	< 0.075	< 0.075
26	$e^\pm\mu^\mp$	< 6.1		< 6.1		< 6.1
27	$\mu^+\mu^-\phi$	< 47		< 2.3	< 3.2 †	< 2.3

†Relative BF converted to absolute BF

Table 76: B_s rare relative branching fractions. Values in red (blue) are new published (preliminary) result since PDG2006 [as of March 15, 2007].

RPP#	Mode	PDG2006 Avg.	CDF	DØ	New Avg.
9	$f_s\mathcal{B}(B_s^0 \to \pi^+\pi^-)/f_d\mathcal{B}(B^0 \to K^+\pi-)$		$0.007 \pm 0.004 \pm 0.005$		0.007 ± 0.006
15	$\mathcal{B}(B_s^0 \to \phi\phi)/\mathcal{B}(B_s^0 \to J/\psi\phi)$		$(10^{+5}_{-4} \pm 1) \times 10^{-3}$		10^{+7}_{-6}
16	$f_s\mathcal{B}(B_s^0 \to K^+\pi^-)/f_d\mathcal{B}(B_d^0 \to K^+\pi^-)$		$0.066 \pm 0.010 \pm 0.010$		0.066 ± 0.014
17	$f_s\mathcal{B}(B_s^0 \to K^+K^-)/f_d\mathcal{B}(B_d^0 \to K^+\pi^-)$		$0.324 \pm 0.019 \pm 0.041$		0.324 ± 0.045
27	$\mathcal{B}(B_s^0 \to \mu^+\mu^-\phi)/\mathcal{B}(B_s^0 \to J/\psi\phi)$		$1.24 \pm 0.60 \pm 0.15$	$< 3.5 \times 10^{-3}$	1.24 ± 0.62

6.6 Charge asymmetries

Table 77: CP asymmetries for charmless hadronic charged B decays. Values in red (blue) are new published (preliminary) result since PDG2006 [as of March 15, 2007].

RPP#	Mode	PDG2006 Avg.	BABAR	Belle	CLEO	CDF	New Avg.
182	$K^0\pi^+$	-0.02 ± 0.07	$-0.029 \pm 0.039 \pm 0.010$	$0.03 \pm 0.03 \pm 0.01$	$0.18 \pm 0.24 \pm 0.02$		0.009 ± 0.025
183	$K^+\pi^0$	0.04 ± 0.04	$0.016 \pm 0.041 \pm 0.012$	$0.07 \pm 0.03 \pm 0.01$	$-0.29 \pm 0.23 \pm 0.02$		0.047 ± 0.026
184	$\eta' K^+$	0.020 ± 0.025	$0.033 \pm 0.028 \pm 0.005$	$0.028 \pm 0.028 \pm 0.021$	$0.03 \pm 0.12 \pm 0.02$		0.031 ± 0.021
185	$\eta' K^{*+}$	New	$0.30^{+0.33}_{-0.37} \pm 0.02$				$0.30^{+0.33}_{-0.37}$
186	ηK^+	-0.25 ± 0.14	$-0.20 \pm 0.15 \pm 0.01$	$-0.39 \pm 0.16 \pm 0.03$			-0.29 ± 0.11
187	ηK^{*+}	0.13 ± 0.14	$0.01 \pm 0.08 \pm 0.02$	$0.03 \pm 0.10 \pm 0.01$			0.02 ± 0.06
–	$\eta K_0^{*+}(1430)$	New	$0.05 \pm 0.13 \pm 0.02$				0.05 ± 0.13
–	$\eta K_2^{*+}(1430)$	New	$-0.45 \pm 0.30 \pm 0.02$				-0.45 ± 0.30
188	ωK^+	-0.02 ± 0.13	$0.05 \pm 0.09 \pm 0.01$	$0.05^{+0.08}_{-0.07} \pm 0.01$			0.05 ± 0.06
192	$K^{*0}\pi^+$	0.07 ± 0.11	$0.07 \pm 0.08 \pm 0.07$	$-0.149 \pm 0.064 \pm 0.022$			-0.085 ± 0.057
193	$K^{*+}\pi^0$	New	$0.04 \pm 0.29 \pm 0.05$				0.04 ± 0.29
194	$K^+\pi^+\pi^-$	-0.013 ± 0.039	$-0.013 \pm 0.037 \pm 0.011$	$0.049 \pm 0.026 \pm 0.020$			0.023 ± 0.025
196	$K^+ f_0(980)$	$0.09^{+0.14}_{-0.12}$	$0.09 \pm 0.10^{+0.10}_{-0.06}$	$-0.077 \pm 0.065^{+0.046}_{-0.026}$			$-0.026^{+0.068}_{-0.064}$
197	$f_2(1270)K^+$	New		$-0.59 \pm 0.22 \pm 0.04$			-0.59 ± 0.22
202	$K^+\rho^0$	$0.32^{+0.16}_{-0.15}$	$0.32 \pm 0.13^{+0.10}_{-0.08}$	$0.30 \pm 0.11^{+0.11}_{-0.05}$			$0.31^{+0.11}_{-0.10}$
203	$K_0^*(1430)^0\pi^+$	$-0.064^{+0.039}_{-0.041}$	$-0.064 \pm 0.032^{+0.023}_{-0.026}$	$0.076 \pm 0.038^{+0.028}_{-0.022}$			-0.002 ± 0.029
211	$K^0\rho^+$	New	$0.12 \pm 0.17 \pm 0.02$				0.12 ± 0.17
213	$K^{*+}\rho^0$	$0.20^{+0.32}_{-0.29}$	$0.20^{+0.32}_{-0.29} \pm 0.04$				$0.20^{+0.32}_{-0.29}$
214	$K^{*0}\rho^+$	New	$-0.01 \pm 0.16 \pm 0.02$				-0.01 ± 0.16
–	$K^{*+} f_0$	New	$-0.34 \pm 0.21 \pm 0.03$				-0.34 ± 0.21
218	$K^+\overline{K^0}$	0.15 ± 0.33	$0.10 \pm 0.26 \pm 0.03$	$0.13^{+0.23}_{-0.24} \pm 0.02$			$0.12^{+0.17}_{-0.18}$
220	$K^+K_SK_S$	-0.04 ± 0.11	$-0.04 \pm 0.11 \pm 0.02$				-0.04 ± 0.11
228	$K^+K^-K^+$	-0.02 ± 0.08	$-0.02 \pm 0.03 \pm 0.02$				-0.02 ± 0.04
229	ϕK^+	0.01 ± 0.07	$0.046 \pm 0.046 \pm 0.017$	$0.01 \pm 0.12 \pm 0.05$		$-0.07 \pm 0.17^{+0.03}_{-0.02}$	0.034 ± 0.044
235	$K^{*+}K^+K^-$	New	$0.11 \pm 0.08 \pm 0.03$				0.11 ± 0.09
–	$K^{*+}\pi^+\pi^-$	New	$0.07 \pm 0.07 \pm 0.04$				0.07 ± 0.08
236	ϕK^{*+}	0.05 ± 0.11	$0.16 \pm 0.17 \pm 0.03$	$-0.02 \pm 0.14 \pm 0.03$			0.05 ± 0.11
239	$\phi\phi K^+$	New		$0.01^{+0.19}_{-0.16} \pm 0.02$			$0.01^{+0.19}_{-0.16}$
242	$K^+\eta\gamma$	-0.16 ± 0.10	$-0.09 \pm 0.12 \pm 0.01$	$-0.16 \pm 0.09 \pm 0.06$			-0.13 ± 0.08
243	$K^+\phi\gamma$	New	$-0.26 \pm 0.14 \pm 0.05$				-0.26 ± 0.15
254	$\pi^+\pi^0$	-0.02 ± 0.07	$-0.02 \pm 0.09 \pm 0.01$	$0.07 \pm 0.06 \pm 0.01$			0.04 ± 0.05
255	$\pi^+\pi^-\pi^+$	-0.01 ± 0.09	$-0.01 \pm 0.08 \pm 0.03$				-0.01 ± 0.09
256	$\rho^0\pi^+$	-0.07 ± 0.13	$-0.07 \pm 0.12^{+0.03}_{-0.06}$				$-0.07^{+0.12}_{-0.13}$
257	$f_0(980)\pi^+$	New	$-0.50 \pm 0.54 \pm 0.06$				-0.50 ± 0.54
258	$f_2(1270)\pi^+$	New	$-0.01 \pm 0.25^{+0.28}_{-0.32}$				$-0.01^{+0.38}_{-0.41}$
264	$\rho^+\pi^0$	0.15 ± 0.12	$-0.01 \pm 0.13 \pm 0.02$	$0.06 \pm 0.17^{+0.04}_{-0.05}$			0.02 ± 0.11
266	$\rho^+\rho^0$	-0.09 ± 0.16	$-0.12 \pm 0.13 \pm 0.10$	$0.00 \pm 0.22 \pm 0.03$			-0.08 ± 0.13
269	$\omega\pi^+$	0.10 ± 0.22	$-0.01 \pm 0.10 \pm 0.01$	$-0.02 \pm 0.09 \pm 0.01$	$-0.34 \pm 0.25 \pm 0.02$		-0.04 ± 0.06
270	$\omega\rho^+$	0.05 ± 0.26	$0.04 \pm 0.18 \pm 0.02$				0.04 ± 0.18
271	$\eta\pi^+$	-0.05 ± 0.10	$-0.13 \pm 0.12 \pm 0.01$	$-0.23 \pm 0.09 \pm 0.02$			-0.19 ± 0.07
272	$\eta'\pi^+$	0.14 ± 0.16	$0.14 \pm 0.16 \pm 0.01$	$0.20^{+0.37}_{-0.36} \pm 0.04$			0.15 ± 0.15
273	$\eta'\rho^+$	New	$-0.04 \pm 0.28 \pm 0.02$				-0.04 ± 0.28
274	$\eta\rho^+$	New	$0.02 \pm 0.18 \pm 0.02$	$-0.04^{+0.34}_{-0.32} \pm 0.01$			0.01 ± 0.16
286	$p\overline{p}\pi^+$	-0.16 ± 0.22		$-0.16 \pm 0.22 \pm 0.01$			-0.16 ± 0.22
289	$p\overline{p}K^+$	-0.05 ± 0.11	$-0.16 \pm 0.08 \pm 0.04$	$-0.05 \pm 0.11 \pm 0.01$			-0.12 ± 0.07
320	$K^+\ell\ell$	New	$-0.07 \pm 0.22 \pm 0.02$				-0.07 ± 0.22

Table 78: Charmless hadronic CP asymmetries for $B^{\pm}/B^0$ admixtures. Values in red (blue) are new published (preliminary) result since PDG2006 [as of March 15, 2007].

RPP#	Mode	PDG2006 Avg.	BABAR	Belle	CLEO	CDF	New Avg.
58	$K^*\gamma$	-0.01 ± 0.07	$-0.013 \pm 0.036 \pm 0.010$	$-0.015 \pm 0.044 \pm 0.012$	$0.08 \pm 0.13 \pm 0.03$		-0.010 ± 0.028
70	$s\gamma$	0.00 ± 0.04	$0.025 \pm 0.050 \pm 0.015$	$0.002 \pm 0.050 \pm 0.030$	$-0.079 \pm 0.108 \pm 0.022$		0.004 ± 0.037
–	$(s+d)\gamma$	New	$-0.11 \pm 0.12 \pm 0.02$				-0.11 ± 0.12
107	$s\ell\ell$	-0.22 ± 0.26	$-0.22 \pm 0.26 \pm 0.02$				-0.22 ± 0.26
113	$K^*\ell\ell$	New	$0.03 \pm 0.23 \pm 0.03$				0.03 ± 0.23

Table 79: CP asymmetries for charmless hadronic neutral B decays. Values in red (blue) are new published (preliminary) result since PDG2006 [as of March 15, 2007].

RPP#	Mode	PDG2006 Avg.	BABAR	Belle	CLEO	CDF	New Avg.
168	$K^+\pi^-$	-0.113 ± 0.020	$-0.107 \pm 0.018^{+0.007}_{-0.004}$	$-0.093 \pm 0.018 \pm 0.008$	$-0.04 \pm 0.16 \pm 0.02$	$-0.086 \pm 0.023 \pm 0.009$	-0.095 ± 0.013
171	$\eta' K^{*0}$	New	$-0.08 \pm 0.25 \pm 0.02$				-0.08 ± 0.25
172	ηK^{*0}	0.02 ± 0.11	$0.21 \pm 0.06 \pm 0.02$	$0.17 \pm 0.08 \pm 0.01$			0.19 ± 0.05
–	$\eta K_0^{*0}(1430)$	New	$0.06 \pm 0.13 \pm 0.02$				0.06 ± 0.13
–	$\eta K_2^{*0}(1430)$	New	$-0.07 \pm 0.19 \pm 0.02$				-0.07 ± 0.19
180	$K^0\overline{K^0}$	New		$-0.58^{+0.73}_{-0.66} \pm 0.04$			$-0.58^{+0.73}_{-0.66}$
183	$K^+\rho^-$	0.26 ± 0.15		$0.22^{+0.22+0.06}_{-0.23-0.02}$			0.22 ± 0.23
182	$K^+\pi^-\pi^0$	0.07 ± 0.11		$0.07 \pm 0.11 \pm 0.01$			0.07 ± 0.11
189	$K^{*+}\pi^-$	-0.05 $\pm$ 0.14	$-0.11 \pm 0.14 \pm 0.05$		$0.26^{+0.33+0.10}_{-0.34-0.08}$		-0.05 ± 0.14
191	$K^{*0}\pi^0$	New					$-0.01^{+0.27}_{-0.26}$
199	$K^{*0}\rho^0$	New	$0.09 \pm 0.19 \pm 0.02$				0.09 ± 0.19
200	$K^{*0}f_0(980)$	New	$-0.17 \pm 0.28 \pm 0.02$				-0.17 ± 0.28
204	ϕK^{*0}	0.01 ± 0.07	$-0.03 \pm 0.07 \pm 0.03$	$0.02 \pm 0.09 \pm 0.02$			-0.01 ± 0.06
–	$\phi K_0^*(1430)^0$	New	$0.17 \pm 0.15 \pm 0.03$				0.17 ± 0.15
–	$\phi K_2^*(1430)^0$	New	$-0.12 \pm 0.14 \pm 0.04$				-0.12 ± 0.15
230	$\pi^0\pi^0$	0.3 ± 0.4	$0.33 \pm 0.36 \pm 0.08$	$0.44^{+0.73+0.04}_{-0.62-0.06}$			$0.36^{+0.33}_{-0.31}$

† Measurements of time-dependent CP asymmetries are listed on the Unitarity Triangle home page. (http://www.slac.stanford.edu/xorg/hfag/triangle/index.html)

6.7 Polarization measurements

Table 80: Longitudinal polarization fraction f_L for B^+ decays. Values in red (blue) are new published (preliminary) result since PDG2006 [as of March 15, 2007].

RPP#	Mode	PDG2006 Avg.	BABAR	Belle	New Avg.
213	$K^{*+}\rho^0$	$0.96^{+0.04}_{-0.15} \pm 0.04$	$0.96^{+0.04}_{-0.15} \pm 0.05$		$0.96^{+0.06}_{-0.16}$
214	$K^{*0}\rho^+$	$0.43 \pm 0.11^{+0.05}_{-0.02}$	$0.52 \pm 0.10 \pm 0.04$	$0.43 \pm 0.11^{+0.05}_{-0.02}$	0.48 ± 0.08
236	ϕK^{*+}	0.50 ± 0.07	$0.46 \pm 0.12 \pm 0.03$	$0.52 \pm 0.08 \pm 0.03$	0.50 ± 0.07
266	$\rho^+\rho^0$	0.96 ± 0.06	$0.905 \pm 0.042^{+0.023}_{-0.027}$	$0.95 \pm 0.11 \pm 0.02$	$0.912^{+0.044}_{-0.045}$
270	$\omega\rho^+$	$0.88^{+0.12}_{-0.15} \pm 0.03$	$0.82 \pm 0.11 \pm 0.02$		0.82 ± 0.11

Table 81: Full angular analysis of $B^+ \to \phi K^{*+}$. Values in red (blue) are new published (preliminary) result since PDG2006 [as of March 15, 2007].

Parameter	PDG2006 Avg.	BABAR	Belle	New Avg.
$f_\perp$	$0.19 \pm 0.08 \pm 0.02$		$0.19 \pm 0.08 \pm 0.02$	0.19 ± 0.08
$\phi_\parallel$	$2.10 \pm 0.28 \pm 0.04$		$2.10 \pm 0.28 \pm 0.04$	2.10 ± 0.28
$\phi_\perp$	$2.31 \pm 0.30 \pm 0.07$		$2.31 \pm 0.30 \pm 0.07$	2.31 ± 0.31

BR, f_L and A_{CP} are tabulated separately.

Table 82: Longitudinal polarization fraction f_L for B^0 decays. Values in red (blue) are new published (preliminary) result since PDG2006 [as of March 15, 2007].

RPP#	Mode	PDG2006 Avg.	BABAR	Belle	CDF	New Avg.
199	$K^{*0}\rho^0$	New	$0.57 \pm 0.09 \pm 0.08$			0.57 ± 0.12
204	ϕK^{*0}	0.48 ± 0.04	$0.506 \pm 0.040 \pm 0.015$	$0.45 \pm 0.05 \pm 0.02$	$0.57 \pm 0.10 \pm 0.05$	0.491 ± 0.032
–	$\phi K_2^*(1430)^0$	New	$0.85 \pm 0.07 \pm 0.04$			0.85 ± 0.08
253	$\rho^0\rho^0$	New	$0.86^{+0.11}_{-0.13} \pm 0.05$			$0.86^{+0.12}_{-0.14}$
257	$\rho^+\rho^-$	$0.967^{+0.022}_{-0.027}$	$0.977 \pm 0.024^{+0.015}_{-0.013}$	$0.941^{+0.034}_{-0.040} \pm 0.030$		0.968 ± 0.023

Table 83: Full angular analysis of $B^0 \to \phi K^{*0}$. Values in red (blue) are new published (preliminary) result since PDG2006 [as of March 15, 2007].

Parameter	PDG2006 Avg.	BABAR	Belle	CDF	New Avg.
$f_\perp = \Lambda_{\perp\perp}$	0.26 ± 0.04	$0.227 \pm 0.038 \pm 0.013$	$0.31^{+0.06}_{-0.05} \pm 0.02$	$0.20 \pm 0.10 \pm 0.05$	0.252 ± 0.031
$\phi_\parallel$	$2.36^{+0.18}_{-0.16}$	$2.31 \pm 0.14 \pm 0.08$	$2.40^{+0.28}_{-0.24} \pm 0.07$	$2.97 \pm 0.52 \pm 0.26$	$2.37^{+0.14}_{-0.13}$
$\phi_\perp$	2.49 ± 0.18	$2.24 \pm 0.15 \pm 0.09$	$2.51 \pm 0.25 \pm 0.06$	$2.77 \pm 0.37 \pm 0.37$	2.36 ± 0.14
A^0_{CP}	0.01 ± 0.09	$-0.03 \pm 0.08 \pm 0.02$	$0.13 \pm 0.12 \pm 0.04$		0.02 ± 0.07
$A^\perp_{CP}$	-0.16 ± 0.15	$-0.03 \pm 0.16 \pm 0.05$	$-0.20 \pm 0.18 \pm 0.04$		-0.11 ± 0.12
$\Delta\phi_\parallel$	0.02 ± 0.28	$0.24 \pm 0.14 \pm 0.08$	$-0.32 \pm 0.27 \pm 0.07$		0.10 ± 0.14
$\Delta\phi_\perp$	0.03 ± 0.33	$0.19 \pm 0.15 \pm 0.08$	$-0.30 \pm 0.25 \pm 0.06$		0.04 ± 0.14

BR, f_L and A_{CP} are tabulated separately.

Table 84: Full angular analysis of $B^0 \to \phi K^*_2(1430)^0$. Values in red (blue) are new published (preliminary) result since PDG2006 [as of March 15, 2007].

Parameter	PDG2006 Avg.	BABAR	Belle	CDF	New Avg.
$f_\perp = \Lambda_{\perp\perp}$	New	$0.045^{+0.049}_{-0.040} \pm 0.013$			$0.045^{+0.051}_{-0.042}$
$\phi_\parallel$	New	$2.90 \pm 0.39 \pm 0.06$			2.90 ± 0.40
$\phi_\perp$	New	$5.7^{+0.6}_{-0.9} \pm 0.1$			$5.7^{+0.6}_{-0.9}$

BR, f_L and A_{CP} are tabulated separately.

7 B Decays to open charm and charmonium final states

This section reports the updated contribution to the HFAG report from the "$B \to$ charm " group[19]. The mandate of the group is to compile measurements and perform averages of all available quantities related to B decays to charmed particles, excluding CP related quantities. To date the group has analyzed a total of 431 measurements reported in 131 papers, principally branching fractions. The group aims to organize and present the copious information on B decays to charmed particles obtained from a combined sample of more than one billion B mesons from the BABAR, Belle and CDF Collaborations.

Branching fractions for rare B-meson decays or decay chains of a few 10^{-7} are being measured with statistical uncertainties typically below 30%. Results for more common decay chains, with branching fractions around 10^{-4}, are becoming precision measurements, with uncertainties typically at the 3% level. Some decays have been observed for the first time, for example $B^- \to \Lambda_c^- \Lambda_c^+ K^-$ or $B^- \to \chi_{c1}\pi^-$, with a branching fraction of $(6.5 \pm 3.7) \times 10^{-4}$ and $(2.2 \pm 0.5) \times 10^{-5}$, respectively.

Among the many results, we highlight the great improvements that have been attained towards a deeper understanding of recently discovered new states with either hidden or open charm content. The $J/\psi\gamma$ decay mode of the $X(3870)$ has been observed by both BABAR and Belle and the average branching fraction is $\mathcal{B}(B^- \to X(3870)K^-) \times \mathcal{B}(X(3870 \to J/\psi\gamma) = (2.4 \pm 0.5) \times 10^{-6}$: this final state allowed to unambiguously establish the positive C parity of the $X(3870)$. Branching fractions for several B decays to $D_{sJ}^{*-}(2317)$ and $D_{sJ}^-(2460)$ have been measured, and also absolute branching fraction measurements have been reported: $\mathcal{B}(\overline{B}^0 \to D_{sJ}^-(2460)D^+) = (0.26 \pm 0.17) \times 10^{-2}$, $\mathcal{B}(\overline{B}^0 \to D_{sJ}^-(2460)D^{*+}) = (0.88 \pm 0.24) \times 10^{-2}$, $\mathcal{B}(B^- \to D_{sJ}^-(2460)D^0) = (0.43 \pm 0.21) \times 10^{-2}$ and $\mathcal{B}(B^- \to D_{sJ}^-(2460)D^{*0}) = (1.12 \pm 0.33) \times 10^{-2}$. The abundance of measurements with many different final states for these particles is of the greatest importance for quantum number assignments, and already some of the proposed theoretical interpretations have been ruled out.

The measurements are classified according to the decaying particle: Charged B, Neutral B or Miscellaneous; the decay products and the type of quantity: branching fraction, product of branching fractions, ratio of branching fractions or other quantities. For the decay product classification the below precedence order is used to ensure that each measurement appears in only one category.

- new particles
- strange D mesons
- baryons
- J/ψ
- charmonium other than J/ψ
- multiple D, D^* or D^{**} mesons
- a single D^* or D^{**} meson
- a single D meson
- other particles

[19]The HFAG/BtoCharm group was formed in the spring of 2005; it performs its work using an XML database backed web application.

Within each table the measurements are color coded according to the publication status and age. Table 85 provides a key to the color scheme and categories used. When viewing the tables with most pdf viewers every number, label and average provides hyperlinks to the corresponding reference and individual quantity web pages on the HFAG/Charm group website http://hfag.phys.ntu.edu.tw. The links provided in the captions of the table lead to the corresponding compilation pages. Both the individual and compilation webpages provide a graphical view of the results, in a variety of formats.

Tables 86 to 123 provide either limits at 90% confidence level or measurements with statistical and systematic uncertainties and in some cases a third error corresponding to correlated systematics. For details on the meanings of the uncertainties and access to the references click on the numbers to visit the corresponding web pages. Where there are multiple determinations of the same quantity by one experiment the table footnotes act to distinguish the methods or datasets used; such cases are visually highlighted in the table by presenting the measurements on the lines beneath the quantity label. Where both limits and measured values of a quantity are available the limits are presented in the tables but are not used in the determination of the average. Where only limits are available the most stringent is presented in the Average column of the tables. Where available the PDG 2006 result is also presented.

Table 85: Key to the colors used to classify the results presented in tables 86 to 123. When viewing these tables in a pdf viewer each number, label and average provides a hyperlink to the corresponding online version provided by the charm subgroup website http://hfag.phys.ntu.edu.tw/b2charm/. Where an experiment has multiple determinations of a single quantity they are distinguished by the table footnotes.

Class	Definition
waiting	Results without a preprint available
pubhot	Results published during or after 2006
prehot	Preprint released during or after 2006
pub	Results published after or during the last PDG year
pre	Preprint released after or during the last PDG year
pubold	Results published before the last PDG year
preold	Preprint released before the last PDG year
error	Incomplete information to classify
superceeded	Results superceeded by more recent measurements from the same experiment
inactive	Results in the process of being entered into the database
noquo	Results without quotes

Table 86: Branching fractions of charged B modes producing new particles in units of 10^{-3}, upper limits are at 90% CL. The latest version is available at: http://hfag.phys.ntu.edu.tw/b2charm/00101.html

Mode	PDG 2006	Belle	*BABAR*	CDF	Average
$X(3872)K^-$	< 0.32		< 0.32		< 0.32
$D_{sJ}^-(2460)D^0$			$4.3 \pm 1.6 \pm 1.3$		4.3 ± 2.1
$D_{sJ}^-(2460)D^{*0}(2007)$			$11.2 \pm 2.6 \pm 2.0$		11.2 ± 3.3

Table 87: Product branching fractions of charged B modes producing new particles in units of 10^{-4}, upper limits are at 90% CL. The latest version is available at: http://hfag.phys.ntu.edu.tw/b2charm/00101.html

Mode	PDG 2006	Belle	*BABAR*	CDF	Average
$K^-X(3872)[\gamma J/\psi(1S)]$		$0.0180 \pm 0.0060 \pm 0.0010$	$0.033 \pm 0.010 \pm 0.003$		$\mathbf{0.022 \pm 0.005}$
$K^-X(3872)[J/\psi(1S)\eta]$	< 0.077		< 0.077		< 0.077
$K^-X(3872)[\pi^+\pi^- J/\psi(1S)]$	0.11 ± 0.02	$0.13 \pm 0.02 \pm 0.01$	$0.101 \pm 0.025 \pm 0.010$		0.12 ± 0.02
$K^-Y(3940)[J/\psi(1S)\gamma]$			< 0.140		$\mathbf{< 0.140}$
$K^-Y(4260)[J/\psi(1S)\pi^+\pi^-]$	< 0.29		$0.20 \pm 0.07 \pm 0.02$		0.20 ± 0.07
$\overline{K}^0X^-(3872)[J/\psi(1S)\pi^-\pi^0]$	< 0.22		< 0.22		< 0.22
$K^-X(3872)[D^+D^-]$	< 0.40	< 0.40			< 0.40
$K^-X(3872)[D^0\overline{D}^0\pi^0]$	< 0.60	< 0.60			< 0.60
$K^-X(3872)[D^0\overline{D}^0]$	< 0.60	< 0.60			< 0.60
$D^0D_{sJ}^-(2460)[D_s^-\pi^+\pi^-]$	< 2.2	< 2.2			< 2.2
$D^0D_{sJ}^-(2460)[D_s^-\pi^0]$	< 2.7	< 2.7			< 2.7
$D^0D_{sJ}^-(2460)[D_s^-\gamma]$	4.7 ± 1.3	$5.6 \pm^{1.6}_{1.5} \pm 1.7$	$6.00 \pm 2.00 \pm 1.00 \pm^{2.00}_{1.00}$		$5.8 \pm^{1.7}_{1.9}$
$D^0D_{sJ}^*(2317)^-[D_s^{*-}\gamma]$	< 7.6	< 7.6			< 7.6
$D^{*0}(2007)D_{sJ}^*(2317)^-[D_s^-\pi^0]$	9.0 ± 7.0		$9.0 \pm 6.0 \pm 2.0 \pm^{3.0}_{2.0}$		$9.0 \pm^{7.0}_{6.6}$
$D^0D_{sJ}^*(2317)^-[D_s^-\pi^0]$	7.4 ± 2.1	$8.1 \pm^{3.0}_{2.7} \pm 2.4$	$10.00 \pm 3.00 \pm 1.00 \pm^{4.00}_{2.00}$		$8.9 \pm^{2.7}_{3.2}$
$D^0D_{sJ}^-(2460)[D_s^{*-}\gamma]$	< 9.8	< 9.8			< 9.8
$D^{*0}(2007)D_{sJ}^-(2460)[D_s^-\gamma]$	14.0 ± 7.0		$14.0 \pm 4.0 \pm 3.0 \pm^{5.0}_{3.0}$		$14.0 \pm^{7.1}_{5.8}$
$D^0D_{sJ}^-(2460)[D_s^{*-}\pi^0]$	14.0 ± 6.0	$11.9 \pm^{6.1}_{4.9} \pm 3.6$	$27.0 \pm 7.0 \pm 5.0 \pm^{9.0}_{6.0}$		$15.0 \pm^{5.3}_{5.8}$
$D^{*0}(2007)D_{sJ}^-(2460)[D_s^{*-}\pi^0]$	76 ± 33		$76 \pm 17 \pm 18 \pm^{26}_{16}$		$76 \pm^{36}_{29}$

Table 88: Branching fractions of charged B modes producing strange D mesons in units of 10^{-4}, upper limits are at 90% CL. The latest version is available at: http://hfag.phys.ntu.edu.tw/b2charm/00102.html

Mode	PDG 2006	Belle	*BABAR*	CDF	Average
$D_s^- \phi(1020)$	< 0.019		< 0.019		< 0.019
$D_s^{*-} \phi(1020)$	< 0.120		< 0.120		< 0.120
$D_s^- \pi^0$	< 1.70		< 0.28		< 0.28
$D_s^{*+} K^- \pi^-$	< 9.8		$1.84 \pm 0.19 \pm 0.40 \pm 0.06$		$\mathbf{1.84 \pm 0.45}$
$D_s^+ K^- \pi^-$	< 7.0		$1.88 \pm 0.13 \pm 0.41 \pm 0.06$		$\mathbf{1.88 \pm 0.43}$
$D_s^{*-} D^0$	72 ± 26		$93 \pm 18 \pm 19$		93 ± 26
$D_s^- D^{*0}(2007)$	100 ± 40		$121 \pm 23 \pm 20$		121 ± 30
$D_s^- D^0$	109 ± 27		$133 \pm 18 \pm 32$		133 ± 37
$D_s^{*-} D^{*0}(2007)$	220 ± 70		$170 \pm 26 \pm 24$		170 ± 35

Table 89: Product branching fractions of charged B modes producing strange D mesons in units of 10^{-4}, upper limits are at 90% CL. The latest version is available at: http://hfag.phys.ntu.edu.tw/b2charm/00102.html

Mode	PDG 2006	Belle	*BABAR*	CDF	Average
$D^{*0}(2007) D_s^- [\phi(1020)\pi^-]$	4.4 ± 1.7		$2.95 \pm 0.65 \pm 0.36$		2.95 ± 0.74
$D_s^{*-} D^0 [D_s^- \to \phi(1020)\pi^-]$	3.2 ± 1.1		$3.13 \pm 1.19 \pm 0.58$		3.1 ± 1.3
$D^0 D_s^- [\phi(1020)\pi^-]$	4.80 ± 1.00		$4.00 \pm 0.61 \pm 0.61$		4.00 ± 0.86
$D_s^{*-} D^{*0}(2007) [D_s^- \to \phi(1020)\pi^-]$	9.7 ± 2.8		$8.6 \pm 1.5 \pm 1.1$		8.6 ± 1.9

Table 90: Branching fractions of charged B modes producing baryons in units of 10^{-5}, upper limits are at 90% CL. The latest version is available at: http://hfag.phys.ntu.edu.tw/b2charm/00103.html

Mode	PDG 2006	Belle	*BABAR*	CDF	Average
$J/\psi(1S)\Sigma^0\overline{p}$	< 1.10	< 1.10			$\mathbf{< 1.10}$
$J/\psi(1S)\Lambda\overline{p}$	1.18 ± 0.31	$1.16 \pm 0.28 \pm^{0.18}_{0.23}$	$1.16 \pm^{0.74}_{0.53} \pm^{0.42}_{0.18}$		$\mathbf{1.16 \pm 0.31}$
$D^{*+}(2010)p\overline{p}$		< 1.50			< 1.50
$D^+p\overline{p}$		< 1.50			< 1.50
$\Sigma_c^{*0}\overline{p}$	< 4.6	< 4.6			< 4.6
$\Sigma_c^0\overline{p}$	< 8.0	< 9.3			< 9.3
$\Lambda_c^+\overline{p}\pi^-$	21.0 ± 7.0	$18.7 \pm^{4.3}_{4.0} \pm 2.8 \pm 4.9$	$35.3 \pm 1.8 \pm 3.1 \pm 9.2$		$24.2 \pm^{5.6}_{5.7}$
$\Lambda_c^+\Lambda_c^-K^-$		$65.0 \pm^{10.0}_{9.0} \pm 11.0 \pm 34.0$			$\mathbf{65 \pm 37}$

Table 91: Product branching fractions of charged B modes producing baryons in units of 10^{-5}, upper limits are at 90% CL. The latest version is available at: http://hfag.phys.ntu.edu.tw/b2charm/00103.html

Mode	PDG 2006	Belle	*BABAR*	CDF	Average
$K^-\eta_c(1S)[\Lambda\overline{\Lambda}]$		$0.095 \pm^{0.025}_{0.022} \pm^{0.008}_{0.011}$			$\mathbf{0.10 \pm 0.03}$
$K^-\eta_c(1S)[p\overline{p}]$	0.12 ± 0.04	$0.14 \pm 0.01 \pm^{0.02}_{0.02}$	$0.18 \pm^{0.03}_{0.02} \pm 0.02$		$\mathbf{0.15 \pm 0.02}$
$K^-J/\psi(1S)[\Lambda\overline{\Lambda}]$		$0.20 \pm^{0.03}_{0.03} \pm 0.03$			$\mathbf{0.20 \pm 0.05}$
$K^-J/\psi(1S)[p\overline{p}]$	0.22 ± 0.01	$0.22 \pm 0.01 \pm 0.01$	$0.22 \pm 0.02 \pm 0.01$		$\mathbf{0.22 \pm 0.01}$
$\Lambda_c^-\Xi_c^0[\Xi^-\pi^+]$		$4.80 \pm^{1.00}_{0.90} \pm 1.10 \pm 1.20$			$\mathbf{4.8 \pm 1.9}$

Table 92: Ratios of branching fractions of charged B modes producing baryons in units of 10^0, upper limits are at 90% CL. The latest version is available at: http://hfag.phys.ntu.edu.tw/b2charm/00103.html

Mode	PDG 2006	Belle	*BABAR*	CDF	Average
$\frac{\mathcal{B}(B^- \to \Lambda_c^+\overline{p}\pi^-)}{\mathcal{B}(\overline{B}^0 \to \Lambda_c^+\overline{p})}$			$16.4 \pm 2.9 \pm 1.3$		16.4 ± 3.2

Table 93: Branching fractions of charged B modes producing $J/\psi(1S)$ in units of 10^{-4}, upper limits are at 90% CL. The latest version is available at: http://hfag.phys.ntu.edu.tw/b2charm/00104.html

Mode	PDG 2006	Belle	*BABAR*	CDF	Average
$J/\psi(1S)D^0\pi^-$	< 0.25	< 0.25	< 0.52		< 0.25
$J/\psi(1S)\phi(1020)K^-$	0.52 ± 0.17		$0.44 \pm 0.14 \pm 0.05 \pm 0.01$		0.44 ± 0.15
$J/\psi(1S)\pi^-$	0.49 ± 0.06	$0.38 \pm 0.06 \pm 0.03$	$0.54 \pm 0.04 \pm 0.02$		0.48 ± 0.04
$J/\psi(1S)\eta K^-$	1.08 ± 0.33		$1.08 \pm 0.23 \pm 0.24 \pm 0.03$		1.08 ± 0.33
$J/\psi(1S)D^-$	< 1.20		< 1.20		< 1.20
$J/\psi(1S)K^-$	10.08 ± 0.35				10.26 ± 0.37
		$10.10 \pm 0.20 \pm 0.70 \pm 0.20$	$10.61 \pm 0.15 \pm 0.44 \pm 0.18$ [1]		
			$10.10 \pm 0.90 \pm 0.60$ [2]		
			$8.10 \pm 1.30 \pm 0.70$ [3]		
$J/\psi(1S)K^-\pi^+\pi^-$	10.7 ± 1.9		$11.60 \pm 0.70 \pm 0.90$	$6.9 \pm 1.8 \pm 1.2$	10.6 ± 1.0
$J/\psi(1S)K^{*-}(892)$	14.10 ± 0.80	$12.80 \pm 0.70 \pm 1.40 \pm 0.20$	$14.54 \pm 0.47 \pm 0.94 \pm 0.25$	$15.8 \pm 4.7 \pm 2.7$	14.03 ± 0.88
$J/\psi(1S)K_1^-(1270)$	18.0 ± 5.2	$18.0 \pm 3.4 \pm 3.0 \pm 2.5$			18.0 ± 5.2

[1] MEASUREMENT OF BRANCHING FRACTIONS AND CHARGE ASYMMETRIES FOR EXCLUSIVE B DECAYS TO CHARMONIUM (124M $B\overline{B}$ pairs) ; $B^- \to J/\psi K^-$ with J/ψ to leptons
[2] MEASUREMENT OF THE $B^+ \to p\overline{p}K^+$ BRANCHING FRACTION AND STUDY OF THE DECAY DYNAMICS (232M $B\overline{B}$ pairs) ; $B^- \to J/\psi K^-$ with $J/\psi \to p\overline{p}$
[3] Measurements of the absolute branching fractions of $B^\pm \to K^\pm X_{c\overline{c}}$ (231.8M $B\overline{B}$ pairs) ; $B^- \to J/\psi K^-$ (inclusive)

Table 94: Product branching fractions of charged B modes producing $J/\psi(1S)$ in units of 10^{-4}, upper limits are at 90% CL. The latest version is available at: http://hfag.phys.ntu.edu.tw/b2charm/00104.html

Mode	PDG 2006	Belle	*BABAR*	CDF	Average
$K^-h_c(1P)[J/\psi(1S)\pi^+\pi^-]$	< 0.034		< 0.034		< 0.034

Table 95: Ratios of branching fractions of charged B modes producing $J/\psi(1S)$ in units of 10^0, upper limits are at 90% CL. The latest version is available at: http://hfag.phys.ntu.edu.tw/b2charm/00104.html

Mode	PDG 2006	Belle	*BABAR*	CDF	Average
$\frac{\mathcal{B}(B^- \to J/\psi(1S)\pi^-)}{\mathcal{B}(B^- \to J/\psi(1S)K^-)}$	0.049 ± 0.006		$0.054 \pm 0.004 \pm 0.001$	$0.0500 \pm^{0.0190}_{0.0170} \pm 0.0010$	0.053 ± 0.004
$\frac{\mathcal{B}(B^- \to J/\psi(1S)K_1^-(1400))}{\mathcal{B}(B^- \to J/\psi(1S)K_1^-(1270))}$	< 0.30	< 0.30			< 0.30
$\frac{\mathcal{B}(B^- \to \chi_{c0}(1P)K^-)}{\mathcal{B}(B^- \to J/\psi(1S)K^-)}$	0.60 ± 0.20	$0.60 \pm^{0.21}_{0.18} \pm 0.05 \pm 0.08$			$0.60 \pm^{0.23}_{0.20}$
$\frac{\mathcal{B}(B^- \to \eta_c(1S)K^-)}{\mathcal{B}(B^- \to J/\psi(1S)K^-)}$	1.33 ± 0.44				1.12 ± 0.20
			$1.28 \pm 0.10 \pm 0.38$ [1]		
			$1.06 \pm 0.23 \pm 0.04$ [2]		
$\frac{\mathcal{B}(B^- \to J/\psi(1S)K^{*-}(892))}{\mathcal{B}(B^- \to J/\psi(1S)K^-)}$	1.39 ± 0.09		$1.37 \pm 0.05 \pm 0.08$	$1.92 \pm 0.60 \pm 0.17$	1.38 ± 0.09
$\frac{\mathcal{B}(B^- \to J/\psi(1S)K_1^-(1270))}{\mathcal{B}(B^- \to J/\psi(1S)K^-)}$		$1.80 \pm 0.34 \pm 0.34$			1.80 ± 0.48

[1] Branching Fraction Measurements of $B \to \eta_c K$ Decays (86.1M $B\overline{B}$ pairs) ; Ratio $B^- \to \eta_c K^-$ to $B^- \to J/\psi K^-$ with $\eta_c \to K\overline{K}\pi$

[2] Measurements of the absolute branching fractions of $B^\pm \to K^\pm X_{c\overline{c}}$ (231.8M $B\overline{B}$ pairs) ; Ratio $B^- \to \eta_c K^-$ to $B^- \to J/\psi K^-$ (inclusive analysis)

Table 96: Branching fractions of charged B modes producing charmonium other than $J/\psi(1S)$ in units of 10^{-4}, upper limits are at 90% CL. The latest version is available at: http://hfag.phys.ntu.edu.tw/b2charm/00105.html

Mode	PDG 2006	Belle	*BABAR*	CDF	Average
$h_c(1P)K^-$		< 0.038			$\mathbf{< 0.038}$
$\chi_{c2}(1P)K^{*-}(892)$	< 0.120		< 0.120		< 0.120
$\chi_{c1}(1P)\pi^-$		$0.22 \pm 0.04 \pm 0.03$			$\mathbf{0.22 \pm 0.05}$
$\chi_{c2}(1P)K^-$	< 0.29		< 0.30		< 0.30
$\chi_{c0}(1P)\pi^-$			< 0.61		< 0.61
$\chi_{c0}(1P)K^-$	1.60 ± 0.50				$\mathbf{1.88 \pm 0.30}$
		$6.00 \pm^{2.10}_{1.80} \pm 0.70 \pm 0.90$	2.70 ± 0.70 [2]		
			$1.84 \pm 0.32 \pm 0.14 \pm 0.28$ [1]		
			$1.34 \pm 0.45 \pm 0.15 \pm 0.14$ [3]		
			< 1.80 [6b]		
$\eta_c(2S)K^-$	3.4 ± 1.8		$3.40 \pm 1.80 \pm 0.30$		3.4 ± 1.8
$\chi_{c1}(1P)K^{*-}(892)$	3.60 ± 0.90	$4.10 \pm 0.60 \pm 0.90$	$2.94 \pm 0.95 \pm 0.93 \pm 0.31$		$\mathbf{3.65 \pm 0.85}$
$\psi(3770)K^-$	4.9 ± 1.3	$4.80 \pm 1.10 \pm 0.70$	$3.50 \pm 2.50 \pm 0.30$		4.5 ± 1.2
$\chi_{c1}(1P)K^-$	5.30 ± 0.70				$\mathbf{5.01 \pm 0.37}$
		$4.50 \pm 0.20 \pm 0.70$	$8.00 \pm 1.40 \pm 0.70$ [6c]	$15.5 \pm 5.4 \pm 2.0$	
			$4.90 \pm 0.20 \pm 0.40$ [4]		
$\psi(2S)K^-$	6.48 ± 0.35				6.32 ± 0.37
		6.90 ± 0.60	$6.17 \pm 0.32 \pm 0.38 \pm 0.23$ [5]	$5.50 \pm 1.00 \pm 0.60$	
			$4.90 \pm 1.60 \pm 0.40$ [6a]		
$\psi(2S)K^{*-}(892)$	6.7 ± 1.4	$8.13 \pm 0.77 \pm 0.89$	$5.92 \pm 0.85 \pm 0.86 \pm 0.22$		7.07 ± 0.85
$\eta_c(1S)K^-$	9.1 ± 1.3				9.8 ± 1.3
		$12.50 \pm 1.40 \pm^{1.00}_{1.20} \pm 3.80$	$12.90 \pm 0.90 \pm 1.30 \pm 3.60$ [7]		
			$13.8 \pm^{2.3}_{1.5} \pm 1.5 \pm 4.2$ [8]		
			8.7 ± 1.5 [6d]		
$\chi_{c0}(1P)K^{*-}(892)$	< 29		< 29		< 29

[1] Dalitz plot analysis of the decay $B^\pm \to K^\pm K^\pm K^\mp$ (226M $B\overline{B}$ pairs) ; $B^\pm \to K^\pm \chi_{c0}$, with $chi_c0 \to K^+K^-$ (Dalitz analysis)
[2] MEASUREMENT OF THE BRANCHING FRACTION FOR $B^\pm \to \chi_{c0}K^\pm$. (88.9M $B\overline{B}$ pairs) ; $B^- \to \chi_{c0}K^-$ with $\chi_{c0} \to K^+K^-, \pi^+\pi^-$
[3] Dalitz-plot analysis of the decays $B^\pm \to K^\pm\pi^\mp\pi^\pm$ (226M $B\overline{B}$ pairs) ; $B^- \to \chi_{c0}K^-$ with $\chi_{c0} \to \pi^+\pi^-$ (Dalitz analysis)
[4] Search for $B \to X(3872)K, X(3872) \to J/\psi\gamma$ (287M $B\overline{B}$ pairs) ; $B^- \to \chi_{c1}K^-$ with χ_{c1} to $J/\psi\gamma$
[5] MEASUREMENT OF BRANCHING FRACTIONS AND CHARGE ASYMMETRIES FOR EXCLUSIVE B DECAYS TO CHARMONIUM (124M $B\overline{B}$ pairs) ; $B^- \to \psi(2S)K^-$ with $\psi(2S)$ to leptons
[6] Measurements of the absolute branching fractions of $B^\pm \to K^\pm X_{c\overline{c}}$ (231.8M $B\overline{B}$ pairs) ; [6a] $B^- \to \psi(2S)K^-$ (inclusive) ; [6b] $B^- \to \chi_{c0}K^-$ (inclusive) ; [6c] $B^- \to \chi_{c1}K^-$ (inclusive) ; [6d] $B^- \to \eta_c K^-$ (inclusive)
[7] Branching Fraction Measurements of $B \to \eta_c K$ Decays (86.1M $B\overline{B}$ pairs) ; $B^- \to \eta_c K^-$ with $\eta_c \to K\overline{K}\pi$
[8] MEASUREMENT OF THE $B^+ \to p\overline{p}K^+$ BRANCHING FRACTION AND STUDY OF THE DECAY DYNAMICS (232M $B\overline{B}$ pairs) ; $B^- \to \eta_c K^-$ with $\eta_c \to p\overline{p}$

Table 97: Ratios of branching fractions of charged B modes producing charmonium other than $J/\psi(1S)$ in units of 10^{-1}, upper limits are at 90% CL. The latest version is available at: http://hfag.phys.ntu.edu.tw/b2charm/00105.html

Mode	PDG 2006	Belle	*BABAR*	CDF	Average
$\frac{\mathcal{B}(B^- \to \chi_{c1}(1P)\pi^-)}{\mathcal{B}(B^- \to \chi_{c1}(1P)K^-)}$		$0.43 \pm 0.08 \pm 0.03$			$\mathbf{0.43 \pm 0.09}$
$\frac{\mathcal{B}(B^- \to \chi_{c1}(1P)K^{*-}(892))}{\mathcal{B}(B^- \to \chi_{c1}(1P)K^-)}$	5.1 ± 2.3		$5.1 \pm 1.7 \pm 1.6$		5.1 ± 2.3
$\frac{\mathcal{B}(B^- \to \psi(2S)K^{*-}(892))}{\mathcal{B}(B^- \to \psi(2S)K^-)}$	9.6 ± 1.7		$9.60 \pm 1.50 \pm 0.90$		9.6 ± 1.7

Table 98: Product branching fractions of charged B modes producing multiple D, D^* or D^{**} mesons in units of 10^{-4}, upper limits are at 90% CL. The latest version is available at: http://hfag.phys.ntu.edu.tw/b2charm/00106.html

Mode	PDG 2006	Belle	*BABAR*	CDF	Average
$\pi^- D_1^0(2420)[D^{*0}(2007)\pi^-\pi^+]$	< 0.060	< 0.060			< 0.060
$\pi^- D_2^{*0}(2460)[D^{*0}(2007)\pi^-\pi^+]$	< 0.22	< 0.22			< 0.22
$\pi^- D_2^{*0}(2460)[D^{*+}(2010)\pi^-]$	1.80 ± 0.50	$1.80 \pm 0.30 \pm 0.30 \pm 0.20$	$1.80 \pm 0.30 \pm 0.50$		1.80 ± 0.36
$\pi^- D_1^0(2420)[D^0\pi^-\pi^+]$	1.90 ± 0.60	$1.85 \pm 0.29 \pm 0.35 \pm^{0.00}_{0.46}$			$1.85 \pm^{0.45}_{0.65}$
$\pi^- D_2^{*0}(2460)[D^+\pi^-]$	3.40 ± 0.80	$3.40 \pm 0.30 \pm 0.60 \pm 0.40$	$2.90 \pm 0.20 \pm 0.50$		3.06 ± 0.44
$\pi^- D_1^0(H)[D^{*+}(2010)\pi^-]$		$5.00 \pm 0.40 \pm 1.00 \pm 0.40$			5.0 ± 1.1
$\pi^- D_0^{*0}[D^+\pi^-]$		$6.10 \pm 0.60 \pm 0.90 \pm 1.60$			6.1 ± 1.9
$\pi^- D_1^0(2420)[D^{*+}(2010)\pi^-]$	6.8 ± 1.5	$6.80 \pm 0.70 \pm 1.30 \pm 0.30$	$5.90 \pm 0.30 \pm 1.10$		6.23 ± 0.91

Table 99: Ratios of branching fractions of charged B modes producing multiple D, D^* or D^{**} mesons in units of 10^0, upper limits are at 90% CL. The latest version is available at: http://hfag.phys.ntu.edu.tw/b2charm/00106.html

Mode	PDG 2006	Belle	*BABAR*	CDF	Average
$\frac{\mathcal{B}(B^- \to D^0 K^-)}{\mathcal{B}(B^- \to D^0 \pi^-)}$	0.083 ± 0.010	$0.077 \pm 0.005 \pm 0.006$	$0.083 \pm 0.003 \pm 0.002$	$0.065 \pm 0.007 \pm 0.004$	$\mathbf{0.079 \pm 0.003}$
$\frac{\mathcal{B}(B^- \to D^{*0}(2007) K^-)}{\mathcal{B}(B^- \to D^{*0}(2007) \pi^-)}$	0.08 ± 0.02	$0.078 \pm 0.019 \pm 0.009$	$0.081 \pm 0.004 \pm^{0.004}_{0.003}$		0.081 ± 0.005
$\frac{\mathcal{B}(B^- \to D_2^{*0}(2460) \pi^-)}{\mathcal{B}(B^- \to D_1^0(2420) \pi^-)}$			$0.80 \pm 0.07 \pm 0.16$		0.80 ± 0.17
$\frac{\mathcal{B}(B^- \to D^{*0}(2007) \pi^-)}{\mathcal{B}(B^- \to D^0 \pi^-)}$			$1.14 \pm 0.07 \pm 0.04$		$\mathbf{1.14 \pm 0.08}$
$\frac{\mathcal{B}(B^- \to D^{**+} \pi^-)}{\mathcal{B}(B^- \to D^0 \pi^-)}$			$1.22 \pm 0.13 \pm 0.23$		$\mathbf{1.22 \pm 0.26}$
$\frac{\mathcal{B}(B^- \to D^0 \pi^-)}{\mathcal{B}(\overline{B}^0 \to D^+ \pi^-)}$				$1.97 \pm 0.10 \pm 0.21$	1.97 ± 0.23

Table 100: Branching fractions of charged B modes producing a single D^* or D^{**} meson in units of 10^{-4}, upper limits are at 90% CL. The latest version is available at: http://hfag.phys.ntu.edu.tw/b2charm/00107.html

Mode	PDG 2006	Belle	*BABAR*	CDF	Average
$D^{*-}(2010)\overline{K}^0$	< 0.090		< 0.090		< 0.090
$D^{*0}(2007)K^-$	3.70 ± 0.40	$3.59 \pm 0.87 \pm 0.41 \pm 0.31$			3.6 ± 1.0
$D^{*0}(2007)K^{*-}(892)$	8.1 ± 1.4		$8.30 \pm 1.10 \pm 0.96 \pm 0.27$		8.3 ± 1.5
$D^{*0}(2007)K^-K^0$	< 10.6	< 10.6			< 10.6
$D^{*+}(2010)\pi^-\pi^-$	13.5 ± 2.2	$12.50 \pm 0.80 \pm 2.20$	$12.20 \pm 0.50 \pm 1.80$		12.3 ± 1.5
$D^{*0}(2007)K^-K^{*0}(892)$	15.0 ± 4.0	$15.3 \pm 3.1 \pm 2.9$			15.3 ± 4.2
$D^{*+}(2010)\pi^-\pi^+\pi^-\pi^-$	26.0 ± 4.0	$25.6 \pm 2.6 \pm 3.3$			25.6 ± 4.2
$D^{*0}(2007)\pi^-$	46.0 ± 4.0				$\mathbf{52.8 \pm 2.8}$
			$55.20 \pm 1.70 \pm 4.20 \pm 0.20$ [2]		
			$51.3 \pm 2.2 \pm 2.8$ [1]		
$D^{**+}\pi^-$			$55.0 \pm 5.2 \pm 10.4$		$\mathbf{55 \pm 12}$
$D^{*0}(2007)\pi^-\pi^+\pi^-\pi^+\pi^-$		$56.7 \pm 9.1 \pm 8.5$			57 ± 12
$D^{*0}(2007)\pi^-\pi^+\pi^-$	103 ± 12	$105.5 \pm 4.7 \pm 12.9$			106 ± 14

[1] Measurement of the Absolute Branching Fractions $B \to D^{(*,**)}\pi$ with a Missing Mass method (231M $B\overline{B}$ pairs) ; $B^- \to D^{*0}\pi^-$

[2] Branching fraction measurements and isospin analyses for $\overline{B} \to D^{(*)}\pi^-$ decays (65M $B\overline{B}$ pairs) ; $B^- \to D^{*0}\pi^-$

Table 101: Branching fractions of charged B modes producing a single D meson in units of 10^{-4}, upper limits are at 90% CL. The latest version is available at: http://hfag.phys.ntu.edu.tw/b2charm/00108.html

Mode	PDG 2006	Belle	*BABAR*	CDF	Average
$D^-\overline{K}^0$	< 0.050		< 0.050		< 0.050
D^0K^-	4.08 ± 0.24	$3.83 \pm 0.25 \pm 0.30 \pm 0.22$			3.83 ± 0.45
$D^0K^{*-}(892)$	6.30 ± 0.80				5.29 ± 0.45
			$5.29 \pm 0.30 \pm 0.34$ [1]		
			$6.30 \pm 0.70 \pm 0.50$ [2]		
$D^0K^-K^0$	5.5 ± 1.6	$5.50 \pm 1.40 \pm 0.80$			5.5 ± 1.6
$D^0K^-K^{*0}(892)$	7.5 ± 1.7	$7.5 \pm 1.3 \pm 1.1$			7.5 ± 1.7
$D^+\pi^-\pi^-$	10.2 ± 1.6	$10.20 \pm 0.40 \pm 1.50$	$8.70 \pm 0.40 \pm 1.30$		9.4 ± 1.0
$D^0\pi^-$	49.2 ± 2.0				$\mathbf{47.5 \pm 1.9}$
			$49.00 \pm 0.70 \pm 2.20 \pm 0.06$ [3]		
			$44.9 \pm 2.1 \pm 2.3$ [4]		

[1] Measurement of the $B^- \to D^0K^{*-}$ branching fraction (232M $B\overline{B}$ pairs) ; Measurement of of the $B^- \to D^0K^{*-}$ branching fraction
[2] Measurement of the Branching Fraction for $B^- \to D^0K^{*-}$ (86M $B\overline{B}$ pairs) ; $B^- \to D^0K^{*-}$
[3] Branching fraction measurements and isospin analyses for $\overline{B} \to D^{(*)}\pi^-$ decays (65M $B\overline{B}$ pairs) ; $B^- \to D^0\pi^-$
[4] Measurement of the Absolute Branching Fractions $B \to D^{(*,**)}\pi$ with a Missing Mass method (231M $B\overline{B}$ pairs) ; $B^- \to D^0\pi^-$

Table 102: Branching fractions of neutral B modes producing new particles in units of 10^{-3}, upper limits are at 90% CL. The latest version is available at: http://hfag.phys.ntu.edu.tw/b2charm/00201.html

Mode	PDG 2006	Belle	*BABAR*	CDF	Average
$X^+(3872)K^-$	< 0.50		< 0.50		< 0.50
$D_{sJ}^-(2460)D^+$			$2.60 \pm 1.50 \pm 0.70$		2.6 ± 1.7
$D_{sJ}^-(2460)D^{*+}(2010)$			$8.8 \pm 2.0 \pm 1.4$		8.8 ± 2.4

Table 103: Product branching fractions of neutral B modes producing new particles in units of 10^{-4}, upper limits are at 90% CL. The latest version is available at: http://hfag.phys.ntu.edu.tw/b2charm/00201.html

Mode	PDG 2006	Belle	*BABAR*	CDF	Average
$\pi^+ D_{sJ}^-(2460)[D_s^-\gamma]$	< 0.040	< 0.040			< 0.040
$\overline{K}^0 X(3872)[J/\psi(1S)\pi^+\pi^-]$	< 0.103		$0.051 \pm 0.028 \pm 0.007$		0.05 ± 0.03
$K^- X^+(3872)[J/\psi(1S)\pi^+\pi^0]$	< 0.054		< 0.054		< 0.054
$K^- D_{sJ}^+(2460)[D_s^+\gamma]$	< 0.094	< 0.086			< 0.086
$\pi^+ D_{sJ}^*(2317)^-[D_s^-\pi^0]$	< 0.25	< 0.25			< 0.25
$K^- D_{sJ}^*(2317)^+[D_s^+\pi^0]$	0.43 ± 0.15	$0.44 \pm 0.08 \pm 0.06 \pm 0.11$			0.44 ± 0.15
$D^+ D_{sJ}^-(2460)[D_s^-\pi^+\pi^-]$	< 2.00	< 2.00			< 2.00
$D^+ D_{sJ}^-(2460)[D_s^-\pi^0]$	< 3.6	< 3.6			< 3.6
$D^+ D_{sJ}^-(2460)[D_s^{*-}\gamma]$	< 6.0	< 6.0			< 6.0
$D^+ D_{sJ}^-(2460)[D_s^-\gamma]$	6.6 ± 1.7	$8.2 \pm^{2.2}_{1.9} \pm 2.5$	$8.00 \pm 2.00 \pm 1.00 \pm^{3.00}_{2.00}$		$8.1 \pm^{2.2}_{2.5}$
$D^+ D_{sJ}^*(2317)^-[D_s^{*-}\gamma]$	< 9.5	< 9.5			< 9.5
$D^+ D_{sJ}^*(2317)^-[D_s^-\pi^0]$	9.7 ± 3.7	$8.6 \pm^{3.3}_{2.6} \pm 2.6$	$18.0 \pm 4.0 \pm 3.0 \pm^{6.0}_{4.0}$		$10.4 \pm^{3.2}_{3.5}$
$D^{*+}(2010) D_{sJ}^*(2317)^-[D_s^-\pi^0]$	15.0 ± 6.0		$15.0 \pm 4.0 \pm 2.0 \pm^{5.0}_{3.0}$		$15.0 \pm^{6.7}_{5.4}$
$D^{*+}(2010) D_{sJ}^-(2460)[D_s^-\gamma]$	23.0 ± 8.0		$23.0 \pm 3.0 \pm 3.0 \pm^{8.0}_{5.0}$		$23.0 \pm^{9.1}_{6.6}$
$D^+ D_{sJ}^-(2460)[D_s^{*-}\pi^0]$	20.0 ± 5.0	$22.7 \pm^{7.3}_{6.2} \pm 6.8$	$28.0 \pm 8.0 \pm 5.0 \pm^{10.0}_{6.0}$		$24.6 \pm^{7.2}_{8.2}$
$D^{*+}(2010) D_{sJ}^-(2460)[D_s^{*-}\pi^0]$	55 ± 23		$55.0 \pm 12.0 \pm 10.0 \pm^{19.0}_{12.0}$		$55 \pm^{25}_{20}$

Table 104: Ratios of branching fractions of neutral B modes producing new particles in units of 10^0, upper limits are at 90% CL. The latest version is available at: http://hfag.phys.ntu.edu.tw/b2charm/00201.html

Mode	PDG 2006	Belle	*BABAR*	CDF	Average
$\frac{\mathcal{B}(\overline{B}^0 \to X(3872)\overline{K}^0)}{\mathcal{B}(B^- \to X(3872)K^-)}$			$0.50 \pm 0.30 \pm 0.05$		0.50 ± 0.30

Table 105: Branching fractions of neutral B modes producing strange D mesons in units of 10^{-3}, upper limits are at 90% CL. The latest version is available at: http://hfag.phys.ntu.edu.tw/b2charm/00202.html

Mode	PDG 2006	Belle	*BABAR*	CDF	Average
$D_s^- \pi^+$	0.022 ± 0.007				0.014 ± 0.003
		$0.024 \pm^{0.010}_{0.008} \pm 0.004 \pm 0.006$	$0.032 \pm 0.009 \pm 0.007 \pm 0.008$ [1c]		
			$0.013 \pm 0.003 \pm 0.001 \pm 0.002$ [2c]		
$D_s^- \rho^+(770)$	< 0.60		< 0.019		< 0.019
$D_s^- a_0^+(980)$			< 0.019		< 0.019
$D_s^{*+} K^-$	< 0.025				0.020 ± 0.006
			$0.020 \pm 0.005 \pm 0.003 \pm 0.003$ [2b]		
			< 0.025 [1b]		
$D_s^+ K^-$	0.031 ± 0.008				0.027 ± 0.005
		$0.046 \pm^{0.012}_{0.011} \pm 0.006 \pm 0.012$	$0.032 \pm 0.010 \pm 0.007 \pm 0.008$ [1a]		
			$0.025 \pm 0.004 \pm 0.002 \pm 0.003$ [2a]		
$D_s^{*-} \pi^+$	< 0.041				0.028 ± 0.008
			$0.028 \pm 0.006 \pm 0.004 \pm 0.003$ [2d]		
			< 0.041 [1d]		
$D_s^{*-} a_0^+(980)$			< 0.036		< 0.036
$D_s^+ \Lambda \overline{p}$		$0.036 \pm 0.009 \pm 0.006 \pm 0.009$			$\mathbf{0.04 \pm 0.01}$
$D_s^- D_s^{*+}$	< 0.130		< 0.130		< 0.130
$D_s^- D_s^+$	< 0.100	< 0.200	< 0.100		< 0.100
$D_s^- a_2^+(1320)$			< 0.190		< 0.190
$D_s^{*-} a_2^+(1320)$			< 0.200		< 0.200
$D_s^{*+} D_s^{*-}$	< 0.24		< 0.24		< 0.24
$D_s^{*-} D^+$	8.6 ± 3.4		$6.7 \pm 2.0 \pm 1.1$		6.7 ± 2.3
$D_s^- D^+$	6.5 ± 2.1	$7.42 \pm 0.23 \pm 1.36$	$9.0 \pm 1.8 \pm 1.4$		7.8 ± 1.2
$D_s^- D^{*+}(2010)$	8.8 ± 1.6				6.8 ± 1.6
			$5.70 \pm 1.60 \pm 0.90$ [3a]		
			$10.3 \pm 1.4 \pm 1.3 \pm 2.6$ [4a]		
$D_s^{*-} D^{*+}(2010)$	17.9 ± 1.6				18.2 ± 1.6
			$18.80 \pm 0.90 \pm 1.60 \pm 0.60$ [5]		
			$16.5 \pm 2.3 \pm 1.9$ [3b]		
			$19.7 \pm 1.5 \pm 3.0 \pm 4.9$ [4b]		
$D_{s1}^-(2536) D^{*+}(2010)$			$92.00 \pm 24.00 \pm 1.00$		$\mathbf{92 \pm 24}$

[1] A study of the rare decays $\overline{B}^0 \to D_s^{-(*)}\pi^+$ and $\overline{B}^0 \to D_s^{+(*)}K^-$ (84.3M $B\overline{B}$ pairs) ; [1a] $\overline{B}^0 \to D_s^+ K^-$; [1b] $\overline{B}^0 \to D_s^{*+} K^-$; [1c] $\overline{B}^0 \to D_s^- \pi^+$; [1d] $\overline{B}^0 \to D_s^{*-} \pi^+$

[2] Observation of Decays $\overline{B}^0 \to D_s^{-(*)}\pi^+$ and $\overline{B}^0 \to D_s^{+(*)}K^-$ (230M $B\overline{B}$ pairs) ; [2a] $\overline{B}^0 \to D_s^+ K^-$; [2b] $\overline{B}^0 \to D_s^{*+} K^-$; [2c] $\overline{B}^0 \to D_s^- \pi^+$; [2d] $\overline{B}^0 \to D_s^{*-} \pi^+$

[3] Study of $\overline{B} \to D^{(*)+,-} X^-$ and $\overline{B} \to D_s^{(*)-} X^{+,0}$ decays and measurement of D_s^- and $D_{sJ}^-(2460)$ absolute branching fractions (230M $B\overline{B}$ pairs) ; [3a] $\overline{B}^0 \to D_s^- D^{*+}$; [3b] $\overline{B}^0 \to D_s^{*-} D^{*+}$)

[4] Measurement of $\overline{B}^0 \to D_s^{(*)} D^*$ Branching Fractions and $D_s^* D^*$ Polarization with a Partial Reconstruction technique (22.7M $B\overline{B}$ pairs) ; [4a] $\overline{B}^0 \to D_s^- D^{*+}$; [4b] $\overline{B}^0 \to D_s^{*-} D^{*+}$

[5] Measurement of the $\overline{B}^0 \to D_s^{*-} D^+$ and $D_s^+ \to \phi\pi^+$ branching fractions (123M $B\overline{B}$ pairs) ; $\overline{B}^0 \to D_s^{*-} D^{*+}$

Table 106: Product branching fractions of neutral B modes producing strange D mesons in units of 10^{-4}, upper limits are at 90% CL. The latest version is available at: http://hfag.phys.ntu.edu.tw/b2charm/00202.html

Mode	PDG 2006	Belle	*BABAR*	CDF	Average
$D^+D_s^-[\pi^-\phi(1020)[K^+K^-]]$	1.41 ± 0.41	$1.47 \pm 0.05 \pm 0.21$			1.47 ± 0.22
$D^+D_s^-[\phi(1020)\pi^-]$	2.90 ± 0.80		$2.67 \pm 0.61 \pm 0.47$		2.67 ± 0.77
$D_s^{*-}D^+[D_s^- \to \phi(1020)\pi^-]$	3.8 ± 1.4		$4.14 \pm 1.19 \pm 0.94$		4.1 ± 1.5
$D^{*+}(2010)D_s^-[\phi(1020)\pi^-]$	3.90 ± 0.50		$5.11 \pm 0.94 \pm 0.72$		5.1 ± 1.2
$D_s^{*-}D^{*+}(2010)[D_s^- \to \phi(1020)\pi^-]$	7.9 ± 1.3		$12.2 \pm 2.2 \pm 2.2$		12.2 ± 3.1

Table 107: Ratios of branching fractions of neutral B modes producing strange D mesons in units of 10^0, upper limits are at 90% CL. The latest version is available at: http://hfag.phys.ntu.edu.tw/b2charm/00202.html

Mode	PDG 2006	Belle	*BABAR*	CDF	Average
$\frac{\mathcal{B}(\overline{B}^0 \to D_s^{*-}D^+)}{\mathcal{B}(\overline{B}^0 \to D_s^-D^+)}$				$0.90 \pm 0.20 \pm 0.10$	0.90 ± 0.22
$\frac{\mathcal{B}(\overline{B}^0 \to D_s^-D^{*+}(2010))}{\mathcal{B}(\overline{B}^0 \to D_s^-D^+)}$				$1.50 \pm 0.50 \pm 0.10$	1.50 ± 0.51
$\frac{\mathcal{B}(\overline{B}^0 \to D_s^-D^+)}{\mathcal{B}(\overline{B}^0 \to D^+\pi^+\pi^-\pi^-)}$				$1.99 \pm 0.13 \pm 0.11 \pm 0.45$	1.99 ± 0.48
$\frac{\mathcal{B}(\overline{B}^0 \to D_s^{*-}D^{*+}(2010))}{\mathcal{B}(\overline{B}^0 \to D_s^-D^+)}$				$2.60 \pm 0.50 \pm 0.20$	2.60 ± 0.54

Table 108: Branching fractions of neutral B modes producing baryons in units of 10^{-5}, upper limits are at 90% CL. The latest version is available at: http://hfag.phys.ntu.edu.tw/b2charm/00203.html

Mode	PDG 2006	Belle	*BABAR*	CDF	Average
$J/\psi(1S)\overline{p}p$	< 0.083	< 0.083	< 0.190		$\mathbf{< 0.083}$
$\Lambda_c^+\overline{p}$	2.20 ± 0.80	$2.19 \pm^{0.56}_{0.49} \pm 0.32 \pm 0.57$	$2.15 \pm 0.36 \pm 0.13 \pm 0.56$		2.17 ± 0.53
$\Sigma_c^{*0}\overline{p}\pi^+$	< 12.1				$\mathbf{< 3.3}$
		< 12.1 [1]			
		< 3.3 [2]			
$D^{*0}(2007)p\overline{p}$					11.1 ± 1.3
		$12.0 \pm^{3.3}_{2.9} \pm 2.1$	$6.70 \pm 2.10 \pm 0.82 \pm 0.36$ [3c]		
			$11.00 \pm 1.00 \pm 0.90$ [4c]		
$D^0p\overline{p}$					11.39 ± 0.91
		$11.8 \pm 1.5 \pm 1.6$	$12.40 \pm 1.40 \pm 1.16 \pm 0.30$ [3b]		
			$11.30 \pm 0.60 \pm 0.80$ [4b]		
$\Sigma_c^{*++}\overline{p}\pi^-$	16.0 ± 7.0				$\mathbf{12.9 \pm^{3.3}_{3.4}}$
		$16.3 \pm^{5.7}_{5.1} \pm 2.8 \pm 4.2$ [1]			
		$12.0 \pm 1.0 \pm 2.0 \pm 3.0$ [2]			
$\Sigma_c^0\overline{p}\pi^+$	10.0 ± 8.0				$\mathbf{14.0 \pm 4.9}$
		$14.0 \pm 2.0 \pm 2.0 \pm 4.0$ [2]			
		< 15.9 [1]			
$\Sigma_c^{++}\overline{p}\pi^-$	28.0 ± 9.0				$\mathbf{21.8 \pm^{5.1}_{5.2}}$
		$23.8 \pm^{6.3}_{5.5} \pm 4.1 \pm 6.2$ [1]			
		$21.0 \pm 2.0 \pm 3.0 \pm 5.0$ [2c]			
$D^+p\overline{p}\pi^-$					33.8 ± 3.2
			$38.00 \pm 3.50 \pm 4.50 \pm 0.95$ [3a]		
			$33.8 \pm 1.4 \pm 2.9$ [4a]		
$D^{*+}(2010)p\overline{p}\pi^-$	65 ± 16				48.1 ± 4.9
			$56.1 \pm 5.9 \pm 6.4 \pm 3.6$ [3d]		
			$48.1 \pm 2.2 \pm 4.4$ [4d]		
$\Lambda_c^+\Lambda_c^-\overline{K}^0$		$79 \pm^{29}_{23} \pm 12 \pm 41$			$\mathbf{79 \pm^{52}_{49}}$
$\Lambda_c^+\overline{p}\pi^+\pi^-$	130 ± 40	$110 \pm^{12}_{12} \pm 19 \pm 29$			110 ± 37

[1] STUDY OF EXCLUSIVE B DECAYS TO CHARMED BARYONS AT BELLE. (31.7M $B\overline{B}$ pairs)

[2] Study of the charmed baryonic decays $\overline{B}^0 \to \Sigma_c^{++}\overline{p}\pi^-$ and $\overline{B}^0 \to \Sigma_c^0\overline{p}\pi^+$ (386M $B\overline{B}$ pairs) ; [2c] B0bar to Sigmac(2455)++ pbar pi

[3] Measurement of the Branching Fraction for the decays $\overline{B}^0 \to D^{*+}p\overline{p}\pi^-$, $\overline{B}^0 \to D^+p\overline{p}\pi^-$, $\overline{B}^0 \to \overline{D}^{*0}p\overline{p}$, $\overline{B}^0 \to \overline{D}^0p\overline{p}$ (124M $B\overline{B}$ pairs) ; [3a] $\overline{B}^0 \to D^+p\overline{p}\pi^-$; [3b] $\overline{B}^0 \to \overline{D}^0p\overline{p}$; [3c] $\overline{B}^0 \to \overline{D}^{*0}p\overline{p}$; [3d] $\overline{B}^0 \to D^{*+}p\overline{p}\pi^-$

[4] Measurements of the Decays $B^0 \to \overline{D}^0p\overline{p}$, $B^0 \to \overline{D}^{*0}p\overline{p}$, $B^0 \to D^-p\overline{p}\pi + -$, and $B^0 \to D^-p\overline{p}\pi^+$ (232M $B\overline{B}$ pairs) ; [4a] $\overline{B}^0 \to D^+p\overline{p}\pi^-$; [4b] $\overline{B}^0 \to \overline{D}^0p\overline{p}$; [4c] $\overline{B}^0 \to \overline{D}^{*0}p\overline{p}$; [4d] $\overline{B}^0 \to D^{*+}p\overline{p}\pi^-$

Table 109: Product branching fractions of neutral B modes producing baryons in units of 10^{-5}, upper limits are at 90% CL. The latest version is available at: http://hfag.phys.ntu.edu.tw/b2charm/00203.html

Mode	PDG 2006	Belle	*BABAR*	CDF	Average
$\Lambda_c^- \Xi_c^+ [\Xi^- \pi^+ \pi^+]$		$9.3 \pm^{3.7}_{2.8} \pm 1.9 \pm 2.4$			$\mathbf{9.3 \pm^{4.8}_{4.1}}$

Table 110: Branching fractions of neutral B modes producing $J/\psi(1S)$ in units of 10^{-4}, upper limits are at 90% CL. The latest version is available at: http://hfag.phys.ntu.edu.tw/b2charm/00204.html

Mode	PDG 2006	Belle	*BABAR*	CDF	Average
$J/\psi(1S)\gamma$	< 0.016		< 0.016		< 0.016
$J/\psi(1S)\phi(1020)$	< 0.092		< 0.090		< 0.090
$J/\psi(1S)\eta$	< 0.27	$0.096 \pm 0.017 \pm 0.007$	< 0.27		$\mathbf{0.10 \pm 0.02}$
$J/\psi(1S)f_2(1270)$		$0.10 \pm 0.04 \pm 0.02$			0.10 ± 0.04
$J/\psi(1S)D^0$	< 0.130	< 0.200	< 0.130		< 0.130
$J/\psi(1S)\pi^0$	0.22 ± 0.04	$0.23 \pm 0.05 \pm 0.02$	$0.19 \pm 0.02 \pm 0.02$		$\mathbf{0.20 \pm 0.02}$
$J/\psi(1S)\rho^0(770)$	0.16 ± 0.07	$0.28 \pm 0.03 \pm 0.03$	$0.16 \pm 0.06 \pm 0.04$		0.25 ± 0.04
$J/\psi(1S)\pi^+\pi^-$	0.46 ± 0.09	< 0.100	$0.46 \pm 0.07 \pm 0.06$		0.46 ± 0.09
$J/\psi(1S)\eta'(958)$	< 0.63		< 0.63		< 0.63
$J/\psi(1S)\eta K^0_S$	0.80 ± 0.40		$0.84 \pm 0.26 \pm 0.27 \pm 0.02$		0.84 ± 0.38
$J/\psi(1S)\phi(1020)\overline{K}^0$	0.94 ± 0.26		$1.02 \pm 0.38 \pm 0.10 \pm 0.02$		1.02 ± 0.39
$J/\psi(1S)\overline{K}^0\rho^0(770)$	5.4 ± 3.0			$5.40 \pm 2.90 \pm 0.90$	5.4 ± 3.0
$J/\psi(1S)\overline{K}^{*0}(892)\pi^+\pi^-$	6.6 ± 2.2			$6.6 \pm 1.9 \pm 1.1$	6.6 ± 2.2
$J/\psi(1S)K^{*-}(892)\pi^+$	8.0 ± 4.0			$7.7 \pm 4.1 \pm 1.3$	7.7 ± 4.3
$J/\psi(1S)\overline{K}^0$	8.72 ± 0.33	$7.90 \pm 0.40 \pm 0.90 \pm 0.10$	$8.69 \pm 0.22 \pm 0.26 \pm 0.15$	$11.5 \pm 2.3 \pm 1.7$	8.63 ± 0.35
$J/\psi(1S)\overline{K}^0\pi^+\pi^-$	10.0 ± 4.0			$10.3 \pm 3.3 \pm 1.5$	10.3 ± 3.6
$J/\psi(1S)\overline{K}^0_1(1270)$	13.0 ± 5.0	$13.0 \pm 3.4 \pm 2.5 \pm 1.8$			13.0 ± 4.6
$J/\psi(1S)\overline{K}^{*0}(892)$	13.30 ± 0.60	$12.90 \pm 0.50 \pm 1.30 \pm 0.20$	$13.09 \pm 0.26 \pm 0.74 \pm 0.22$	$17.4 \pm 2.0 \pm 1.8$	13.32 ± 0.68

Table 111: Ratios of branching fractions of neutral B modes producing $J/\psi(1S)$ in units of 10^0, upper limits are at 90% CL. The latest version is available at: http://hfag.phys.ntu.edu.tw/b2charm/00204.html

Mode	PDG 2006	Belle	*BABAR*	CDF	Average
$\frac{\mathcal{B}(\overline{B}^0 \to J/\psi(1S)\overline{K}_1^0(1270))}{\mathcal{B}(B^- \to J/\psi(1S)K^-)}$		$1.30 \pm 0.34 \pm 0.28$			1.30 ± 0.44
$\frac{\mathcal{B}(\overline{B}^0 \to \eta_c(1S)\overline{K}^0)}{\mathcal{B}(\overline{B}^0 \to J/\psi(1S)\overline{K}^0)}$	1.39 ± 0.49		$1.34 \pm 0.19 \pm 0.13 \pm 0.38$		1.34 ± 0.44
$\frac{\mathcal{B}(\overline{B}^0 \to J/\psi(1S)\overline{K}^{*0}(892))}{\mathcal{B}(\overline{B}^0 \to J/\psi(1S)\overline{K}^0)}$	1.50 ± 0.09		$1.51 \pm 0.05 \pm 0.08$	$1.39 \pm 0.36 \pm 0.10$	1.50 ± 0.09

Table 112: Miscellaneous quantities of neutral B modes producing $J/\psi(1S)$ in units of 10^0, upper limits are at 90% CL. The latest version is available at: http://hfag.phys.ntu.edu.tw/b2charm/00204.html

Mode	PDG 2006	Belle	*BABAR*	CDF	Average
$\frac{\lvert\mathcal{A}_0\rvert^2(\overline{B}^0 \to J/\psi(1S)K^{*0}(892))}{\lvert\mathcal{A}_0\rvert^2(B^0 \to J/\psi(1S)K^{*0}(892))}$			< 0.26		< 0.26
$\frac{\lvert\mathcal{A}_0\rvert^2(B^0 \to J/\psi(1S)\overline{K}^{*0}(892))}{\lvert\mathcal{A}_0\rvert^2(\overline{B}^0 \to J/\psi(1S)\overline{K}^{*0}(892))}$			< 0.32		< 0.32

Table 113: Branching fractions of neutral B modes producing charmonium other than $J/\psi(1S)$ in units of 10^{-3}, upper limits are at 90% CL. The latest version is available at: http://hfag.phys.ntu.edu.tw/b2charm/00205.html

Mode	PDG 2006	Belle	*BABAR*	CDF	Average
$\chi_{c2}(1P)\overline{K}^{*0}(892)$	< 0.036		< 0.036		< 0.036
$\chi_{c2}(1P)\overline{K}^{0}$	< 0.026		< 0.041		< 0.041
$\chi_{c1}(1P)\overline{K}^{*0}(892)$	0.32 ± 0.06	$0.31 \pm 0.03 \pm 0.07$	$0.33 \pm 0.04 \pm 0.05 \pm 0.03$		$\mathbf{0.32 \pm 0.05}$
$\chi_{c1}(1P)\overline{K}^{0}$	0.39 ± 0.04	$0.35 \pm 0.03 \pm 0.05$	$0.45 \pm 0.04 \pm 0.02 \pm 0.05$		$\mathbf{0.40 \pm 0.04}$
$\psi(2S)\overline{K}^{0}$	0.62 ± 0.06	0.67 ± 0.11	$0.65 \pm 0.06 \pm 0.04 \pm 0.02$		0.65 ± 0.07
$\psi(2S)\overline{K}^{*0}(892)$	0.72 ± 0.08	$0.72 \pm 0.04 \pm 0.06$	$0.65 \pm 0.06 \pm 0.09 \pm 0.02$	$0.90 \pm 0.22 \pm 0.09$	0.71 ± 0.06
$\chi_{c0}(1P)\overline{K}^{*0}(892)$	< 0.77		< 0.77		< 0.77
$\eta_c(1S)\overline{K}^{0}$	0.99 ± 0.19	$1.23 \pm 0.23 \pm^{0.12}_{0.16} \pm 0.38$	$1.14 \pm 0.15 \pm 0.12 \pm 0.32$		1.18 ± 0.29
$\chi_{c0}(1P)\overline{K}^{0}$	< 0.50		< 1.24		< 1.24
$\eta_c(1S)\overline{K}^{*0}(892)$	1.60 ± 0.70	$1.62 \pm 0.32 \pm^{0.24}_{0.34} \pm 0.50$			$1.62 \pm^{0.64}_{0.68}$

Table 114: Ratios of branching fractions of neutral B modes producing charmonium other than $J/\psi(1S)$ in units of 10^{0}, upper limits are at 90% CL. The latest version is available at: http://hfag.phys.ntu.edu.tw/b2charm/00205.html

Mode	PDG 2006	Belle	*BABAR*	CDF	Average
$\frac{\mathcal{B}(\overline{B}^0 \to \chi_{c1}(1P)\overline{K}^{*0}(892))}{\mathcal{B}(\overline{B}^0 \to \chi_{c1}(1P)\overline{K}^{0})}$	0.72 ± 0.16		$0.72 \pm 0.11 \pm 0.12$		0.72 ± 0.16
$\frac{\mathcal{B}(\overline{B}^0 \to \eta_c(1S)\overline{K}^{0})}{\mathcal{B}(B^- \to \eta_c(1S)K^-)}$			$0.87 \pm 0.13 \pm 0.07$		0.87 ± 0.15
$\frac{\mathcal{B}(\overline{B}^0 \to \psi(2S)\overline{K}^{*0}(892))}{\mathcal{B}(\overline{B}^0 \to \psi(2S)\overline{K}^{0})}$	1.00 ± 0.17		$1.00 \pm 0.14 \pm 0.09$		1.00 ± 0.17
$\frac{\mathcal{B}(\overline{B}^0 \to \eta_c(1S)\overline{K}^{*0}(892))}{\mathcal{B}(\overline{B}^0 \to \eta_c(1S)\overline{K}^{0})}$	1.30 ± 0.40	$1.33 \pm 0.36 \pm^{0.24}_{0.33}$			$1.33 \pm^{0.43}_{0.49}$

Table 115: Branching fractions of neutral B modes producing multiple D, D^* or D^{**} mesons in units of 10^{-3}, upper limits are at 90% CL. The latest version is available at: http://hfag.phys.ntu.edu.tw/b2charm/00206.html

Mode	PDG 2006	Belle	*BABAR*	CDF	Average
$D^0\overline{D}^0$			< 0.060		< 0.060
$D^{*0}(2007)\overline{D}^{*0}(2007)$	< 27		< 0.090		< 0.090
$D^0\overline{D}^0\pi^0\overline{K}^0$		$0.17 \pm 0.07 \pm^{0.03}_{0.05}$			$\mathbf{0.17 \pm 0.08}$
$D^0\overline{D}^{*0}(2007)$			< 0.29		< 0.29
D^-D^+	0.19 ± 0.06	$0.32 \pm 0.06 \pm 0.05$	$0.28 \pm 0.04 \pm 0.03 \pm 0.04$		0.30 ± 0.05
$D^{*-}(2010)D^+$	< 0.63	$1.17 \pm 0.26 \pm^{0.20}_{0.24} \pm 0.08$	$0.57 \pm 0.07 \pm 0.06 \pm 0.04$		0.62 ± 0.09
$D^{*+}(2010)D^{*-}(2010)$	0.83 ± 0.11				0.81 ± 0.08
		$0.81 \pm 0.08 \pm 0.11$	$0.81 \pm 0.06 \pm 0.09 \pm 0.05$ [1]		
			$0.83 \pm 0.16 \pm 0.12$ [2]		
$D^{*+}(2010)D^-$	< 0.63		$0.88 \pm 0.10 \pm 0.11 \pm 0.06$		0.88 ± 0.16
$D^0\overline{D}^0\overline{K}^0$	< 1.40		< 1.40		< 1.40
$D^+D^-\overline{K}^0$	< 1.70		< 1.70		< 1.70
$D^+\overline{D}^0K^-$	1.70 ± 0.40		$1.70 \pm 0.30 \pm 0.30$		1.70 ± 0.42
$D^{*+}(2010)\overline{D}^0K^-$	3.10 ± 0.60		$3.10 \pm^{0.40}_{0.30} \pm 0.40$		$3.10 \pm^{0.57}_{0.50}$
$D^0\overline{D}^{*0}(2007)\overline{K}^0$	< 3.7		< 3.7		< 3.7
$D^{*-}(2010)D^{*+}(2010)K^0_S$			$4.40 \pm 0.40 \pm 0.70 \pm 0.04$		$\mathbf{4.40 \pm 0.81}$
$D^+\overline{D}^{*0}(2007)K^-$	4.60 ± 1.00		$4.60 \pm 0.70 \pm 0.70$		4.60 ± 0.99
$D^{*+}(2010)D^-\overline{K}^0$	6.5 ± 1.6		$6.50 \pm 1.20 \pm 1.00$		6.5 ± 1.6
$D^{*0}(2007)\overline{D}^{*0}(2007)\overline{K}^0$	< 6.6		< 6.6		< 6.6
$D^{*-}(2010)D^{*+}(2010)\overline{K}^0$	8.8 ± 1.9		$8.8 \pm^{1.5}_{1.4} \pm 1.3$		$8.8 \pm^{2.0}_{1.9}$
$D^{*+}(2010)\overline{D}^{*0}(2007)K^-$	11.8 ± 2.0		$11.80 \pm 1.00 \pm 1.70$		11.8 ± 2.0

[1] Measurement of Branching Fraction and CP-violating charge asymmetried for B meson decays to $D^{(*)}D^{(*)}$ and implications for the CKM angle γ (232M $B\overline{B}$ pairs) ; $\overline{B}^0 \to D^{*+}D^{*-}$

[2] Measurement of the branching fraction and CP content for the decay B^0 to D^*D^* (23M $B\overline{B}$ pairs) ; $\overline{B}^0 \to D^{*-}D^{*+}$

Table 116: Product branching fractions of neutral B modes producing multiple D, D^* or D^{**} mesons in units of 10^{-4}, upper limits are at 90% CL. The latest version is available at: http://hfag.phys.ntu.edu.tw/b2charm/00206.html

Mode	PDG 2006	Belle	*BABAR*	CDF	Average
$K^- D_2^{*+}(2460)[D^0\pi^+]$	0.18 ± 0.05		$0.18 \pm 0.04 \pm 0.03$		0.18 ± 0.05
$\pi^- D_2^{*+}(2460)[D^{*+}(2010)\pi^-\pi^+]$	< 0.24	< 0.24			< 0.24
$\pi^- D_1^{+}(2420)[D^{*+}(2010)\pi^-\pi^+]$	< 0.33	< 0.33			< 0.33
$\pi^- D_1^{+}(H)[D^{*0}(2007)\pi^+]$		< 0.70			< 0.70
$\pi^- D_1^{+}(2420)[D^+\pi^-\pi^+]$	0.89 ± 0.29	$0.89 \pm 0.15 \pm 0.17 \pm^{0.00}_{0.26}$			$0.89 \pm^{0.23}_{0.34}$
$\pi^- D_0^{*+}[D^0\pi^+]$		< 1.20			< 1.20
$\pi^- D_2^{*+}(2460)[D^{*0}(2007)\pi^+]$		$2.45 \pm 0.42 \pm^{0.35}_{0.45} \pm^{0.39}_{0.17}$			$2.45 \pm^{0.67}_{0.64}$
$\pi^- D_2^{*+}(2460)[D^0\pi^+]$		$3.08 \pm 0.33 \pm 0.09 \pm^{0.15}_{0.02}$			$3.08 \pm^{0.37}_{0.34}$
$\pi^- D_1^{+}(2420)[D^{*0}(2007)\pi^+]$		$3.68 \pm 0.60 \pm^{0.71}_{0.40} \pm^{0.65}_{0.30}$			$3.68 \pm^{1.13}_{0.78}$
$\omega(782) D_1^{0}(H)[D^{*+}(2010)\pi^-]$			$4.10 \pm 1.20 \pm 1.00 \pm 0.40$		4.1 ± 1.6

Table 117: Ratios of branching fractions of neutral B modes producing multiple D, D^* or D^{**} mesons in units of 10^0, upper limits are at 90% CL. The latest version is available at: http://hfag.phys.ntu.edu.tw/b2charm/00206.html

Mode	PDG 2006	Belle	*BABAR*	CDF	Average
$\frac{\mathcal{B}(\overline{B}^0 \to D^+ K^-)}{\mathcal{B}(\overline{B}^0 \to D^+ \pi^-)}$	0.07 ± 0.02	$0.068 \pm 0.015 \pm 0.007$			0.07 ± 0.02
$\frac{\mathcal{B}(\overline{B}^0 \to D^{*+}(2010) K^-)}{\mathcal{B}(\overline{B}^0 \to D^{*+}(2010) \pi^-)}$	0.07 ± 0.02	$0.074 \pm 0.015 \pm 0.006$	$0.078 \pm 0.003 \pm 0.003$		0.077 ± 0.004
$\frac{\mathcal{B}(\overline{B}^0 \to D^{**0} \pi^-)}{\mathcal{B}(\overline{B}^0 \to D^+ \pi^-)}$			$0.77 \pm 0.22 \pm 0.29$		$\mathbf{0.77 \pm 0.36}$
$\frac{\mathcal{B}(\overline{B}^0 \to D^{*+}(2010) \pi^-)}{\mathcal{B}(\overline{B}^0 \to D^+ \pi^-)}$			$0.99 \pm 0.11 \pm 0.08$		$\mathbf{0.99 \pm 0.14}$
$\frac{\mathcal{B}(\overline{B}^0 \to D^0 \rho^0(770))}{\mathcal{B}(\overline{B}^0 \to D^0 \omega(782))}$		1.60 ± 0.80			1.60 ± 0.80
$\frac{\mathcal{B}(\overline{B}^0 \to D^+ \mu^- \overline{\nu}_\mu)}{\mathcal{B}(\overline{B}^0 \to D^+ \pi^-)}$				$9.80 \pm 1.00 \pm 0.60 \pm 1.20$	9.8 ± 1.7
$\frac{\mathcal{B}(\overline{B}^0 \to D^{*+}(2010) \mu^- \overline{\nu}_\mu)}{\mathcal{B}(\overline{B}^0 \to D^{*+}(2010) \pi^-)}$				$17.70 \pm 2.30 \pm 0.60 \pm 1.20$	17.7 ± 2.7

Table 118: Branching fractions of neutral B modes producing a single D^* or D^{**} meson in units of 10^{-4}, upper limits are at 90% CL. The latest version is available at: http://hfag.phys.ntu.edu.tw/b2charm/00207.html

Mode	PDG 2006	Belle	*BABAR*	CDF	Average
$D^{*0}(2007)\overline{K}^0$	< 0.66				0.36 ± 0.12
		< 0.66	$0.45 \pm 0.19 \pm 0.05$ [2]		
			$0.36 \pm 0.12 \pm 0.03$ [1]		
$\overline{D}^{*0}(2007)\overline{K}^{*0}(892)$	< 0.40	< 0.40			< 0.40
$D^{*0}(2007)\overline{K}^{*0}(892)$	< 0.69	< 0.69			< 0.69
$D^{*0}(2007)\eta'(958)$	1.23 ± 0.35	$1.21 \pm 0.34 \pm 0.22$	< 2.6		1.21 ± 0.40
$D^{*0}(2007)\pi^0$	2.70 ± 0.50	$1.39 \pm 0.18 \pm 0.26$	$2.90 \pm 0.40 \pm 0.46 \pm 0.19$		$\mathbf{1.69 \pm 0.28}$
$D^{*0}(2007)\eta$	2.60 ± 0.60	$1.40 \pm 0.28 \pm 0.26$	$2.60 \pm 0.40 \pm 0.37 \pm 0.16$		$\mathbf{1.77 \pm 0.32}$
$f_2(1270)D^{*0}(2007)$		$1.86 \pm 0.65 \pm 0.60 \pm^{0.80}_{0.52}$			$1.9 \pm^{1.2}_{1.0}$
$D^{*+}(2010)K^-$	2.14 ± 0.20	$2.04 \pm 0.41 \pm 0.17 \pm 0.16$			2.04 ± 0.47
$D^{*0}(2007)\omega(782)$	4.2 ± 1.1	$2.29 \pm 0.39 \pm 0.40$	$4.20 \pm 0.70 \pm 0.86 \pm 0.27$		$\mathbf{2.66 \pm 0.50}$
$D^{*+}(2010)K^0\pi^-$	3.00 ± 0.80		$3.00 \pm 0.70 \pm 0.22 \pm 0.20$		3.00 ± 0.76
$D^{*+}(2010)K^{*-}(892)$	3.30 ± 0.60		$3.20 \pm 0.60 \pm 0.27 \pm 0.12$		3.20 ± 0.67
$D^{*0}(2007)\rho^0(770)$	< 5.1				3.73 ± 0.99
		$3.73 \pm 0.87 \pm 0.46 \pm^{0.18}_{0.08}$ [4]			
		< 5.1 [3]			
$D^{*+}(2010)K^-K^0$	< 4.7	< 4.7			< 4.7
$D^{*0}(2007)\pi^+\pi^-$	6.2 ± 2.2				9.0 ± 1.4
		$6.2 \pm 1.2 \pm 1.8$ [3]			
		$10.90 \pm 0.80 \pm 1.60$ [4]			
$D^{*+}(2010)K^-K^{*0}(892)$	12.9 ± 3.3	$12.9 \pm 2.2 \pm 2.5$			12.9 ± 3.3
$D^{**0}\pi^-$			$23.4 \pm 6.5 \pm 8.8$		$\mathbf{23 \pm 11}$
$D^{*0}(2007)\pi^-\pi^+\pi^-\pi^+$	27.0 ± 5.0	$26.0 \pm 4.7 \pm 3.7$			26.0 ± 6.0
$D^{*+}(2010)\pi^-$	27.6 ± 2.1				$\mathbf{26.2 \pm 1.3}$
		$23.00 \pm 0.60 \pm 1.90$	$27.90 \pm 0.80 \pm 1.70 \pm 0.05$ [5]		
			$29.9 \pm 2.3 \pm 2.4$ [6]		
$D^{*+}(2010)\omega(782)\pi^-$			$28.8 \pm 2.1 \pm 2.8 \pm 1.4$		28.8 ± 3.8
$D^{*+}(2010)\pi^-\pi^+\pi^-\pi^+\pi^-$		$47.2 \pm 5.9 \pm 7.1$			47.2 ± 9.2
$D^{*+}(2010)\pi^-\pi^+\pi^-$	76 ± 18	$68.1 \pm 2.3 \pm 7.2$			68.1 ± 7.6

[1] A study of the $\overline{B}^0 \to D^{(*)0}K^{(*)0}$ decays (226M $B\overline{B}$ pairs) ; $\overline{B}^0 \to D^{*0}\overline{K}^0$
[2] A study of the $\overline{B}^0 \to D^{(*)0}K^{(*)0}$ decays (124M $B\overline{B}$ pairs) ; $B \to D^{*0}\overline{K}^0$
[3] Study of $\overline{B^0} \to D^{(*)0}\pi^+\pi^-$ Decays (31.3M $B\overline{B}$ pairs)
[4] Study of $\overline{B}^0 \to D^{(*)0}\pi^+\pi^-$ decays ; Dalitz fit analysis (152M $B\overline{B}$ pairs)
[5] Branching fraction measurements and isospin analyses for $\overline{B} \to D^{(*)}\pi^-$ decays (65M $B\overline{B}$ pairs) ; $\overline{B}^0 \to D^{*+}\pi^-$
[6] Measurement of the Absolute Branching Fractions $B \to D^{(*,**)}\pi$ with a Missing Mass method (231M $B\overline{B}$ pairs) ; $\overline{B}^0 \to D^{*+}\pi^-$

Table 119: Branching fractions of neutral B modes producing a single D meson in units of 10^{-4}, upper limits are at 90% CL. The latest version is available at: http://hfag.phys.ntu.edu.tw/b2charm/00208.html

Mode	PDG 2006	Belle	*BABAR*	CDF	Average
$\overline{D}^0\overline{K}^{*0}(892)$	< 0.180				< 0.110
		< 0.180	< 0.41 [2c]		
			< 0.110 [1c]		
$\overline{D}^0 K^-\pi^+$	< 0.190		< 0.190		< 0.190
$D^0\overline{K}^{*0}(892)$	0.53 ± 0.08				0.42 ± 0.06
		$0.48 \pm^{0.11}_{0.10} \pm 0.05$	$0.62 \pm 0.14 \pm 0.06$ [2b]		
			$0.40 \pm 0.07 \pm 0.03$ [1b]		
$D^0\overline{K}^0$	0.50 ± 0.14				0.52 ± 0.07
		$0.50 \pm^{0.13}_{0.12} \pm 0.06$	$0.62 \pm 0.12 \pm 0.04$ [2a]		
			$0.53 \pm 0.07 \pm 0.03$ [1a]		
$D^0 K^-\pi^+$	0.88 ± 0.17		$0.88 \pm 0.15 \pm 0.09$		0.88 ± 0.17
$D^0\eta'(958)$	1.25 ± 0.23	$1.14 \pm 0.20 \pm^{0.10}_{0.13}$	$1.70 \pm 0.40 \pm 0.18 \pm 0.10$		1.26 ± 0.21
$f_2(1270)D^0$		$1.95 \pm 0.34 \pm 0.38 \pm^{0.32}_{0.02}$			$1.95 \pm^{0.60}_{0.51}$
$D^0\eta$	2.20 ± 0.50	$1.77 \pm 0.16 \pm 0.21$	$2.50 \pm 0.20 \pm 0.29 \pm 0.11$		$\mathbf{2.02 \pm 0.21}$
D^+K^-	2.00 ± 0.60	$2.04 \pm 0.45 \pm 0.21 \pm 0.27$			2.04 ± 0.57
$D^0\omega(782)$	2.50 ± 0.60	$2.37 \pm 0.23 \pm 0.28$	$3.00 \pm 0.30 \pm 0.38 \pm 0.13$		$\mathbf{2.59 \pm 0.29}$
$D^0\pi^0$	2.91 ± 0.28	$2.25 \pm 0.14 \pm 0.35$	$2.90 \pm 0.20 \pm 0.27 \pm 0.13$		$\mathbf{2.59 \pm 0.26}$
$D^0\rho^0(770)$	2.9 ± 1.1				$2.91 \pm^{0.58}_{0.40}$
		$2.90 \pm 1.00 \pm 0.40$ [3]			
		$2.91 \pm 0.28 \pm 0.33 \pm^{0.08}_{0.54}$ [4]			
$D^+K^-K^0$	< 3.1	< 3.1			< 3.1
$D^+K^{*-}(892)$	4.50 ± 0.70		$4.60 \pm 0.60 \pm 0.47 \pm 0.16$		4.60 ± 0.78
$D^+K^0\pi^-$	4.90 ± 0.90		$4.90 \pm 0.70 \pm 0.38 \pm 0.32$		4.90 ± 0.86
$D^+K^-K^{*0}(892)$	8.8 ± 1.9	$8.8 \pm 1.1 \pm 1.5$			8.8 ± 1.9
$D^0\pi^+\pi^-$	8.0 ± 1.6				9.78 ± 0.95
		$8.00 \pm 0.60 \pm 1.50$ [3]			
		$10.70 \pm 0.60 \pm 1.00$ [4]			
$D^+\pi^-$	34.0 ± 9.0				$\mathbf{26.5 \pm 1.5}$
			$25.50 \pm 0.50 \pm 1.60 \pm 0.10$ [6]		
			$30.3 \pm 2.3 \pm 2.3$ [5]		

[1] A study of the $\overline{B}^0 \to D^{(*)0}K^{(*)0}$ decays (226M $B\overline{B}$ pairs) ; [1a] $\overline{B}^0 \to D^0\overline{K}^0$; [1b] $\overline{B}^0 \to D^0\overline{K}^{*0}$; [1c] $\overline{B}^0 \to \overline{D}^0\overline{K}^{*0}$
[2] A study of the $\overline{B}^0 \to D^{(*)0}K^{(*)0}$ decays (124M $B\overline{B}$ pairs) ; [2a] $B \to D^0\overline{K}^0$; [2b] $\overline{B}^0 \to D^0K^{*0}$; [2c] $\overline{B}^0 \to \overline{D}^0\overline{K}^{*0}$
[3] Study of $\overline{B^0} \to D^{(*)0}\pi^+\pi^-$ Decays (31.3M $B\overline{B}$ pairs)
[4] Study of $\overline{B}^0 \to D^{(*)0}\pi^+\pi^-$ decays ; Dalitz fit analysis (152M $B\overline{B}$ pairs)
[5] Measurement of the Absolute Branching Fractions $B \to D^{(*,**)}\pi$ with a Missing Mass method (231M $B\overline{B}$ pairs) ; $\overline{B}^0 \to D^+\pi^-$
[6] Branching fraction measurements and isospin analyses for $\overline{B} \to D^{(*)}\pi^-$ decays (65M $B\overline{B}$ pairs) ; $\overline{B}^0 \to D^+\pi^-$

Table 120: Product branching fractions of neutral B modes producing a single D meson in units of 10^{-5}, upper limits are at 90% CL. The latest version is available at: http://hfag.phys.ntu.edu.tw/b2charm/00208.html

Mode	PDG 2006	Belle	*BABAR*	CDF	Average
$D^0\overline{K}^{*0}(892)[K^-\pi^+]$			$3.80 \pm 0.60 \pm 0.40$		3.80 ± 0.72

Table 121: Branching fractions of miscellaneous modes producing charmed particles in units of 10^{-3}, upper limits are at 90% CL. The latest version is available at: http://hfag.phys.ntu.edu.tw/b2charm/00300.html

Mode	PDG 2006	Belle	*BABAR*	CDF	Average
$\mathcal{B}(B \to D^0 \overline{D}^0 \pi^0 K)$		$0.13 \pm 0.03 \pm^{0.02}_{0.04}$			$\mathbf{0.13 \pm 0.04}$
$\mathcal{B}(\overline{\Lambda}_b^0 \to J/\psi(1S)\overline{\Lambda})$	0.47 ± 0.28			$0.47 \pm 0.21 \pm 0.19$	0.47 ± 0.28
$\mathcal{B}(\overline{D}^0 \to D^{*0}(2007)D^-)$			$0.63 \pm 0.14 \pm 0.08 \pm 0.06$		0.63 ± 0.17
$\mathcal{B}(\overline{B}_s^0 \to J/\psi(1S)\phi(1020))$	0.93 ± 0.33			$0.93 \pm 0.28 \pm 0.17$	0.93 ± 0.33

Table 122: Product branching fractions of miscellaneous modes producing charmed particles in units of 10^{-5}, upper limits are at 90% CL. The latest version is available at: http://hfag.phys.ntu.edu.tw/b2charm/00300.html

Mode	PDG 2006	Belle	*BABAR*	CDF	Average
$\mathcal{B}(B \to KY(3940)[\omega(782)J/\psi(1S)])$	7.1 ± 3.4	$7.1 \pm 1.3 \pm 3.1$			7.1 ± 3.4

Table 123: Ratios of branching fractions of miscellaneous modes producing charmed particles in units of 10^0, upper limits are at 90% CL. The latest version is available at: http://hfag.phys.ntu.edu.tw/b2charm/00300.html

Mode	PDG 2006	Belle	*BABAR*	CDF	Average
$\frac{\mathcal{B}(\overline{B}_s^0 \to \psi(2S)\phi(1020))}{\mathcal{B}(\overline{B}_s^0 \to J/\psi(1S)\phi(1020))}$				$0.52 \pm 0.13 \pm 0.07$	0.52 ± 0.15
$\frac{\mathcal{B}(\overline{B}_s^0 \to D_s^+\pi^+\pi^-\pi^-)}{\mathcal{B}(\overline{B}^0 \to D^+\pi^+\pi^-\pi^-)}$				$1.05 \pm 0.10 \pm 0.23$	1.05 ± 0.25
$\frac{\mathcal{B}(\overline{B}_s^0 \to D_s^+\pi^-)}{\mathcal{B}(\overline{B}^0 \to D^+\pi^-)}$				$1.13 \pm 0.08 \pm 0.05 \pm 0.15$	1.13 ± 0.18
$\frac{\mathcal{B}(\overline{B}_s^0 \to D_s^- D_s^+)}{\mathcal{B}(\overline{B}^0 \to D_s^- D^+)}$				$1.67 \pm 0.41 \pm 0.12 \pm 0.46$	1.67 ± 0.63
$\frac{\mathcal{B}(\overline{\Lambda}_b^0 \to \Lambda_c^-\pi^+)}{\mathcal{B}(\overline{B}^0 \to D^+\pi^-)}$				$3.30 \pm 0.30 \pm 0.40 \pm 1.10$	3.3 ± 1.2
$\frac{\mathcal{B}(\overline{\Lambda}_b^0 \to \Lambda_c^-\mu^+\nu_\mu)}{\mathcal{B}(\overline{\Lambda}_b^0 \to \Lambda_c^-\pi^+)}$				$20.00 \pm 3.00 \pm 1.20 \pm^{0.90}_{2.20}$	$20.0 \pm^{3.4}_{3.9}$

Table 124: Miscellaneous quantities of miscellaneous modes producing charmed particles in units of 10^0, upper limits are at 90% CL. The latest version is available at: http://hfag.phys.ntu.edu.tw/b2charm/00300.html

Mode	PDG 2006	Belle	*BABAR*	CDF	Average
$\delta_{\parallel}(B \to J/\psi(1S)K^*)$		$-2.887 \pm 0.090 \pm 0.008$	$-2.93 \pm 0.08 \pm 0.04$		$\mathbf{-2.91 \pm 0.06}$
$\delta_{\parallel}(B \to \psi(2S)K^*)$			$-2.80 \pm 0.40 \pm 0.10$		$\mathbf{-2.80 \pm 0.41}$
$\delta_{\parallel}(B \to \chi_{c1}(1P)K^*)$			$0.00 \pm 0.30 \pm 0.10$		$\mathbf{0.00 \pm 0.32}$
$\lvert\mathcal{A}_{\perp}\rvert^2(B \to \chi_{c1}(1P)K^*)$			$0.03 \pm 0.04 \pm 0.02$		$\mathbf{0.03 \pm 0.04}$
$\lvert\mathcal{A}_{\parallel}\rvert^2(B \to \chi_{c1}(1P)K^*)$			$0.20 \pm 0.07 \pm 0.04$		$\mathbf{0.20 \pm 0.08}$
$\lvert\mathcal{A}_{\perp}\rvert^2(B \to J/\psi(1S)K^*)$		$0.195 \pm 0.012 \pm 0.008$	$0.233 \pm 0.010 \pm 0.005$		$\mathbf{0.219 \pm 0.009}$
$\lvert\mathcal{A}_{\parallel}\rvert^2(B \to J/\psi(1S)K^*)$		$0.231 \pm 0.012 \pm 0.008$	$0.211 \pm 0.010 \pm 0.006$		$\mathbf{0.219 \pm 0.009}$
$\lvert\mathcal{A}_{\parallel}\rvert^2(B \to \psi(2S)K^*)$			$0.22 \pm 0.06 \pm 0.02$		$\mathbf{0.22 \pm 0.06}$
$\lvert\mathcal{A}_{\perp}\rvert^2(B \to \psi(2S)K^*)$			$0.30 \pm 0.06 \pm 0.02$		$\mathbf{0.30 \pm 0.06}$
$\lvert\mathcal{A}_{0}\rvert^2(B \to \psi(2S)K^*)$			$0.48 \pm 0.05 \pm 0.02$		$\mathbf{0.48 \pm 0.05}$
$\lvert\mathcal{A}_{0}\rvert^2(B \to J/\psi(1S)K^*)$		$0.574 \pm 0.012 \pm 0.009$	$0.556 \pm 0.009 \pm 0.010$		$\mathbf{0.56 \pm 0.01}$
$\lvert\mathcal{A}_{0}\rvert^2(B \to \chi_{c1}(1P)K^*)$			$0.77 \pm 0.07 \pm 0.04$		$\mathbf{0.77 \pm 0.08}$
$\delta_{\perp}(B \to \psi(2S)K^*)$			$2.80 \pm 0.30 \pm 0.10$		$\mathbf{2.80 \pm 0.32}$
$\delta_{\perp}(B \to J/\psi(1S)K^*)$		$2.938 \pm 0.064 \pm 0.010$	$2.91 \pm 0.05 \pm 0.03$		$\mathbf{2.92 \pm 0.04}$

8 Summary

This article provides the updated world averages for b-hadron properties as of at the end of 2006. A small selection of highlights of the results described in Sections 3-7 is given in Table 125.

Concerning the lifetime and mixing averages, the most significant changes since the end of 2005 [3] are due to new measurements from the Tevatron experiments, mainly in the areas of heavy b-baryon lifetimes and B_s^0 mixing parameters. After more than a decade of effort at LEP, SLC, and Tevatron, B_s^0 oscillations have been observed by CDF with a frequency in agreement with the Standard Model prediction. First results on CP violation in B_s^0 mixing have also been obtained from Tevatron data, consistent with no CP violation. In the mean time, B_s^0 production at the $\Upsilon(5S)$ has been established.

Measurements by *BABAR* and Belle of the time-dependent CP violation parameter $S_{b\to c\bar{c}s}$ in B decays to charmonium and a neutral kaon have established CP violation in B decays, and allow a precise extraction of the Unitarity Triangle parameter $\sin 2\beta \equiv \sin 2\phi_1$. Recent studies of $B \to J/\psi K^*$ (Sec. 4.4.2), $B \to D^{(*)}h^0$, where $h^0 = \pi^0$ *etc.*. (Sec. 4.5) and $B \to D^{*+}D^{*-}K_S^0$ (Sec. 4.4.3) allow to resolve the ambiguity in the solutions for $\beta \equiv \phi_1$ from the measurement of $\sin 2\beta \equiv \sin 2\phi_1$. Measurements of time-dependent CP asymmetries in hadronic $b \to s$ penguin decays continue to provide insight into possible new physics. In this update, results from both *BABAR* and Belle have been updated. A particularly notable change is that the CP violation effect in $B \to \eta' K^0$ is now established with more than 5σ significance in both experiments. Also noteworthy is that *BABAR* has performed the first time-dependent Dalitz plot analysis of the $B \to K^+K^-K^0$ decay, and quasi-two-body CP violation parameters for the decays $B \to \phi K^0$ and $B \to f_0 K^0$ are obtained from this analysis. Compared to the previous round of averages, the consistency with the Standard Model expectation remains at about the same level, in terms of significance. Results from time-dependent analyses with the decays $B^0 \to \pi^+\pi^-, \rho^\pm\pi^\mp$ and $\rho^+\rho^-$ provide constraints on the Unitarity Triangle angle $\alpha \equiv \phi_2$ (Sec. 4.10). Both *BABAR* and Belle now observed CP violation in $B^0 \to \pi^+\pi^-$ with more than 5σ significance, and both experiments have now performed time-dependent Dalitz plot analyses of $B^0 \to (\rho\pi)^0 \to \pi^+\pi^-\pi^0$. Progress continues to constrain the third Unitarity Triangle angle $\gamma \equiv \phi_3$. Both *BABAR* and Belle are using $B^- \to D^{(*)}K^-$ decays (Sec. 4.12), with multiple $D^{(*)}$ decays to final states accessible to both $D^{(*)0}$ and $\overline{D}^{(*)0}$. At present, the most constraining results arise from the Dalitz plot analysis of the $D \to K_S^0\pi^+\pi^-$ decay.

Progress in the determination of properties of semileptonic B-meson decays has been steady over the last year. *BABAR* made new measurements of the D^* form factor ratios R_1 and R_2, which were a factor of 5 more precise than the older CLEO measurements. They caused the value of $|V_{cb}|F(1)$ to shift by -1.7σ but had no impact on it's precision, which is dominated by the branching fraction. For the first time we computed averages for the inclusive semileptonic branching fraction of neutral and charged B-mesons separately and their ratio. The latter was found to be, as one would expect, consistent with the corresponding lifetime ratio. We extracted $|V_{ub}|$ from inclusive measurements using in addition to BLNP, DGE and BLL. The average found using the DGE method was found to be in very good agreement with that of BLNP, while BLL, which makes use of a subsample of the available measurements, is also in agreement with DGE and BLNP. New and updated measurements of the $B \to \pi l\nu$ branching fraction have reduced the error on the average by 25%. As was the case last year, the precision with which $|V_{ub}|$ is known is limited by the uncertainty on the form factor, which is at the level of 15–20%. Significant strides have been made in reducing uncertainties from the shape of the

Table 125: Brief summary of the world averages as of at the end of 2006.

b-hadron lifetimes	
$\tau(B^0)$	1.527 ± 0.008 ps
$\tau(B^+)$	1.643 ± 0.010 ps
$\tau(B_s^0 \to$ flavour specific)	1.440 ± 0.036 ps
$\overline{\tau}(B_s^0) = 1/\Gamma_s$	$1.451^{+0.029}_{-0.028}$ ps
$\tau(B_c^+)$	0.460 ± 0.066 ps
$\tau(\Lambda_b^0)$	1.393 ± 0.049 ps
b-hadron fractions	
f^{+-}/f^{00} in $\Upsilon(4S)$ decays	1.021 ± 0.034
f_s in $\Upsilon(5S)$ decays	0.199 ± 0.032
$f_d = f_u$ at high energy	0.401 ± 0.010
f_s at high energy	0.106 ± 0.013
$f_{\rm baryon}$ at high energy	0.092 ± 0.018
B^0 and B_s^0 mixing parameters	
Δm_d	0.507 ± 0.004 ps^{-1}
$\lvert q/p\rvert_d$	1.0024 ± 0.0023
Δm_s	17.77 ± 0.12 ps^{-1}
$\Delta\Gamma_s/\Gamma_s = (\Gamma_{\rm L} - \Gamma_{\rm H})/\Gamma_s$	$+0.104^{+0.076}_{-0.084}$
$\lvert q/p\rvert_s$	0.9998 ± 0.0046
Measurements related to Unitarity Triangle angles	
$\sin 2\beta \equiv \sin 2\phi_1$	0.675 ± 0.026
$\beta \equiv \phi_1$	$(21.2 \pm 1.0)^\circ$
$-\eta S_{\eta' K^0}$	0.61 ± 0.07
$S_{\pi^+\pi^-}$	-0.59 ± 0.09
Semileptonic B decay parameters	
$\mathcal{B}(\overline{B}^0 \to D^{*+}\ell^-\overline{\nu})$	$(5.28 \pm 0.18)\%$
$\mathcal{B}(\overline{B}^0 \to D^{+}\ell^-\overline{\nu})$	$(2.09 \pm 0.18)\%$
$\mathcal{B}(\overline{B} \to X\ell\overline{\nu})$	$(10.95 \pm 0.15)\%$
$\lvert V_{cb}\rvert F(1)$ $(\overline{B}^0 \to D^{*+}\ell^-\overline{\nu})$	$(36.0 \pm 0.6) \times 10^{-3}$
$\lvert V_{cb}\rvert G(1)$ $(\overline{B}^0 \to D^{+}\ell^-\overline{\nu})$	$(42.4 \pm 4.5) \times 10^{-3}$
$\mathcal{B}(\overline{B} \to \pi\ell\overline{\nu})$	$(1.39 \pm 0.08) \times 10^{-4}$
Rare B decays	
$\mathcal{B}(B^+ \to \tau^+\nu)$	$(132 \pm 49) \times 10^{-6}$

q^2 spectrum, with a new measurement made in q^2 bins of size $2\,\mathrm{GeV}^2$.

For rare B decays, branching fractions and charge asymmetries of many new decay modes have been measured recently, mostly by *BABAR* and Belle. There are several hundred measurements in the tables in Sec. 6. Particularly noteworthy is the measurement of $B \to \tau\nu$; Belle sees evidence for this decay while *BABAR* reports a somewhat smaller branching fraction. There are new results from *BABAR* on the vector-vector decays $B \to \phi K^*$ and $B \to \rho K^*$. They confirm earlier indications that the longitudinal polarization is about 0.5 for the penguin-dominated modes, while it is $\sim$1.0 for tree-dominated decays. This pattern still has no theoretical explanation. The branching fractions for inclusive charmless B decays with a kaon and the full angular analysis of B decays into a vector-tensor final state are added for this update.

In the sector of B decays to charmed particles, reduction in the uncertainties and new measurements have steadily continued to be obtained. Branching fractions for rare B-meson decays or decay chains of a few 10^{-7} are being measured with statistical uncertainties typically below 30%. Results for more common decay chains, with branching fractions around 10^{-4}, are becoming precision measurements, with uncertainties typically at the 3% level. Some decays have been observed for the first time, for example $B^- \to \Lambda_c^- \Lambda_c^+ K^-$ or $B^- \to \chi_{c1}\pi^-$, with a branching fraction of $(6.5 \pm 3.7) \times 10^{-4}$ and $(2.2 \pm 0.5) \times 10^{-5}$, respectively. Great improvements have been attained towards a deeper understanding of recently discovered new states with either hidden or open charm content. The $J/\psi\gamma$ decay mode of the $X(3870)$ has been observed by both *BABAR* and Belle and the average branching fraction is $\mathcal{B}(B^- \to X(3870)K^-) \times \mathcal{B}(X(3870 \to J/\psi\gamma) = (2.4 \pm 0.5) \times 10^{-6}$: this final state allowed to unambiguously establish the positive C parity of the $X(3870)$. Branching fractions for several B decays to $D_{sJ}^{*-}(2317)$ and $D_{sJ}^-(2460)$ have been measured, and also absolute branching fraction measurements have been reported: $\mathcal{B}(\overline{B}^0 \to D_{sJ}^-(2460)D^+) = (0.26 \pm 0.17) \times 10^{-2}$, $\mathcal{B}(\overline{B}^0 \to D_{sJ}^-(2460)D^{*+}) = (0.88 \pm 0.24) \times 10^{-2}$, $\mathcal{B}(B^- \to D_{sJ}^-(2460)D^0) = (0.43 \pm 0.21) \times 10^{-2}$ and $\mathcal{B}(B^- \to D_{sJ}^-(2460)D^{*0}) = (1.12 \pm 0.33) \times 10^{-2}$. The abundance of measurements with many different final states for these particles is of the greatest importance for quantum number assignments, and already some of the proposed theoretical interpretations have been ruled out.

Acknowledgments

We would like to thank collaborators of *BABAR*, Belle, CDF, CLEO, DØ, LEP, and SLD experiments who provided fruitful results on b-hadron properties and cooperated with the HFAG for averaging. These results are thanks to the excellent operations of the accelerators and collaborations with experimental groups by the accelerator groups of PEP-II, KEKB, CESR, Tevatron, LEP, and SLC.

References

[1] N. Cabibbo, Phys. Rev. Lett. 10, 531 (1963); M. Kobayashi and T. Maskawa, Prog. Theor. Phys. **49**, 652 (1973).

[2] ALEPH, CDF, DELPHI, L3, OPAL, and SLD collaborations, "Combined results on b-hadron production rates and decay properties", CERN-EP-2000-096, hep-ex/0009052 (2000); updated in CERN-EP-2001-050, hep-ex/0112028 (2001).

[3] Heavy Flavor Averaging Group (HFAG), "Averages of b-hadron Properties at the End of 2005", hep-ex/0603003 (2006).

[4] W.-M. Yao *et al.* (Particle Data Group), J. Phys. G **33**, 1 (2006).

[5] J.P. Alexander *et al.* (CLEO Collaboration), Phys. Rev. Lett. **86**, 2737 (2001).

[6] B. Aubert *et al.* (*BABAR* Collaboration), Phys. Rev. D **65**, 032001 (2002).

[7] S.B. Athar *et al.* (CLEO Collaboration), Phys. Rev. D **66**, 052003 (2002).

[8] N.C. Hastings *et al.* (Belle Collaboration), Phys. Rev. D **67**, 052004 (2003).

[9] B. Aubert *et al.* (*BABAR* Collaboration), Phys. Rev. D **69**, 071101 (2004).

[10] B. Aubert *et al.* (*BABAR* Collaboration), Phys. Rev. Lett. **95**, 042001 (2005).

[11] B. Aubert *et al.* (*BABAR* Collaboration), Phys. Rev. Lett. **96**, 232001 (2006);
A. Sokolov, M. Shapkin *et al.* (Belle Collaboration), Phys. Rev. D **75**, 071103 (2007).

[12] B. Barish *et al.* (CLEO Collaboration), Phys. Rev. Lett. **76**, 1570 (1996).

[13] G.S. Huang *et al.* (CLEO Collaboration), Phys. Rev. D **75**, 012002 (2007); this supersedes the results of Ref. [15]

[14] A. Drutskoy *et al.* (Belle Collaboration), Phys. Rev. Lett. **98**, 052001 (2007).

[15] M. Artuso *et al.* (CLEO Collaboration), Phys. Rev. Lett. **95**, 261801 (2005).

[16] G. Bonvicini *et al.* (CLEO Collaboration), Phys. Rev. Lett. **96**, 022002 (2006).

[17] K. Abe *et al.* (Belle Collaboration), hep-ex/0610003 v4, March 2007, submitted to Phys. Rev. D.

[18] P. Abreu *et al.* (DELPHI Collaboration), Phys. Lett. B **289**, 199 (1992);
P.D. Acton *et al.* (OPAL Collaboration), Phys. Lett. B **295**, 357 (1992);
D. Buskulic *et al.* (ALEPH Collaboration), Phys. Lett. B **361**, 221 (1995).

[19] P. Abreu *et al.* (DELPHI Collaboration), Z. Phys. C **68**, 375 (1995).

[20] R. Barate *et al.* (ALEPH Collaboration), Eur. Phys. J. C **2**, 197 (1998).

[21] D. Buskulic *et al.* (ALEPH Collaboration), Phys. Lett. B **384**, 449 (1996).

[22] J. Abdallah *et al.* (DELPHI Collaboration), Eur. Phys. J. C **44**, 299 (2005).

[23] P. Abreu *et al.* (DELPHI Collaboration), Z. Phys. C **68**, 541 (1995).

[24] R. Barate *et al.* (ALEPH Collaboration), Eur. Phys. J. C **5**, 205 (1998).

[25] J. Abdallah *et al.* (DELPHI Collaboration), Phys. Lett. B **576**, 29 (2003).

[26] T. Affolder *et al.* (CDF Collaboration), Phys. Rev. Lett. **84**, 1663 (2000).

[27] F. Abe *et al.* (CDF Collaboration), Phys. Rev. D **60**, 092005 (1999).

[28] CDF Collaboration, CDF note 8140, 28 March 2006,
`http://www-cdf.fnal.gov/physics/new/bottom/060216.blessed-fqFractions/`

[29] LEP collaborations ALEPH, CDF, DELPHI, L3, OPAL, LEP Electroweak Working Group, SLD Electroweak and Heavy Flavour Working Groups, "Precision electroweak measurements on the Z resonance", Phys. Reports **427**, 257 (2006); we use the average given in Eq. 5.39 of this paper, obtained from a 10-parameter global fit of all electroweak data where the asymmetry measurements have been excluded.

[30] D. Acosta *et al.* (CDF Collaboration), Phys. Rev. D **69**, 012002 (2004).

[31] V.M. Abazov *et al.* (DØ Collaboration), Phys. Rev. D **74**, 092001 (2006).

[32] M.A. Shifman and M.B. Voloshin, Sov. Phys. JETP **64**, 698 (1986);
J. Chay, H. Georgi and B. Grinstein, Phys. Lett. B **247**, 399 (1990);
I.I. Bigi, N.G. Uraltsev and A.I. Vainshtein, Phys. Lett. B **293**, 430 (1992), erratum ibid. B **297**, 477 (1993).

[33] I. Bigi, UND-HEP-95-BIG02 (1995);
G. Bellini, I. Bigi and P. Dornan, Phys. Reports **289**, 1 (1997).

[34] M. Ciuchini, E. Franco, V. Lubicz and F. Mescia, Nucl. Phys. B **625**, 211 (2002);
M. Beneke, G. Buchalla, C. Greub, A. Lenz and U. Nierste, Nucl. Phys. B **639**, 389 (2002);
E. Franco, V. Lubicz, F. Mescia and C. Tarantino, Nucl. Phys. B **633**, 212 (2002).

[35] C. Tarantino, hep-ph/0310241, Eur. Phys. J. C **33**, S895 (2004);
F. Gabbiani, A. Onishchenko and A. Petrov, Phys. Rev. D **68**, 114006 (2003).

[36] F. Gabbiani, A. Onischenko and A. Petrov, Phys. Rev. D **70**, 094031 (2004).

[37] L. Di Ciaccio *et al.*, internal note by former B lifetime working group (1996),
`http://lepbosc.web.cern.ch/LEPBOSC/lifetimes/ps/final_blife.ps`

[38] D. Buskulic *et al.* (ALEPH Collaboration), Phys. Lett. B **314**, 459 (1993).

[39] P. Abreu *et al.* (DELPHI Collaboration), Z. Phys. C **63**, 3 (1994).

[40] P. Abreu *et al.* (DELPHI Collaboration), Phys. Lett. B **377**, 195 (1996).

[41] J. Abdallah *et al.* (DELPHI Collaboration), Eur. Phys. J. C **33**, 307 (2004).

[42] M. Acciarri *et al.* (L3 Collaboration), Phys. Lett. B **416**, 220 (1998).

[43] K. Ackerstaff *et al.* (OPAL Collaboration), Z. Phys. C **73**, 397 (1997).

[44] K. Abe *et al.* (SLD Collaboration), Phys. Rev. Lett. **75**, 3624 (1995).

[45] D. Buskulic *et al.* (ALEPH Collaboration), Phys. Lett. B **369**, 151 (1996).

[46] P.D. Acton *et al.* (OPAL Collaboration), Z. Phys. C **60**, 217 (1993).

[47] F. Abe *et al.* (CDF Collaboration), Phys. Rev. D **57**, 5382 (1998).

[48] R. Barate *et al.* (ALEPH Collaboration), Phys. Lett. B **492**, 275 (2000).

[49] D. Buskulic *et al.* (ALEPH Collaboration), Z. Phys. C **71**, 31 (1996).

[50] P. Abreu *et al.* (DELPHI Collaboration), Z. Phys. C **68**, 13 (1995).

[51] W. Adam *et al.* (DELPHI Collaboration), Z. Phys. C **68**, 363 (1995).

[52] P. Abreu *et al.* (DELPHI Collaboration), Z. Phys. C **74**, 19 (1997).

[53] M. Acciari *et al.* (L3 Collaboration), Phys. Lett. B **438**, 417 (1998).

[54] R. Akers *et al.* (OPAL Collaboration), Z. Phys. C **67**, 379 (1995).

[55] G. Abbiendi *et al.* (OPAL Collaboration), Eur. Phys. J. C **12**, 609 (2000).

[56] G. Abbiendi *et al.* (OPAL Collaboration), Phys. Lett. B **493**, 266 (2000).

[57] K. Abe *et al.* (SLD Collaboration), Phys. Rev. Lett. **79**, 590 (1997).

[58] F. Abe *et al.* (CDF Collaboration), Phys. Rev. D **58**, 092002 (1998).

[59] D. Acosta *et al.* (CDF Collaboration), Phys. Rev. D **65**, 092009 (2003).

[60] D. Acosta *et al.* (CDF Collaboration), Phys. Rev. Lett. **94**, 101803 (2005).

[61] CDF Collaboration, CDF note 7514, 1 March 2005, `http://www-cdf.fnal.gov/physics/new/bottom/050224.blessed-bsemi-life/`

[62] CDF Collaboration, CDF note 7386, 23 March 2005, `http://www-cdf.fnal.gov/physics/new/bottom/050303.blessed-bhadlife/`

[63] A. Abulencia *et al.* (CDF Collaboration), hep-ex/0609021, September 2006, submitted to Phys. Rev. Lett.

[64] V.M. Abazov *et al.* (DØ Collaboration), Phys. Rev. Lett. **95**, 171801 (2005).

[65] V.M. Abazov *et al.* (DØ Collaboration), Phys. Rev. Lett. **94**, 042001 (2005).

[66] V.M. Abazov *et al.* (DØ Collaboration), DØ note 5179, contribution to ICHEP06, August 2006.

[67] B. Aubert *et al.* (*BABAR* Collaboration), Phys. Rev. Lett. **87**, 201803 (2001).

[68] B. Aubert *et al.* (*BABAR* Collaboration), Phys. Rev. Lett. **89**, 011802 (2002), erratum ibid. **89**, 169903 (2002).

[69] B. Aubert *et al.* (*BABAR* Collaboration), Phys. Rev. D **67**, 072002 (2003).

[70] B. Aubert *et al.* (*BABAR* Collaboration), Phys. Rev. D **67**, 091101 (2003).

[71] B. Aubert *et al.* (*BABAR* Collaboration), Phys. Rev. D **73**, 012004 (2006).

[72] K. Abe *et al.* (Belle Collaboration), Phys. Rev. D **71**, 072003 (2005).

[73] CDF Collaboration, CDF note 7409, 9 May 2004, `http://www-cdf.fnal.gov/physics/new/bottom/040428.blessed-lft/`

[74] V.M. Abazov *et al.* (DØ Collaboration), Phys. Rev. Lett. **94**, 182001 (2005).

[75] A. Lenz and U. Nierste, hep-ph/0612167, TTP06-31, December 2006; M. Beneke *et al.*, Phys. Lett. B **459**, 631 (1999).

[76] K. Hartkorn and H.-G. Moser, Eur. Phys. J. C **8**, 381 (1999).

[77] D. Buskulic *et al.* (ALEPH Collaboration), Phys. Lett. B **377**, 205 (1996).

[78] F. Abe *et al.* (CDF Collaboration), Phys. Rev. D **59**, 032004 (1999).

[79] P. Abreu *et al.* (DELPHI Collaboration), Eur. Phys. J. C **16**, 555 (2000).

[80] K. Ackerstaff *et al.* (OPAL Collaboration), Phys. Lett. B **426**, 161 (1998).

[81] V.M. Abazov *et al.* (DØ Collaboration), Phys. Rev. Lett. **97**, 241801 (2006).

[82] CDF Collaboration, CDF note 7386, 23 March 2005, submitted to Moriond 2005.

[83] CDF Collaboration, CDF note 7757, 13 August 2005.

[84] D. Buskulic *et al.* (ALEPH Collaboration), Eur. Phys. J. C **4**, 367 (1998).

[85] P. Abreu *et al.* (DELPHI Collaboration), Eur. Phys. J. C **18**, 229 (2000).

[86] K. Ackerstaff *et al.* (OPAL Collaboration), Eur. Phys. J. C **2**, 407 (1998).

[87] CDF Collaboration, D. Tonelli, FPCP 2006 proceedings, FPCP06_112, hep-ex/0605038.

[88] F. Abe *et al.* (CDF Collaboration), Phys. Rev. Lett. **81**, 2432 (1998).

[89] A. Abulencia *et al.* (CDF Collaboration), Phys. Rev. Lett. **97**, 012002 (2006).

[90] V.M. Abazov *et al.* (DØ Collaboration), DØ note 4539, contribution 11-0559 to ICHEP04, August 2004.

[91] D. Acosta *et al.* (CDF Collaboration), Phys. Rev. Lett. **96**, 082002 (2006).

[92] D. Acosta *et al.* (CDF Collaboration), Phys. Rev. Lett. **96**, 202001 (2006).

[93] D. Buskulic *et al.* (ALEPH Collaboration), Phys. Lett. B **365**, 437 (1996).

[94] F. Abe *et al.* (CDF Collaboration), Phys. Rev. Lett. **77**, 1439 (1996).

[95] V.M. Abazov *et al.* (DØ Collaboration), DØ note 5263, contribution to DPF06, October 2006.

[96] P. Abreu *et al.* (DELPHI Collaboration), Eur. Phys. J. C **10**, 185 (1999).

[97] P. Abreu *et al.* (DELPHI Collaboration), Z. Phys. C **71**, 199 (1996).

[98] R. Akers *et al.* (OPAL Collaboration), Z. Phys. C **69**, 195 (1996).

[99] M. Beneke, G. Buchalla and I. Dunietz, Phys. Rev. D **54**, 4419 (1996);
Y. Keum and U. Nierste, Phys. Rev. D **57**, 4282 (1998).

[100] M.B. Voloshin, Phys. Rep. **320**, 275 (1999);
B. Guberina, B. Melic and H. Stefancic, Phys. Lett. B **469**, 253 (1999);
M. Neubert and C.T. Sachrajda, Nucl. Phys. B **483**, 339 (1997).

[101] N. Uraltsev, Phys. Lett. B **376**, 303 (1996);
D. Pirjol and N. Uraltsev, Phys. Rev. D **59**, 034012 (1999);
P. Colangelo and F. De Fazio, Phys. Lett. B **387**, 371 (1996);
M. Di Pierro, C. Sachrajda, C. Michael, Phys. Lett. B **468**, 143 (1999).

[102] J. Bartelt *et al.* (CLEO Collaboration), Phys. Rev. Lett. **71**, 1680 (1993).

[103] B.H. Behrens *et al.* (CLEO Collaboration), Phys. Lett. B **490**, 36 (2000).

[104] D.E. Jaffe *et al.* (CLEO Collaboration), Phys. Rev. Lett. **86**, 5000 (2001).

[105] F. Abe *et al.* (CDF Collaboration), Phys. Rev. D **55**, 2546 (1997).

[106] K. Ackerstaff *et al.* (OPAL Collaboration), Z. Phys. C **76**, 401 (1997).

[107] R. Barate *et al.* (ALEPH Collaboration), Eur. Phys. J. C **20**, 431 (2001).

[108] B. Aubert *et al.* (*BABAR* Collaboration), Phys. Rev. Lett. **92**, 181801 (2004) and Phys. Rev. D **70**, 012007 (2004).

[109] B. Aubert *et al.* (*BABAR* Collaboration), Phys. Rev. Lett. **88**, 231801 (2002).

[110] B. Aubert *et al.* (*BABAR* Collaboration), Phys. Rev. Lett. **96**, 251802 (2006).

[111] B. Aubert *et al.* (*BABAR* Collaboration), BABAR-CONF-06/013, hep-ex/0607091, submitted to ICHEP06.

[112] E. Nakano *et al.* (Belle Collaboration), Phys. Rev. D **73**, 112002 (2006).

[113] G. Abbiendi *et al.* (OPAL Collaboration), Eur. Phys. J. C **12**, 609 (2000).

[114] M. Beneke, G. Buchalla and I. Dunietz, Phys. Lett. B **393**, 132 (1997);
I. Dunietz, Eur. Phys. J. C **7**, 197 (1999).

[115] D. Buskulic *et al.* (ALEPH Collaboration), Z. Phys. C **75**, 397 (1997).

[116] P. Abreu *et al.* (DELPHI Collaboration), Z. Phys. C **76**, 579 (1997).

[117] J. Abdallah *et al.* (DELPHI Collaboration), Eur. Phys. J. C **28**, 155 (2003).

[118] M. Acciarri *et al.* (L3 Collaboration), Eur. Phys. J. C **5**, 195 (1998).

[119] K. Ackerstaff *et al.* (OPAL Collaboration), Z. Phys. C **76**, 417 (1997).

[120] K. Ackerstaff *et al.* (OPAL Collaboration), Z. Phys. C **76**, 401 (1997).

[121] G. Alexander *et al.* (OPAL Collaboration), Z. Phys. C **72**, 377 (1996).

[122] G. Abbiendi *et al.* (OPAL Collaboration), Phys. Lett. B **493**, 266 (2000).

[123] F. Abe *et al.* (CDF Collaboration), Phys. Rev. Lett. **80**, 2057 (1998) and Phys. Rev. D **59**, 032001 (1999).

[124] F. Abe *et al.* (CDF Collaboration), Phys. Rev. D **60**, 051101 (1999).

[125] F. Abe *et al.* (CDF Collaboration), Phys. Rev. D **60**, 072003 (1999).

[126] T. Affolder *et al.* (CDF Collaboration), Phys. Rev. D **60**, 112004 (1999).

[127] CDF Collaboration, CDF note 8235, April 26, 2006, `http://www-cdf.fnal.gov/physics/new/bottom/060406.blessed-semi_B0mix/`

[128] CDF Collaboration, CDF note 7920, November 15, 2005, `http://www-cdf.fnal.gov/physics/new/bottom/050804.hadr_B0mix/`

[129] V.M. Abazov *et al.* (DØ Collaboration), Phys. Rev. D **74**, 112002 (2006).

[130] B. Aubert *et al.* (*BABAR* Collaboration), Phys. Rev. Lett. **88**, 221802 (2002) and Phys. Rev. D **66**, 032003 (2002).

[131] B. Aubert *et al.* (*BABAR* Collaboration), Phys. Rev. Lett. **88**, 221803 (2002).

[132] Y. Zheng *et al.* (Belle Collaboration), Phys. Rev. D **67**, 092004 (2003).

[133] H. Albrecht *et al.* (ARGUS Collaboration), Z. Phys. C **55**, 357 (1992); Phys. Lett. B **324**, 249 (1994).

[134] V.M. Abazov *et al.* (DØ Collaboration), hep-ex/0701007, to appear in Phys. Rev. Lett.

[135] R. Aleksan, Phys. Lett. B **316**, 567 (1993).

[136] V.M. Abazov *et al.* (DØ Collaboration), Phys. Rev. Lett. **98**, 121801 (2007).

[137] U. Nierste, private communication, September 2006.

[138] R. Barate *et al.* (ALEPH Collaboration), Phys. Lett. B **486**, 286 (2000).

[139] V.M. Abazov *et al.* (DØ Collaboration), hep-ex/0702049, February 2007, submitted to Phys. Rev. Lett.

[140] CDF Collaboration, CDF note 7925, March 2006.

[141] A. Abulencia *et al.* (CDF Collaboration), Phys. Rev. Lett. **97**, 242003 (2006); this result supersedes A. Abulencia *et al.* (CDF Collaboration), Phys. Rev. Lett. **97**, 062003 (2006).

[142] M. Okamoto, plenary talk at the XXIIIth International Symposium on Lattice Field Theory, Dublin, July 2005, hep-lat/0510113; this estimate is obtained by combining the unquenched lattice QCD calculations from A. Gray *et al.* (HPQCD Collaboration), Phys. Rev. Lett. **95**, 212001 (2005) and S. Aoki *et al.* (JLQCD Collaboration), Phys. Rev. Lett. **91**, 212001 (2003).

[143] H.-G. Moser and A. Roussarie, Nucl. Instrum. Methods A **384**, 491 (1997).

[144] A. Heister *et al.* (ALEPH Collaboration), Eur. Phys. J. C **29**, 143 (2003).

[145] F. Abe *et al.* (CDF Collaboration), Phys. Rev. Lett. **82**, 3576 (1999).

[146] V.M. Abazov *et al.* (DØ Collaboration), Phys. Rev. Lett. **97**, 021802 (2006).

[147] DØ Collaboration, DØ notes 5172-CONF, 5174-CONF, and 5254-CONF, July and October 2006, submitted to summer and fall 2006 conferences.

[148] J. Abdallah *et al.* (DELPHI Collaboration), Eur. Phys. J. C **35**, 35 (2004).

[149] G. Abbiendi *et al.* (OPAL Collaboration), Eur. Phys. J. C **11**, 587 (1999).

[150] G. Abbiendi *et al.* (OPAL Collaboration), Eur. Phys. J. C **19**, 241 (2001).

[151] K. Abe *et al.* (SLD Collaboration), Phys. Rev. D **67**, 012006 (2003).

[152] K. Abe *et al.* (SLD Collaboration), Phys. Rev. D **66**, 032009 (2002).

[153] SLD Collaboration, SLAC-PUB-8568, contrib. to 30th Int. Conf. on High-Energy Physics, Osaka, Japan (2000).

[154] CDF Collaboration, CDF notes 7907 and 7941, October and November 2005, submitted to fall 2005 conferences.

[155] DØ Collaboration, DØ notes 4878 and 4881, July 2005, submitted to summer 2005 conferences.

[156] L.L. Chau and W.Y. Keung, Phys. Rev. Lett. **53**, 1802 (1984).

[157] L. Wolfenstein, Phys. Rev. Lett. **51**, 1945 (1983).

[158] A.J. Buras, M.E. Lautenbacher and G. Ostermaier, Phys. Rev. D **50**, 3433 (1994).

[159] A.B. Carter and A.I. Sanda, Phys. Rev. D **23**, 1567 (1981). I.I.Y. Bigi, A.I. Sanda, Nucl. Phys. B **193**, 85 (1981).

[160] B. Aubert *et al.* (*BABAR* Collaboration), Phys. Rev. Lett. **86**, 2515 (2001).

[161] K. Abe *et al.* (Belle Collaboration), Phys. Rev. Lett. **87**, 091802 (2001).

[162] B. Aubert *et al.* (*BABAR* Collaboration), BABAR-CONF-06/043 (hep-ex/0607081).

[163] R. Itoh, Y. Onuki, *et al.* (Belle Collaboration), Phys. Rev. Lett. **95**, 091601 (2005).

[164] B. Aubert *et al.* (*BABAR* Collaboration), BABAR-CONF-06/036 (hep-ex/0607107).

[165] K.-F. Chen, K. Hara *et al.* (Belle Collaboration), Phys. Rev. Lett. **98** (2007) 031802.

[166] R. Barate *et al.* (ALEPH Collaboration), Phys. Lett. B **492**, 259 (2000).

[167] K. Ackerstaff *et al.* (OPAL Collaboration), Eur. Phys. J C **5**, 379 (1998).

[168] T. Affolder *et al.* (CDF Collaboration), Phys. Rev. D **61**, 072005 (2000).

[169] CKMfitter Group (J. Charles *et al.*), Eur. Phys. J. C **41**, 1 (2005). Updated results available at `http://www.slac.stanford.edu/xorg/ckmfitter/`

[170] UTfit Collaboration (M. Bona *et al.*) JHEP **0507**, 028 (2005). Updated results available at `http://www.utfit.org/`

[171] I. Dunietz, H. Quinn, A. Snyder, W. Toki, H.J. Lipkin, Phys. Rev. D **43**, 2193 (1991).

[172] D. Aston *et al.* (LASS Collaboration), Nucl. Phys. B **296**, 493 (1988).

[173] M. Suzuki, Phys. Rev. D **64**, 117503 (2001).

[174] B. Aubert *et al.* (*BABAR* Collaboration), Phys. Rev. D **71**, 032005 (2005).

[175] T.E. Browder, A. Datta, P.J. O'Donnell, S. Pakvasa, Phys. Rev. D **61**, 054009 (2000).

[176] B. Aubert *et al.* (*BABAR* Collaboration), Phys. Rev. D **74**, 091101 (2006).

[177] I. Dunietz, R. Fleischer and Ulrich Nierste Phys. Rev. D **63**, 114015 (2001).

[178] V. Abazov *et al.* (DØ Collaboration), hep-ex/0702030.

[179] Yu. Grossman, M.P. Worah, Phys. Lett. B **395**, 241 (1997).

[180] R. Fleischer, Phys. Lett. B **562**, 234 (2003); Nucl. Phys. B **659**, 321 (2003).

[181] A. Bondar, T. Gershon, P. Krokovny, Phys. Lett. B **624**, 1 (2005).

[182] P. Krokovny *et al.* (Belle Collaboration), Phys. Rev. Lett. **97**, 081801 (2006).

[183] B. Aubert *et al.* (*BABAR* Collaboration), BABAR-CONF-06/017 (hep-ex/0607105).

[184] See, for example, Y. Grossman, Z. Ligeti, Y. Nir, H. Quinn, Phys. Rev. D **68**, 015004 (2003), M. Gronau, Y. Grossman, J. Rosner, Phys. Lett. B **579**, 331 (2004), M. Gronau, J. Rosner, J. Zupan, Phys. Lett. B **596**, 107 (2004), H.Y. Cheng, C.K. Chua, A. Soni, Phys. Rev. D **72**, 014006 (2005), M. Gronau, J. Rosner, Phys. Rev. D **71**, 074019 (2005), M. Beneke, Phys. Lett. B **620**, 143 (2005), G. Engelhard, Y. Nir, G. Raz, Phys. Rev. D **72**, 075013 (2005), H.Y. Cheng, A. Soni, Phys. Rev. D **72**, 094003 (2005), and references therein.

[185] B. Aubert *et al.* (*BABAR* Collaboration), Phys. Rev. D **71**, 091102(R) (2005).

[186] B. Aubert *et al.* (*BABAR* Collaboration), Phys. Rev. Lett. **98** (2007) 031801.

[187] B. Aubert *et al.* (*BABAR* Collaboration), BABAR-CONF-06/18 (hep-ex/0607108).

[188] B. Aubert *et al.* (*BABAR* Collaboration), BABAR-CONF-06/030 (hep-ex/0607096).

[189] K. Abe *et al.* (Belle Collaboration), BELLE-CONF-0648 (hep-ex/0609006).

[190] B. Aubert *et al.* (*BABAR* Collaboration), Phys. Rev. Lett. **98**, 051803 (2007).

[191] B. Aubert *et al.* (*BABAR* Collaboration), BABAR-CONF-06/012 (hep-ex/0607101).

[192] B. Aubert *et al.* (*BABAR* Collaboration), BABAR-CONF-04/019 (hep-ex/0408095).

[193] B. Aubert *et al.* (*BABAR* Collaboration), BABAR-CONF-05/020 (hep-ex/0508017).

[194] B. Aubert *et al.* (*BABAR* Collaboration), BABAR-CONF-05/002 (hep-ex/0507016).

[195] B. Aubert *et al.* (*BABAR* Collaboration), BABAR-CONF-06/040 (hep-ex/0607112).

[196] A. Garmash *et al.* (Belle Collaboration), Phys. Rev. D **71**, 092003 (2005).

[197] B. Aubert *et al.* (*BABAR* Collaboration), Phys. Rev. D **74**, 032003 (2006)

[198] B. Aubert *et al.* (*BABAR* Collaboration), Phys. Rev. D **74**, 011101 (2006).

[199] S.U. Kataoka *et al.* (Belle Collaboration), Phys. Rev. Lett. **93**, 261801 (2004).

[200] B. Aubert *et al.* (*BABAR* Collaboration), Phys. Rev. Lett. **95**, 131802 (2005).

[201] See talk by S. Fratina at CKM2006.

[202] B. Aubert *et al.* (*BABAR* Collaboration), Phys. Rev. Lett. **95**, 151804 (2005).

[203] H. Miyake, M. Hazumi, *et al.* (Belle Collaboration), Phys. Lett. B **618**, 34 (2005).

[204] T. Aushev, Y. Iwasaki *et al.* (Belle Collaboration), Phys. Rev. Lett. **93**, 201802 (2004).

[205] B. Aubert *et al.* (*BABAR* Collaboration), Phys. Rev. Lett. **97**, 171805 (2006).

[206] D. Atwood, M. Gronau and A. Soni, Phys. Rev. Lett **79**, 185 (1997).

[207] D. Atwood, T. Gershon, M. Hazumi and A. Soni, Phys. Rev. D **71**, 076003 (2005).

[208] B. Grinstein, Yu. Grossman, Z. Ligeti and D. Pirjol, Phys. Rev. D **71**, 011504 (2005).

[209] B. Aubert *et al.* (*BABAR* Collaboration), Phys. Rev. D **72**, 051103 (2005).

[210] Y. Ushiroda, K. Sumisawa *et al.* (Belle Collaboration), Phys. Rev. D **74**, 111104 (2006).

[211] A.E. Snyder and H.R. Quinn, Phys. Rev. D **48**, 2139 (1993).

[212] H.R. Quinn and J.P. Silva, Phys. Rev. D **62**, 054002 (2000).

[213] B. Aubert *et al.* (*BABAR* Collaboration), BABAR-CONF-06/039 (hep-ex/0607106).

[214] H. Ishino *et al.*, (Belle Collaboration), BELLE-CONF-0649 (hep-ex/0608035).

[215] B. Aubert *et al.* (*BABAR* Collaboration), BABAR-CONF-06/016 (hep-ex/0607098).

[216] K. Abe *et al.* (Belle Collaboration), BELLE-CONF-0678 (hep-ex/0702009).

[217] B. Aubert *et al.* (*BABAR* Collaboration), Phys. Rev. Lett. **91**, 201802 (2003).

[218] C.C. Wang *et al.* (Belle Collaboration), Phys. Rev. Lett **94**, 121801 (2005).

[219] B. Aubert *et al.* (*BABAR* Collaboration), BABAR-CONF-06/037 (hep-ex/0608002).

[220] K. Abe *et al.* (Belle Collaboration), BELLE-CONF-0650 (hep-ex/0609003); A. Kusaka, C.C. Wang, H. Ishino BELLE-PREPRINT-2007-4 (hep-ex/0701015).

[221] B. Aubert *et al.* (*BABAR* Collaboration), BABAR-PUB-06/071 (hep-ex/0612050).

[222] M. Gronau and J.L. Rosner, Phys. Rev. D **65**, 093012 (2002).

[223] B. Aubert *et al.* (*BABAR* Collaboration), Phys. Rev. Lett. **98**, 111801 (2007).

[224] M. Gronau and D. London, Phys. Rev. Lett. **65**, 3381 (1990).

[225] H.J. Lipkin, Y. Nir, H.R. Quinn and A.E. Snyder, Phys. Rev. D **44**, 1454 (1991).

[226] B. Aubert *et al.* (*BABAR* Collaboration), Phys. Rev. D **73**, 111101 (2006).

[227] F.J. Ronga, T. Sarangi *et al.* (Belle Collaboration), Phys. Rev. D **73**, 092003 (2006).

[228] B. Aubert *et al.* (*BABAR* Collaboration), Phys. Rev. D **71**, 112003 (2005).

[229] T. Gershon *et al.* (Belle Collaboration), Phys. Lett. B **624** 11 (2005).

[230] O. Long, M. Baak, R.N. Cahn, D. Kirkby, Phys.Rev. D **68**, 034010 (2003).

[231] R. Fleischer, Nucl. Phys. B **671**, 459 (2003).

[232] I.I. Bigi and A.I. Sanda, Phys. Lett. B **211**, 213 (1988).

[233] M. Gronau and D. London, Phys. Lett. B **253**, 483 (1991), M. Gronau and D. Wyler, Phys. Lett. B **265**, 172 (1991).

[234] D. Atwood, I. Dunietz, and A. Soni, Phys. Rev. Lett. **78**, 3257 (1997), Phys. Rev. D **63**, 036005 (2001).

[235] A. Giri, Y. Grossman, A. Soffer and J. Zupan, Phys. Rev. D **68**, 054018 (2003); A. Poluektov *et al.* (Belle Collaboration), Phys. Rev. D **70**, 072003 (2004).

[236] A. Bondar and T. Gershon, Phys. Rev. D **70**, 091503(R) (2004).

[237] B. Aubert *et al.* (*BABAR* Collaboration), Phys. Rev. D **73**, 051105 (2006).

[238] K. Abe *et al.* (Belle Collaboration), Phys. Rev. D **73**, 051106 (2006).

[239] B. Aubert *et al.* (*BABAR* Collaboration), Phys. Rev. D **71**, 031102 (2005).

[240] B. Aubert *et al.* (*BABAR* Collaboration), Phys. Rev. D **72**, 071103(R) (2005).

[241] B. Aubert *et al.* (*BABAR* Collaboration), Phys. Rev. D **72**, 032004 (2005).

[242] K. Abe *et al.* (Belle Collaboration), BELLE-CONF-0552 (hep-ex/0508048).

[243] B. Aubert *et al.* (*BABAR* Collaboration), Phys. Rev. D **72**, 071104 (2005).

[244] B. Aubert *et al.* (*BABAR* Collaboration), BABAR-CONF-06/007 (hep-ex/0607065).

[245] M. Gronau, Phys. Lett. B **557**, 198 (2003).

[246] B. Aubert *et al.* (*BABAR* Collaboration), BABAR-CONF-06/038 (hep-ex/0607104).

[247] A. Poluektov *et al.* (Belle Collaboration), Phys. Rev. D **73**, 112009 (2006).

[248] B. Aubert *et al.* (*BABAR* Collaboration), BABAR-CONF-05/018 (hep-ex/0507101).

[249] B. Aubert [BABAR Collaboration], arXiv:hep-ex/0607076.

[250] J. E. Duboscq *et al.* [CLEO Collaboration], Phys. Rev. Lett. **76**, 3898 (1996).

[251] D. Buskulic *et al.* (ALEPH Collaboration), Phys. Lett. B **395**, 373 (1997).

[252] G. Abbiendi *et al.* (OPAL Collaboration), Phys. Lett. B **482**, 15 (2000) [arXiv:hep-ex/0003013].

[253] P. Abreu *et al.* (DELPHI Collaboration), Phys. Lett. B **510**, 55 (2001) [arXiv:hep-ex/0104026].

[254] K. Abe *et al.* (Belle Collaboration), Phys. Lett. B **526**, 247 (2002) [arXiv:hep-ex/0111060].

[255] N. E. Adam *et al.* (CLEO collaboration), Phys. Rev. D **67**, 032001 (2003) [arXiv:hep-ex/0210040].

[256] J. Abdallah *et al.* (DELPHI Collaboration), Eur. Phys. J. C **33**, 213 (2004) [arXiv:hep-ex/0401023].

[257] S. Hashimoto, A. S. Kronfeld, P. B. Mackenzie, S. M. Ryan and J. N. Simone, Phys. Rev. D **66**, 014503 (2002) [arXiv:hep-ph/0110253].

[258] J. Bartelt *et al.* (CLEO Collaboration), Phys. Rev. Lett. **82**, 3746 (1999) [arXiv:hep-ex/9811042].

[259] K. Abe *et al.* (Belle Collaboration), Phys. Lett. B **526**, 258 (2002) [arXiv:hep-ex/0111082].

[260] N. Uraltsev, Phys. Lett. B **585**, 253 (2004) [arXiv:hep-ph/0312001].

[261] O. Buchmuller and H. Flacher, Phys. Rev. D **73**, 073008 (2006) [arXiv:hep-ph/0507253].

[262] P. Gambino and N. Uraltsev, Eur. Phys. J. C **34**, 181 (2004) [arXiv:hep-ph/0401063].

[263] H. Albrecht *et al.* [ARGUS Collaboration], Phys. Lett. B **318**, 397 (1993).

[264] K. Abe *et al.* [Belle Collaboration], Phys. Lett. B **547**, 181 (2002) [arXiv:hep-ex/0208033].

[265] A. H. Mahmood *et al.* [CLEO Collaboration], Phys. Rev. D **70**, 032003 (2004) [arXiv:hep-ex/0403053].

[266] B. Aubert *et al.* [BABAR Collaboration], Phys. Rev. D **69**, 111104 (2004) [arXiv:hep-ex/0403030].

[267] B. Aubert *et al.* [BABAR Collaboration], Phys. Rev. D **74**, 091105 (2006) [arXiv:hep-ex/0607111].

[268] P. Urquijo *et al.* [Belle Collaboration],, Phys. Rev. D **75**, 032001 (2007) [arXiv:hep-ex/0610012].

[269] E. Barberio *et al.* [Heavy Flavor Averaging Group(HFAG)], arXiv:hep-ex/0603003.

[270] M. Artuso *et al.* [CLEO Collaboration], Phys. Lett. B **399**, 321 (1997) [arXiv:hep-ex/9702007].

[271] S. Henderson *et al.* [CLEO Collaboration], Phys. Rev. D **45**, 2212 (1992).

[272] H. Albrecht *et al.* [ARGUS Collaboration], Phys. Lett. B **324**, 249 (1994).

[273] See, for example, I. I. Y. Bigi, M. A. Shifman and N. Uraltsev, Ann. Rev. Nucl. Part. Sci. **47**, 591 (1997); M. Neubert, Nucl. Phys. Proc. Suppl. **59**, 101 (1997); A. H. Hoang, Z. Ligeti and A. V. Manohar, Phys. Rev. D **59**, 074017 (1999), and references therein.

[274] M. Battaglia *et al.*, Phys. Lett. B **556**, 41 (2003) [arXiv:hep-ph/0210319].

[275] A. H. Mahmood *et al.* [CLEO Collaboration], Phys. Rev. D **67**, 072001 (2003) [arXiv:hep-ex/0212051].

[276] B. Aubert *et al.* (*BABAR* Collaboration), Phys. Rev. Lett. **93**, 011803 (2004) [arXiv:hep-ex/0404017].

[277] C. W. Bauer, Z. Ligeti, M. Luke, A. V. Manohar and M. Trott, Phys. Rev. **D70**, 094017 (2004).

[278] P. Urquijo for the Belle Colloboration, Results presented at the XXXIII INTERNATIONAL CONFERENCE ON HIGH ENERGY PHYSICS, see http://ichep06.jinr.ru/reports/

[279] B. Aubert *et al.* (BABAR Collab.), Phys. Rev. **D69**:111103 (2004).

[280] B. Aubert *et al.* (BABAR Collab.), Phys. Rev. **D69**:111104 (2004).

[281] B. Aubert *et al.* (BABAR Collab.), Phys. Rev. Lett. **93**:011803 (2004).

[282] B. Aubert *et al.* (BABAR Collab.), Phys. Rev. **D72**:052004 (2005).

[283] B. Aubert *et al.* (BABAR Collab.), hep-ex/0507001.

[284] BELLE Collab., hep-ex/0408139 (2004).

[285] BELLE Collab., hep-ex/0409015 (2004).

[286] P. Koppenburg *et al.* (BELLE Collab.), Phys. Rev. Lett. **93**:061803 (2004), K. Abe *et al.* [Belle Collaboration], arXiv:hep-ex/0508005.

[287] S. E. Csorna *et al.* (CLEO Collab.), Phys. Rev. **D70**:032002 (2004).

[288] A. H. Mahmood *et al.* (CLEO Collab.), Phys. Rev. **D70**:032003 (2004).

[289] S. Chen *et al.* (CLEO Collab.), Phys. Rev. Lett. **87**:251807 (2001).

[290] D. Acosta *et al.* (CDF Collab.), Phys. Rev. **D71**:051103 (2005).

[291] DELPHI Collab., CERN-PH-EP/2005-015 (2005).

[292] S. B. Athar *et al.* (CLEO Collab.), Phys. Rev. **D68**:072003 (2003).

[293] B. Aubert *et al.* (BABAR Collaboration), Phys. Rev. Lett. **98** (2007) 091801 [arXiv:hep-ex/0612020].

[294] T. Hokuue *et al.* [Belle Collaboration], arXiv:hep-ex/0604024.

[295] B. Aubert [BABAR Collaboration], Phys. Rev. Lett. **97** (2006) 211801 [arXiv:hep-ex/0607089].

[296] K. Abe [Belle Collaboration], arXiv:hep-ex/0610054.

[297] P. Ball and R. Zwicky, Phys. Rev. **D71** (2005) 014015

[298] J. Shigemitsu *et al.* (HPQCD), Nucl. Phys. Proc. Suppl. **140**, 464 (2005)

[299] M. Okamoto *et al.* (Fermilab/MILC), Nucl. Phys. Proc. Suppl. **140**, 461 (2005)

[300] A. Abada, D. Becirevic, P. Boucaud, J. P. Leroy, V. Lubicz and F. Mescia, Nucl. Phys. B **619**, 565 (2001) [arXiv:hep-lat/0011065].

[301] B. H. Behrens *et al.* (CLEO Collab.), Phys. Rev. **D61**:052001 (2000).

[302] BABAR Collab., hep-ex/0408068.

[303] BABAR Collab., hep-ex/0301001.

[304] K. Abe *et al.* (BELLE Collab.), Phys. Rev. Lett. **93**:131803 (2004).

[305] [BABAR Collaboration], arXiv:hep-ex/0607066.

[306] B. O. Lange, M. Neubert and G. Paz, Phys. Rev. D **72**, 073006 (2005)

[307] J. R. Andersen and E. Gardi, JHEP **0601**, 097 (2006) [arXiv:hep-ph/0509360].

[308] C. W. Bauer, Z. Ligeti and M. E. Luke, Phys. Rev. D **64**, 113004 (2001) [arXiv:hep-ph/0107074].

[309] I. Bizjak *et al.* (Belle Collaboration), Phys. Rev. Lett. **95** (2005) 241801 [arXiv:hep-ex/0505088].

[310] A. K. Leibovich, I. Low and I. Z. Rothstein, Phys. Rev. D **61**, 053006 (2000) [arXiv:hep-ph/9909404].

[311] B. Aubert *et al.* [BABAR Collaboration], Phys. Rev. Lett. **96**, 221801 (2006) [arXiv:hep-ex/0601046].

[312] R. Kowalewski and S. Menke, Phys. Lett. B **541**:29 (2002).

[313] A. Bornheim *et al.* (CLEO Collab.), Phys. Rev. Lett. **88**:231803 (2002).

[314] B. Aubert *et al.* (BABAR Collab.) Phys. Rev. Lett. **95**, 111801 (2005).

[315] BABAR Collab., ICHEP 2004 conference contribution, hep-ex/0408075.

[316] A. Limosani *et al.* (BELLE Collab.) Phys. Lett. B **621**, 28 (2005).

[317] BABAR Collab., hep-ex/0507017. This is an update of B. Aubert *et al.* (BABAR Collab.), Phys. Rev. Lett. **92**:071802 (2004).

[318] H. Kakuno *et al.* (BELLE Collab.), Phys. Rev. Lett. **92**:101801 (2004).

[319] S.W. Bosch, B.O. Lange, M. Neubert and G. Paz, Nucl. Phys. B **699**:335 (2004).

[320] S.W. Bosch, M. Neubert and G. Paz, JHEP **0411**:073 (2004).

[321] M. Neubert, Eur. Phys. J. C **44** (2005) 205 [arXiv:hep-ph/0411027].

[322] M. Neubert, Phys. Lett. B **612**:13 (2005).

[323] D. Benson, I.I. Bigi and N. Uraltsev, Nucl. Phys. **B710**, 371 (2005); hep-ph/0410080.

[324] S.W. Bosch, B.O. Lange, M. Neubert and G. Paz, Nucl. Phys. **B699**, 335 (2004); hep-ph/0402094.

[325] A.L. Kagan and M. Neubert, Eur. Phys. Jour. **C7**, 5 (1999); hep-ph/9805303.

[326] R. Barate *et al.*(ALEPH Collaboration), Phys. Lett. B **429**, 169 (1998).

[327] S. Chen *et al.*(CLEO Collaboration), Phys. Rev. Lett. **87**, 251807 (2001).

[328] K. Abe *et al.*(Belle Collaboration), Phys. Lett. B **511**, 151 (2001).

[329] P. Koppenburg *et al.*(Belle Collaboration), Phys. Rev. Lett. **93**, 061803 (2004).

[330] B. Aubert *et al.*(*BABAR* Collaboration), Phys. Rev. D **72**, 052004 (2005).

[331] B. Aubert *et al.*(*BABAR* Collaboration), Phys. Rev. Lett. **97**, 171803 (2006).